CERN Yellow Reports: Monographs CERN-2025-004

Report from the Conventional Beams Working Group to the Physics Beyond Colliders Study and to the 2026 European Strategy for Particle Physics Update

Editors: Johannes Bernhard
Lau Gatignon
Silvia Schuh

CERN Yellow Reports: Monographs
Published by CERN, CH-1211 Geneva 23, Switzerland

ISBN 978-92-9083-686-5 (paperback)
ISBN 978-92-9083-687-2 (PDF)
ISSN 2519-8068 (Print)
ISSN 2519-8076 (Online)
DOI https://doi.org/10.23731/CYRM-2025-004

This volume should be cited as:

Report from the Conventional Beams Working Group to the Physics Beyond Colliders Study and to the 2026 European Strategy for Particle Physics Update,
Editors: Johannes Bernhard, Lau Gatignon, and Silvia Schuh
CERN Yellow Reports: Monographs, CERN-2025-004 (CERN, Geneva, 2025)
https://doi.org/10.23731/CYRM-2025-004.

Corresponding editor: Johannes Bernhard (johannes.bernhard@cern.ch).

Accepted in Jun. 2025, by the CERN Reports Editorial Board (contact Carlos.Lourenco@cern.ch).

Published by the CERN Scientific Information Service (contact Jens.Vigen@cern.ch).

Indexed in the CERN Document Server and in INSPIRE.

Published Open Access to permit its wide dissemination, as knowledge transfer is an integral part of the mission of CERN.

Preface

This document reports the work and results of the Conventional Beams Working Group, which focuses on studies of the beam-related and technical requirements and requests from proposals submitted to the Physics Beyond Colliders Study (PBC) for the North Area at the CERN SPS and the East Area at the CERN PS accelerators. Previous CBWG reports have been published in 2018 [1] and 2022 [2], providing inputs to the European Strategy for Particle Physics (ESPP) discussions that took place in those years. This new document provides updated and supplementary material relevant for the 2025–2026 ESPP Update, including detailed results regarding the HIKE, SHADOWS, DICE/NA60+, ENUBET, NuTag, and SBN projects. Please note that BDF/SHiP was studied in an independent PBC Working Group [3,4].

Since its inception, the working group has presented results on feasibility, requirements, compatibility between proposals, and, where possible, cost estimates at all PBC Annual Workshops and group meetings. Following the renewed mandate of the PBC Study in 2021, the Conventional Beams Working Group continued its studies for previously received proposals, as well as for new initiatives, including ENUBET, NuTag, a potential Short-Baseline tagged neutrino beam (SBN), SHADOWS, and HIKE. Work relevant to these studies has progressed since the Annual PBC Workshop in 2019 [5], which this document summarises. This edition also includes information on installation work already carried out for some proposals and presents initial studies for the more recent ones.

The physics interest, sensitivity reach, and worldwide competitiveness of the proposals are discussed in the PBC working groups for Beyond Standard Model (BSM) physics and Quantum ChromoDynamics (QCD), as well as in the newly established working group on Feebly Interacting Particles (FIPs). These physics-focused working groups collaborate in close synergy with the Conventional Beams Working Group.

Geneva, March 2025.

Authors

D. Banerjee, A. Baratto Roldan, J. Bernhard, M. Brugger, N. Charitonidis, M. van Dijk, N. Doble, L.A. Dyks, L. Gatignon, M.A. Jebramcik, F. Metzger, R. Murphy, C.A. Mussolini, L.J. Nevay, E.G. Parozzi, S. Schuh, F. Stummer, on behalf of the Physics Beyond Colliders Conventional Beams working group.

Contents

Executive Summary

Introduction

The Conventional Beams Working Group (CBWG) is part of the Accelerators and Technology Domain within the framework of the Physics Beyond Colliders Study Group (PBC). A first report was presented to the PBC in 2018 [1] and an Executive Summary from the CBWG was submitted to the European Strategy for Particle Physics Update (ESPPU) at the same time. These documents in 2018 provided input for the direction of CERN's fixed-target programme, encompassing several facilities and experiments at the Booster, PS and SPS, and spanning the period until the 2040s.

In 2021, the mandate of the PBC study was renewed and extended. Since then, the CBWG continued and refined the ongoing studies, and also adopted the study of new proposals. The Conventional Beams study is complementary to and works in synergy with the PBC Physics Working Groups on Physics Beyond the Standard Model (BSM) and the one on Quantum Chromodynamics (QCD), as well as the Feebly Interacting Particles Physics Centre (FPC). All four working groups support mainly proposals in the North Area at the SPS as most ideas have been brought forward for this particular accelerator complex, now even beyond 2040.

During the PBC kick-off workshop in September 2016, a large number of fixed-target proposals was presented. It was deemed important to perform pre-proposal studies as input for the physics groups to make informed progress with their evaluations. These first indications were published in the above-mentioned PBC report from the CBWG in 2018 [1]. Several of these preliminary studies have been completed since and have been published in 2022 [2]. A few new proposals have been submitted since the PBC mandate was renewed in 2021. The updated list of proposals studied within the CBWG is shown in Table 1.

The North Area [6] comprises two surface halls, EHN1 and EHN2, and an underground cavern, ECN3. EHN1 is the biggest surface hall at CERN with a size of about 330 by 50 m^2, and is served by the H2, H4, H6 and H8 beamlines. EHN2 is served by the M2 beamline for muon, hadron and electron beams and hosted the COMPASS experiment until end 2022. In ECN3, the NA62 experiment for ultra-rare kaon decay measurements will be served by the K12 beamline until LS3, currently planned to start in September 2026. The CBWG groups all proposals per experimental hall. Only the recently added ENUBET and NuTag neutrino beam proposals, now merged into the Short Baseline Neutrino beam (SBN) proposal, are not yet attributed to a specific hall.

The studies summarised in this executive summary are further detailed in the respective chapters within the present report on the CBWG studies.

Proposals for EHN1

Introduction

In EHN1, the NA61/SHINE experiment, installed in the H2 beamline, continues to drive the SPS heavy ion programme. It explores mainly the phase transition to Quark-Gluon Plasma (QGP) and continues open charm measurements and provides hadron production measurements for cosmic ray physics and neutrino beams, and neutrino beams, the latter with replica targets for T2K, LBNF/DUNE, and NuMI. The experiment now profits from a significant, 10-fold increase of the beam intensity in the H2 beamline, but has also requested a study for an in-situ low-energy beamline.

NA64 plans to continue its search for dark photons and dark matter employing the missing energy technique using pure electron beams with continuously increasing beam intensities and, in the future, expand to various types of hadron beams, possibly also in the H4 line or the CERN East Area. To optimise beam time, they plan to maximise the electron beam intensity while maintaining comparable purity and quality. Additionally, they now propose running with medium-energy positron beams.

Table 1: List of proposals followed by the Conventional Beams Working Group.

Experiment	Brief description and comments
AMBER/NA66	Study new requests for QCD physics-related measurements, including RF separated beams and improvements to the conventional beamline for Phase 1 and 2 proposals.
BDF/SHiP	Beam dump experiment to search for feebly interacting particles (FIPs). Formally not part of the CBWG, beam delivery studies in synergy with those for HIKE. Approved in 2024 for a TDR phase followed within the HI-ECN3 project.
DIRAC++	Measurement of pionium to test low-energy QCD. Proposal withdrawn.
ENUBET/NP06	A monitored neutrino beam, now merged into SBN.
HIKE	Detailed study for a next-gen. kaon experiment, measuring $K^+ \to \pi^+\nu\bar{\nu}$ and other (ultra-)rare decays at high precision. Study discontinued as BDF/SHiP was approved for ECN3.
KLEVER	Measurement of $K_L \to \pi^0\nu\bar{\nu}$ in ECN3. Study discontinued as BDF/SHiP was approved for ECN3.
DICE/NA60+	Quark-Gluon Plasma and dilepton production measurements in heavy-ion collisions. Originally considered for ECN3, now studied for delivering lead and proton beams to H8 (EHN1).
NA61++	Hadron production measurements for cosmic-ray physics, neutrino experiments, and heavy-ion studies. Studied higher intensities and implications plus design of a new low energy beam.
NA64e,h	Search for dark sector particles using missing energy technique. Increase electron flux and optimise hadron beams in H4.
NA64μ	Implementation of a NA64-like experiment with muons in M2.
NuTag	A tagged muon neutrino beam, now merged into SBN.
MUonE	Implementation of MUonE for operation with muon beams to study the hadronic contribution to the vacuum polarisation.
SBN	Tagged ν_μ and ν_e neutrino beams, fusion of ENUBET and NuTag.
SHADOWS	Search for off-axis production of FIPs in ECN3, running in parallel with HIKE. Study discontinued as BDF/SHiP was approved for ECN3.
True Muonium	Search for true muonium with a positron beam at resonance threshold. Study on hold.

DICE/NA60+ proposes to study electromagnetic and hard probes of the Quark-Gluon Plasma in heavy-ion collisions using lead beams at various energies at the CERN SPS. The experiment will investigate, among other topics, open charm production and will need proton beam matching the lead beam energies to perform reference measurements. DICE/NA60+ was initially proposed for the underground ECN3 cavern, where higher beam intensities could be made available. However, since this would be incompatible with NA62, HIKE/SHADOWS and BDF/SHiP, the team has opted for an experiment location in EHN1, accepting a trade-off of lower maximum beam intensity and smaller detector dimensions.

NA61++

At the time of the previous ESPPU in 2020, NA61/SHINE requested to continue measurements with ion and hadron beams at ten times higher beam intensity. Radiation measurements and simulations indicated that, at such intensities, the shielding around the new Projectile Spectator Detector (PSD) calorimeter needed significant reinforcement. Furthermore, NA61/SHINE planned several detector upgrades, requiring local modifications to the infrastructure. These modifications have since been successfully implemented, and NA61/SHINE now routinely exploits the higher beam intensities.

At the same time, NA61++ had expressed interest in an in-situ low-energy beam with momenta up to 13 GeV/c. The Conventional Beams Working Group has completed and documented the design for such a beam, incorporating a performant particle identification scheme covering the full range from 2 to 13 GeV/c. The Collaboration submitted a proposal for such a beamline to the SPSC, which supported the physics case. However, the CERN Research Board has placed the request on hold until further notice.

DICE/NA60+

DICE/NA60+ is proposed as follow-up of the NA60 experiment. While an installation in the underground ECN3 cavern would have, in principle, allowed for the highest lead ion beam intensities, strong competition for ECN3 has led the Collaboration to revise its plans. It is proposed to be located at the H8 beamline in the EHN1 surface hall. The CBWG has conducted a detailed study of this proposal and identified the H8 beamline as the only viable location. Extensive integration and radiation protection studies have been completed, and the Collaboration is almost ready to submit a proposal to the SPSC. The experiment requests Pb ion beams ranging from 20 to 150 AGeV/c as well as proton beams in the same range, with very small spot sizes in both planes of $\sigma < 0.6\,\mathrm{mm}$, where σ denotes the standard deviation of the transverse beam profile. The beam has been studied extensively in simulation and in-situ testbeam, showing promising results. The feasibility of the lowest ion and proton beam momenta remains to be confirmed.

NA64: NA64e and NA64h

NA64e has been successfully operating with secondary electron beams in the H4 beamline, utilising synchrotron radiation tagging and tracking, as well as calorimetry to effectively eliminate the effects of beam contamination, which typically occurs at the percent level. Over the years, the beam intensity has been steadily increased, reaching over 10^7 electrons per spill in 2024, while maintaining excellent background conditions. Before LS2, a major limitation was the lengthy setup time at the beginning of each run due to the absence of a permanent location. Following a recommendation from PBC, a new user zone, PPE144, was established just downstream of the previous NA64e location. This allows the experiment to keep its critical detectors in place and connected, significantly improving startup efficiency. As a result, NA64e has achieved the measurement of the most stringent limits to date on dark photons via the $\mathrm{A}' \to$ invisible channel within the covered mass range.

Additionally, NA64 has successfully initiated data-taking with positron beams to search for Light Dark Matter (LDM) with masses above 100 MeV/c^2. The positron programme uses beams of 40 to 60 GeV/c to explore the LDM parameter space in the mass range between 135 to 250 MeV/c^2. This will enable the first probe of the so-called “thermal target lines”, which represent the dark sector coupling values predicted by astrophysical and cosmological arguments for selected model parameter values in the aforementioned mass range.

NA64 is also considering running with hadron beams and studies have been initiated to explore a potential extension of its programme in this direction.

True Muonium

True muonium, the bound state of a positive and a negative muon, was proposed to be studied in the H4 beamline with 43.7 GeV/c positrons, which corresponds to the threshold for di-muon production in a fixed-target configuration. Hadronic contamination was studied in the context of NA64 running with positrons in H4. The maximal beam intensity at H4 today is about 10^7 e^+/spill while the energy spread is estimated to be around 1 %. Recently, a study for the target optimisation (40 low-Z Lithium foils) was conducted showing that, in principle, a discovery of true muonium at the 5σ-level could be achieved during three months of data taking. A detailed study is planned to understand the feasibility of such a search within NA64. Such a project would profit if higher intensity and smaller momentum resolution of the beamline would become possible.

Proposals for EHN2

Introduction

In the EHN2 hall, COMPASS continued its programme using the existing M2 muon and hadron beam options until the end of 2022, when the experiment officially completed its data-taking. The AMBER/NA66 Collaboration, which emerged from several institutes of the COMPASS Collaboration, proposes to continue an extensive QCD physics programme in EHN2 using both muon and hadron beams. This programme has been developed through the CBWG and has officially been approved as the NA66 experiment. It encompasses a measurement of the proton radius and antimatter production measurements. A Drell–Yan measurement with kaon and pion beams is currently planned for post-LS3.

The NA64 Collaboration uses the M2 muon beam for dark matter searches, for instance investigating invisible decays of a potential Z' boson as a low-mass explanation for the muon $(g-2)_\mu$ anomaly. This part of the programme is also known as NA64μ. The required muon beam properties are well within the capabilities of the existing M2 muon beamline. Compatibility with AMBER has been assessed, and an implementation plan has been developed. The changeover between NA64μ and AMBER requires only a few days and can be carried out within a run period, as demonstrated in the recent years. In a more advanced stage, NA64μ aims to establish a parasitic installation within the AMBER spectrometer, though this approach requires further detailed studies.

MUonE aims to measure μ-e elastic scattering, providing an independent measurement of the hadronic contribution to the vacuum polarisation, which might contribute to the interpretation of the latest precision measurements of $(g-2)_\mu$ and their implications for new physics. The required muon beam properties are well within the capabilities of the existing M2 beamline. Scenarios for the installation of a full MUonE setup in parallel with AMBER have been investigated.

A new user zone, PPE211, located in the beam tunnel upstream of the experimental hall, has been completed during LS2. This zone has successfully hosted several test beam runs for all three experiments.

AMBER

The AMBER/NA66 Collaboration utilises the M2 beamline as a versatile QCD facility, enabling a wide range of QCD-related physics measurements under various beam conditions. The first phase, developed with significant support from the CBWG, was in large parts approved by the SPSC in 2020, and data-taking is currently underway. The approved AMBER physics programme includes a measurement of the proton radius using muon beams and antimatter production measurements to contribute to the interpretation of the latest AMS results. Phase 1 also consists of Drell–Yan data collection with hadron beams, possibly after LS3. The beam requirements generally align with the standard capabilities of the M2 beamline, both in hadron and muon modes.

In recent years, the Collaboration has been preparing for a second phase of its physics programme. The primary challenge for the CBWG is the request for a high-intensity kaon beam for a Drell–Yan experiment. Due to the low kaon production rate, combined with the short kaon lifetime and the M2 beamline's length of over 1100 m, the kaon content at the AMBER experimental site is relatively low, at only the percent level. Furthermore, radiation protection constraints in and around the experimental hall limit the total beam intensity, hence limiting the maximum achievable kaon rate.

Kaons are tagged using two differential Cherenkov counters (CEDAR), which are insensitive to other particle species in the beam. These counters could handle much higher kaon beam rates if available. However, for optimal kaon identification efficiency and rejection of other species, the CEDARs require a highly parallel beam. Currently, the M2 beam exhibits significant divergence at the CEDAR location due to over 80 m of beamline at atmospheric pressure, which increases beam spread.

To enhance K-π separation in the beam, the option of a radio-frequency (RF) separated kaon beam was explored to increase the kaon fraction. The CBWG conducted a detailed pre-study in collaboration with the CERN RF group to assess the feasibility of such a beamline, employing 3.9 GHz cavities with 30 mm diameter irises, based on the ILC crab cavity design. This cavity configuration was deemed the only technically and economically viable option. However, the cavity frequency and available space between cavities limit the kaon momentum to a maximum of approximately 80 GeV/c. For a kaon purity of around 20 %, the maximum achievable K^- flux would be 3×10^6 per SPS spill, roughly a factor of 30 below the AMBER requirement for the Drell–Yan programme. While such a kaon-enhanced beam might still be beneficial for lower-intensity components of the AMBER programme, like the Primakoff experiment, similar kaon intensities could be achieved using the conventional hadron beam, without incurring the substantial costs of RF cavities and associated infrastructure (estimated at several tens of MCHF). Moreover, even with RF separation, the CEDAR detectors' limited tagging efficiency remains a bottleneck for kaon intensity at the AMBER site.

As an alternative, upgrading the existing M2 beamline to improve vacuum conditions and particle identification presents a cost-effective solution. Placing as many beam sections as possible under vacuum significantly reduces beam divergence at the CEDAR detectors. The M2 beamline, originally designed exclusively for muon operation, included atmospheric sections that had little impact on muon performance. Most of these sections are located at nine 5 m-long magnetic collimators, which are toroidal magnets with adjustable apertures and, therefore, not under vacuum. For muon beams, precise aperture adjustments are critical, but for hadron beams, the aperture positions can be fixed, allowing racetrack-shaped vacuum tubes to be installed without damaging the collimators. Additionally, a 10 m-long atmospheric section exists where mobile hadron absorbers are positioned to absorb hadrons after the 700 m decay section for muon beam operations. These absorbers can also be modified to be vacuum-compatible.

Detailed studies have assessed the performance of the M2 hadron beam with improved vacuum conditions. Simulations suggest that enhanced vacuum maintains the beam characteristics at the experimental hall as defined by collimators far upstream. This allows for increased sine-like transfer matrix elements (R_{12} and R_{34}), which improves beam parallelism at the CEDARs without the need for tight re-collimation just before the CEDARs and the AMBER experiment. This improvement addresses background issues from collimators close to the experiment, as previously encountered by the COMPASS experiment at the same location.

Technical solutions for implementing vacuum inside the scrapers and absorber regions are planned. With these improvements, beam parallelism is expected to meet the requirements for all phases of AMBER. However, the impact of enhanced vacuum on high-intensity muon beams remains to be determined. If negatively affected, studies will be required to evaluate the resources needed for switching magnetic collimators between muon and hadron modes.

The first part of improving the beamline vacuum is underway, with costs significantly lower than those for an RF-separated beamline. Furthermore, the CEDAR counters have been recently refurbished and upgraded, enhancing their intrinsic kaon identification efficiency and rate capabilities. Further improvements are planned for LS3.

Another potential future option for AMBER was a low-energy negative hadron beam in the range of 12 to 20 GeV/c. At these low energies, the majority of pions and kaons decay over the 1.1 km beamline, resulting in a beam highly enriched in antiprotons. This allows for high antiproton rates without exceeding radiation limits due to overall beam flux. This option also benefits from the aforementioned vacuum improvements. However, CEDAR detectors are unsuitable for such low momenta, and the use of high-rate, upgraded threshold Cherenkov detectors is under study for these low-energy beams. However, AMBER has, for the moment, put on hold this part of the programme.

Additionally, AMBER, like the COMPASS experiment before it, intends to use tertiary electron beams for calibration purposes. The atmospheric pressure sections of the beamline have been particularly detrimental for electron beams. With improved vacuum in the M2 beamline, the performance of tertiary electron beams may become comparable, at least in intensity, to those in EHN1. If needed, the magnetic collimators and hadron absorbers could be replaced with standard vacuum tubes at a modest cost. This change would also significantly enhance the rate of tertiary electron beams.

NA64μ

NA64μ utilises the M2 muon beam for missing energy searches, similar to NA64e in the H4 beamline. The use of a muon beam extends the accessible mass range for dark sector particles and enables dedicated searches for particles that couple exclusively to muons, such as a hypothetical Z' boson, which has been proposed as a potential low-mass explanation for the $(g-2)_\mu$ anomaly. The existing M2 muon beam already meets the experimental requirements in terms of both beam momentum and flux.

However, the proposed experiment extends over 20 m and cannot be accommodated within the existing AMBER experimental zone without the removal of a significant portion of that setup. A feasible installation solution has been identified upstream of the AMBER zone, at the end of the beam tunnel. By removing two quadrupoles and adding two dipoles, a 20 m long free region can be created in zone PPE211 within a few days, providing sufficient space to host the NA64μ experiment. The beam optics have been locally modified to meet the specific local beam conditions required for NA64μ.

The experiment is currently running under stable conditions and is expected to continue well beyond LS3. A future high-rate upgrade would enable it to fully exploit the higher muon intensities achievable with M2.

MUonE

The MUonE Collaboration proposes a measurement of muon-electron elastic scattering, which is an independent way of determining the hadronic contribution to vacuum polarisation and would help to interpret the latest $(g-2)_\mu$ results. The experiment will utilise the M2 muon beam under standard operating conditions, with minor local optics modifications just upstream of the experimental setup. While the beam parameter constraints are similar to those of NA64μ, they are not identical, and MUonE requires a significantly longer detector setup of about 40 m.

The proposal suggests placing the MUonE experiment at the same location planned for NA64μ, with some additional modifications. Simultaneous operation of MUonE and NA64μ is not feasible due to incompatible layouts and conflicting beam rate requirements. Similarly, MUonE and AMBER cannot operate concurrently because the presence of MUonE equipment negatively impacts muon beam performance.

To date, MUonE has successfully operated with up to two target modules out of the 40 planned for the final setup. Cohabitation with other users has been smooth, with straightforward and time-efficient changeovers. However, with the full 40-module setup, changeovers will become more complex. Integration studies are underway to identify the best cohabitation scenario for all three experiments. Approximately 60 m of the M2 beamline will need to be cleared for MUonE runs.

Initially, MUonE requested relatively modest muon beam rates. However, to significantly reduce the required data-taking period, the Collaboration is now considering intensities up to 10^9 muons per SPS spill, which is substantially higher than the current limit of 2×10^8 muons per spill in EHN2. Further studies and beam tests are ongoing to mitigate radiation limitations, investigating the possibility of deflecting the muon beam downward after the MUonE setup to minimise radiation dose on the surface at the edge of the CERN site.

ECN3 Proposals

Introduction

Located in the underground cavern ECN3, the NA62 experiment currently measures the branching ratio of the very rare decay mode $K^+ \to \pi^+\nu\bar{\nu}$. During occasional shorter runs, the beamline is operated in beam dump mode, creating relatively clean conditions for Hidden Sector searches. Prior to LS2, CBWG studies suggested that background rejection could be significantly improved in beam dump mode by re-cabling the first four dipoles in the K12 kaon beamline. This re-cabling was completed during LS2, and data collected from 2021 onwards have confirmed a substantial reduction in background, as expected, thereby greatly enhancing the sensitivity of these searches.

KLEVER was an independent proposal aimed at collecting a significant sample of $K_L \to \pi^0\nu\bar{\nu}$ decays in a newly designed setup, ideally situated in ECN3. This would have necessitated the creation of an entirely new neutral K12 beamline with a proton flux seven times higher than that used for NA62, specifically 2×10^{13} protons/pulse (or protons/spill, abbreviated as ppp) on the T10 target. This increase would have had major implications for radiation protection, TCC8 target complex, machine safety, and equipment design. While relevant studies were detailed in the 2018 Conventional Beams Working Group Report [1], the Collaboration later identified unmanageable background contributions from $\Lambda \to \pi^0 n$ decays. Potential mitigation strategies from the beam dynamics perspective involved lengthening the beamline and increasing the production angle from 2.4 to 8 mrad, as documented in the 2022 CBWG Report.

The previous European Strategy Update report strongly endorsed the physics case for an ambitious kaon physics programme at CERN, while also emphasising the importance of searching for Dark Sector particles and Feebly Interacting Particles (FIPs). The BDF/SHiP proposal, submitted to the SPSC in 2015, was designed to search for Heavy Neutral Leptons and other Dark Sector particles in a new underground cavern, ECN4.

Although the European Strategy Update strongly supported the BDF/SHiP physics case, it concluded that the experiment could not be funded within the next years. As a result, BDF/SHiP explored alternative locations and identified ECN3 as the most suitable and cost-effective solution, culminating in the submission of a Letter of Intent to the SPSC to install BDF/SHiP in ECN3.

The NA62 community accelerated studies for a continued kaon programme in ECN3 post-LS3. This led to the formation of the HIKE Collaboration, which submitted a Letter of Intent to the SPSC, coinciding with the BDF/SHiP submission, and outlining two phases of a future kaon programme. The first phase focused on improving the measurement of the $K^+ \to \pi^+\nu\bar{\nu}$ branching ratio to 5 % accuracy, while the second phase aimed to measure the branching ratios of $K_L \to \pi^0 e^+ e^-$, $K_L \to \pi^0 \mu^+ \mu^-$, and several other important decay channels. Additionally, HIKE proposed spending a significant portion of time operating in beam dump mode during the first phase.

The SHADOWS Collaboration proposed an off-axis experiment, running in parallel with HIKE in beam dump mode to search for Neutral Heavy Leptons and Dark Sector particles. Their detector would be positioned immediately after the proton dump of the K12 beamline for HIKE but laterally offset, ensuring full compatibility with HIKE.

All three Collaborations requested beam intensities per pulse between 4 and 14 times higher than those provided for NA62, leading to substantial implications for the beamline, infrastructure, and radiation protection measures. Until the submission of the respective Letters of Intent, BDF/SHiP was included in PBC within a dedicated working group. Following the submission of the three Letters of Intent, CERN established a special ECN3 Beam Delivery Taskforce to assess the feasibility, implications, requirements, and costs of the proposed facility upgrades. This task force included personnel from both the BDF/SHiP and Conventional Beams working groups, with all teams prioritising the ECN3 studies until the taskforce proposals were submitted to the SPSC in September 2023. PBC contributed actively to evaluating the physics potential of the experiments, and all findings were submitted to the SPSC at that time.

The SPSC carefully reviewed the three proposals, comparing two primary scenarios in detail: the implementation of either BDF/SHiP or HIKE combined with SHADOWS. Both physics cases were deemed outstanding and of significant scientific importance, though difficult to compare directly. The SPSC was unable to express a clear preference, leading CERN management to approve BDF/SHiP as a strategic choice. Following this decision, studies for HIKE, SHADOWS, and KLEVER in ECN3 were concluded, and the ECN3 taskforce evolved into the HI-ECN3 project.

Two additional experiments were initially proposed for high-intensity proton or heavy ion beam usage: DIRAC++ and DICE/NA60+. Both were discussed in the 2018 Conventional Beams Working Group report. Since then, the DIRAC++ proposal has been withdrawn, and DICE/NA60+ has been relocated to EHN1.

HIKE

The NA62 Collaboration had long envisioned continuing the measurement of the $K^+ \to \pi^+ \nu\bar{\nu}$ branching ratio with a 4-fold increase in beam intensity after LS3. During this phase, the Collaboration also planned to dedicate a significant portion of time to data collection in beam dump mode. A potential second experiment phase could have been as the KLEVER experiment. However, given the time constraints imposed by the ECN3 studies, investigations related to the KLEVER proposal were put on hold. Instead, the Collaboration proposed focusing on the measurement of the $K_L \to \pi^0 e^+ e^-$ and $K_L \to \pi^0 \mu^+ \mu^-$ branching ratios as the primary objectives for the second phase. Numerous other important decay modes were also planned to be addressed across both phases.

CBWG provided strong support to the HIKE Collaboration in preparing its Letter of Intent, proposing an initial design of the neutral kaon beam based on the KLEVER beamline studies.

Conceptually, the charged kaon beamline could remain largely unmodified. However, to provide the higher beam intensities requested, several magnet replacements in the front-end of the kaon beamline would be necessary. These upgrades were thoroughly studied by the CBWG. As these upgrades would largely overlap with those required for BDF/SHiP, the newly formed ECN3 Beam Delivery Taskforce conducted a detailed study of all infrastructure needs. In any case, all efforts rely heavily on a comprehensive consolidation of the North Area infrastructure, a process already underway through the approved NA-CONS project.

The design of the neutral kaon beam was inspired by the K_L beamline used in the NA48 experiment and, more specifically, by the beamline description provided for KLEVER. Minor modifications were introduced to further reduce background from K_S regeneration. Detailed studies were conducted on the front-end of the neutral beam, where protons are dumped, along with comprehensive analyses of muon background contributions.

These studies were subsequently halted and documented in the present document, following the decision to approve the BDF/SHiP proposal for ECN3.

SHADOWS

The SHADOWS experiment was designed to search for Feebly Interacting Particles (FIPs) and was intended to be located in close proximity to the proton beam dump of the kaon beamline used for HIKE. The experiment was planned to run in parallel with HIKE whenever HIKE operated in beam dump mode. Positioned off-axis, SHADOWS would have just fit within the available space in the TCC8 cavern. Despite the tight spatial constraints on the detector dimensions, SHADOWS would have achieved a large acceptance due to its proximity to the proton dump at a relatively moderate cost.

The CBWG conducted detailed studies to mitigate muon backgrounds, which would otherwise have been prohibitive at such close distances to the dump. Other backgrounds would predominantly propagate downstream and would be minimal at the SHADOWS location. The physics reach of SHADOWS was designed to be complementary to and transparent to HIKE during beam dump mode operations, with

SHADOWS focusing on particles produced at larger angles, while HIKE was sensitive primarily to forward-directed particles.

Integration studies were carried out to assess the feasibility and compatibility of the SHADOWS concept within the ECN3 taskforce framework. There studies would have continued after a positive decision for a TDR phase of SHADOWS and HIKE, which was not the case.

Proposals for Neutrino Beams

Two proposals for tagged and monitored neutrino beams became part of the CBWG mandate in 2021. Both approaches offer significant advantages over conventional neutrino beams, particularly for measurements of CP violation in the neutrino sector. At the same time, they provide an opportunity to improve knowledge of neutrino cross sections, which remain among the least well-constrained parameters in neutrino physics. These uncertainties limit the precision of oscillation experiments and hinder a full understanding of electroweak interactions in the nuclear medium. The energy ranges accessible at CERN cover both the regime relevant for long-baseline experiments such as Hyper-Kamiokande and DUNE and the higher-energy domain probed by IceCube and KM3NeT. High-statistics experiments with a well-characterised neutrino beam would enable precise studies of neutrino energy reconstruction and kinematic distributions, which are usually accessible only in electron scattering experiments.

The ENUBET/NP06 proposal is a conceptual study focused on the development of a monitored ν_e beam. This low-energy neutrino beam features a long, flat top time structure, enabling monitoring of the ν_e fraction within the beam. This is achieved by detecting electrons from K_{e3} decays using detectors positioned around the decay tunnel. NuTag is a parallel proposal aimed at developing a tagged ν_μ and $\bar{\nu}_\mu$ beam.

Through CBWG, a strong synergy between ENUBET and NuTag has been identified, resulting in the initiation of a joint study under the name Short Baseline Neutrino beamline (SBN). This unified effort aims to harness the strengths of both concepts to advance the site-independent design and implementation of next-generation neutrino beams. First explorations of a potential installation of a Short Baseline Neutrino facility on and off the CERN site have commenced.

Apart from the two novel concepts of ENUBET and NuTag, the NA61++ experiment proposes the development of a conventional low-energy beamline, specifically dedicated to measurements for neutrino beams. This project has been reassigned from the CBWG EHN1 subgroup to the CBWG Neutrino Beams subgroup.

ENUBET

An initial beam design was already in place when ENUBET joined the PBC study in 2021. Since then, significant enhancements have been made to the design of both, the target complex and the beamline, notably allowing the beam to be configured for different neutrino energies. The ENUBET design is now considered completed and has been thoroughly documented.

NuTag

NuTag is a proposal for a tagged ν_μ and $\bar{\nu}_\mu$ beam, featuring a long flat top and employing quadrupoles instead of a magnetic horn, similar to ENUBET. A notable advantage of this design is its ability to simultaneously select π^+ and π^- beams with identical momentum, thereby producing ν_μ and $\bar{\nu}_\mu$ beams concurrently. The decay section would be surrounded by tagging counters, providing event-by-event information on the neutrino species.

Short Baseline Neutrino Beamline

The CBWG has developed a new optics design that enables tagging not only around the decay tunnel but also in the forward region. The acceptance and performance have been significantly optimised from the already improved ENUBET and NuTag designs. The feasibility of the proposed neutrino beam concept has been shown.

This study has since progressed from a site-independent conceptual phase to an implementation study at CERN. One potential location has been identified near the old West Area target zone TCC6, utilising the TT61 tunnel towards the West Area. This implementation location would require a new slow extraction system, for which a conceptual pre-study has been completed. The detector could potentially be one of the existing ProtoDUNE liquid argon cryostats, currently installed in the Neutrino Platform part of EHN1. However, the implementation study remains in its early stages and requires further development.

Costs

Cost estimates remain largely very preliminary. Table 2 lists the current estimates, categorised into four cost groups as an initial reference. Notably, consolidation costs, such as those for electrical systems, cooling, ventilation, and civil engineering infrastructure, are not included. Additionally, these estimates pertain solely to beam and infrastructure upgrades and do not account for the costs of the experiments themselves.

The cost categories are defined as follows:

- C0: Up to 300 kCHF
- C1: From 300 kCHF to 2 MCHF
- C2: From 2 to 10 MCHF
- C3: Above 10 MCHF

Please note that some of these upgrades have already been partly or completely implemented, including the new shielding for NA61/SHINE, the newly established PPE144 zone with NA64e already taking data in it, and the re-cabling of the first achromat in the K12 beam.

Final remarks and conclusions

The Conventional Beams Working Group has conducted extensive studies and made significant contributions to all proposals submitted for its review. A common requirement across nearly all proposals is the need for higher proton fluxes, with the most demanding requests coming from proposals for the ECN3 underground cavern. Following the submission of Letters of Intent from BDF/SHiP, HIKE+SHADOWS, the priority request for increased primary proton beam intensity to ECN3 was initially transferred to a dedicated task force and, more recently, to the HIECN3 working group.

No major obstacles were identified, and the cost estimates for BDF/SHiP and HIKE plus SHADOWS were comparable. Ultimately, CERN management made a strategic decision in favour of BDF/SHiP. Consequently, the HIKE and SHADOWS studies were finalised and documented in the present report, along with the original KLEVER studies.

Since publishing our previous report in 2022, several experiments have been approved and implemented, either fully or partially. These include AMBER Phase 1, NA64e in a dedicated zone, NA64μ, a MUonE pilot detector, and an increased intensity for NA61/SHINE. The electron fluxes for NA64e have been steadily increased while maintaining excellent background conditions.

A detailed study for AMBER Phase 2 has shown that an RF-separated kaon beam falls significantly short of delivering the required kaon fluxes at the momenta needed for the Drell–Yan programme and can only marginally support the lower-intensity components of the physics programme. However, a conventional beamline with substantially improved vacuum conditions should be capable of providing the

Table 2: Preliminary cost estimates for the initial proposals where available. The definition of cost categories is explained in the text.

Location	Proposal	Foreseen upgrades	Cost category	Comment
EHN1	NA61++	Shielding, interlocks	C1	Done.
	DICE/NA60+	Shielding, magnets, power, beam instrumentation (TT20+H8)	C2	
	NA64e	Semi-permanent location	C0	Done.
EHN2	NA64μ	New location in beamline	C0	Done.
	NA64μ	Phase 2, detector installation in SM2	C0	
	MUonE	Installation in M2 beamline	C1	
	AMBER	Static vacuum improvements	C1	Ongoing.
	AMBER	Magnetic collimator upgrade	C2	
	AMBER	New RF-separated beam	C3	
ECN3	NA62/HIKE-BD	Re-cabling for μ sweeping	C0	Done.
	HIKE-K+	Compatibility with high intensity operation	C3	
	HIKE-KL	Replacement of K12 with neutral beamline	C2	
	HIKE-KLEVER	Upgrades, civil engineering, and new beamline	C3	
	SHADOWS	Integration of experiment	C2	
	DIRAC++	New K12 beamline	C2	
other	ENUBET[1]	New beamline (site-independent)	N/A	
	NuTag[1]	New beamline (site-independent)	N/A	
	SBN	New slow extraction from SPS	C3	

necessary kaon flux with suitable conditions for kaon tagging. Technical studies for its implementation are well underway.

These improvements would also benefit both NA64μ and MUonE. The latter wants to perform measurements also with an electron beam which, thanks to improved vacuum conditions in M2, can be made available at the MUonE location with adequate quality. However, since the vacuum implementation affects the magnetic collimators and hadron absorbers in the muon beamline, it may impact muon beam performance or introduce operational constraints.

In EHN1, NA61++ continues the NA61/SHINE hadron programme, focusing on particle production for cosmic ray studies and neutrino beams, as well as its ion beam programme for open charm production and fragmentation studies. Local improvements have been made to shielding and interlocks to mitigate intensity and beam position variations. A dedicated local low-intensity beam design has been completed. While the physics case has been endorsed by the SPSC, the proposal is still under consideration for potential future approval from the Research Board. Studies for the implementation of NA60+ are underway; however, the feasibility of low-energy ion and primary proton beams remains to be clarified.

The ENUBET and NuTag proposals for monitored or tagged neutrino beams have now been merged into a combined Short Baseline Neutrino study. This study is progressing very fast and has already provided a site-independent SBN concept. Preliminary studies for a potential SBN implementation at CERN have just started.

[1] Conceptual design, now superseded by SBN.

Chapter 1

Introduction

Johannes Bernhard, Markus Brugger, Lau Gatignon, Silvia Schuh

1.1 The Physics Beyond Colliders Study

The Physics Beyond Colliders (PBC) Study at CERN [7] continues to provide a platform for exploratory studies aimed at fully exploiting the scientific potential of CERN's accelerator complex and its infrastructure through projects complementary to the objectives of the main experiments of the laboratory's collider programme.

This study shall provide input for the future of CERN's fixed-target programme, which currently spans several facilities and experiments at the Booster, PS and SPS, covering the period until the 2040s. Efforts shall be made to ensure complementarity with similar initiatives worldwide, optimising resources of the particle physics field globally, fostering synergies with other laboratories and institutions, and attracting the international particle physics community. The proposed projects or experiments shall:

- Enrich and extend CERN's scientific programme,
- Make optimal use of the unique opportunities offered by CERN's existing accelerator complex and scientific infrastructure,
- Complement the flagship experiments of CERN's collider programme (LHC, HL-LHC and possible future colliders).

Physics objectives include searches for rare processes and feebly interacting particles, QCD physics, searches for physics beyond the Standard Model, as well as precision measurements of electric dipole moments, among others.

The mandate for the Physics Beyond Colliders study was renewed at the beginning of 2021 [7] and the first Annual Workshop under the renewed mandate was held in early March 2021 [8]. Since 2021, the PBC study has been structured into two main domains, each comprising multiple subgroups:

- The physics domain features three working groups, each focusing on specific research areas:
  - BSM (Beyond Standard Model),
  - QCD physics,
  - FIP (Feebly Interacting Particles) Physics Centre (FPC), newly created in 2021.
- The accelerator and technology domain (PBC-Accelerators & Technology committee) [9], composed of a number of working groups, including the Conventional Beams working groups.

The overall organisation of PBC from 2021 onwards is illustrated in Fig. 1. Pictures of the experimental hall EHN1, of the AMBER/COMPASS experiment in EHN2, and of the NA62 experiment in ECN3, are provided in Figs. 2–4.

1.2 The Conventional Beams Working Group

During the initial PBC kick-off workshop in September 2016 [10], a substantial number of fixed-target (FT) proposals were presented. It was deemed essential to conduct pre-proposal studies to enable the PBC working groups to effectively evaluate the scientific merit of these FT proposals.

The Conventional Beams working group is tasked with examining a broad range of proposals that could be accommodated within the existing non-LHC experimental areas. Given the extensive list of

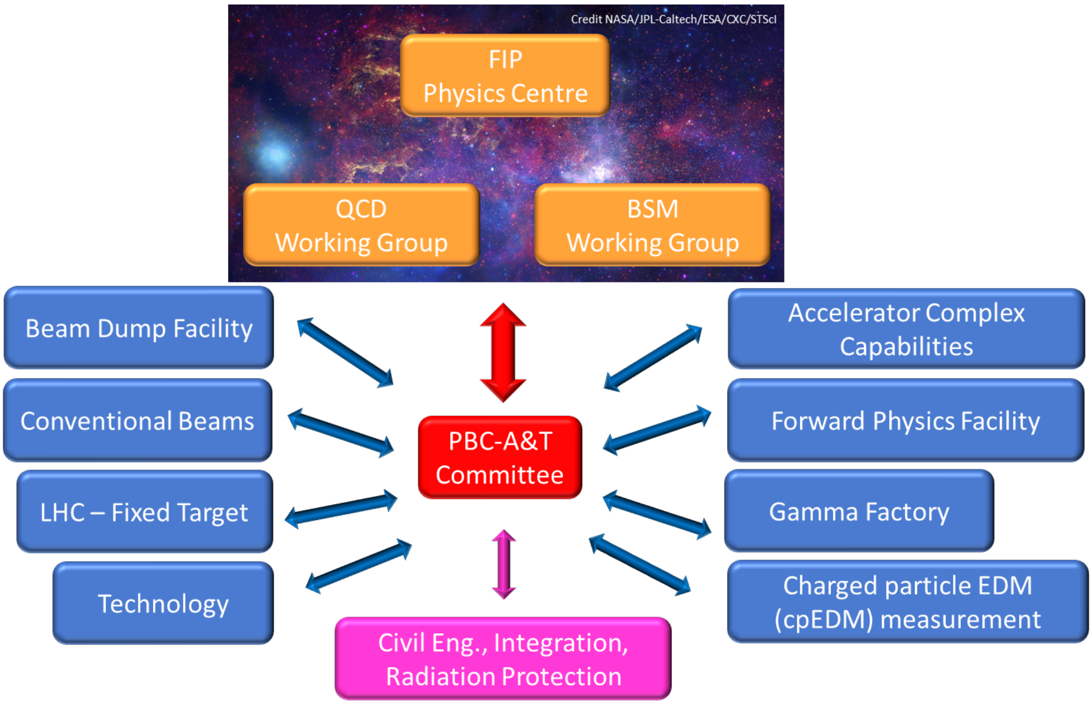

Fig. 1: The overall structure of the Physics Beyond Colliders study.

Fig. 2: Overview picture of the experimental hall EHN1.

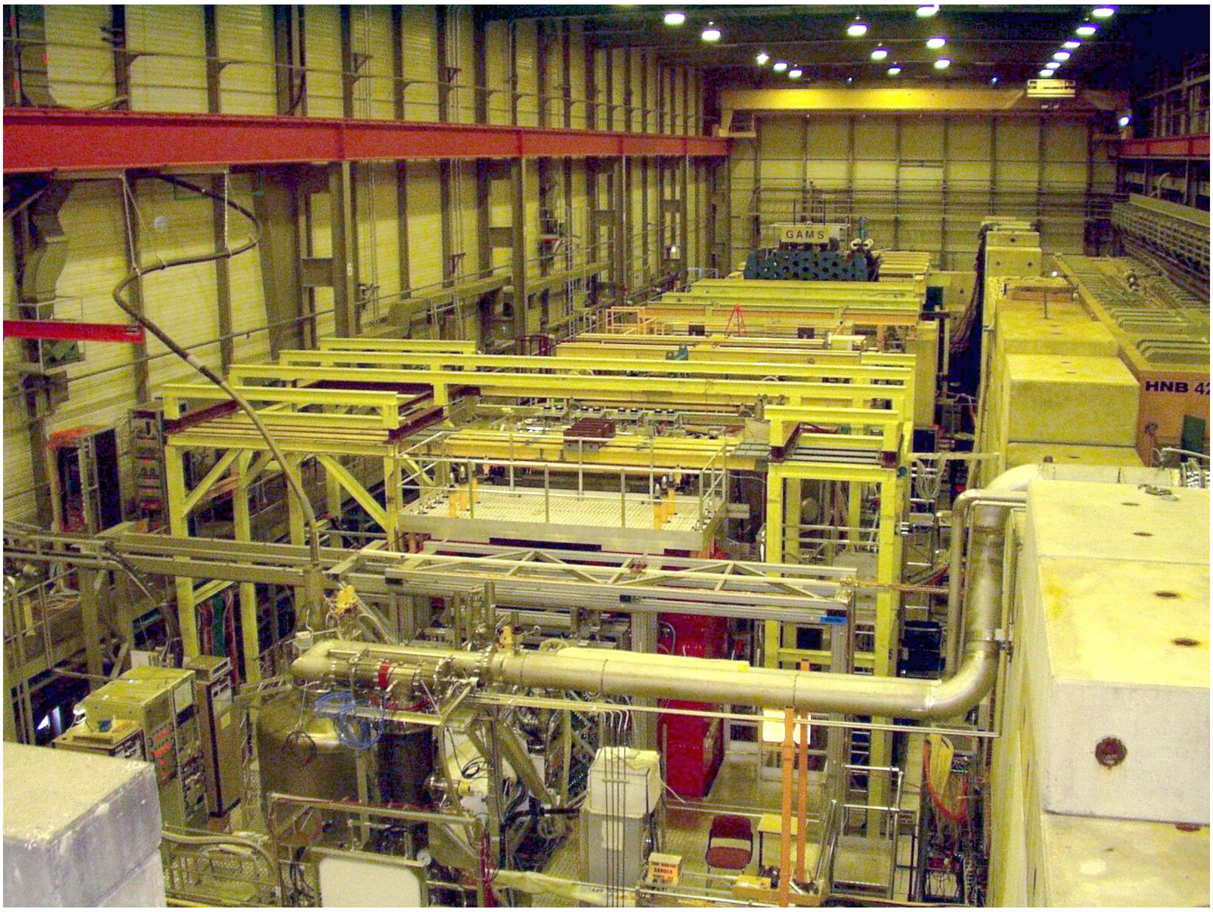

Fig. 3: The AMBER/COMPASS experiment in the EHN2 hall.

studies, initial efforts were concentrated on proposals that offer the potential for short- and medium-term implementation with limited resource requirements, as well as those that appeared the most advanced and competitive from a physics standpoint. This prioritisation was based on available input following the initial kick-off event and an initial feasibility analysis regarding their FT implementation.

In 2021, a new set of proposals was added to the CBWG mandate and corresponding studies have been initiated or continued where appropriate. The current list of proposed experiments is shown in Table 3. In the meantime, some proposals, like DIRAC++ and KLEVER, have been either withdrawn or suspended.

1.3 Existing Beamlines and Experimental Areas

Based on the list of proposals in Table 3, the Conventional Beams working group primarily focuses on the North Experimental Area at the CERN Super Proton Synchrotron (SPS), commonly referred to as the North Area. The North Area receives a primary proton beam with a momentum of 400 GeV/c from the CERN SPS[1], or primary ion beams of corresponding or lower rigidity.

The full SPS proton beam is slowly extracted to the North Area during a flat top phase typically 4.8 s. This duration can be adjusted based on the requirements of the specific physics programme — for instance, shortened for the Beam Dump Facility or extended for cases of cohabitation with the Beam Dump Facility within the same super-cycle (i.e., the accelerator operation sequence that is cyclically repeated). The typical duty cycle, defined as the ratio between the useful flat top length and the full

[1] Beams of up to a maximum of 450 GeV/c can be delivered and transported up to the production targets.

Fig. 4: The NA62 experiment in the ECN3 underground cavern.

super-cycle duration, ranges between 20 % and 30 %. The maximum routinely extracted proton intensity per spill (ppp) during standard physics operations using slow extraction was approximately 3.5×10^{13} ppp, with future plans aiming to reach 4×10^{13} ppp. This proton flux is transported to and directed through two series of splitter magnets onto three primary targets (T2, T4 and T6) from which the North Area beamlines are derived.

The North Area consists of two surface halls, EHN1 and EHN2, along with an underground cavern, ECN3. EHN1 is the largest surface hall at CERN, measuring 330 m×50 m, and hosts the H2, H4, H6 and H8 beamlines.

EHN2 is served by the almost 1200 m long M2 beamline [41], which provides muon, hadron and electron beams, currently serving three experiments : AMBER [11–13], MUonE [36] and NA64μ [33].

In ECN3, the NA62 experiment [42], dedicated to studying rare kaon decays, is served by the K12 beamline.

Figure 5 presents a schematic layout of the North Area beamlines and experiment complex as implemented in 2025.

The T2 target serves the H2 and H4 beamlines. These two lines are normally operated as versatile secondary or tertiary beamlines but can occasionally be configured to transport ions or attenuated primary proton beams. The two beams exit the target at a relative angle of 11.2 mrad, and their momenta are coupled through the angle of incidence of the proton beam on the production target.

This relative angle between the two beams and the resulting distribution of different momenta between the two beamlines can be adjusted with different settings of the T2 wobbling station. This station comprises two sets of dipole magnets upstream and one pair of dipole magnets downstream of the primary target, enabling precise control over beam trajectories and momenta.

The H2 beamline hosts the NA61/SHINE experiment [27–30], which supports an extensive physics

Table 3: List of proposals currently being followed by the Conventional Beams working group.

Experiment	Brief description and comments
AMBER/NA66 [11–13]	Study new requests, including RF separated beams and improvements to the conventional beamline.
BDF/SHiP [14–20]	Formally not part of the CBWG, but beam studies are in synergy with those for HIKE. Fully approved in 2024 and from then on followed within the HI-ECN3 project.
ENUBET/NP06 [21, 22]	A monitored electron neutrino beam, now merged into SBN.
HIKE [23, 24]	Performed detailed study for a next kaon experiment in ECN3. Study discontinued as BDF/SHiP was approved for ECN3.
DICE/NA60+ [25, 26]	Study implementation options for focused high-intensity Pb and proton beams down to low SPS energy. Originally considered for ECN3, now studied for EHN1 (H8 beamline).
NA61++ [27–30]	Exploit NA61/SHINE at higher intensity and with better machine protection. A study for a new Very Low Energy beam has been completed.
NA64e,h [31, 32]	Increase electron flux and optimise hadron beams in H4.
NA64μ [33]	Implementation of a NA64-like experiment with muons in M2.
NuTag [34, 35]	A monitored muon neutrino beam, now merged into SBN.
MUonE [36]	Implementation of MUonE for operation with muon beams to study the hadronic contribution to the vacuum polarisation
SBN [37]	Tagged (monitored) neutrino beam, for ν_μ and ν_e beams simultaneously, integration of ENUBET and NuTag.
SHADOWS [38, 39]	Beam study to search for FIPs in ECN3, running in parallel with HIKE. Study discontinued as BDF/SHiP was approved for ECN3.
True Muonium [40]	A search for true muonium with an e^+ beam at resonance threshold. Study is on hold.

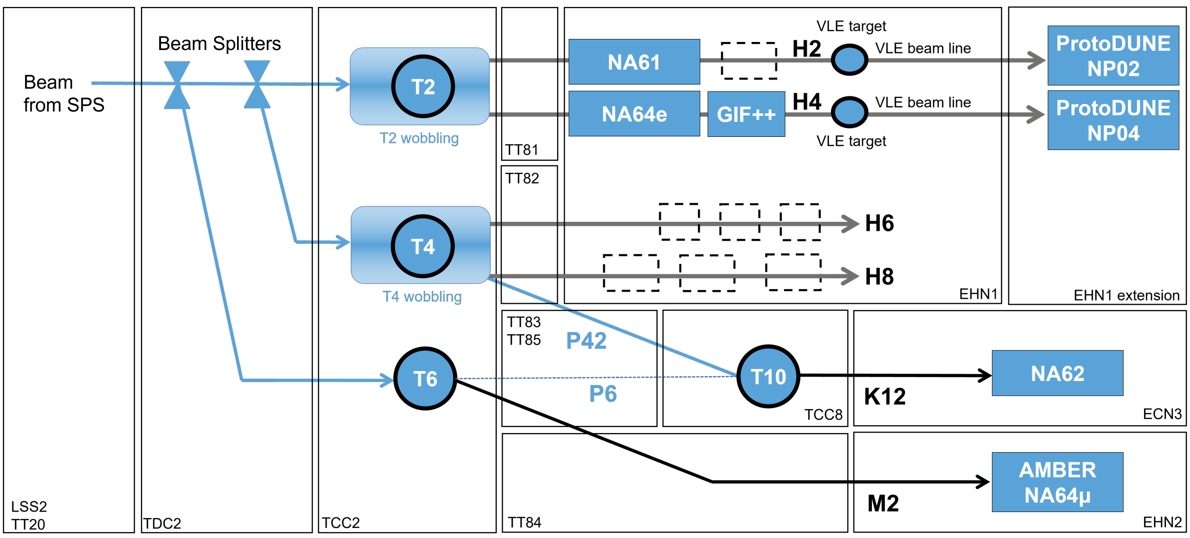

Fig. 5: A schematic layout of the 2025 North Area beamlines and experiment complex.

programme utilising both hadron and heavy ion beams. The H4 beamline provides a particularly clean electron beam, while also offering high-quality hadron or muon beams to its users. Currently, the primary physics experiment in H4 is NA64 [43], which focuses on dark photon searches using high-purity electron beams [44].

The above configurations highlight the versatility of the T2 target and its associated beamlines, H2 and H4, supporting a broad spectrum of physics research through flexible beam tuning and specialised facilities.

The H6 and H8 beamlines originate from the T4 target and are designed as versatile beamlines capable of transporting hadron and electron beams, as well as providing low- to medium-intensity muon beams. These beamlines are primarily utilised for test beam activities, supporting a wide range of detector development and calibration efforts.

Occasionally, the H8 beamline can be configured to operate as a low-intensity, low-emittance, attenuated primary proton beam. This specialised configuration, referred to as the micro-beam option, offers good beam parallelism, making it ideal for specific studies. The UA9 experiment [45] took advantage of this micro-beam setup to conduct crystal channelling and collimation experiments, as well as the crystal studies for the NA48 K_S beamline [46, 47], exploring innovative methods for loss reduction in high-energy accelerators and beam steering.

This flexibility in beam configurations underscores the adaptability of the H6 and H8 beamlines, serving beam tests, fundamental research and applied accelerator studies.

Most of the time, the protons hitting the T4 target are directed towards the P42 beamline, while the secondary particles produced in the target supply secondary or tertiary beams to the H6 and H8 beamlines. Protons that do not interact with the T4 target are transported by the P42 beamline to the T10 target, located 838 meters downstream of T4. The T10 target generates a high-intensity mixed secondary beam, which is then transported by the K12 beamline to the NA62 experiment, dedicated to rare kaon decay studies and located in the ECN3 underground cavern. Within this setup, the KTAG Cherenkov detector identifies and tags the kaon component of the beam, which constitutes approximately 6 % of the total flux.

This T4 wobbling configuration enables efficient use of the proton beam, supporting multiple experiments across different beamlines while ensuring precise kaon tagging for the NA62 experiment.

The T6 target produces the M2 beamline, which serves the AMBER experiment located in the EHN2 hall. The M2 beamline offers a globally unique, high-energy, high-intensity muon beam. In addition to its muon configuration, its initial purpose as a muon beamline, it can now be also operated as a high-intensity hadron beam, extending its versatility for various physics programmes. While there is the option to operate the M2 beamline as a tertiary electron beam, the currently achievable rates in this mode are low, limiting it to test or calibration applications. As will be discussed in more detail in Chapter 4, planned vacuum improvements in the M2 beamline will also significantly enhance the available electron rates in the M2 beamline.

A detailed overview of the characteristics of the North Area beamlines is provided in Table 4. The maximum intensities in all beamlines are primarily constrained by radiation protection guidelines, especially within the surface halls. Additionally, factors such as beam momentum, production angle, and particle type can further limit achievable intensities due to their impact on particle production rates.

1.4 Input from Experiments and Physics Working Groups

NA62 is conducting a last data taking run for the measurement of the very rare decay mode $K^+ \to \pi^+ \nu\bar{\nu}$ until LS3. The experiment operates the beamline also in beam dump mode. In this condition the T10 primary target is moved into OUT position and the full proton beam of up to 3×10^{12} ppp is dumped onto the K12 dump collimators (TAX) while the muon sweeping system is left active. Prior to LS2, CBWG studies suggested that background rejection could be significantly improved in beam dump mode by re-cabling the first four dipoles in the K12 kaon beamline. This re-cabling was completed during LS2,

Table 4: Overview of the characteristics of the North Area beamlines. If multiple entries are provided for a specific value, the first one corresponds to primary beam operation, while the second one refers to secondary beams. The following abbreviations are used for particle types: p (protons), h (hadrons), e (electrons), μ (muons). Intensities are given for a typical spill of 4.8 s.

Parameter	H2	H4	H6	H8	M2	K12	P42
Max. momentum (GeV/c)	400/360	400/360	205	400/360	280	75	400
Max. acceptance (μsr)	1.5	1.5	2	2.5	5(h)	12.7	1.4(p) 0.3(e,h)
Maximum $\Delta p/p$ (%)	± 2.0	± 1.4	± 1.5	± 1.5	± 4.0	± 2.0	± 0.5(p)
Typical $\Delta p/p$ (%)						± 1.0	
Maximum intensity/spill	$10^7/10^5$	$10^7/10^5$	$10^7/10^5$	$10^7/10^5$	5×10^8	2.2×10^9	6×10^{12}
Particle types (typical)	p, h, μ, e, ions	p, h, μ, e, ions	h, μ, e	p, h, μ, e, ions	μ, h, e	h, μ	p, h, μ, e, ions

and data collected from 2021 onwards have confirmed a substantial reduction in background, as expected, thereby creating relatively clean conditions for heavy neutral lepton and axion searches.

KLEVER [48] was an independent proposal designed to collect a substantial sample of $K_L \to \pi^0 \nu\bar{\nu}$ decays in a newly developed experimental setup, ideally located in ECN3. This would have required the creation of an entirely new neutral K12 beamline. Due to the smaller angular acceptance in the absence of focusing, achieving the desired event rate would have necessitated a proton flux on the T10 target approximately seven times higher than that used for NA62. Specifically, a flux of 2 to 2.4×10^{13} ppp would have been required on the T10 target, compared to the nominal 3×10^{12} ppp used by NA62.

This significant increase in proton flux would have had major implications for radiation protection, ventilation, machine safety, and equipment design. While relevant studies were detailed in the 2018 Conventional Beams Working Group Report [1], the Collaboration later identified unmanageable background contributions from $\Lambda \to \pi^0 n$ decays. Potential mitigation strategies from the beam dynamics perspective involved lengthening the beamline and increasing the production angle from 2.4 to 8 mrad, as documented in the 2022 Conventional Beams Working Group Report. Nevertheless, the KLEVER Collaboration has not presented a final validation of this approach, and as a result, KLEVER has not been included in any subsequent proposals.

The previous European Strategy report strongly endorsed the physics case for an ambitious kaon physics programme at CERN, while also emphasising the importance of searching for Dark Sector particles and Feebly Interacting Particles (FIPs). The BDF/SHiP proposal, submitted to the PS and SPS Scientific Committee (SPSC) in 2015, was designed to search for Heavy Neutral Leptons and other Dark Sector particles in a new underground cavern, ECN4.

Although the European Strategy strongly supported the BDF/SHiP physics case, it concluded that the experiment could not be funded within the time-frame covered by the previous European Strategy, finalised in 2020. As a result, BDF/SHiP explored alternative locations and identified ECN3 as the most suitable and cost-effective solution after the end of NA62. This culminated in the submission of a Letter of Intent to the SPSC to install BDF/SHiP in ECN3.

As studies for high-intensity operation in ECN3 progressed, the NA62 community intensified its exploration of a continued kaon programme for the post-LS3 era. This led to the formation of the HIKE Collaboration, which submitted a Letter of Intent to the SPSC, coinciding with the BDF/SHiP submission, and outlining two phases of a future kaon programme. The first phase focused on improving the measurement of the $K^+ \to \pi^+ \nu\bar{\nu}$ branching ratio to 5 % accuracy, while the second phase aimed to measure the branching ratios of $K_L \to \pi^0 e^+ e^-$, $K_L \to \pi^0 \mu^+ \mu^-$, and several other important decay channels. Additionally, HIKE proposed spending a significant portion of time operating in beam dump mode during the first phase.

The SHADOWS Collaboration [38] presented at the 2021 Annual PBC Workshop and proposed operating in parallel with HIKE in beam dump mode to search for Neutral Heavy Leptons and Dark Sector particles. The SHADOWS detector would be strategically placed immediately downstream of the proton dump in the K12 beamline for HIKE but laterally offset to ensure full compatibility with HIKE operations. SHADOWS would have significantly benefited from an increased proton flux in the P42/K12 beamline, as its operation was not constrained by rate limitations. Several critical considerations required detailed studies by the Conventional Beams team, including radiation protection, integration with existing infrastructure, and the mitigation of muon background. Additionally, it was essential to ensure that SHADOWS could operate fully transparently alongside the ongoing NA62 experiment without causing interference.

All three Collaborations requested beam intensities per pulse between 4 and 14 times higher than those provided for NA62, leading to substantial implications for the beamline, infrastructure, and radiation protection measures. Until the submission of the Letters of Intent, the BDF/SHiP request was studied by PBC within a dedicated working group. Following the submission of the three Letters of Intent, CERN established a special ECN3 task force to assess the feasibility, implications, requirements, and costs of the proposed intensity upgrades. This task force included personnel from both the BDF/SHiP and Conventional Beams working groups, with all teams prioritising the ECN3 studies until the task force proposals were submitted to the SPSC in September 2023. PBC contributed actively to evaluating the physics potential of the experiments, and all findings were submitted to the SPSC at that time.

The SPSC carefully reviewed the three proposals, comparing two primary scenarios in detail: the implementation of either BDF/SHiP or HIKE+SHADOWS. Both physics cases were deemed outstanding and of highly significant scientific importance, though difficult to compare directly. The SPSC was unable to express a clear preference, leading the CERN management to approve BDF/SHiP as a strategic choice. Following this decision, studies for HIKE, SHADOWS, and KLEVER were concluded, and the ECN3 task force evolved into the HI-ECN3 project. Chapter 4 of this document, along with its references, presents the final results of the aforementioned studies.

Two other experiments, namely DIRAC++ and DICE/NA60+, were initially proposed for very high proton or heavy ion beam intensities in ECN3. Both were discussed in the 2018 Conventional Beams working group report. Since then, the DIRAC++ proposal has been withdrawn and DICE/NA60+ has been reassigned to a new location in EHN1.

In the EHN2 hall, the COMPASS experiment continued its physics programme using the existing M2 muon and hadron beam options until its official conclusion at the end of 2022. The AMBER Collaboration, also known as NA66 and the direct successor of COMPASS, was approved for a first phase to extend QCD-related research activities. While AMBER utilises largely the same apparatus and continues to exploit the existing M2 beam options, it pursues different physics goals, marking a new direction in the experimental programme.

This AMBER Phase 1 programme has been developed through the PBC CBWG and it encompasses a measurement of the proton radius, a deep virtual Compton scattering experiment with a muon beam, Dark Matter searches using low-momentum antiproton beams, and a Drell–Yan measurement programme with kaon and pion beams.

In recent years, the AMBER Collaboration has been preparing for the second phase of its physics programme, with a primary focus on conducting a high-intensity kaon beam experiment for Drell–Yan studies. This effort has brought to light several technical challenges, notably the low kaon production rate, the short kaon lifetime, and the considerable length (1100 m) of the M2 beamline, which collectively result in a limited kaon intensity at the AMBER site. Additional constraints from radiation protection guidelines further limit the total beam intensity and thereby the kaon rate. Although the use of differential Cherenkov counters (CEDAR) allows efficient kaon tagging, the existing beamline's significant divergence reduces their effectiveness. While a potential RF-separated kaon beamline was explored, its current technical limitations and high costs made it unsuitable for meeting the stringent intensity requirements of the Drell–Yan programme.

As an alternative, upgrading the existing M2 beamline to improve vacuum conditions and particle identification presents a cost-effective solution to reduce beam divergence and increase the CEDAR tagging efficiency, thereby effectively enhancing kaon intensity at the AMBER experimental site. Studies show that placing key sections of the beamline under vacuum, particularly around magnetic collimators and hadron absorbers, significantly improves beam parallelism and overall performance. This approach not only benefits the kaon beam but also enhances tertiary electron beam quality for calibration purposes. Additionally, the Collaboration has considered future options, such as a low-energy antiproton-rich beam, though this part of the programme is currently on hold. If muon beam operations are discontinued in the future, further cost-effective upgrades could permanently optimise the beamline for hadron and electron experiments, potentially significantly expanding AMBER's scientific reach.

NA64μ recently proposed a search for the invisible decays of a Z' boson as a potential low-mass explanation for the $(g-2)_\mu$ anomaly, using the existing M2 muon beam, which already meets the required momentum and flux. While the experiment spans 20 m and cannot fit within the AMBER zone without major modifications, a suitable alternative location was identified upstream in zone PPE211 by reconfiguring the beamline. Local beam optics adjustments and the removal of two quadrupoles, replaced by two dipoles, created the necessary space and functionality. Efforts to reduce hadronic contamination, primarily originating from the NA64μ detectors themselves, successfully limited it to around 10^{-6}. The experiment is currently running under stable conditions and is expected to continue until LS3. Future plans for a higher-rate version, potentially integrated with the AMBER experiment's SM2 spectrometer magnet, are on hold pending further studies.

The MUonE Collaboration aims to measure muon-electron elastic scattering to precisely determine the hadronic contribution to the muon magnetic moment, $(g-2)_\mu$. It uses the M2 muon beam under standard operating conditions with minor upstream optics adjustments. The experiment requires a 40 m long detector setup, planned for the same location as NA64μ, though simultaneous operation is not possible due to conflicting layouts and beam rate requirements. Similarly, MUonE cannot run concurrently with AMBER, as its equipment strongly impacts muon beam performance for AMBER. While initial tests with up to two target modules have been successful and cohabitation with other users has been smooth, full implementation will complicate changeovers. To shorten the data-taking period, MUonE now aims for beam intensities up to 10^9 muons per SPS spill, significantly exceeding the current M2 limit of 2×10^8 muons. This increase has prompted studies to address radiation management, including strategies such as deflecting the beam downward after the experiment to reduce the radiation dose at the surface. Integration studies are underway to develop optimised cohabitation strategies for MUonE, NA64μ, and AMBER, aiming to ensure efficient use of the M2 beamline while minimising operational conflicts and maintaining optimal performance for all experiments.

In EHN1, the NA61/SHINE experiment, located in the H2 beamline, continues to lead the SPS heavy-ion programme, focusing on the exploration of the phase transition to Quark-Gluon Plasma (QGP). Post-LS2, NA61/SHINE has expanded its research to include open charm measurements, cosmic ray physics studies, and particle production measurements using neutrino beam replica targets. The experiment now benefits from a tenfold increase in beam intensity in the H2 beamline and has requested a study for an in-situ low-energy beamline. This study has been completed since, but its implementation is on hold, pending CERN Research Board approval.

NA64e plans to advance its search for dark photons and other dark matter candidates using pure electron beams, with future expansions to hadron beams, possibly also in the H4 beamline. To optimise beam time, NA64 aims to maximise electron beam intensity while maintaining purity and has also proposed running with medium-energy positron beams. To reduce setting-up time, they had requested a dedicated beam zone for a quasi-permanent installation in the H4 line, which has been made available and has already been successfully used by NA64e since 2021.

DICE/NA60+ proposes studying electromagnetic and hard probes of the Quark-Gluon Plasma in heavy-ion collisions using lead beams at varying energies at the CERN SPS, with a focus on open charm production. Initially proposed for the underground ECN3 cavern to access higher beam intensities, the experiment was relocated to EHN1 due to incompatibilities with NA62, HIKE+SHADOWS, or BDF/SHiP, accepting lower maximum beam intensity and reduced detector dimensions as a trade-off.

Ideally all the above addressed studies shall conclude with an evaluation of feasibility and an estimate of their respective, associated cost.

Additional studies concern the delivery of a sufficient number of protons to the North Area. These studies continue to be done in synergy with the Injector Capabilities and BDF working groups within the PBC Accelerators and Technology domain.

The role of the Physics Beyond Collider study and the Conventional Beam working group has been, and continues to be, crucial in supporting participating experiments in preparing formal proposals for submission to CERN's scientific committees.

Chapter 2

Organisation of the Conventional Beams Working Group

Johannes Bernhard, Markus Brugger

The different proposals submitted to the Conventional Beams working group exhibit correlations and synergies, lending themselves to being grouped into four distinct categories, based on the following rationale:

- Standard Operation Enhancements: NA61++ and NA64e are closely aligned with standard operation and primarily require enhanced shielding and targeted beamline improvements. Both experiments are located in EHN1.
- Revised Requirements and Layout: The DICE/NA60+ Collaboration has significantly reduced its intensity and space requirements and shifted its baseline location from ECN3 to the H8 beamline in EHN1.
- High-Intensity ECN3 Experiments: HIKE, SHADOWS, and DIRAC++ can only be considered for implementation in ECN3 due to their high-intensity requirements.
- High-Intensity Muon Beams in EHN2: AMBER, MUonE and NA64μ all request access to a high-intensity muon beam, which is exclusively available through the M2 beamline serving the EHN2 hall. Notably, the COMPASS experiment concluded its programme in 2022, freeing up space in this area.
- Neutrino Beam Studies: ENUBET and NuTaG are not tied to any specific experimental area and are therefore evaluated within a dedicated subgroup focused on neutrino beam studies (CBWG-NB). Additionally, the low-energy beamline branch for NA61++ (denoted NA61 LE) is included in this category due to its potential role in characterising hadron production for neutrino beams.

Conveniently, three of these categories align directly with the existing experimental halls and caverns: EHN1, EHN2, and ECN3. Each facility hosts projects with shared infrastructure needs, enabling efficient planning and resource allocation.

In EHN1, the proposals require similar enhancements, including improved shielding and beamline modifications, which necessitate similar approaches and expertise for their studies. In EHN2, the proposals compete for the same limited space and access to the M2 beamline, necessitating careful co-habitation coordination. Meanwhile, in ECN3, all proposed experiments require similar and correlated studies on radiation protection, target complex configuration, and ventilation, as they aim to be installed within the same underground cavern.

To streamline coordination and optimise resources, the Conventional Beams working group has been organised into four dedicated subgroups, as illustrated in Fig. 6.

The Conventional Beams working group is supported by expert advisors and maintains close coordination with representatives from the PBC physics group, as well as with referees for experiments that have advanced to either Letter-of-Intent (LoI) or Proposal status under the PS and SPS Scientific Committee (SPSC)[1].

The core activities of the CBWG are carried out within the four sub-working groups, which organise meetings either with individual experiments or collectively with all concerned experiments, whenever required. The full Conventional Beams working group convenes several times a year. These sessions bring together all supported experiments along with the involved technical experts involved. In parallel, regular dedicated meetings are held within the BE-EA-LE section, which hosts the beam physicists responsible for

[1] https://committees.web.cern.ch/spsc

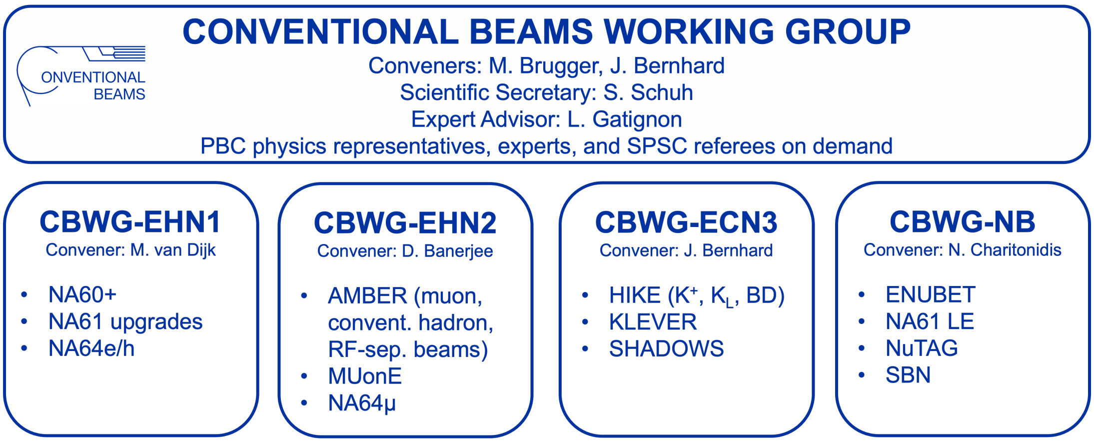

Fig. 6: The internal structure of the Conventional Beams working group.

the CERN's North and East experimental areas. These meetings focus on optimising the use of available resources and enhancing synergies across projects.

The primary deliverable of the Conventional Beams working group for 2025 is the present comprehensive final report, supplementing both the experiment proponents' input and the overall PBC summary input to the current Update of the European Strategy for Particle Physics (ESPPU). Given the continuous influx of new experimental ideas, some studies remain ongoing and will continue beyond the ESPPU process. Previous editions of this report, which partly include more extensive details on experiments studied for the first two phases of the Physics Beyond Colliders study, can be found in Refs. [1, 2]. Additionally, detailed documentation of specific studies is published in ATS and/or PBC Notes, Reports, and made accessible via EDMS[2]. References to these materials are interspersed throughout this document. The meeting agendas and the presentation material are available on the CBWG Indico site[3].

[2] https://edms.cern.ch/

[3] https://indico.cern.ch/category/8813/

Chapter 3

Projects in EHN1

Nikolaos Charitonidis, Maarten van Dijk, Luke Aidan Dyks, Elisabetta Giulia Parozzi

3.1 Introduction

The North Area Experimental Halls [6] are multi-purpose facilities that host large fixed-target experiments alongside numerous test beam stands. The EHN1 experimental hall serves as a general-purpose experimental area, accommodating four secondary beamlines: H2, H4, H6 and H8. These beamlines originate from two primary targets (T2 supplying H2 and H4, and T4 serving H6 and H8), and extend approximately 600 meters, with the final 250 meters located inside the EHN1 hall.

In the context of the conventional beam studies for PBC, the H2 beamline is designated to serve the NA61/SHINE experiment, while the H4 beamline supplies the NA64 experiment with electron beams. Within the NA64 community, a new idea has emerged to search for true muonium, the bound state of a positive and a negative muon. Although a specific location for this experiment has yet to be determined, the H4 beamline appears promising due to its ability to provide high-quality, high-purity positron beams and the beamline's synergies with the existing and the newly proposed NA64e programme.

The proposed search for true muonium would be based on 43.7 GeV/c positrons in the H4 beamline, matching the threshold for dimuon production in a fixed-target setup. Hadronic contamination in the H4 positron beam has been investigated in the context of NA64e operations using positrons. These measurements indicate that the H4 beam can deliver up to 10^7 e^+/spill with an energy spread estimated to be around 1 %. A recent target optimisation study, utilising 40 low-Z lithium foils, indicated that a 5 σ discovery of true muonium could be achieved within just three months of data collection. A comprehensive study of such an experiment is foreseen during LS3 to further evaluate the potential for conducting this search within the NA64 framework. Enhancements to the beamline, such as higher intensity and reduced energy spread, could significantly benefit this project.

The T4 primary target is at the origin of the H6 and H8 beamlines. For the DICE/NA60+ experiment, the H8 beamline is now considered a viable alternative to the ECN3 cavern.

3.2 NA61++

NA61/SHINE [27] is a fixed-target experiment permanently installed in the most upstream experimental area of the H2 beamline (zone PPE152). A view from the top of the EHN1 experimental hall, including the beamlines, is shown in Fig. 7. The location of the NA61/SHINE experiment is also indicated.

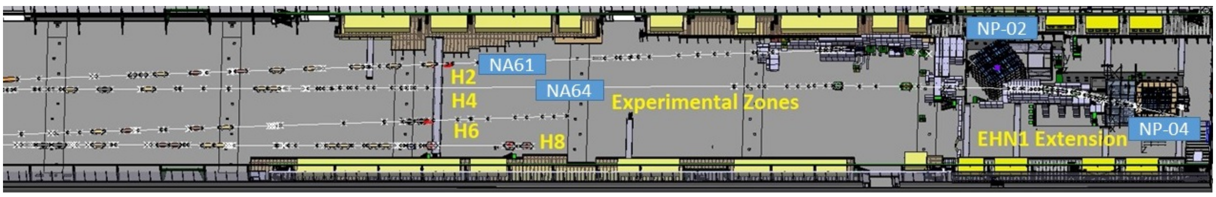

Fig. 7: Top view of the EHN1 experimental hall. The four beamlines H2, H4, H6, H8 are indicated, as well as the EHN1 extension [49]. NA61/SHINE is located in the H2 beamline, in zone PPE152.

The proposal for the NA61++ programme focuses on three primary research objectives:

– Conducting open charm measurements in $\mathrm{Pb} + \mathrm{Pb}$ collisions to investigate the onset of deconfinement and search for the critical point of the QCD phase transition.

- Measuring fragmentation cross-sections of light nuclei and anti-nuclei.
- Performing hadron production measurements using both thick and thin targets, across a momentum range from below 10 GeV/c up to 120 GeV/c.

3.2.1 High Intensity Pb Beam for Open Charm Measurements in $\mathrm{Pb}+\mathrm{Pb}$ Collisions

The H2 beamline is equipped to transport various ion species to the experimental areas, with safety constraints limiting the momentum per charge to below 380 GeV/c. For fully stripped Pb ions, this corresponds to a maximum energy of 150 GeV per nucleon. Prior to LS2, the maximum intensity of primary ions deliverable to the hall was limited to approximately 10^5 heavy ions per 10 second spill. Although the SPS can provide higher intensities, radiation protection studies conducted by the CBWG indicated the necessity for enhanced shielding, particularly around the zone housing the Projectile Spectator Detector (PSD) calorimeter. These studies have been completed [50, 51], and the recommended shielding reinforcements were implemented during LS2. Figure 8 shows the upgraded PPE152 area, including the enhanced shielding around the PSD calorimeter.

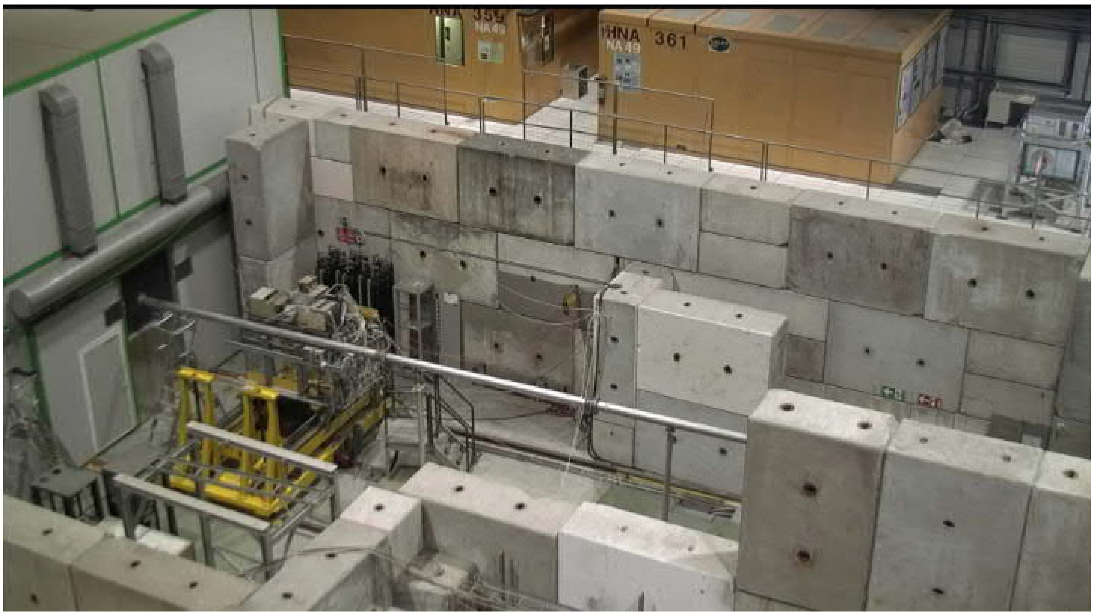

Fig. 8: The downstream section of PPE152 featuring the Projectile Spectator Detector (PSD) calorimeter. To tolerate higher beam intensities in this zone, additional shielding was designed and implemented during LS2.

In parallel to the shielding upgrades, a software interlock system was implemented to safeguard the experiment against fluctuations in beam intensity and position caused by power supply instabilities. This interlock system, triggered by a signal from part of the experimental setup, can switch the power supply of magnet MBNH.021.405 (BEND6) to STANDBY mode within a single spill duration of approximately 4.8 s. The interlock system is remotely resettable by the beamline physicist or the CERN Control Center (CCC). The implementation required significant effort on the controls software side, but only minimal additional cabling between the NA61/SHINE detector, the beam instrumentation electronics, and the power supply located in building BA81.

3.2.2 Measurement of Fragmentation Cross-Sections and Fragmented Beams

Fragmented ion beams were already delivered to NA61/SHINE in 2010 and 2011 [52]. In 2018, fragmented beams of ^{12}C and ^{16}O were successfully produced using a 300 mm beryllium target and transported to NA61/SHINE under a new beamline configuration. For this setup, the H2 beamline was optimised using FLUKA simulations to determine the ideal collimator settings and to maximise the ratio of desired ions to the total ion flux within the selected momentum bite. The predicted beam composition, which showed excellent agreement with experimental measurements, is shown in Fig. 9. Moreover, in 2024, a 13.5 AGeV/c lead ion beam was once again provided to NA61/SHINE as part of its cosmic-ray programme, utilising a beamline configuration closely resembling that of 2018. The measured fragmentation data for this beam is presented in Fig. 10. Fragmented ion beams are now exploited by NA61/SHINE on a regular basis.

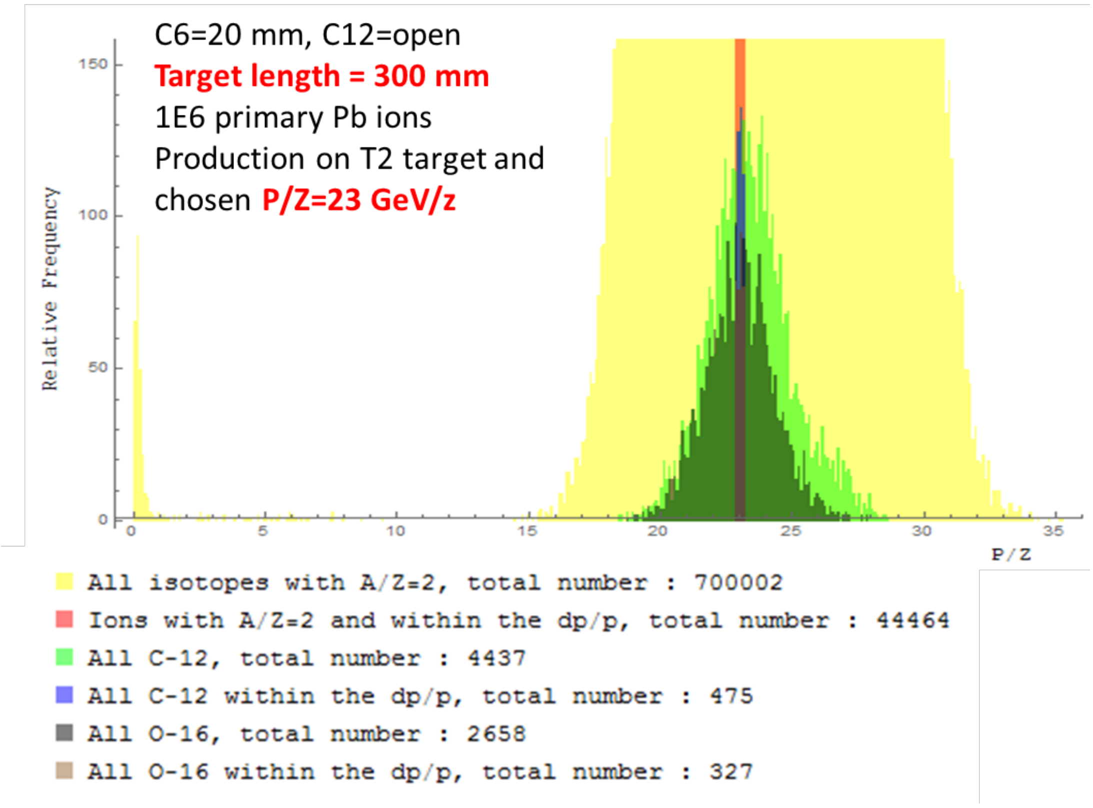

Fig. 9: Results of the FLUKA simulation of the fragmented beam composition delivered to NA61/SHINE in 2018. The 300 mm beryllium target was used as T2 target, with the momentum collimators fully open. The yellow distribution is the total number of all isotopes produced with an $A/Z = 2$, while the cut-off is done purely for visualisation purposes. The wanted ion species corresponds to the overlap of the orange band and the green distribution.

3.2.3 Hadron Production Measurements at Low Momenta

Since data below 10 GeV/c are crucial for reducing neutrino production uncertainties in several experiments worldwide, a dedicated low-energy beamline for NA61++ has been proposed. This study has now been integrated into the newly established Neutrino Beams working group of the CBWG and is discussed in Section 6.2.

3.3 NA64e

The proposed future NA64e research programme significantly expands upon previous runs by incorporating searches for a broader range of dark sector physics, including new sub-GeV states coupled to leptons and/or quarks, novel symmetries, and further beyond-the-Standard-Model phenomena [53–55]. The proposed programme would use leptonic (e, μ) and hadronic $(\pi, \mathrm{K}$, and p) beams provided by the

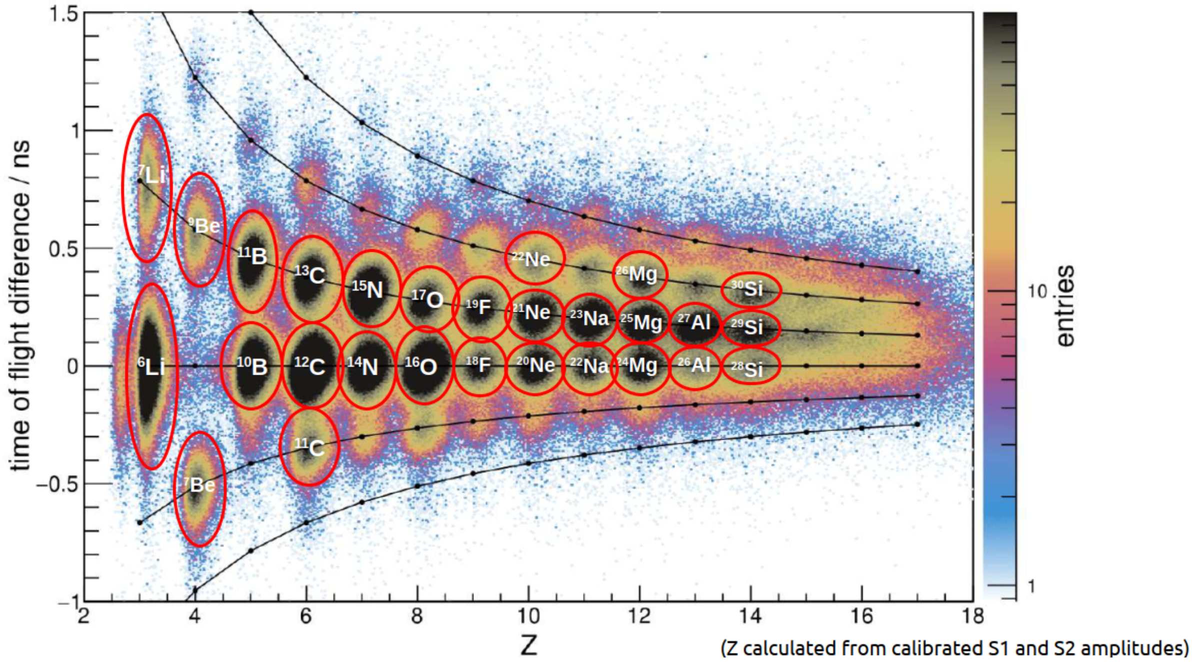

Fig. 10: Measured fragmented beam composition for $A/Z = 2$ at NA61/SHINE in 2024 derived from a 13.5 AGeV/c beam hitting the 300 mm beryllium primary target (Courtesy of the NA61/SHINE collaboration).

CERN SPS. The requirements and necessary modifications to the secondary beamlines, depending on the particle type, are summarised below.

- Electron beams: The primary physics goal remains the search for invisible and visible decays of A′, requiring electron beams in H4 to accumulate 10^{13} electrons on target at 100 GeV/c. Future plans include the possible use of positron beams. In principle, no significant modifications to the H4 beamline would be required.
- Hadron beams: The main physics focus would be on measuring the invisible decays of π^0, η, η', K_S and K_L via meson charge-exchange production. This would require medium-energy (20 to 50 GeV/c) hadron beams. The existing H4 beamline is already capable of delivering these beams without modification.
- Muon beams: The primary objective is the search for missing energy events. Discussions regarding installation and test runs for this experiment have now shifted to the M2 beamline in EHN2. The NA64μ programme is detailed in Chapter 4.

Given the current NA64e proposals within the framework of PBC, no significant modifications to the beamline are required. Hadrons and electrons (or positrons, for the ERC-funded project POKER [56]) with sufficient energy and intensity can already be delivered to NA64.

The NA64e experiment would benefit from further improvements in beam quality. There is optimisation potential in divergence, density (number of electrons mm^2), and the suppression of halo particles reaching the experiment's trigger system. Currently, the halo in the first trigger counter (V0) is approximately 5 %. Measurements in 2024 indicated that increasing the intensity to about 10^7 electrons/spill raises the halo to around 9 %, which may negatively impact data quality.

To reduce the halo and enhance tagging efficiency for hadronic background suppression, a potential reconfiguration of the upstream area (PPE134) is under study. Proposed upgrades include installing new particle identification devices (PID), such as threshold or differential Cherenkov counters, and adding two new QNL quadrupoles to optimise the beam size and divergence in the NA64 experimental area (PPE144).

Fig. 11: The NA64e experiment, installed in the PPE144 zone (July 2021).

These quadrupoles could be mounted on rails to allow easy movement in or out of the beamline, without restricting the beam acceptance for CMS tests located downstream in the experimental area PPE164. For the NA64 hadron programme, which focuses on the search for charge exchange reactions with pions and the decay of π^0, η, and η' into invisible modes, achieving kaon suppression at the level of 10^{-8} is imperative while maintaining reasonable efficiency for pions. To meet this requirement, the feasibility of adding three new Cherenkov counters after LS3 in PPE134 is currently under study.

3.4 True Muonium

Expanding the physics scope of NA64e, it has been proposed that true muonium, the bound state of a positive and a negative muon, could be produced in the H4 beamline using 43.7 GeV positrons, which corresponds to the threshold for dimuon production in a fixed-target configuration [40]. The production cross section is given by:

$$\begin{aligned} \sigma_n^{e^+e^-\to\mu^+\mu^-}(E_+) &= \frac{3\pi\alpha}{2}\cdot\frac{\delta E_n}{\Delta E_+}\cdot\sigma^{e^+e^-\to\mu^+\mu^-}(E_+) \\ &\simeq \frac{\delta E_n}{\Delta E_+}\cdot 9.11\times 10^{-32}\,\mathrm{cm}^2, \end{aligned} \tag{3.1}$$

where $\delta E_n = \alpha^2 m_\mu/(4n^2)$ represents the effective energy window for bound-state production, and ΔE_+ denotes the beam energy spread.

In the context of NA64 data taking with positrons in the H4 beamline, hadronic contamination has been studied [57]. The maximum achievable beam intensity in H4 is approximately 10^7 e^+/spill, with an estimated energy spread of around 1 %. A recent target optimisation study, employing 40 low$-Z$ lithium foils, demonstrated that, in principle, a 5 σ discovery of true muonium could be achieved within three months of data collection [58].

A detailed study is planned for the LS3 period, led by the NA64 Collaboration in partnership with ETH Zurich, to further assess the potential for such a search within the NA64 framework. The experiment would significantly benefit from an increased beam intensity and a reduced momentum spread.

3.5 DICE/NA60+

DICE/NA60+ [26] is a proposed heavy-ion experiment aiming to study open charm and dimuon production using lead-ion beams across beam energies ranging from 20 to 150 AGeV/c. Since the submission of the Letter of Intent (LOI), the highest requested energy has been adjusted downward from 158 to 150 AGeV/c to comply with the effective energy limits for ion beams directed toward EHN1. These limits, defined as 380.488 GeV/c in proton-equivalent terms for lead beams ($A/Z = 2.536$), constrain the maximum achievable beam energy. The experiment aims to submit a full proposal for consideration by the SPSC by May 2025.

DICE/NA60+ requires a lead beam incident on a lead target, generating a set of observables expected to be influenced by the formation of Quark-Gluon Plasma (QGP). To distinguish these signatures from those arising from conventional hadronic interactions, a reference dataset using proton beams incident on a lead target is essential, in addition to the lead-lead data. It is therefore necessary to have proton beams with the same momenta per nucleon, i.e. covering a range of 20 to 150 GeV/c. A dedicated note detailing the need for this reference measurement has been prepared by the DICE/NA60+ proponents [59].

An extensive testbeam campaign was carried out in 2022, 2023 and 2024, culminating in testing detector prototypes with lead beams at 150 AGeV/c and in 2024 also at 13.5 AGeV/c. The testbeam campaigns are discussed in detail in Section 3.5.6. Additionally, extensive studies were conducted to assess various options for proton beams for the reference measurement, as reported in Ref. [60] and summarised in Section 3.5.7.

3.5.1 The DICE/NA60+ Detector

While a detailed description of the experiment is beyond the scope of this document, a brief overview is provided for completeness. Further details can be found in the LoI [26].

The original NA60 experiment operated in ECN3 from 2001 to 2004. Its successor, the DICE/NA60+ experiment, was initially proposed for the same location, but is now proposed for installation in the experimental area PPE138 along the H8 beamline. This choice was driven by strong competition for the single available underground site, which was ultimately allocated to the BDF/SHiP experiment. As a result, the DICE/NA60+ detector design and intensity requirements have been adapted to fit the new location. Whenever the DICE/NA60+ experiment is not operational, the beam path will be cleared to allow regular beam use in the downstream experimental zones PPE158 and PPE168.

The experimental setup consists of two sections:

- Upstream Section: A set of thin lead targets, followed by a vertex detector positioned inside the strong magnetic field of the MEP48 spectrometer magnet, and immediately followed by a thick absorber.
- Muon Spectrometer: A large dipole magnet (MNP33) surrounded by a set of tracking chambers. A second absorber is placed after the magnet and before the final set of tracking stations.

The absorber composition and thickness will be adjusted depending on the ion beam energy and the proton reference beam, with higher-energy beams requiring a thicker absorber. The MNP33 magnet will be accordingly positioned further downstream as the primary absorber increases in size.

The lead target in the current design of DICE/NA60+ consists of five discs, each 1.0 mm in radius and 1.5 mm thick. The vertex detector is expected to be constructed using large-area Monolithic Active Pixel Sensors, developed in synergy with the project of the ALICE ITS3 detector. The absorber is a complex structure comprising tungsten on-axis elements arranged with stepwise increasing radius. Upstream of the absorber there are beryllium-oxide blocks, partially inside the aperture of the MEP48 magnet, with a re-entrant hole (beam catcher) at the beam impact point, and followed by a series of graphite blocks. The target, vertex detector and the most upstream absorber section will be housed within the MEP48 aperture. The absorber's role is to contain the particle showers induced by lead-ion and proton beams while minimising scattering of muons.

A set of muon tracking stations are positioned upstream and downstream the MNP33 magnet, followed by a graphite wall and a final set of muon stations. The muon stations will likely use MWPC (Multi-Wire Proportional Chamber) technology, operating with an Ar/CO_2 (70 % / 30 %) gas mixture. A rendering of the full experimental setup is shown in Fig. 12.

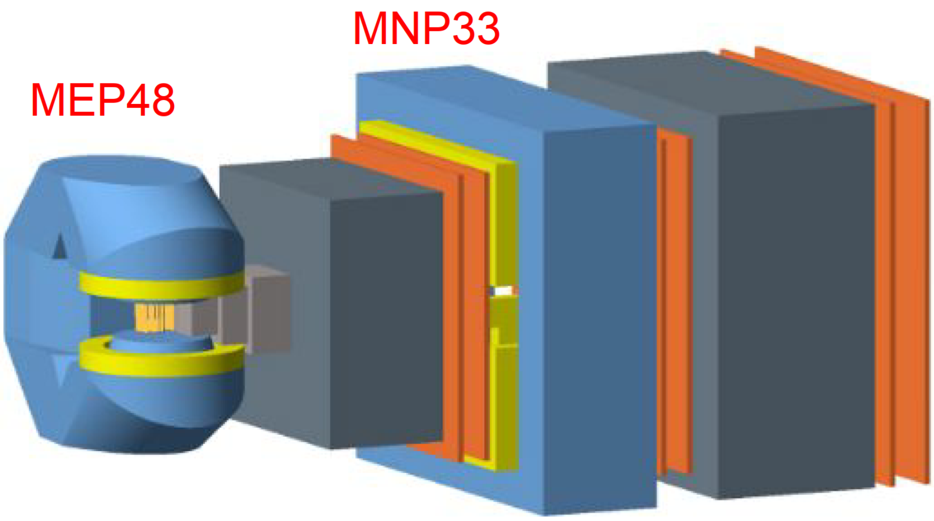

Fig. 12: Schematic view of the DICE/NA60+ setup in EHN1.

Several components from the original NA60 experiment have been identified as potential candidates for reuse in DICE/NA60+. These include graphite and BeO elements, which may be repurposed if they can be located.

A new detector for beam diagnostics is under discussion for DICE/NA60+ (see Section 3.5.6 for details). This detector would enable the distinction between primary and non-primary ion beam components. Additionally, the final beam focus must be verified to ensure a sigma below 0.6 mm in both the horizontal and vertical planes. One proposed method involves using a single ALPIDE sensor in the front-end region for this purpose.

The integration of the experiment into the zone is still under way. With the selection of the MNP33 magnet, excavation work in the zone is no longer required. Most of the access infrastructure, including the zone's access door and its access system, are expected to remain mostly unchanged, though the stairs leading to the beam level will need to be adjusted to fit the new layout. The exit door on the upstream side of the zone will be removed. Additional modifications to the zone layout, particularly those related to radiation shielding, are discussed in Section 3.5.5. A preliminary version of the 40 AGeV/c setup integrated in the PPE138 zone can be seen in Fig. 13, and for the 150 AGeV/c setup in Fig. 14. Known issues to still be addressed include placement of the stairs in the 150 AGeV/c setup, and some overlaps with the shielding. It is found that the full experiment and shielding as currently envisioned is expected to fit entirely within the current footprint of the zone. There will be no need to move the two quadrupoles in the downstream part of the zone. With these layout changes it is expected that the zone door on the upstream side will need to be suppressed, as such a new entrance to the zone may need to be added.

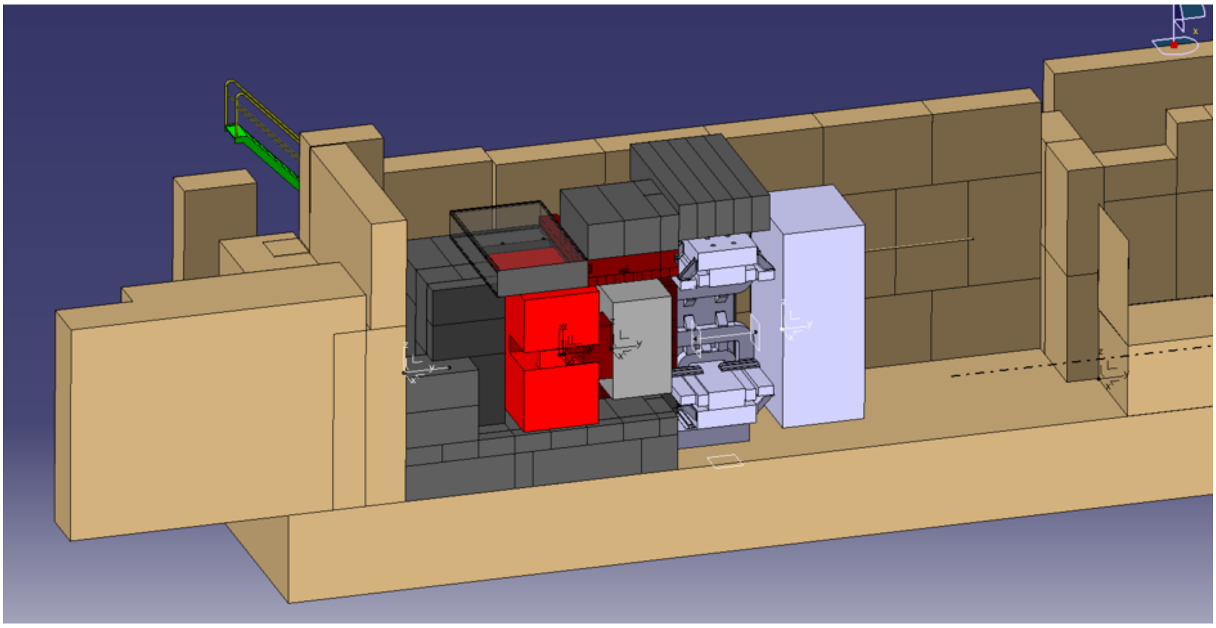

Fig. 13: View of the preliminary integration result of the 40 AGeV/c DICE/NA60+ setup in the EHN1 PPE138 experimental zone.

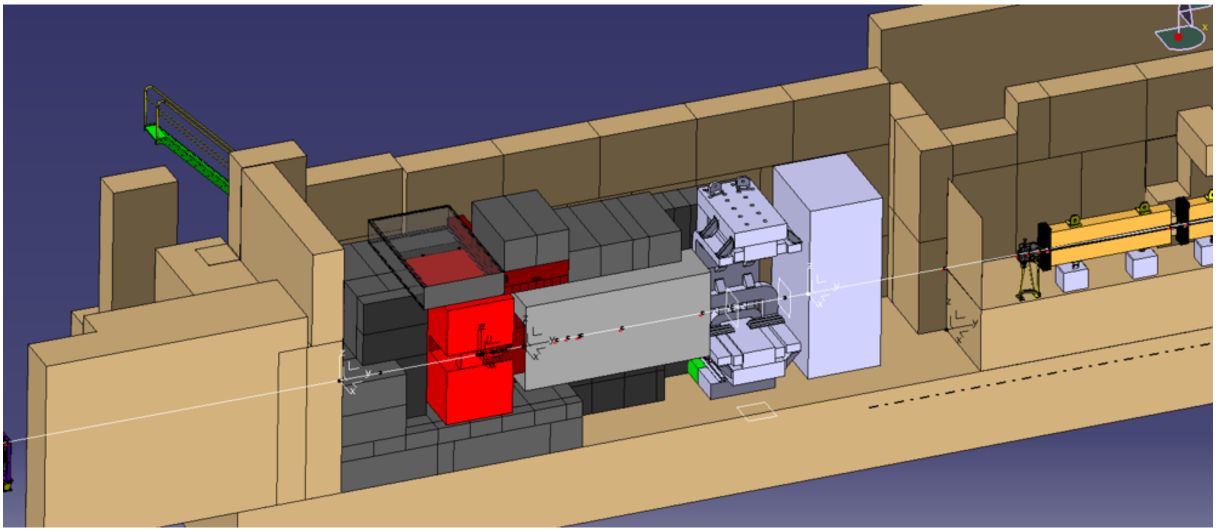

Fig. 14: View of the preliminary integration result of the 150 AGeV/c DICE/NA60+ setup in the EHN1 PPE138 experimental zone.

3.5.2 Magnets for DICE/NA60+

Two large experimental magnets have been identified for reuse in the DICE/NA60+ experiment. The MEP48 magnet is proposed as the vertex magnet, while the MNP33 is suggested for the muon spectrometer.

Notably, the lower coil of MEP48 is shorted. Both coils will be replaced if the magnet is repurposed for DICE/NA60+, as a new tooling setup would have to be prepared in any case.

The large muon spectrometer magnet was initially specified as a hexagonal toroidal magnet, similar to the ACM magnet in the original NA60 experiment. This has since been reconsidered and instead, the existing large experimental magnet MNP33 is proposed for reuse. Constructed in 1975 for the b19 beamline in the East Hall, MNP33 was built as an H-shaped spectrometer magnet featuring a useful aperture width of 2450 mm (full aperture 3100 mm) and a pole gap of 600 mm. Around 1991, it was modified for the NA48 experiment with a new return yoke, expanding the vertical gap to 2400 mm, and a second set of coils was added to create its current configuration. It is currently in use in NA62 and is scheduled to become available in LS3 when NA62 and the K12 beamline will be dismantled.

Simulation studies have compared the performance of the toroidal configuration with the dipole configuration provided by MNP33 [61, 62]. The results indicate that using MNP33 improves the figures of merit for the experiment: notably, the number of reconstructed ω mesons from dimuons increases by a factor 3, and reconstructed J/ψ mesons from dimuons increase by 15 %. These improvements are primarily due to the fact that the toroidal magnet's central dead zone does not exist in the dipole configuration. Additionally, the power consumption of the latest toroidal magnet design would be comparable to that of MNP33, offering no substantial power consumption advantage for the construction of a new magnet. Moreover, the reuse of MNP33 offers cost savings, reduces construction time, and benefits from existing field maps and operational expertise. Finally, MNP33 has a full height of 4 m, compared to the proposed toroid's height of 6.96 m. With a beam height over the floor of 2.86 m, this reduced size eliminates the need for floor excavation to accommodate the muon spectrometer magnet.

For operational efficiency, the MNP33 magnet should be mounted on a rail system to enable movement along the z-direction, allowing adjustments for different incident particle energies.

3.5.3 Field Maps of MEP48 and MNP33

Field maps for MEP48 and MNP33 have been simulated, respectively in Ansys Maxwell (MEP48, N. Pacifico) and OPERA3D (MNP33, F. Stummer). The simulated field map for MNP33 has been compared to measured data from the NA62 experiment with good agreement. A combined field map for the 40 AGeV/c version of the experiment (including the MEP48 and MNP33 magnets plus the iron shielding) is shown in Fig. 15. Also shown are the integrated field maps along the longitudinal axis, with and without the shielding implemented. Considered in isolation, the MNP33 magnet has an integrated strength of 0.9 T m, operating with 1250 A in the old coil and 2500 A in the new coil. The presence of MEP48 reduces this by around 3 %, and adding the shielding for this configuration by another 7 %, for a total of 10 %. The field map has been made available [63]. The magnetic fields of MEP48 and MNP33 will be oriented vertically and of opposite polarity, with regular polarity flips to control experimental systematics. The simulation of the full 150 AGeV/c layout remains to be performed, it is expected that the magnet cross-talk will be less due to larger distance, and the effect of the iron shielding on the integrated field will also be reduced due to a longer distance between the shielding blocks and MNP33.

3.5.4 Power Converters for the Experimental Magnets

The power converters serving the two large experimental magnets MNP33 and MEP48 will be located in BA81. Groups of power converters have been identified which can power the three required circuits: the "old coil" and "new coil" of MNP33, and the single coil for MEP48.

Presently in NA62, the old coil of MNP33 runs at 1250 A with a resistance of 0.484 Ω, corresponding to a power consumption of approximately 750 kW. The new coil is driven at 2500 A with a resistance of 0.190 Ω and consuming around 1.19 MW, bringing the total power consumption to 1.94 MW. The maximum possible power draw for these converters, based on the above resistances, is 2.3 MW, corresponding to 1500 A and 2500 A for the old and new coils, respectively.

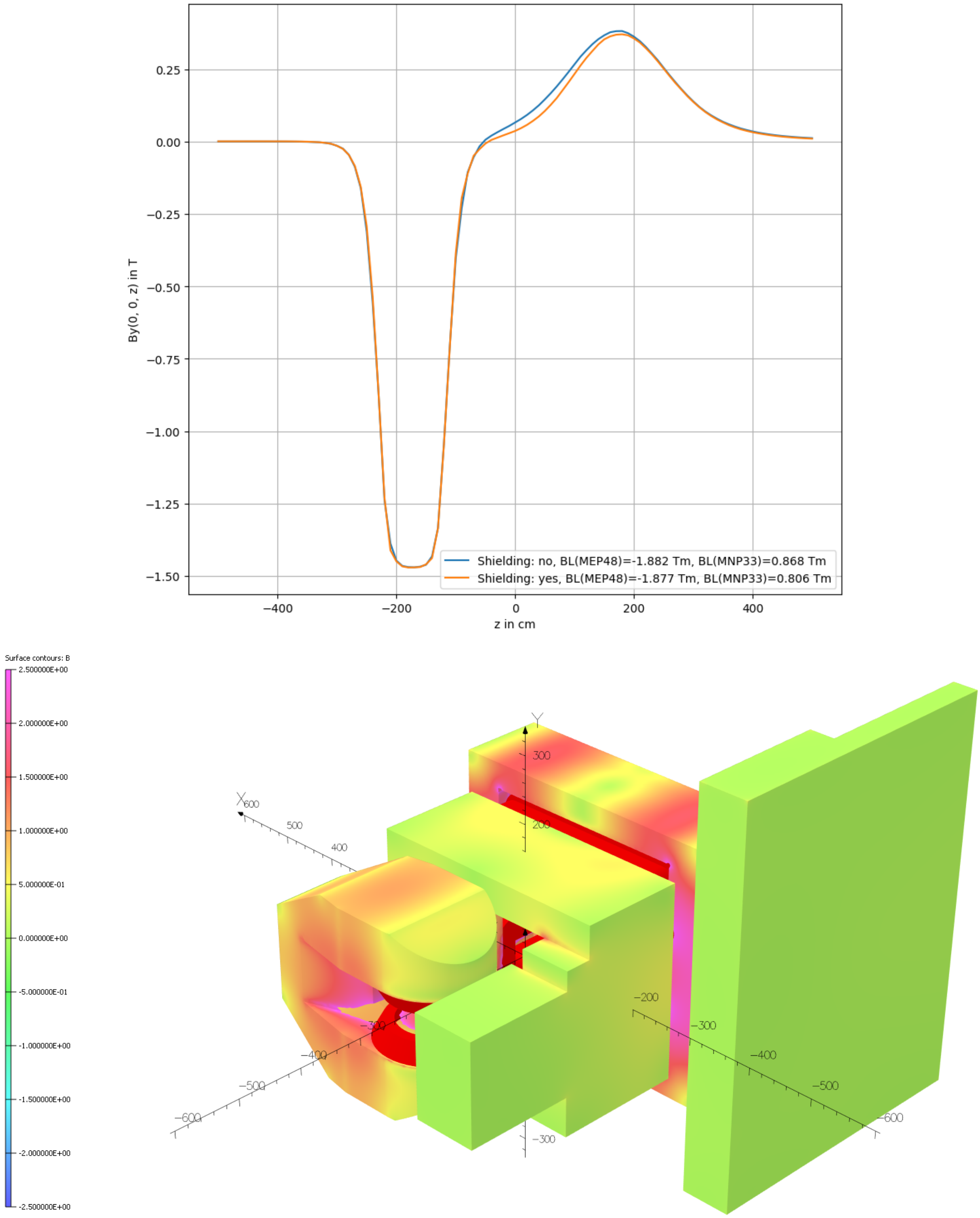

Fig. 15: Simulated integrated magnetic field for the 40 AGeV/c setup (top), with iron shielding as laid out in Section 3.5.5 and visualisation with field strength overlaid on elements (bottom).

The old coil can initially be supplied using two NR22 and one ND21 converters, while the new coil will require one NR31 plus one ND31 converter. MEP48 operates with a single coil operated at 2000 A, with a power consumption of 400 kW. These values should be reassessed after the coil replacement. A single NR31 power converter may be sufficient for MEP48. All these power converters are existing units and can be available for this purpose from LS3 onward. The only remaining requirement is a 400 VAC / 2000 A feed at BA81, presently under discussion with the EN-EL group.

The NA-CONS project, organising the renovation of the North Area, will focus on the consolidation of the TCC2 target cavern and the BA80 power converter building during LS3, while LS4 will include the consolidation of EHN1 and BA81. For MNP33, the new power converters will include one BOREAL 2S for the old coil and one BOREAL 2S-2P converter for the new coil. These replacements were initially planned within the NA-CONS budget, but were removed from the baseline following the decision in favour of the BDF/SHiP experiment in ECN3. Funding for these converters, as well as for a BOREAL 2P converter required for MEP48 has yet to be secured.

Cooling of the magnets will dominate the overall cooling requirements for the DICE/NA60+ experiment. The MNP33 magnet requires approximately 56 $m^3\,h^{-1}$, while MEP48 will need around 12 $m^3\,h^{-1}$. Discussions with EN-CV have indicated that, at present, these cooling needs cannot be guaranteed. But substantial upgrades to the cooling infrastructure of the magnets in EHN1 are currently underway. Once these modifications are completed, the required capacity should become available. The BDF/SHiP experiment, to be installed from ECN3, is also still finalising its cooling requirements. Once all these requirements are established, the cooling needs of DICE/NA60+ and BDF/SHiP will be evaluated together.

The additional cooling requirements for the experiment itself, including detectors and related services, remain to be determined in detail. Depending on the specific needs, it may be possible to integrate these directly into the cooling system for the magnets.

3.5.5 Radiation Protection Considerations

The assessment of the required shielding configuration for DICE/NA60+ comprises two parts. The first is the assessment of the shielding of the transfer line to the experiment, specifically the section in beam zone PPE128, just upstream of the DICE/NA60+ detectors. Simulations indicate that the radiation field around PPE128 will be acceptable if it is shielded by at least 160 cm concrete in all directions. All access doors must be protected by means of chicanes. The shielding of PPE128 must be significantly strengthened to meet these requirements. An adequate shielding layout, shown in Fig. 16, has been proposed and costed.

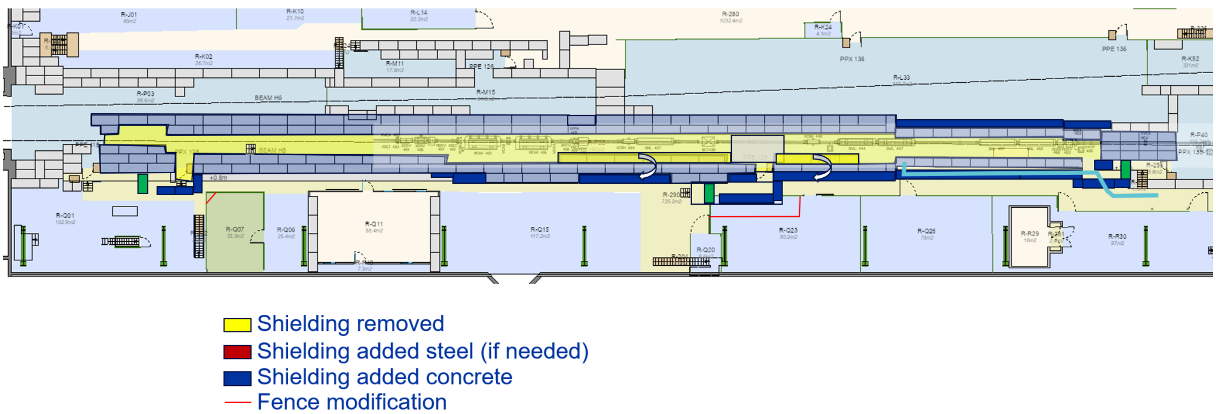

Fig. 16: Proposed modification to the shielding of PPE128, so that there is at least 160 cm of concrete in all directions from any point along the beam axis and that the access points are suitably protected by a chicane.

The RP situation for the proposed setups of DICE/NA60+ in PPE138 was also studied in detail by the CERN HSE/RP experts [64, 65]. It was found that with suitable configurations of shielding, the radiation doses can indeed be brought down to an acceptable level. Two separate setups have been evaluated: the low energy (40 AGeV/c) configuration and the high energy (150 AGeV/c) layout of the experiment. The two proposed layouts, shielding included, are shown in Fig. 17.

Fig. 17: Top views of the proposed shielding configurations for DICE/NA60+ in PPE138 at beam level. The top figure depicts the 40 AGeV/c setup, while the 150 AGeV/c setup is shown in the bottom figure.

One important feature of the shielding in PPE138 is that an 80 cm concrete roof shielding is necessary. The main access door will not move, but it may be necessary to modify the stairs from the PPE entry door to the beam level. The simulated radiation levels for the two setups, with the proposed shielding, are shown in Figs. 18 and 19.

In all cases, the dose rates with this shielding configuration are found compatible with the zone classifications. The situation with the proton reference beams in the required energy range remains to be

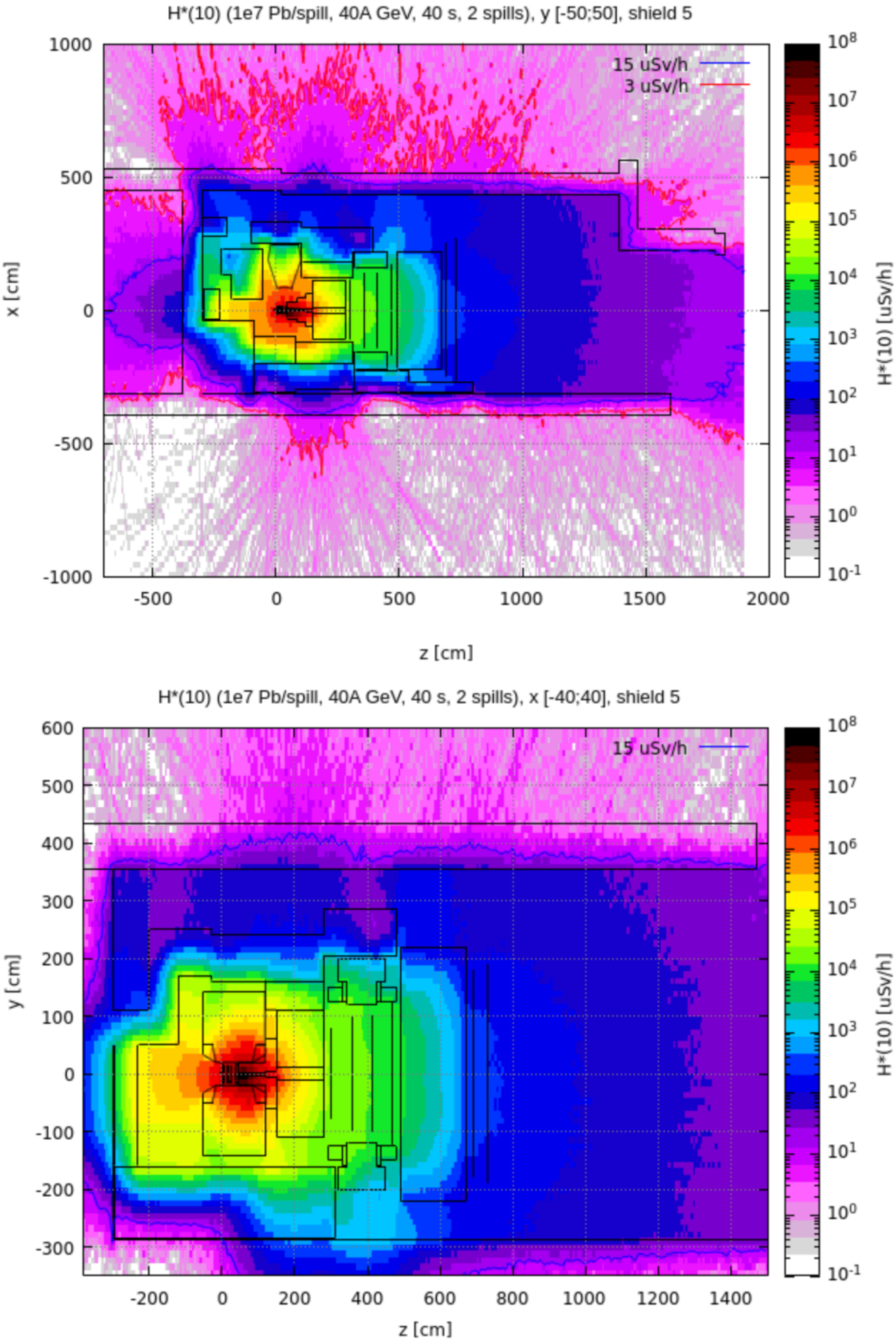

Fig. 18: Simulation results of prompt dose levels for PPE138, with shielding implemented as proposed for the 40 AGeV/c setup. Shown are horizontal (top) and vertical (bottom) slices at beam height.

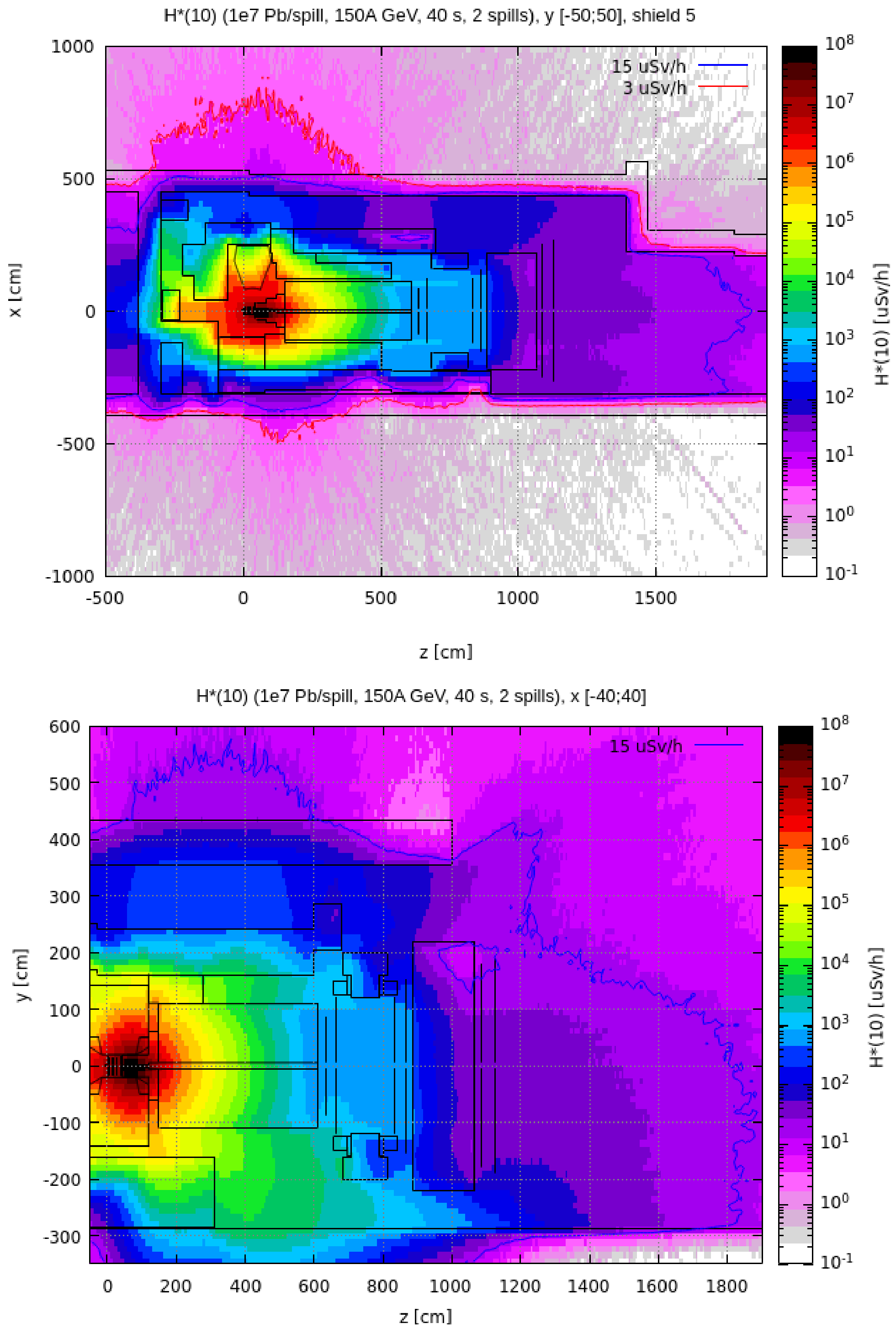

Fig. 19: Simulation results of prompt dose levels for PPE138, with shielding implemented as proposed for the 150 AGeV/c setup. Shown are horizontal (top) and vertical (bottom) slices at beam height.

assessed, but is expected to not be limiting compared to the equivalent Pb ion beam situation. It is noted that three additional RP monitors are foreseen to be placed at the most critical locations.

At the start and end of each operational period of DICE/NA60+, the absorber blocks must be moved out of the beam to allow the downstream zones to receive beam when DICE/NA60+ is not running. The radiological impact of this operation and how it should be minimised will be assessed once the experiment is approved. Similarly, an inventory will be made for activated items and for their disposal.

3.5.6 Ion Beams for DICE/NA60+

DICE/NA60+ will use lead ion beams spanning the range from 20 to 150 AGeV/c. In the operational years 2022, 2023 and 2024, runs were taken with DICE/NA60+ prototypes at 150 AGeV/c. In 2024, a special run was made at 13.5 AGeV/c. This is lower than the desired minimal energy of DICE/NA60+ but provided a good opportunity to assess the feasibility of such low-energy lead ion beams. This section will describe results obtained mainly over the 2024 run period.

The beam size at the experiment is a key parameter for DICE/NA60+. It depends on the beam size and divergence at the T4 target and on the optics of the beamline. The beam size at the T4 target location is measured with a so-called BBS detector, which uses secondary emission from a thin wire that is scanned through the beam, one position per spill. The divergence is measured by means of a monitor located after the last TT20[1] transfer line quadrupoles, 25.99 m upstream of the T4 target. This so-called BSM (mobile split-foil monitor) has two semi-circular secondary emission foils, each covering opposite halves of its sensitive area. Scanning this detector through the beam and measuring the asymmetry of the signals on the two foils allows for a determination of the beam shape at the monitor position. From this beam size one can assess the angular spread of the beam at the T4 target. Normally, these BSM monitors are blocked in nominal position on the beam axis and are used to ensure continuously good steering of the beam onto the target. More details on its definition can be found in [66]. Figure 20 shows the lead ion beam sizes as measured for low and high energies at the T4 target location. At low energy (13.5 AGeV/c), it was found that the beam intensity and size are so diluted that it was challenging to find the signals. Only the horizontal beam size was established, and even that only by averaging over five repetitions of the measurement. The asymmetry was measured and from there the beam size was fitted as shown in Fig. 21. The angular spread of the beam was derived by dividing the size at the BSM by the distance between the BSM and the target (25.99 m) and is shown in Fig. 21. Table 5 contains a synopsis of the derived measurement results.

Table 5: Beam size and divergence (values quoted are at 1 σ), as measured at the T4 target for the high- and low-energy optics used in TT20.

Momentum	150 AGeV/c	13.5 AGeV/c
Optics	Old	New
T4 horizontal size	0.39 mm	1.3 mm
T4 vertical size	0.19 mm	
T4 divergence (x)	52 µrad	350 µrad
T4 divergence (y)	120 µrad	140 µrad

During the ion beam period in 2024, two weeks were allotted in H8 to DICE/NA60+, one week at high (150 AGeV/c) and one week at low (13.5 AGeV/c) energy. At low energy it was expected that, for the same optics settings, the beam size would grow by a factor of $\sqrt{150/13.5} = 3.33$ as expected from emittance growth as a function of momentum. For the standard TT20 optics, the beam is large at

[1]Transfer line that transports particles from the SPS to the production targets in TCC2, here referring to the transport to the T4 target.

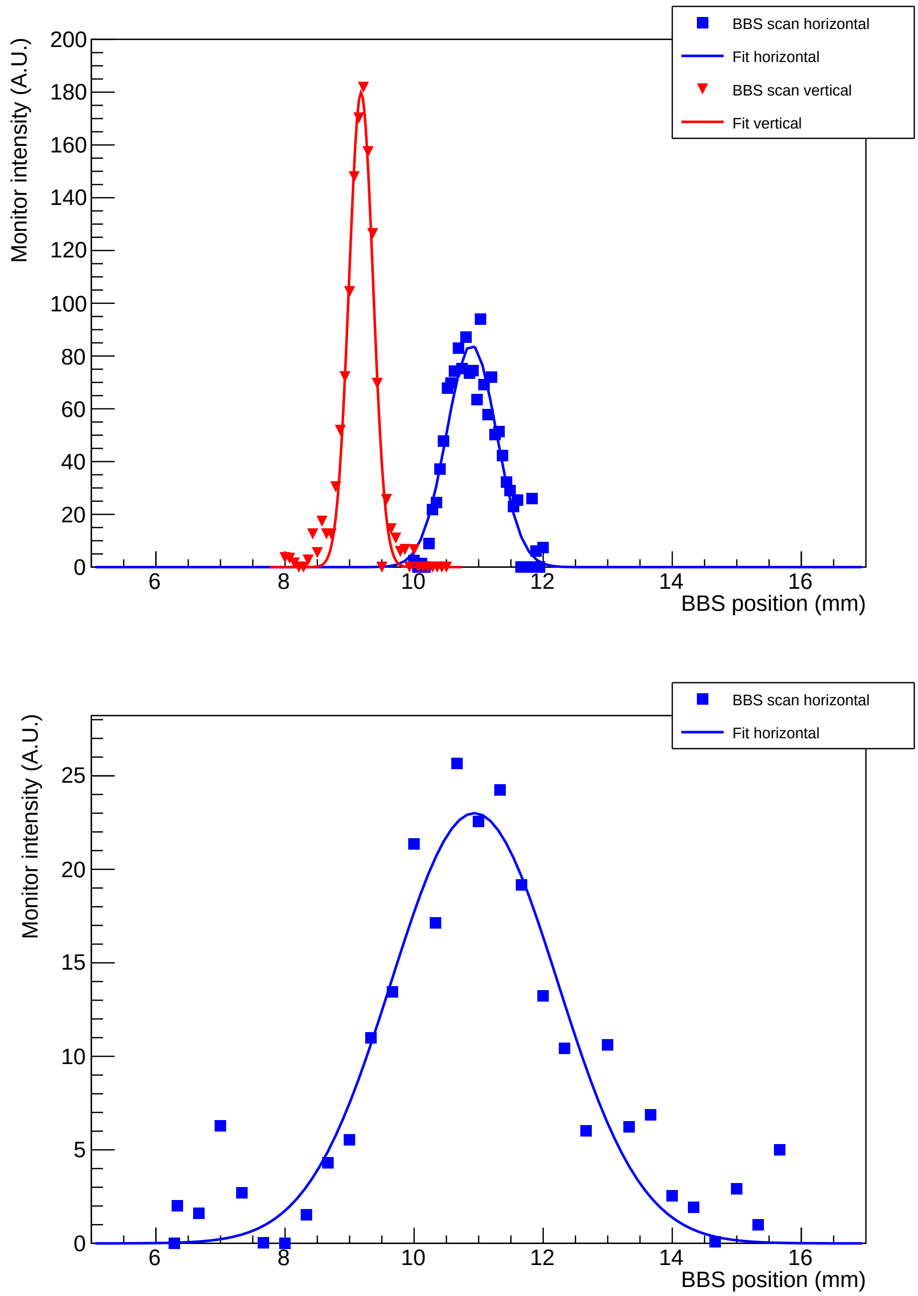

Fig. 20: Beam size as measured on the T4 target, (top) for high-energy beams (150 AGeV/c) and (bottom) for low-energy beams (13.5 AGeV/c). Fitted values for the beam shape are summarised in Table 5.

the splitters to minimise losses on the septum blades. At substantially lower energy, the beam becomes even larger and consequently a substantial fraction is lost on the splitter apertures. The TT20 optics was adjusted to compensate and hence labelled in Table 5 as "New" TT20 optics. For H8, the same optics were used.

Taking measurements with the BBS scanner at low-energy proved to problematic. The size at the target was found to be substantially larger in the horizontal plane than at high energy, leading at approximately the same intensity to a much lower signal on the BBS. This was compensated by averaging over a series of five scans. Even then the signal in the vertical plane was not found, suggesting that the

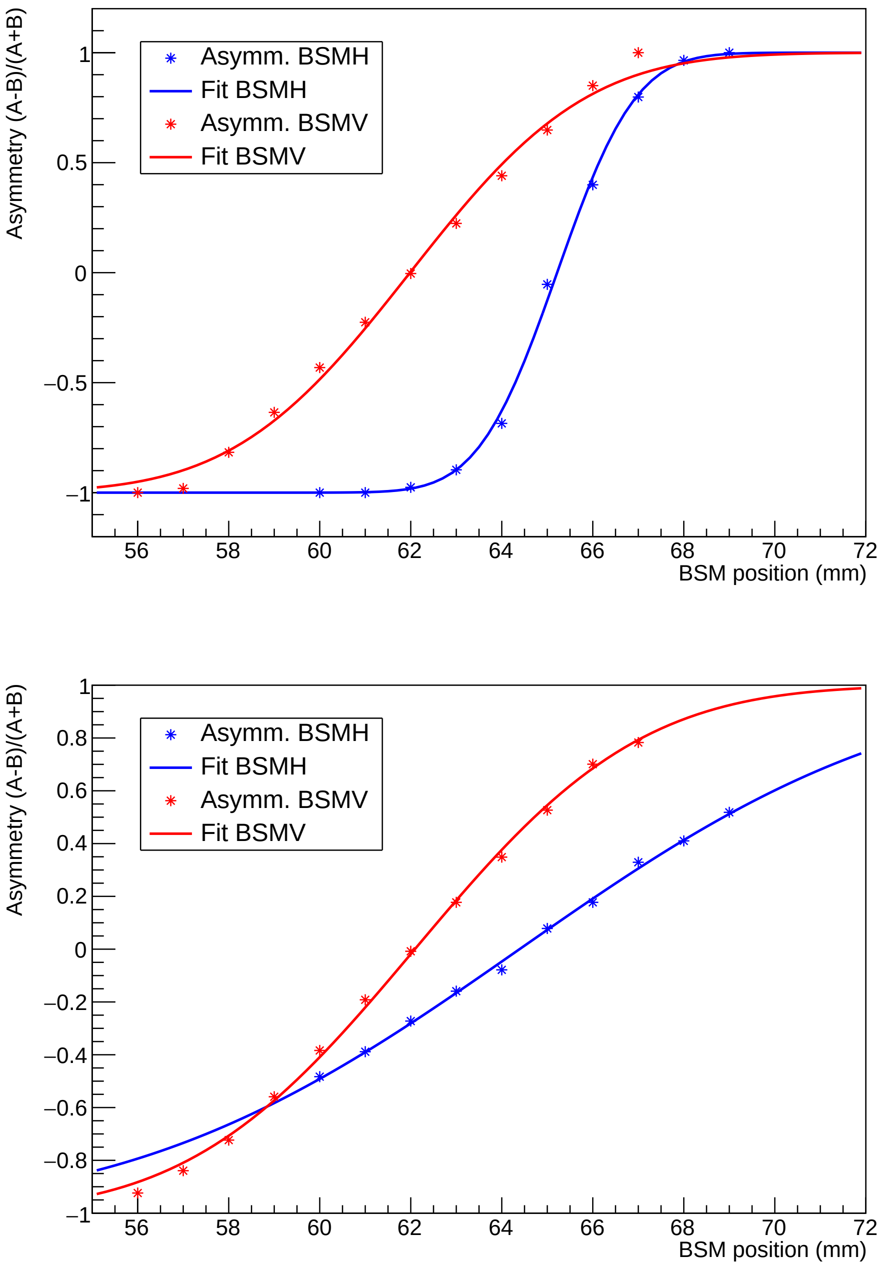

Fig. 21: Measurement of beam asymmetry as measured with the BSM 25.99 m upstream the T4 target, (top) for high-energy beams (150 AGeV/c) and (bottom) for low-energy beams (13.5 AGeV/c). Results of the fit are summarised in Table 5.

beam size in vertical plane was even larger than in the horizontal plane. The beam size increased in the horizontal plane by a factor of 3.3, in the vertical potentially by a factor of 7 or more. This in turn affected the transmission to the experiment, as these terms propagate through the H8 beamline and affect the beam size at the experimental location.

The optical terms for the optics used [67], and shown in Fig. 22, were rescaled to the source terms as measured in Table 5. In this way, a direct assessment of the impact of each term can be made. It should be noted that the terms add up, so while an aperture may not appear limiting to the passage of a single ray it can still represent a substantial cut on the beam as a whole.

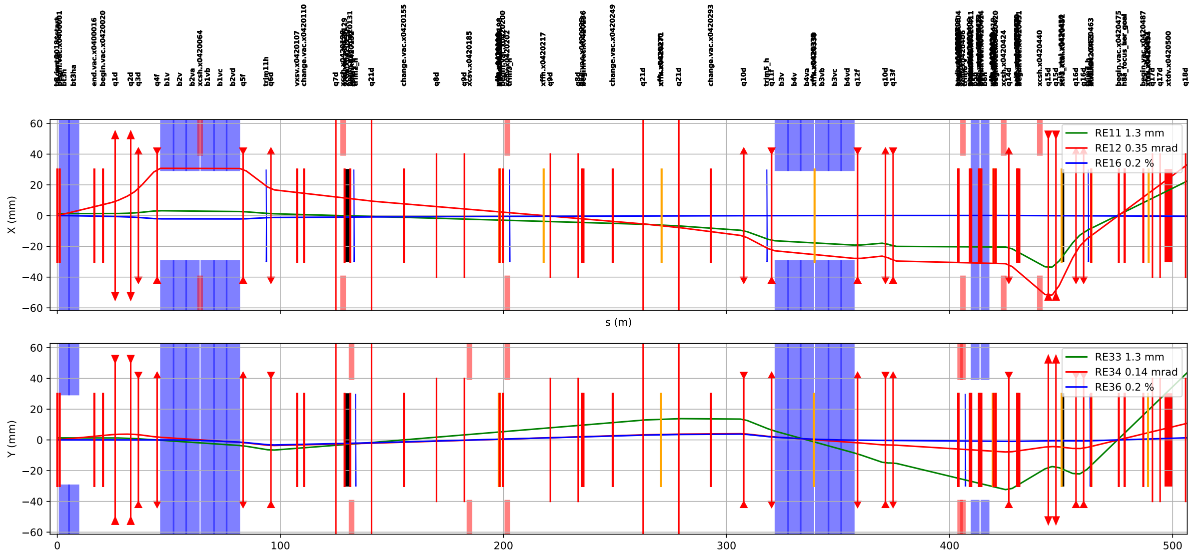

Fig. 22: Optics of H8 beamline for the the DICE/NA60+ experiment as used during the 2024 test beam period. The optical terms shown are scaled according to the source terms (one sigma) as measured at the T4 target (Table 5, at low energy).

The maximum intensity accepted by the line is assessed with fully open collimators. Two high-intensity tests were performed, with the intention of reaching the DICE/NA60+ nominal intensity (10^7 primary Pb ions per spill) for both energy settings. The beam size is a combination of the source terms at T4 multiplied with the relevant R-matrix (transport matrix) elements. In the horizontal plane, there is a multiplicative factor defined by the R_{11} term in the beamline optics (for the component of the beam size stemming from the horizontal beam size at the T4 target, also called magnification) and from the horizontal angle at the T4 target (by the R_{12} matrix element). In the vertical plane, the corresponding matrix elements are R_{33} and R_{34}. At a focus, the terms R_{12} and R_{34} are constrained to be zero. In that case the size of the beam is a direct function of the size at the target. This applies if the momentum spread is small or if the optics eliminates any dependence on the individual particle momentum (R_{16} and R_{36} are zero). The momentum spread is indeed very small for a primary beam. For the optics employed (see Fig. 22) the magnification terms are $R_{11} = 0.33$, $R_{33} = 0.4$. The beam sizes were measured at the experiment for low and for high energy, at the target intensity.

For the high-energy high-intensity test, all collimators were opened to ± 40 mm except for C_1 (horizontal, at $s = 64$ m) and C_3 (vertical, at $s = 130$ m). These were gradually opened and an intensity of 9.6×10^6 spill was reached on the two scintillators XSCI.042.198 and XSCI.042.475, for C_1 at ± 1.8 mm, and C_3 at ± 2.0 mm.

The spot size measured at the experiment at high energy was then found to be (σ_x, σ_y) = (0.207, 0.098) mm at high energy, as shown in Fig. 23. Based solely on the expectation from the optics and the initial conditions, a spot size of (0.127, 0.074) mm could be the best achievable from projecting the initial conditions onto the optics at the location of the experiment, provided no beam scattering and no aperture restrictions are present along the line (which was indeed not the case here). This comfortably meets the requirement from the experiment, defined to be $\sigma < 0.6$ mm in both planes.

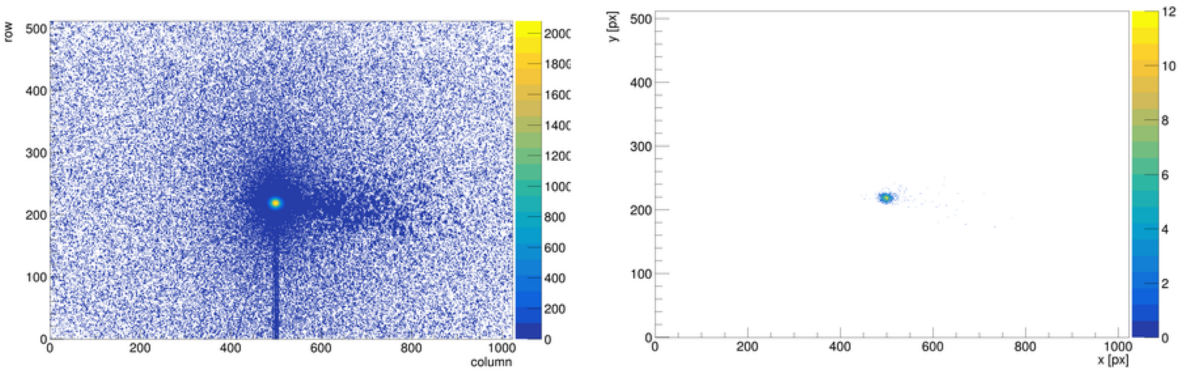

Fig. 23: Beam spot as observed by DICE/NA60+, with (σ_x, σ_y) = (0.207, 0.098) mm for 150 AGeV/c. The plot on the top displays the raw hitmap, while the plot on the bottom shows the map after applying a selection for primary ions only.

The spot size measured at low energy for the same optics was found to be (σ_x, σ_y) = (1.6, 0.18) mm at low intensity, as shown in Fig. 24 and around (1.8, 0.45) mm at high intensity, with fully open collimators. In the latter case, an intensity of close to 10^7 ions was observed in scintillator XSCI.042.198. Nevertheless, only around 2.4×10^6 ions were simultaneously observed in scintillator XSCI.042.475. This loss can be attributed to the large values of the optics terms in between the scintillators. From optics considerations, two apertures appear to be limiting horizontally, the group of vertical bending magnets BEND1 and BEND2 in the region 50 to 80 m from T4 and the quadrupoles that generate the final focus near the experiment (located at around 475 m). The combination of the two initial conditions and R_{11} and R_{12} in the horizontal plane implies a calculated loss rate of 55 %, with 75 % observed. A hotspot was confirmed to exist in the final focus region by specialists of the HSE/RP group. Possibly, the remaining 20 % are lost in the vertical plane, but this assessment could not be completed as the vertical beam size in T4 was not known. Still, our observations clearly demonstrate that at this very low energy and with this optics the initial conditions lead to large losses along the H8 line. Adjustment of the H8 optics will be studied, and additionally the potential of reducing the size of the beam at the T4 target should be investigated. Both can help improving transmission and reducing the beam size at the experiment. Some margin exists as the lowest ion energy requested for DICE/NA60+ is 20 AGeV/c (13.5 AGeV/c was used in this test). This would already result in some improvement. It is recommended to foresee a detector close to the DICE/NA60+ target location to check the beam properties at the final focus. During this series of tests, the beam intensity per spill observed on the BSI upstream of the T4 target varied strongly from 1.2×10^{10} to 2.6×10^{10} charges (or 1.4×10^8 to 3.2×10^8 primary ions).

Despite the intensity fluctuations by a factor of approximately 2 on the upstream BSI, the intensity on the scintillator at $s = 198$ m was much more stable. Even more problematic was the observation that the intensities at the BSI and at the scintillator at $s = 198$ m clearly do not match. With fully open collimators, we expected that a good fraction of the full intensity (if not all of it) should be able to pass through the H8 beamline. Nevertheless, with a maximum of 1.3×10^7 per spill observed in the scintillator and 2.6×10^8 per spill in the BSI, there is a discrepancy of about a factor of 20, which cannot be resolved. Further clarification will be sought from the SY/BI group on the behaviour of the BSI.

Independently, it is recommended that a separate detector be set up, capable of providing an accurate count of the beam rate up to the limits of the available ion intensity, at all required energies. The exact detector type and its location remain to be identified by the beam instrumentation specialists. Up to a factor of 2–4 of losses could be explained by losses from the beamline (horizontal restriction in BEND1

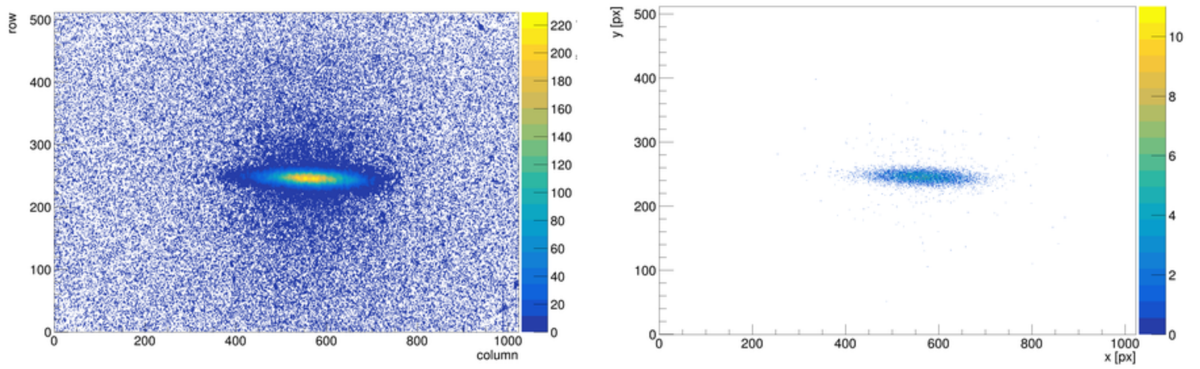

Fig. 24: The beam spot as observed by NA60+ at 13.5 AGeV/c (regular optics), with (σ_x, σ_y) = (1.6, 0.18) mm. The plot on the top shows the raw hitmap, the one on the bottom the map after filtering for primary ions.

and BEND2 plus any errors possibly resulting from the beam steering), but finally observing only up to 5 % of the expected beam implies possibly a detector issue.

The observed maximum beam intensity was never as high as expected and it is unclear if this is a beam-loss issue or a detector issue. Better instrumentation offers the best path forward. LS3 will see the installation of secondary emission grids in the BSM and TBIU locations close to the T4 target [68, 69], and would be available in time for the operation of DICE/NA60+. These replace the existing BBS and BSM and will provide reliable measurements spill-by-spill. This upgrade would greatly enhance the ability of NA60+ to smoothly set up the beamline correctly and take data in good conditions.

Finally, it is imperative to identify the exact loss locations, because optimised collimation will be the only handle the experiment will have on the beam size and shape. If the beam entering the beamline is already of too low intensity, the collimation cannot be done in such a controlled fashion and the final spot size will necessarily be enlarged when collimating for the right intensity at the end of the beamline.

We have shown that at higher energies the focused optics developed for DICE/NA60+ can serve the experiment adequately. A growth in the beam spot of a factor of 3.33, expected from momentum scaling, is allowable from the viewpoint of the experiment. Already near 150 AGeV/c, the beam is expected to scrape apertures along the line, assuming it retains the same size and divergence at T4 as today. This effect might be mitigated by collimation if the incident intensity is sufficiently high, although this has not yet been tested.

It is important for DICE/NA60+ to control the non-primary component of the beam. Preliminary analysis of test beam data indicates that this component amounted to some 10 to 20 % of the primary content of the high-energy beam. Another series of tests will be set up for improving the beam purity, under the assumption that ion beam time will be approved for DICE/NA60+ for 2025. A more effective collimation scheme will be developed in parallel with a redefinition of the lower-energy optics. We recommend that a detector will be developed, in collaboration with SY/BI experts, that is capable of separating the primary from the other components. This will also be a key contributor in developing the collimation scheme. It is finally noted that a veto counter with a small hole for the beam passage will be very helpful, as the fragments by their generation mechanism and different rigidity distribution have a larger spot size than the primary component of the beam.

3.5.7 Proton Beams for DICE/NA60+

A study has been performed to investigate the various options for the proton beams requested by DICE/NA60+ [60]. The proton energies of interest span the range from 20 to 150 GeV/c, although the final list of energies will be constrained by the available time and is still under discussion. The required intensity is 5×10^8 protons/spill, assuming a spill of 4.8 s. For different spill lengths, the required intensity scales linearly.

Three possibilities have been identified to provide protons to DICE/NA60+. The first option is primary beam, accelerated to the right energy by the SPS and transported through TT20 and H8 to PPE138. The second option is to produce a secondary beam in the primary target T4, which corresponds to the standard way of operating the H8 beamline for test beam users. The final option is to use a tertiary beam, where the secondary beam impinges on an intermediate target inside the H8 beamline and the tertiary beam is derived from there.

The three options have distinct advantages and limitations. Typically, the addition of each target for production of a lower energy (secondary or tertiary) beam implies a reduction of the available beam intensity by typically a factor of 10^3 to 10^4. With a primary beam of at most 2×10^{13} protons (limited by target and proton beam dump heating considerations), it is excluded to derive a tertiary beam of the required intensity. The secondary beam option merits further consideration. It was assessed by simulating a primary proton beam on a 300 mm beryllium target, using both FLUKA and Geant4. In both cases, the angular and momentum acceptances of the secondary beam (effectively ± 1.32 mrad horizontally, ± 0.61 mrad vertically and a momentum acceptance of ± 1.5 % for the standard optics) were applied. The result is shown in Fig. 25. The so-called Atherton parametrisation is also shown as it is one of the usual cross-checks for the production of secondary particle beams. It is in principle only valid above 60 GeV/c and is therefore drawn as a dashed line for momenta lower than that.

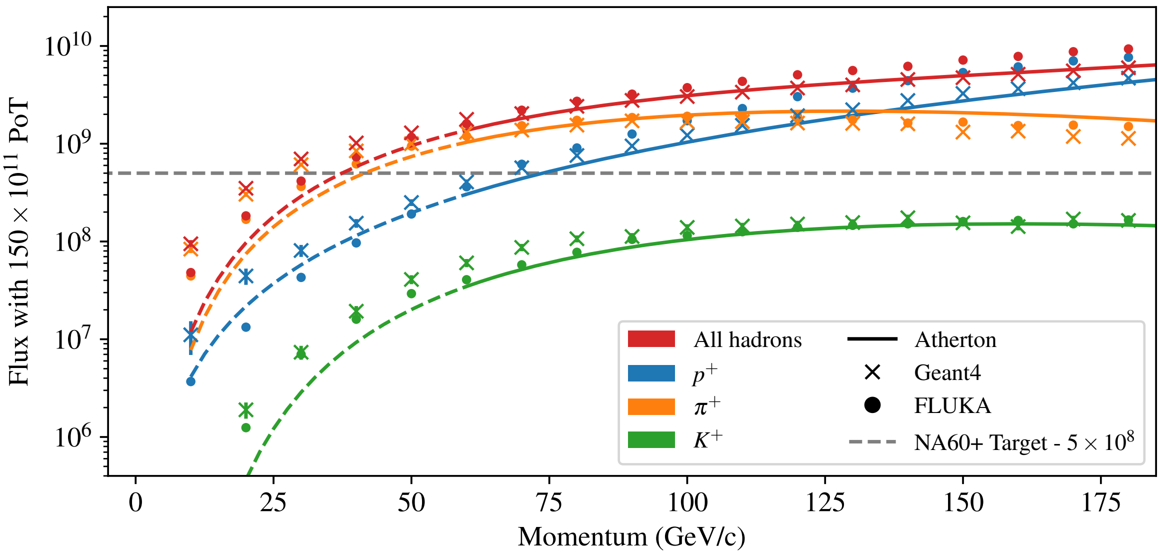

Fig. 25: Expected secondary hadron flux at the DICE/NA60+ experiment versus particle momentum from a primary beam intensity of 150×10^{11} impinging on a 300 mm beryllium target plate. Pion and kaon decay along the beam up to DICE/NA60+ was accounted for.

Two key conclusions emerge. First, only secondary beams with momenta of approximately 70 GeV/c or higher would be able to meet the proton flux requirement for DICE/NA60+. Second, even at the maximum energy of 150 GeV/c, the beam has significant contamination from other hadrons, highlighting the need for some form of particle tagging. To investigate this further, the fractional proton content of the beam was estimated through simulation and compared with data taken in the H6 and H8 beamlines during the 2024 run. Additionally, three momentum points were evaluated using a full beamline simulation. All of these data and simulation points are shown together in Fig. 26.

For all measured points the proton purity is lower than expected from simulation. Even at the highest energy the experiment intends to operate at, 150 GeV/c, the proton purity is only 60 %. To operate

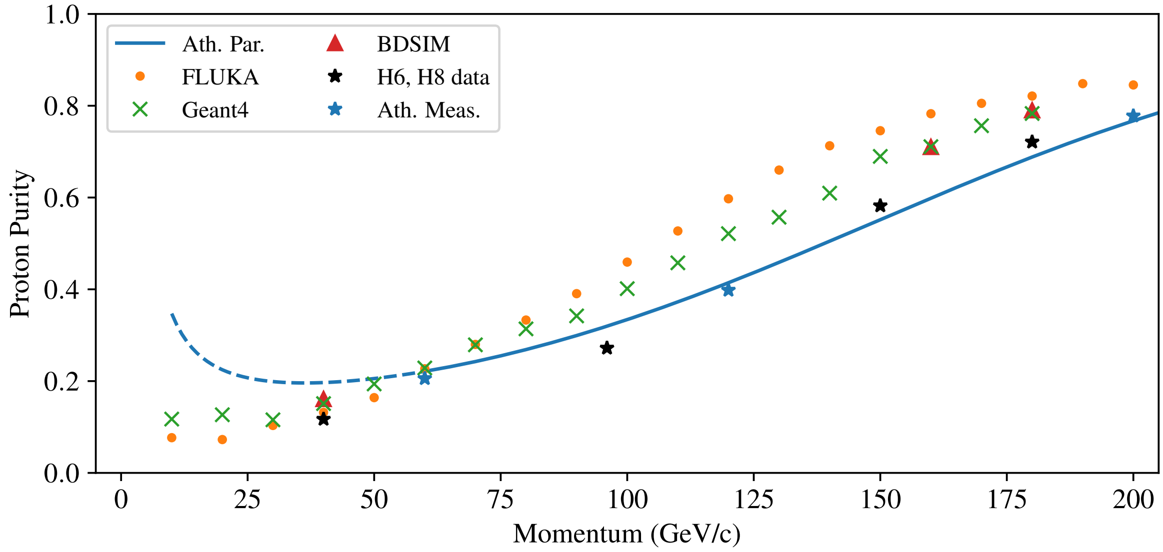

Fig. 26: Proton purity as measured in the H6 and H8 beamlines and calculated proton purity at the DICE/NA60+ experiment as a function of the secondary beam momentum.

with secondary beams, the DICE/NA60+ experiment requires a proton purity of 90 % or higher. This requirement could be met by using a complex particle identification system, which would need to surpass the rate of the highest-performing currently existing example of such a system, the KTAG of NA62 [70], by a factor of three. Developing such a detector within the available timeframe was considered unrealistic by the experiment team and was therefore ruled out as an option.

Consequently, the use of primary protons from the SPS remains the viable option. In 2004, the original NA60 experiment operated with reference protons at 158 GeV/c, demonstrating that it is possible in a technical sense. Since then, the addition of a series of safety elements have made this more difficult. The possibility to extract a regular, full-intensity beam with an intensity of $\mathcal{O}(10^{13})$ protons to the surface experimental halls has to be avoided at all cost for safety reasons. The slow extraction from the SPS for protons towards the North Area is chosen to be 400 GeV/c during regular operation. It would be technically feasible to extract protons of different energy under the so-called ion interlock, which limits the total charge in the ring to the equivalent of 2×10^{11} protons, but has no limitation on the energy. As the DICE/NA60+ experiment requires around 5×10^{8} protons/spill, this would be a possibility. As the name suggests, the ion interlock is normally used for ions, and would require adjustment of a number of imposed software limitations. The required investigation for safety and feasibility is still to be made. The final difficulty is one of planning and availability. The SPS normally serves a wide community of users, and likely only a limited subset of users could be served under these conditions, possibly exclusively the DICE/NA60+ experiment. Despite these difficulties, it is concluded that the use of primary protons is the only feasible way to accumulate the proton reference data for DICE/NA60+. The number of energy points and the required accumulated protons will have to be minimised. The exact way in which these protons could be safely extracted from the SPS remains to be discussed with the relevant machine experts, transfer line experts, safety experts and RP specialists.

3.5.8 Services for DICE/NA60+

A number of items have been identified as required services for DICE/NA60+ and are listed here:

– Gas infrastructure: MWPCs require an Ar/CO_2 70 % / 30 % mix, flow rate to be identified but

small,
- Transport: Lifting capacity of the cranes adequate for the transport of the largest MNP33 and MEP48 components,
- The power usage in the zone (apart from magnets), which is expected to be well within the limitations of the existing electrical infrastructure,
- Required cooling water for the experimental magnets, likely feasible.
- A powering solution for the magnets, which has been identified.

It is expected that only minimal further studies are required for these items. Services and items for which the assessment is not yet complete have been added to Section 3.5.9.

3.5.9 Open Aspects for DICE/NA60+

From the items investigated so far, no real showstoppers have been identified, but a number of open items merit further attention. CBWG is committed to finalising the preliminary requirements and estimates together with the experiment to allow for a timely submission of the DICE/NA60+ proposal to the SPSC. In addition, a complete cost estimate shall be provided in this proposal.

Experiment Magnets

For successful operation of MEP48, its coils need to be replaced. This work falls under the responsibility of the EP Magnets Working Group, whose experts are already following the developments of the project. The effects of cross-talk between the $\mathbf{B}$-fields of the magnets on each other, and the impact of the iron shielding, were studied within the CBWG. Power converters for both magnets have been identified and costed. The only open item for powering the magnets is a missing 400 VAC / 2000 A feed at BA81, to be followed up with EN/EL. Possible local changes to the beamline magnets will be studied within the BE/EA group once the optics has been revisited. The effect of the displacement of the beam in the vertex spectrometer due to the field of MEP48 is under study by the DICE/NA60+ Collaboration. The rail mounting of MNP33 needs to be prepared for the movement of the 132 t-magnet along the beam axis for DICE/NA60+.

Integration

The integration of the experiment in the PPE138 zone is being followed within the CBWG, including the shielding and a rails system to allow MNP33 to move longitudinally. Once the costing for the shielding has been completed, the responsibility for these costs will be attributed. Items in the zone that would impede the installation of the experiment or the shielding around it, will be moved, removed or modified as needed, such as for example the XCET.042.474 currently in place upstream, and the FISC detectors on the upstream and downstream side. Once the experiment is approved, an acceptable solution for the quadrupole magnets in the downstream part of the zone will be identified, either moving them further downstream or removing them altogether. A solution will be identified for the final location of the stairs to floor level in the PPE138 zone. The PPX exit door on the upstream side of the zone will be removed. Finally, an inventory of still-existing elements of the NA50/NA60 absorber will be made. All these items are to be followed within the BE/EA group.

The readout for the experiment, IT infrastructure, any cabling, and the required space to in the counting room remains to be identified by DICE/NA60+. Once these are clarified a plan will be drawn up by the BE/EA group and relevant equipment groups. It is noted that the beam timing information will be moving to the White Rabbit system in LS3 [71]. A renewal of the counting rooms is foreseen already under NA-CONS in LS4.

On request of the experiment, alignment of detectors will be requested from the survey teams.

Beam Optics and Related Items

Substantial needs for further study have been identified for both proton and ion beams, relating to the beam size and intensity on the T4 target. The experiment would substantially benefit from further minimisation of the beam size on the T4 target at all energies, both for protons and ions. The SY/ABT group has the required expertise and would be well placed to perform such a study.

Similarly, the optics of the H8 beamline has substantial room for improvement. The optics will be optimised further within the BE/EA group, with input from the transfer line experts on the TT20 optics, as the initial conditions on T4 set the margins for beam size evolution along H8. Based on the improved optics, a collimation scheme will be developed to optimise the transmission through H8 and minimise any backgrounds to the experiment.

It is currently not permitted to extract protons to EHN1 that are not at 400 GeV/c. The possibility to do lower-energy slow extraction of protons for DICE/NA60+ under the ion interlock is being considered and is technically feasible on the level of the SPS accelerator. The ion interlock as it is today limits the beam intensity to around 2×10^{11} protons, well above the 5×10^{8} protons required for DICE/NA60+. Further discussion with the experts in EN/AA, BE/OP, HSE/RP, BE DSO, and other groups will be necessary, to investigate whether such an interlock could be implemented safely and which restrictions apply. Pending approval of the experiment by the SPSC and Research Board, this discussion should be coordinated by BE/EA to ensure safe conditions also for the other North Area beamlines and experimental areas. Further potential synergies with other experiments that might be interested in lower energy primary protons will be followed by the experimental areas teams.

Beam Instrumentation

On the beam instrumentation side, a number of needs has been identified. Further collaboration is foreseen with the SY/BI group to develop a detector capable of rejecting non-primary components in the DICE/NA60+ primary ion beam. The technical requirements for such a detector are to be specified by the DICE/NA60+ Collaboration. When appropriate, the BE/EA group can be involved in following this development.

The check of the final focus at the experiment requires a detector capable of quantifying beam sizes with good precision down to around 100 μm. This detector should likely be mounted on a movement stage that can move out of the beam during data taking, to minimise material on the beam axis. The DICE/NA60+ Collaboration will check the possibility to use an ALPIDE-based detector for this purpose.

The beam intensity in the line was found to be difficult to quantify during the beam tests in 2024. It was not clear at which point losses occurred, though some hotspots were clearly identified. A counter able to withstand and quantify the primary intensity in H8 (for both ion and proton beam) is to be identified in collaboration with the SY/BI experts. This detector function could also overlap with those of the monitor identified above that rejects non-primary components of the ion beam. Additionally, the BSIs already present in the beamline should be re-calibrated for use with primary ions, possibly by means of activation foils. Expertise for these measurements has been developed in close collaboration between SY/BI and BE/EA.

Radiation Protection

Three additional RP monitors need to be placed along the line and/or in the zone. The HSE/RP group shall further specify what type of devices and where they are to be located. An assessment of the expected activation of the DICE/NA60+ absorber will be requested to the HSE/RP experts, and if needed a procedure will be drawn up in collaboration with DICE/NA60+ for moving in/out the absorber. This movement is required at the beginning and end of each running period. If any further items are expected to be substantially activated, an inventory can be drawn up together with HSE/RP.

Other Required Services

The additional cooling needs for the detector of DICE/NA60+ remain to be defined by the Collaboration. Once this is clarified, a solution will be investigated within the CBWG in collaboration with the EN/CV group.

Chapter 4

Projects in EHN2

Dipanwita Banerjee, Johannes Bernhard, Lau Gatignon, Fabian Metzger, Silvia Schuh

4.1 Introduction

The M2 beamline [41] at the North Area delivers high-energy, high-intensity muon and hadron beams to the experimental hall EHN2, along with low-intensity electron beams for calibration purposes. The schematic layout of the M2 beamline is depicted in Fig. 27.

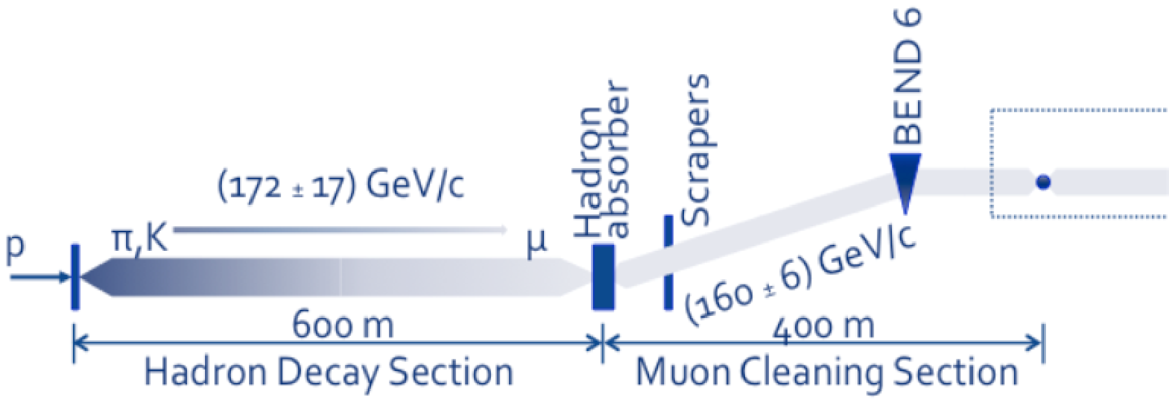

Fig. 27: Schematic layout of the M2 beamline. The specific momenta for the most common operation mode are indicated, namely the 160 GeV/c muon beam.

At present, the M2 line transports secondary particles from the T6 target over a distance of about 1200 m. The upstream end of the beamline consists of six high-gradient quadrupoles designed to maximise the acceptance of secondary hadrons. This is followed by a momentum selection system, consisting of horizontal dipoles and collimators, that allows for a maximum momentum bite $\Delta p/p$ of ±10 % in the horizontal plane. The beam is then matched to a FODO section of about 600 meters allowing some of the pions and kaons to decay. For the muon mode, a set of up to nine motorised beryllium absorbers, each 1.1 m long, can be inserted at the end of the FODO into a series of three vertical dipole magnets to absorb the remaining hadrons. These absorbers are instrumental in achieving hadron suppression levels of about 10^{-6} to 10^{-5}. Beyond these absorbers, a 450 m long section, equipped with motorised magnetised collimators (Scrapers) and magnetised iron blocks (MIBs) serves to transport the muons to the experiment while selecting the final muon momentum and cleaning the beam from muon halo. In hadron beam mode, the momentum selection can be refined with a downstream collimator (COLL05) located 850 m from the T6 target.

Once the beam reaches the surface, it is made level by a combination of BEND6 and BEND8, a system of three 5 m long, consecutive dipole magnets (BEND6) and one 2 m long dipole (BEND8). The final section includes beam instrumentation for momentum measurements (BMS) and space for beam particle identification detectors (CEDARs) in hadron beam mode. This section is followed by a final quadrupole triplet that focuses the beam on the target of the experiment. The different modes of operation are summarised in Table 6.

Table 6: Summary of the available operation modes of the M2 beamline.

Beam Mode	Momentum (GeV/c)	Intensity per 4.8 s spill	Typical $\Delta p/p(\%)$	Spot size at target (mm^2)	Polarisation	Absorber
Muons	$+208/190$ $+172/160$	$\approx 10^8$ 2×10^8	$3\,\%$	8×8	$80\,\%$	IN
Hadrons	$+190$, -190 Max. 280	10^8 (RP) 4×10^8 (with dedicated dump)	$1\,\%$	5×5	-	OUT
Electrons	-10 to -40	$< 2 \times 10^4$	-	$> 10 \times 10$	-	OUT

4.2 Experiment Proposals

The EHN2 Working Group is a sub-group of the Conventional Beams working group, to which it reports regularly. The proposals currently under study by this subgroup include the recently approved AMBER Phase 1 QCD Facility [13], MUonE [36] and NA64µ [33]. These studies are categorised according to the different beam modes:

– Muon Beams
– Hadron and Electron Beams

The final section is dedicated to studies concerning beam instrumentation.

The muon beam studies focus on the compatibility of the three proposals in terms of spatial allocation, required muon momentum and intensity, as well as potential future upgrades to accommodate higher-intensity demands.

The hadron beam studies include the RF-separated beam study and upgrades to the conventional hadron and electron beam.

The RF-separated beam study investigated the feasibility of delivering high-intensity kaon or antiproton beams for AMBER, with requirements summarised in Table 7.

The conventional hadron and electron beam studies explore possible upgrades to the M2 beamline to enhance its ability to deliver higher-intensity and higher-quality hadron and electron beams. These improvements include optimising beamline optics, enhancing beamline shielding for radioprotection considerations, and minimising material in the beamline to reduce interaction effects.

Studies have also been conducted on upgrades to beam instrumentation for both muon and hadron beams. These include an upgrade of the differential Cherenkov detectors (CEDARs) for beam particle identification and an upgrade to or replacement of the existing beam momentum station (BMS) around BEND6.

During Run 3, meetings of the working group were held about twice per year, with additional ad hoc meetings to track progress on both experimental and beam-related studies. Presentations have been archived via Indico and meetings minutes are available on EDMS. Parts of the studies reported below have been included in Ref. [13].

Table 7: Summary of requirements for the AMBER experiment [13].

Programme	Physics Goals	Beam Momentum GeV/c	Beam Intensity 1/s	Trigger Rate 10^3/s	Beam Type	Target	Earliest start time, duration	Hardware Additions
μp elastic scattering	Precision proton radius measurements	100	4×10^6	100	$\mu^\pm$	high-pr. H2	2022 1 year	active TPC SciFi trigger silicon veto
Hard exclusive reactions	GPD E	160	10^7	10	$\mu^\pm$	$NH_3^\uparrow$	2022 2 years	recoil silicon modified PT magnet
Input for DMS	$\overline{p}$ production cross-section	$20 - 280$	5×10^5	25	p	LH2, LHe	2022 1 month	LHe target
$\overline{p}$-induced spectroscopy	Heavy quark exotics	12, 20	5×10^7	25	$\overline{p}$	LH2	2022 2 years	target spectr. tracking, calorimetry
Drell–Yan	Pion PDFs	190	7×10^7	25	$\pi^\pm$	C/W	2022 $1 - 2$ years	
Drell–Yan (RF)	Kaon PDFs Nucleon TMDs	≈ 100	10^8	$25 - 50$	$K^\pm, \overline{p}$	$NH_3^\uparrow$, C/W	2026 $2 - 3$ years	"active absorber", vertex det.
Primakoff (RF)	Kaon polarisability and pion lifetime	~ 100	5×10^6	> 10	K^-	Ni	n/e 2026 1 year	
Prompt Photons (RF)	Meson gluon PDFs	≥ 100	5×10^6	$10 - 100$	$K^\pm$ $\pi^\pm$	LH2, Ni	n/e 2026 $1 - 2$ years	hodoscope
K-induced spectroscopy (RF)	High-precision strange-meson spectrum	$50 - 100$	5×10^6	25	K^-	LH2	2026 1 year	recoil TOF forward PID
Vector mesons (RF)	Spin density matrix elements	$50 - 100$	5×10^6	$10 - 100$	$K^\pm, \pi$	from H to Pb	2026 1 year	

4.3 Muon Beams

4.3.1 Experiment Requests

AMBER

The first phase of AMBER [13] includes a measurement of the proton radius using muon beams. The Collaboration requires a standard muon beam with lower intensities of 10^7 μ/s (particles per second of spill for this chapter). The focused beam shall have a divergence of less than 1 mrad in both planes with a beam spot below 1 cm RMS. The hadron contamination in the muon beam shall be below 10^{-5}.

MUonE

The MUonE experiment aims to measure the hadronic vacuum polarisation contribution to $(g-2)_\mu$ [72,73]. It requires a parallel 160 GeV/c muon beam with maximum intensity, currently 5×10^7 μ/s, with potential increase post-LS3. The beam shall have a divergence below 300 μrad RMS in both planes and fit within tentative detector dimensions of 10 cm × 10 cm. The final experimental setup requires 40 m of space along the beam. The hadron contamination of the muon beam shall remain below 10^{-5}.

***NA64*μ**

NA64μ aims to search for dark matter coupling specifically to the muon [33]. The Collaboration requests muon beams with momenta between 100 to 160 GeV/c, a divergence of less than 500 μrad RMS in both planes and a beam spot size optimised at the location of the active target. The required beam intensity shall be in the range of 10^5 to 10^6 μ/s, with a potential increase to 5×10^7 μ/s post-LS3. The setup requires 25 m of space along the beamline, two large-aperture MBPL dipole magnets as spectrometer magnets, and the possibility of using the existing beam momentum station (BMS) or additional tracking detectors around BEND6 to measure the incoming beam momentum with a resolution of $\lesssim$1 %. Post-LS3, NA64μ also requests to have a semi-permanent location in the M2 beamline to reduce installation time and minimise systematic errors due to potential realignments.

4.3.2 Compatibility and Integration

Given these user requirements, each experiment could be installed as a stand-alone setup in EHN2 without technical difficulties, as all configurations fit within the available space, while leaving enough flexibility for dedicated optics and necessary modifications to the M2 beamline elements. Nevertheless, the possibility of simultaneously installing and even operating two out of the three proposals could be of particular interest, provided that both beam momentum and intensity match across all experiments under consideration.

Several configurations have been studied with the aim to minimise installation changes and allow switching between setups within a time frame of weeks. Since removing the AMBER (former COMPASS) spectrometer would require major works, the baseline approach remains to remove parts of the existing spectrometer only if no other solution could be found. Two potential experimental locations were analysed: upstream of AMBER (starting from BEND6 in zone PPE211) and downstream of AMBER (replacing the existing hadron beam dump,with the option to extend the EHN2 hall if necessary).

The downstream option was found to be a natural choice for test beam or pilot runs, as short setups (up to 7 m) could be accommodated with minimal modifications to the AMBER spectrometer. The removal of the HI05 hodoscope would facilitate the test beam campaign for the AMBER TPC, required in preparation for the proton radius measurements, and a test setup for the MUonE proposal (see Section 4.3.3). Removing the downstream hadron absorber would free an additional 7.5 m, providing a total of 14.5 m of longitudinal space, see Fig. 28. For this mode of operation, M2 would need to be restricted to muon beams only as long as the final beam dump is not present. Additionally, this would require blocking the beamline absorbers at the end of the decay section (at $s = 700$ m) to remain in the

IN position and would require approval from radiation protection. The main drawback of this location is its limited space that, in addition, would not allow re-shaping of the beam using quadrupoles. This last constraint makes the downstream location incompatible with simultaneous operation of another experiment with a beam that is focused further upstream, e.g., at the AMBER target location. Extending the EHN2 hall further downstream could provide the required space for both, beamline elements and a downstream experimental area, but would require extensive civil engineering and infrastructure investments of a magnitude necessitating feasibility studies with SCE, EN-CV, SY-EPC and TE-MSC. Furthermore, the amount of material present in the AMBER spectrometer causes energy loss and scattering, resulting in a broader beam momentum distribution. Given the sensitivity of both the NA64μ and MUonE proposals, an additional spectrometer stage would be required to remeasure the incident beam momentum. This, in turn, necessitates additional space and the installation of one or more additional dipole magnets.

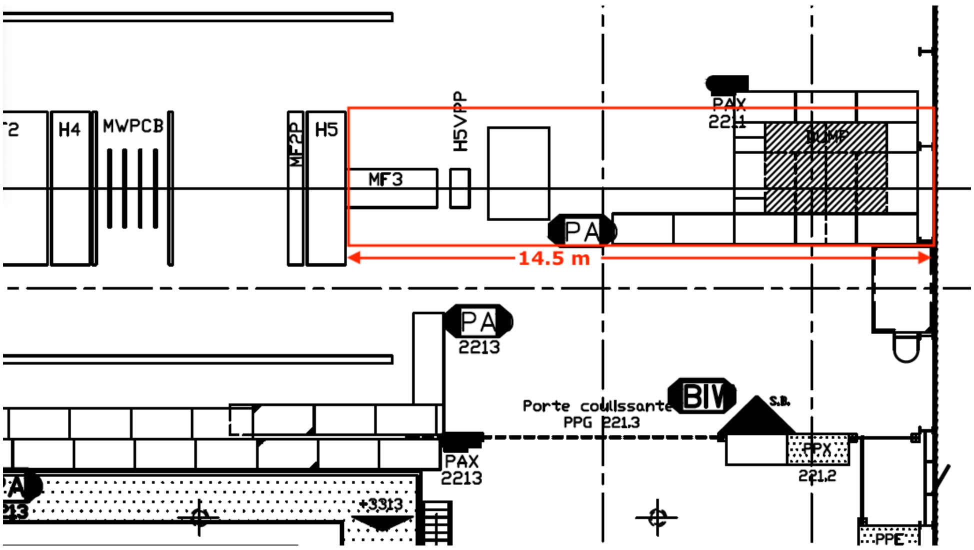

Fig. 28: Downstream option for test beam or demonstration run installation. Removal of the final beam dump would provide a longitudinal space of 14.5 m.

The upstream option, shown in Fig. 29, involves rearranging of the presently installed beamline elements. Removing the CEDAR detectors, which is a standard operation when switching from hadron to muon beams, would free about 15 m of space (left side of Fig. 29). In order to achieve the full 25 m required for NA64μ, a minor rearrangement would be required including removal of Quad34 (QPL 095/ QPL 097), shifting BEND7 (MBPH 101) upstream by 20 m to serve as the first spectrometer (MS1), and placing an additional MBPL of 140 mm aperture 3 m downstream as the second spectrometer (MS2).

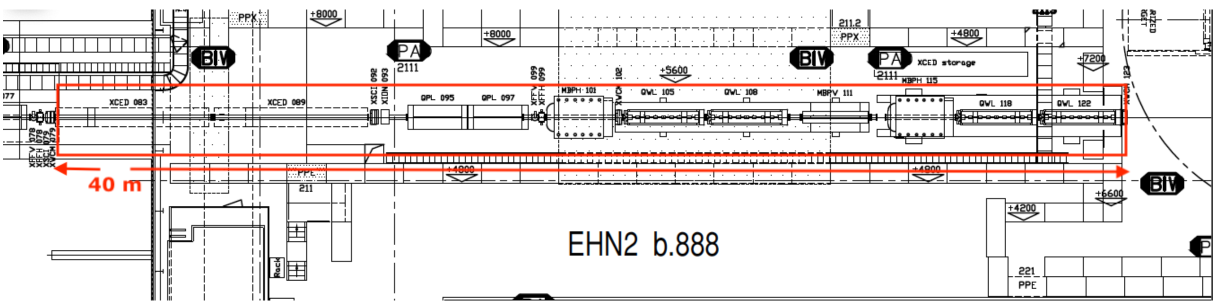

Fig. 29: Upstream option for installation of the final NA64μ and MUonE experiment. Rearranging presently installed beamline elements would provide up to 40 m of additional space.

During Long Shutdown 2, the beam area upstream of COMPASS (now AMBER) was prepared to accommodate (at different times) the test setups of NA64μ, MUonE and the AMBER TPC prototype. The current layout is shown in Fig. 30. Given the limited proposed data-taking period for NA64μ, rapid changeover is desirable. A common mechanical platform with pre-installed detectors significantly reduces installation and alignment duration from weeks to days.

A preliminary design and cost estimate for a platform that allows for a quick installation, possibly with auto-aligning fixation (plug-in), was completed by the BE-EA group, and the first stage has been installed. It includes a rail system for quick placement of MBPL magnets for NA64μ and the CEDAR detectors.

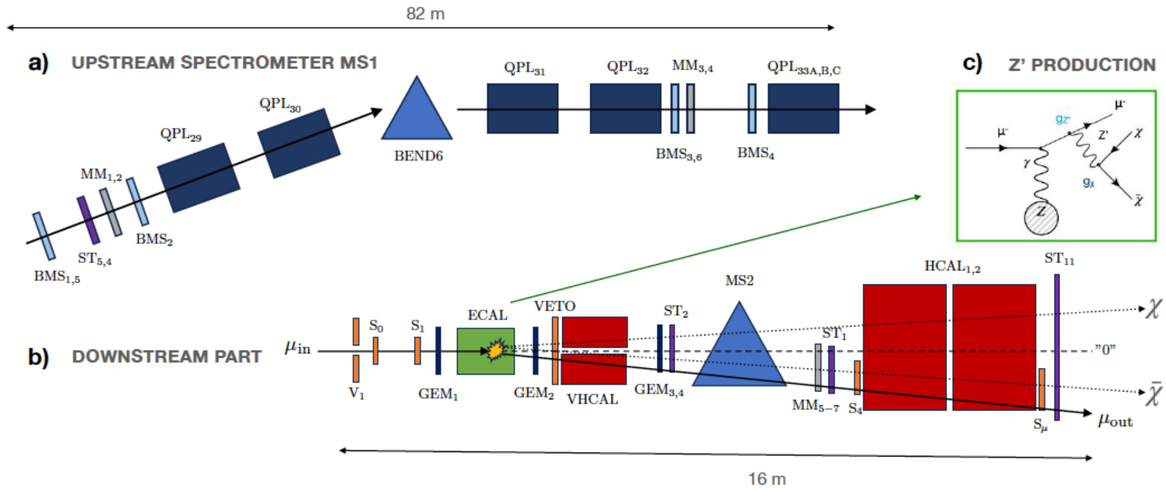

Fig. 30: The current layout of NA64μ. The beam enters from the left An additional MBPL magnet may be requested to be added for post-LS3 operation requiring close to 25 m.

An advantage of the upstream location for NA64μ would be the ability to use the existing beam momentum station (BMS) of AMBER near BEND6, which measures the beam momentum with a precision of about 1 % as part of MS1. The two MBPLs requested by NA64μ would function as spectrometer magnets to either cross-check or refine the BMS momentum measurement as part of MS1 and measure the momentum of the outgoing scattered muon as part of MS2. Since BEND7 is planned to be used as part of MS1, its existing power supply can be reused. For the MBPL requested as second spectrometer (MS2), the existing power supply from Quad34 can be repurposed. As the necessary infrastructure for the operation of these MBPLs is already in place nearby, only minor investments amounting to a few tens of kCHF are required to extend cables and cooling lines, plus some small installation expenses. NA64μ will utilise a downgraded version of the AMBER DAQ system, with an expected data rate of 40 MB s^{-1}. For Run 3, the experiment requested space for two DAQ racks near the setup, which could be accommodated, along with gas connections for tracking detectors operating with an Ar-CO_2 gas mixture.

The calculated optics for this upstream option, shown in Fig. 31, meets the requirements outlined in Section 4.3.1. While this optics configuration would preserve beam focusing at the AMBER target location, minor degradation in spot size or divergence is expected due to the material presence of the NA64μ HCAL. Results of simulations for a 160 GeV/c muon beam with halo are shown in Figs. 32–34. They show a Gaussian beam spot with $\sigma_x = 13$ mm and $\sigma_y = 22$ mm, a corresponding divergence of 0.23 mrad in both x and y, and a momentum spread of about 6 GeV/c.

For the installation of the full MUonE setup in the upstream location, up to 40 m of space must be made available. The calculated optics, shown in Fig. 35, meets the requirements detailed in Section 4.3.1. Making this space available requires removing the final focus quadrupoles, thereby excluding parallel operation with any other experiment downstream.

A drawback in the upstream location is that the material of the MUonE setup, including a 3 m iron

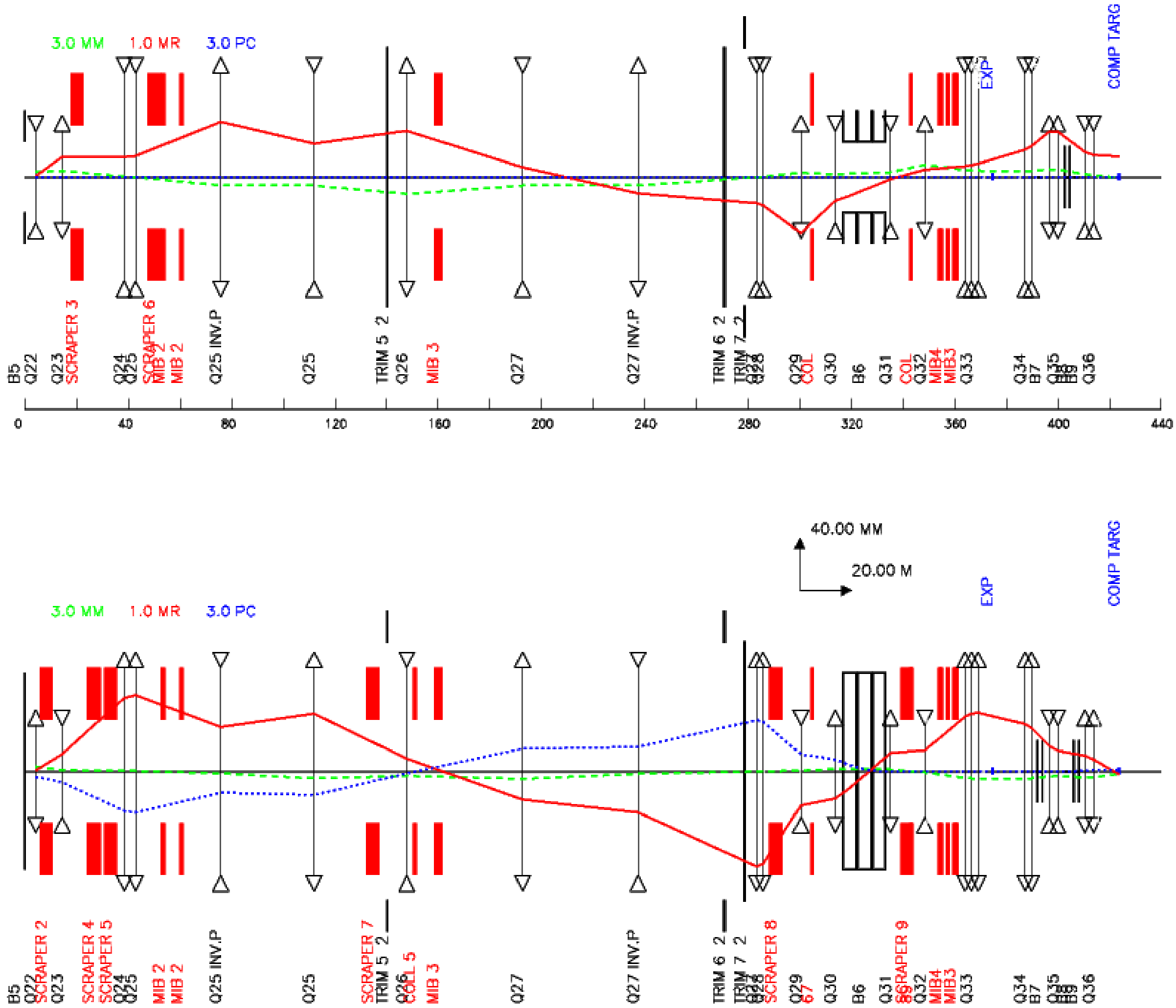

Fig. 31: Optics for NA64µ Phase 1 in the so-called upstream location. The notation follows B6 = BEND6, B7 = BEND7, Q34 = QUAD34 and so on.

block for muon identification and requiring a parallel beam, leads to a non-negligible growth of phase space due to multiple scattering. This cannot be mitigated with optics downstream. Figure 36 illustrates this phase space broadening effect caused by the MUonE material traversed by the beam. Mitigation strategies, including the selection of an optimal material for the muon ID, have been documented in the 2022 edition of this report [2].

As a data acquisition system, MUonE plans to use the baseline CMS upgrade solution with an acquisition rate of 40 MHz. The expected data flux is 0.5 TB s^{-1}, requiring around 10 computers, based on the experience and solutions of LHCb. The system will operate in a trigger-less mode. Given the required stability of the tracking detectors, a very precise alignment is essential, which could benefit from a single-platform support. Additionally, detector cooling will require either a dedicated gas or cooling water infrastructure.

4.3.3 2018 Beam Test

During the 2018 beam time, when COMPASS was the main user conducting a scheduled Drell–Yan physics run with a negative hadron beam, the MUonE Collaboration installed a small tracker setup in the

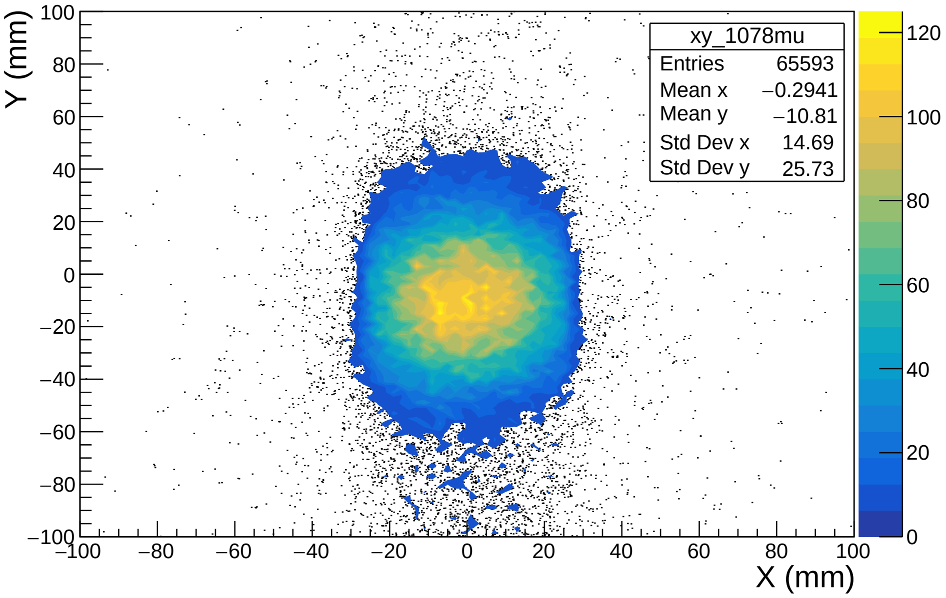

Fig. 32: Beam spot for NA64μ Phase 1 in the upstream location with $\sigma_x = 13$ mm and $\sigma_y = 22$ mm.

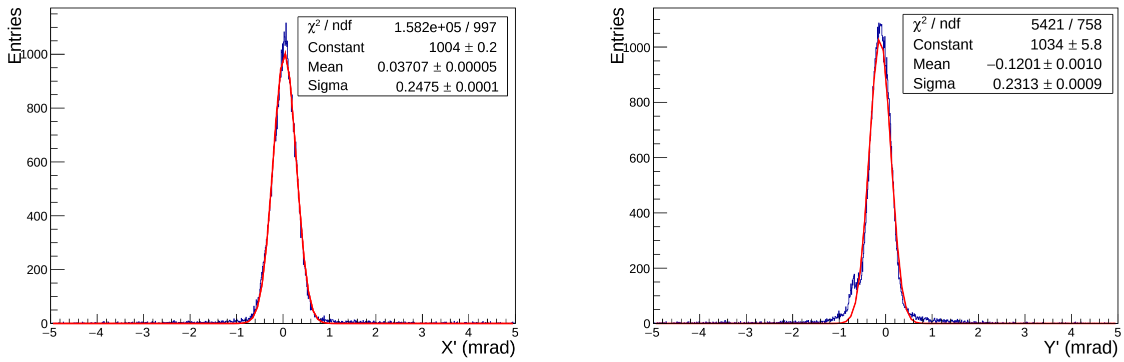

Fig. 33: Beam divergence for NA64μ Phase 1 in the upstream location with $\sigma_{x'} = 0.24$ mrad and $\sigma_{y'} = 0.23$ mrad.

downstream dump location for testing. Simulations were carried out to estimate the muon flux and beam characteristics at the test location, accounting for COMPASS optics and materials in the setup. The details of the simulation, along with their validation with data have been summarised and documented in the 2018 version of this report [1]. Results from the test beam and initial experimental conclusions have also been reported. They provide an invaluable benchmark for our simulations.

4.3.4 2021–2024 Beam Test and Data Taking

Between 2021 and 2024, all proponents successfully conducted pilot runs in the upstream location of EHN2 (PPE211), with NA64μ also acquiring its first physics data. The muon beams used for COMPASS data taking in 2021 and 2022 provided valuable opportunities for parasitic detector and components tests, exploiting valuable beam time during COMPASS target re-polarisation periods. To facilitate these tests, a trolley system was installed in PPE211, enabling rapid insertion of a small MUonE setup into the beamline, effectively adding about a week of extra test beam time to the tight M2 schedule. The downstream location also proved highly useful for parasitic detector tests. It was equipped with additional

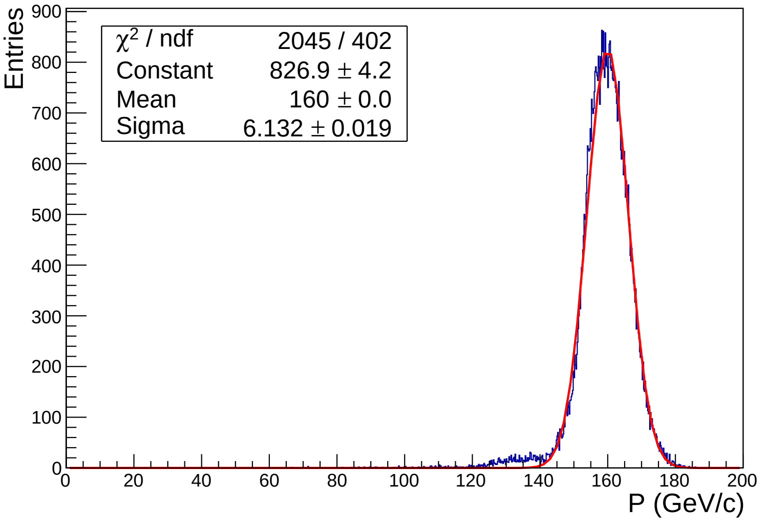

Fig. 34: Beam momentum distribution for NA64μ Phase 1 in the upstream location for a 160 GeV/c nominal beam momentum with $\sigma_p = 6\,\text{GeV}/c$.

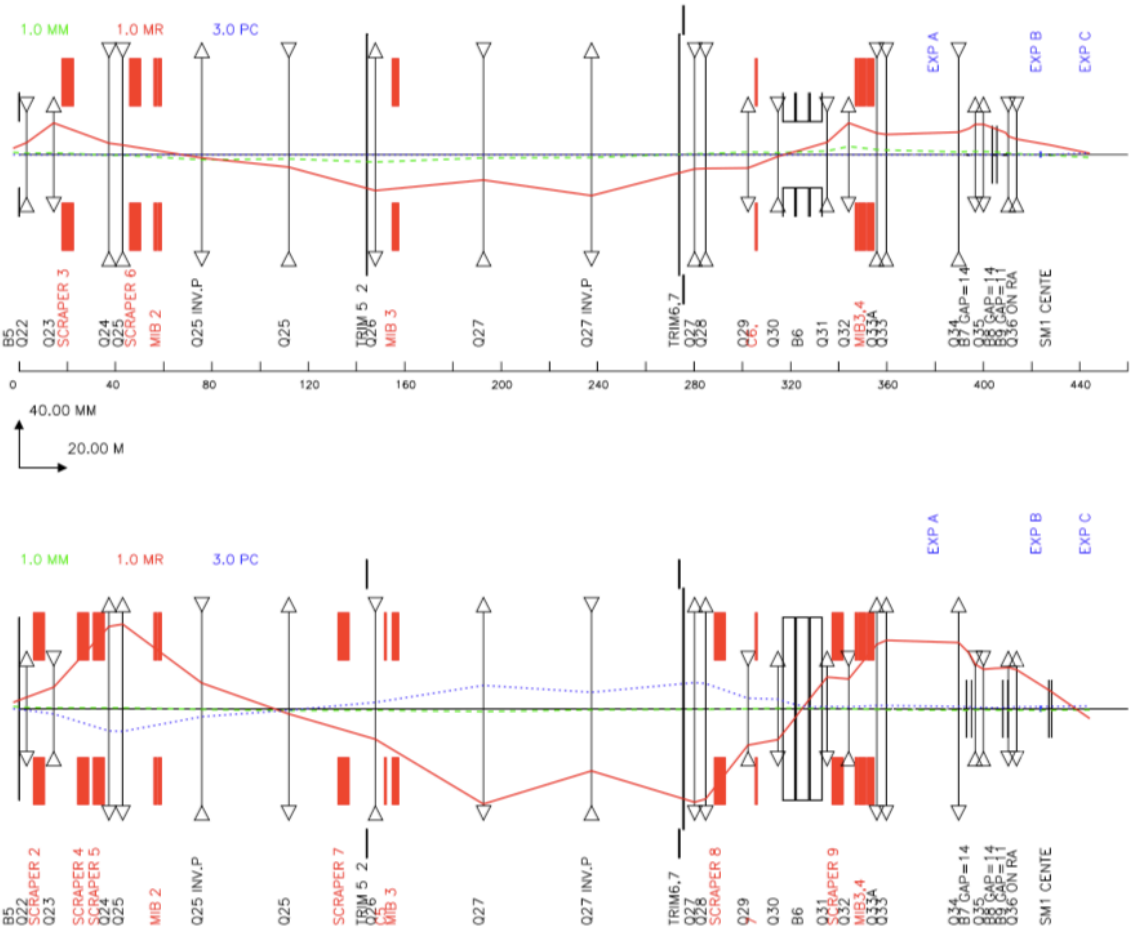

Fig. 35: Optics for MUonE in the upstream location. The notation follows B6 = BEND6, B7 = BEND7, Q34 = QUAD34 and so on.

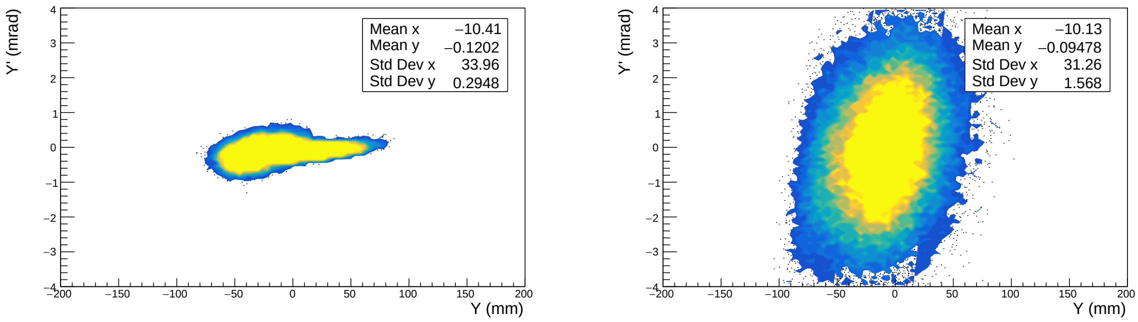

Fig. 36: Example of phase space change for the beam in y coordinate for MUonE in the upstream location: at the entrance (left) and after the experimental setup (right), accounting for tracker (Si + Be) and Muon ID (3 m of Fe) materials.

beam instrumentation and allowed for extended test periods using muon beams without interfering with data taking by upstream experiments.

AMBER took advantage of this setup to test their TPC using the muon beam parasitically during this period. Following the conclusion of the COMPASS experiment in 2022, all proponents utilised the 2023 and 2024 operation years for dedicated data taking or tests. AMBER collected physics data to measure the antiproton production cross-section with hadron beams and completed this part of their programme. Additionally, AMBER evaluated the performance of the particle identification with the CEDAR detectors, a critical component of their planned post-LS3 Drell–Yan programme. Details are provided in Section 4.4 for the hadron beams. NA64μ continued its physics data collection using the muon beam, accumulating a total of 3.2×10^{11} μ on target. Meanwhile, MUonE expanded its setup, testing two tracking stations and an electromagnetic calorimeter. To ensure setup stability and mitigate temperature variations, MUonE installed a tent around their setup. Additionally, the ventilation system of the CEDAR detectors was modified and integrated with the tent as shown in Fig. 37 to maintain a controlled temperature environment. The test beams were highly successful, providing input for the MUonE proposal, which was submitted to the SPSC at the end of 2024 [74].

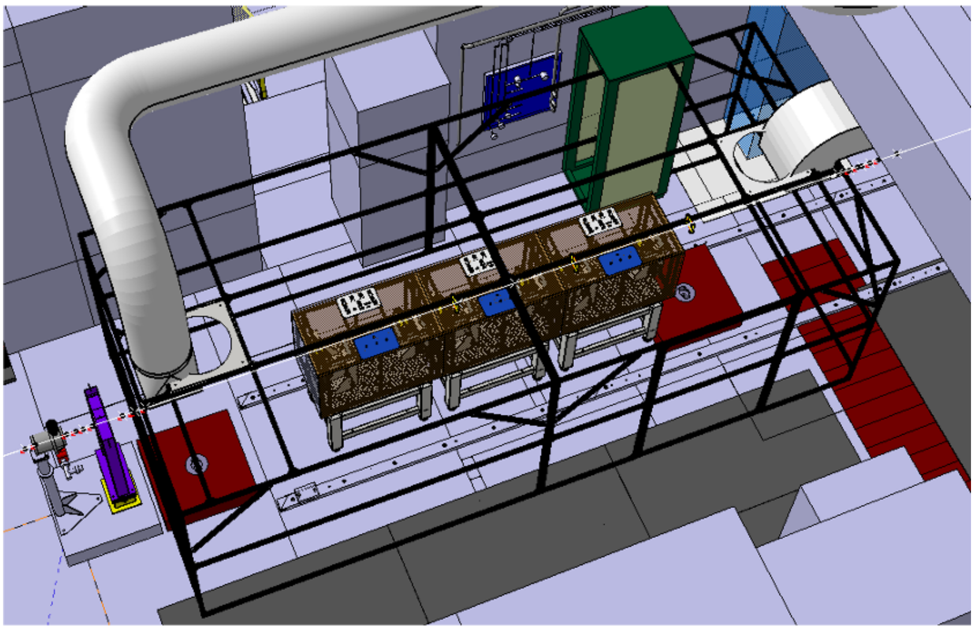

Fig. 37: MUonE cooling tent integrated with the CEDAR ventilation ducts.

4.3.5 Infrastructure Changes Post-LS3

Post-LS3, NA64μ has requested a semi-permanent location in the M2 beamline to minimise installation time and reduce the need for repeated alignment measurements. This would also help reduce systematic uncertainties associated with frequent installation and de-installation of the setup. Similarly, MUonE would benefit from a semi-permanent location for their 40 tracking stations, significantly reducing the time required to connect and disconnect the modules. As noted earlier, without removing any magnets downstream the CEDAR location, the available space is limited to 13 m. Removing these magnets would free up a total of 40 m. Nevertheless, these downstream magnets are essential to tune the beam for AMBER downstream. To address this challenge, an initial study performed by BE-EA explored a solution to accommodate NA64μ, MUonE and the necessary magnets on a transverse rail system. This system would indeed minimise changeover time between experiments and allow setups to be positioned as needed for scheduled beam runs while ensuring reproducible alignment with millimetre-level precision. Implementing this solution would require modifications to the tunnel, as summarised in Figs. 38 and 39. The preliminary cost estimate for these infrastructure changes is around 700 kCHF. Further studies are underway to finalise the design, with a potential installation timeline aligned with LS3.

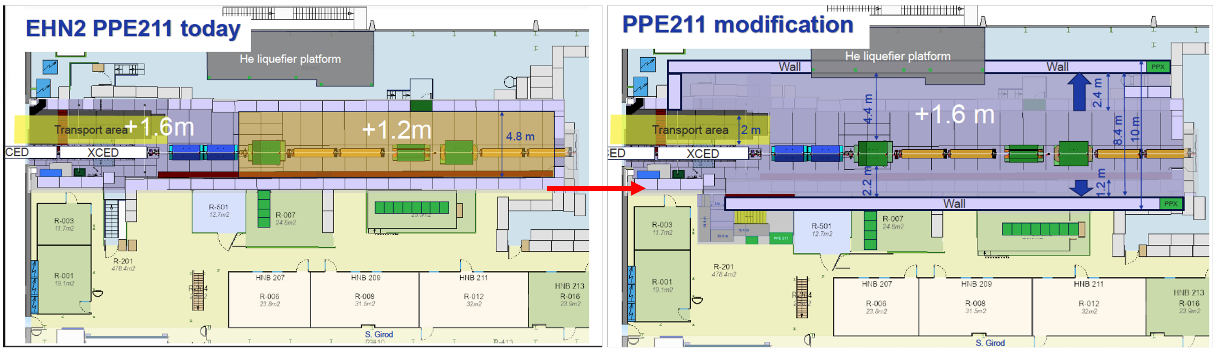

Fig. 38: A first proposal for modifying the PPE211 area (current CEDAR location) to accommodate NA64μ, MUonE and the required magnets for AMBER beam.

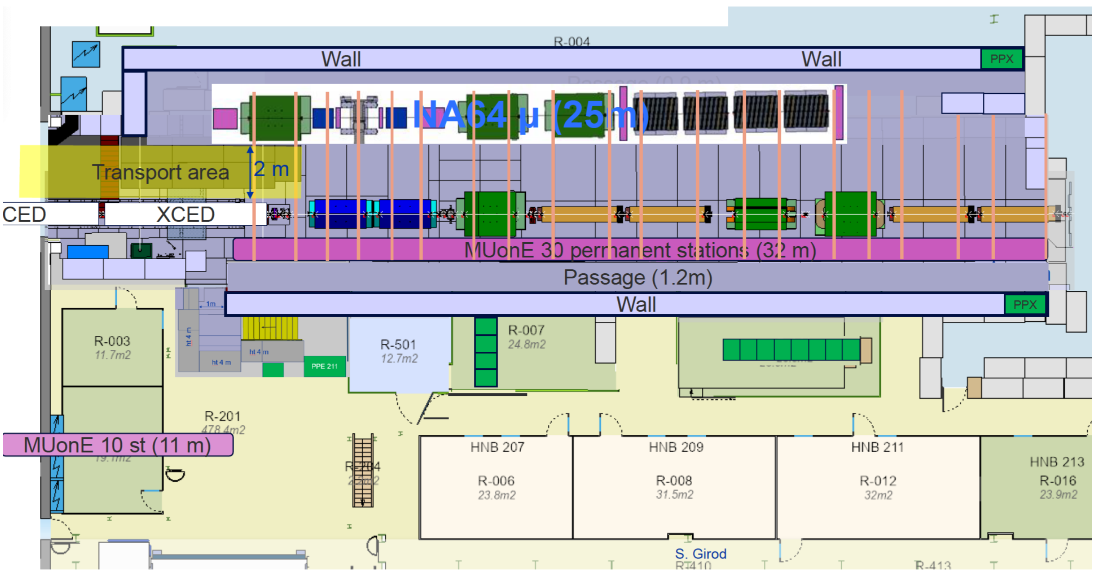

Fig. 39: A first proposal for the modified tunnel layout, including NA64μ, MUonE and magnets needed for AMBER beam on a rail system to allow flexible and rapid transitions between setups.

4.3.6 High Intensity Muon Beam Post-LS3

The M2 beamline currently delivers a maximum muon beam rate of 2×10^8 μ per 4.8 s spill. This rate is limited by the environmental radiation monitor, SMS823, located downstream of the EHN2 building, as shown in Fig. 40. To assess the feasibility of increasing the muon beam rate in M2, as requested by MUonE for post-LS3 operation, a test was conducted in collaboration with HSE-RP during the 2024 operation. The test involved deflecting the beam downward by 5 mrad using the final vertical bending magnet, BEND8, in the M2 beamline. Radiation levels at the environmental monitors were then measured to determine the radiation impact of this deflection. The results showed that deflecting the beam downward reduced the measured radiation dose downstream by nearly a factor of three. The measured dose levels at the monitor during deflection downward were at the background noise level of the monitor. The findings, summarised in Ref. [75], demonstrate the potential to increase the muon beam intensity in M2 by mitigating radiation constraints through downward beam deflection after MUonE. Following this successful test, further studies are planned to optimise beam transmission in M2, and determine the optimal positioning of the final downward deflection magnet to ensure efficient beam steering for the MUonE physics run.

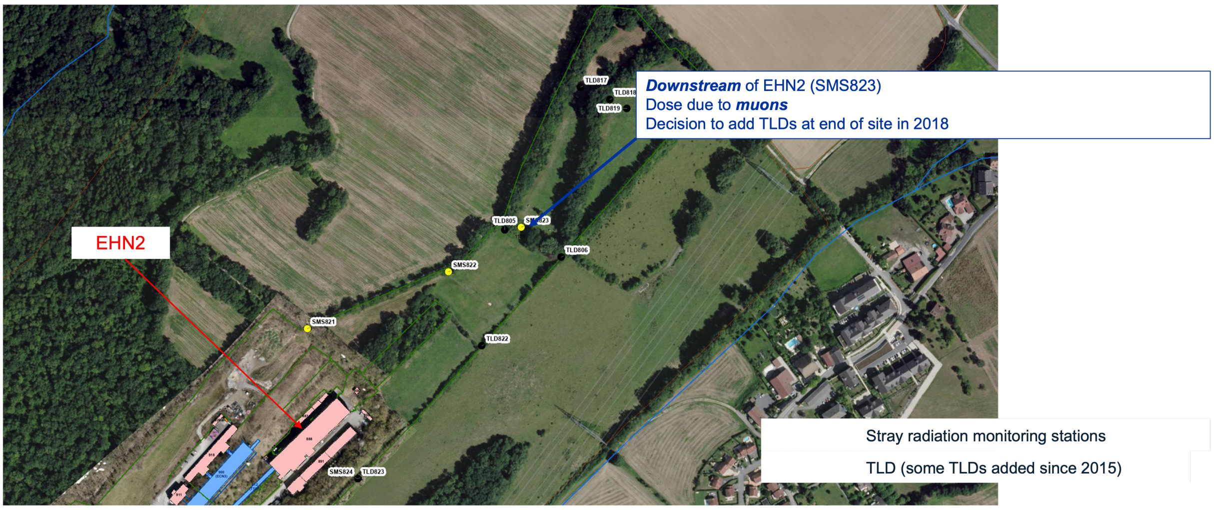

Fig. 40: Location of the environmental radiation monitor SMS823 downstream of the EHN2 building.

4.4 Hadron and Electron Beams

4.4.1 Experiment Requests

Dark Matter Searches at AMBER

The AMBER proposal includes a measurement of antimatter production cross-sections, in particular antiproton production, to provide input for Dark Matter Searches conducted by AMS and other experiments. The proponents request the standard M2 hadron beam, as used in 2008 and 2009, at intensities of 5×10^5 hadrons/s over a momentum range of 20 to 280 GeV/c. The focused beam shall have a divergence of less than 1 mrad in both planes, with a beam spot radius of less than 1 cm.

During the 2023 and 2024 runs, AMBER successfully completed its antiproton production cross-section measurement programme using the standard hadron beam at various momenta, and data analysis is ongoing.

Pion- and Kaon-Induced Drell–Yan Measurements at AMBER

The measurement of pion and kaon Parton Distribution Functions (PDFs) via the Drell–Yan process on nuclear targets is proposed with positive and negative pion and kaon beams of 190 GeV/c. The proponents request beam intensities exceeding 7×10^7 hadrons/s. The focused beam shall have a divergence of less than 1 mrad in both planes with a beam spot radius of less than 2 cm. To ensure identification of the pion and kaon components or to account for potential beam contamination, the use of CEDAR or threshold Cherenkov detectors capable of handling high intensities is required. Performant kaon identification is a prerequisite for this programme to be successful. Alternatively, we considered ways to enrich the beam in either kaon or antiproton content. This would not only ease the kaon or antiproton identification, but also reduce the impact of radiation constraints that limit the full beam intensity on the kaon or antiproton flux. Several methods for kaon or antiproton enrichment were looked at, but in the end only the RF-separation technique was retained as an option to be studied in detail.

Prompt-Photon Measurements at AMBER with Conventional Pion Beams

The measurement of Gluon Parton Distribution Functions (GPDs) in mesons via the production of prompt photons is proposed using positive and negative pion beams of 190 GeV/c. The proponents request beam intensities of 5×10^6 hadrons/s. The focused beam shall have a divergence of less than 1 mrad in both planes with a beam spot radius of no more than 1 cm. As for the Drell–Yan measurements, identification of the pion component or mitigation of beam contamination shall be achieved using CEDAR or threshold Cherenkov detectors.

Hadron Spectroscopy with Low-Energy Antiproton Beams at AMBER

In the first phase of the PBC study, there was a proposal for antiproton-induced spectroscopy at AMBER, and in particular the measurement of heavy quark exotica, using low momentum antiproton beams in the range of 12 to 20 GeV/c. At sufficiently low beam momenta, pions and kaons in the beam would mostly decay before reaching the experiment. As a result, the beam at the experiment would be highly enriched in antiprotons, which are stable. Since then, the experiment has not pursued this proposal, and at the time of the present CBWG report update, there no longer seems to be a requirement for a low-momentum hadron beam in M2. More details on studies of the PBC CBWG concerning such beams can be found in the 2022 edition of this report [2].

4.4.2 Electron Beams

A low-intensity tertiary electron beam is currently used for calibration purposes for the experiments. This electron beam is derived from a 5 mm thick secondary lead target, where due to bremsstrahlung, a spectrum of lower energy tertiary electrons or positrons is produced. The part of the beamline downstream of this secondary target is set to the required electron or positron momentum and from there the tertiary electron beam is transported to the experiment. Almost all of the hadrons traverse the target without interaction and just undergo multiple Coulomb scattering. The electron beam intensity, typically a few 10^4 electrons per spill, is primarily determined by two factors: the lack of continuous vacuum along the beamline, which causes losses due to bremsstrahlung in the air (corresponding to about one-third of a radiation length), and multiple Coulomb scattering. The bremsstrahlung in the air close to the experiments leads also to a long tail on the lower side of the energy spectrum. Upgrades to the vacuum system, as outlined in Section 4.6, will enhance electron beam intensity and quality significantly.

A secondary electron beam directly from the T6 target would be highly contaminated by hadrons, due to the particle production process. At around 100 GeV, the electron fraction in the beam is only $\mathcal{O}(10\,\%)$. At very high energies, electrons loose energy due to synchrotron radiation, mainly in the strong bends. Hadrons do not suffer energy loss and therefore the hadron and electron trajectories separate and the hadrons can be collimated away. The M2 tunnel has only relatively small angles and therefore this technique is not very efficient. Moreover, this separation between hadrons and electrons becomes sufficient only well above 150 GeV, whereas the requests from COMPASS and AMBER have so far been for energies below 50 GeV.

4.5 RF-separated Hadron Beams

4.5.1 Principle of RF-separated Beams and Initial Study

At low momenta, pions and kaons mostly decay over the length of the beam from the T6 target to the AMBER experiment (1138 m). At higher momenta the natural enrichment of antiprotons through particle decays along a beamline is negligible due to the increased decay lengths of the particles in the laboratory frame. The AMBER proposal [13] requires an increased fraction of kaons or positive pions in the beam, depending on the specific measurement to be performed. Naturally, for a 100 GeV/c negative beam as an example, the kaon content of the beam at production is about 6.2 %, which reduces to 1.75 % at the AMBER experiment. Several methods exist for enriching the content of a wanted particle species in the beam, usually by suppression of unwanted particles. Electrostatic separators are ineffective at beam energies beyond a few GeV due to their $1/p^3$ dependence [76]. While, in principle, an enrichment by differential absorption could be a possibility, its very low efficiency, high losses, and small suppression factors for unwanted particles make it an impractical solution. The only remaining option for high-momentum beams could be RF-separation.

The method of RF-separation was first employed at CERN in the 1960s based on the ideas of Panofsky and Schnell, as for instance described in Ref. [77]. RF-separation exploits the velocity differences between particle species in a beam with well-defined momentum. As illustrated in Fig. 41, two dipole RF cavities (RF1 and RF2), operating at frequency f, are placed at a fixed distance L apart. Depending on the phase difference between the two cavities, the transverse kick delivered by RF1 is either amplified or cancelled by RF2, effectively steering different particle species along separate paths.

For two species i and j with masses m_i and velocities β_i, the phase difference is given by

$$\Delta\Phi = \frac{2\pi L f}{c}\left(\frac{1}{\beta_1} - \frac{1}{\beta_2}\right).$$

In the limit of large momenta, this can be approximated in terms of mass difference

$$\Delta\Phi \approx \frac{2\pi L f}{c}\frac{m_1^2 - m_2^2}{2p^2}.$$

For a kaon-enriched beam, the phase difference can be set to $\Delta\Phi_{\pi\mathrm{p}} = 2\pi$, which results in $\Delta\Phi_{\pi\mathrm{K}} = 94^\circ$, ensuring that for both protons and pions, the kick from RF1 is exactly cancelled by RF2 and these particles are absorbed in the beam stopper. The kaons, however, receive a nearly maximum transverse kick and mostly bypass the stopper. For an antiproton beam, the phase difference could be optimally set to $\Delta\Phi_{\bar{\mathrm{p}}\pi} = \pi$, leading to $\Delta\Phi_{\bar{\mathrm{p}}\mathrm{K}} = 133^\circ$ and $\Delta\Phi_{\bar{\mathrm{p}}\mathrm{e}} = 184^\circ$. In this case, the antiprotons would receive an acceptable deflection while kaons and pions would be dumped effectively.

Electrons, which are also a non-negligible fraction of the beam, can be removed by placing a degrader, e.g., a lead sheet of 5 to 10 mm thickness, at an intermediate focus in the beamline. Electrons would loose a significant amount of momentum due to bremsstrahlung and no longer be transportable to the experiment. Hadrons mostly traverse the degrader without interacting and continue their way.

Based on a study by J. Doornbos at TRIUMF for CKM, we assume an RF cavity frequency of $f = 3.9$ GHz and a transverse momentum kick of $\Delta p_\mathrm{T} = 15$ MeV/c per 3 m long cavity. Such a design is used for instance for the ILC crab cavities [78]. Given the 1.1 km length of the M2 beamline, the distance L between cavities is constrained. Under these conditions, the maximum achievable momentum for an RF-separated kaon beam is 75 GeV/c, while an RF-separated antiproton beam could reach 108 GeV/c. A realistic beamline design must include a section for momentum selection, a section to align the beam with the RF cavities and space for dispersion recombination, final focusing and beam particle identification. All these dedicated beam sections reduce the total available length between RF cavities accordingly.

Since the phase difference scales quadratically with momentum, efficient separation is only feasible within a narrow momentum band beam. The beam momentum spread $\Delta p/p$ must be limited to about

1 %, in order to limit the phase shift of $\Delta\Phi_f = \Delta\Phi_1(1 - 2\Delta p/p)$ which would otherwise reduce the separation efficiency.

As an example, using the given acceptance values and the maximum target efficiency of 40 % for the 500 mm T6 target, a calculation was performed for the case of a 100 GeV/c antiproton beam. Assuming that 80 % of the antiprotons would bypass the beam stopper and an optimisation of the solid angle to 10πμsr could be achieved, one would expect about 8×10^7 antiprotons in EHN2 per 10^{13} incident protons at the T6 target. Due to the current radiation protection limit for EHN2 of 10^8 particles per 4.8 s spill for experimental setups without a hadron absorber, the actual limit would depend on the achieved beam purity. Assuming a 50 % purity, up to 5×10^7 antiprotons per spill could be delivered.

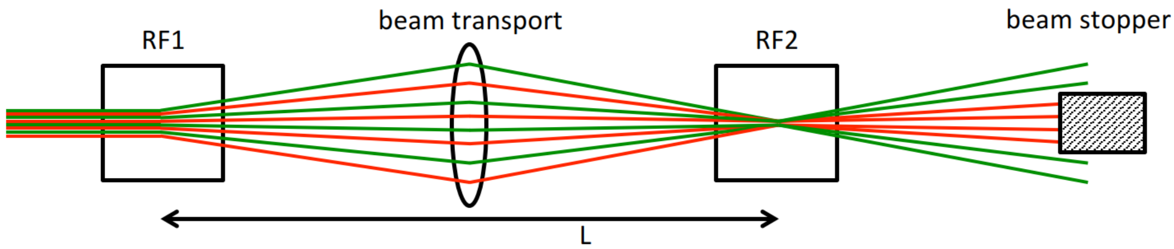

Fig. 41: Panofsky-Schnell method [77] for RF-separated beams. Unwanted particles (red) are stopped by a beam stopper, while the desired particles (green) receive a net deflection from the combined effect of the RF1 and RF2 dipole RF cavities out of the central axis.

4.5.2 Quantitative Studies and Feasibility Assessment

Following discussions at the Plenary PBC workshop 2021 [8], more detailed studies of RF-separated beam were initiated. In parallel, a feasibility study was conducted for a potential RF-separated kaon beam for HIKE at 75 GeV/c [79]. Preliminary results indicated that the very high intensities required for HIKE Phase 1 (named NA62x4 at the time) are well out of reach. Still, the significantly lower intensity requirements of AMBER could make an RF-separated beam a plausible option. A kick-off workshop for this study was held in September 2021 to coordinate efforts and define future steps [80], which was followed up with a second workshop in 2022 [81].

4.5.3 Optics and Beamline Design

One of the key challenges in the design of the RF-separated beam is integrating the new layout within the already existing M2 tunnel. The tunnel features multiple slope changes, where vertical dipoles introduce deflection and dispersion which must be controlled. Another constraint is the front-end section, which currently consists of six high-gradient quadrupoles (see Fig. 42). These quadrupoles provide the high angular acceptance required for the RF-separated beam but are located in TCC2, in close proximity to both the T6 target and the two Target Attenuators (TAX), where the hadron beam is pre-collimated and the primary protons are dumped. Due to the very high residual radiation levels in this region, long installation times are not possible and this particular section should remain in its present configuration.

As the angles in the tunnel are mostly quite small, the corresponding bending magnets are relatively weak. While this is helpful for enabling large momentum acceptance and thus achieving highest muon fluxes in the muon mode, these small angles restrict the formation of large dispersion regions in the beamline section that could be exploited for precise momentum selection for hadron beams. To address this, the new design incorporates a new vertical so-called achromat, consisting of 4 bending magnets, as illustrated in Fig. 42. The first vertical dipole magnet in this achromat, BV1, introduces a vertical deflection angle of 22.5 mrad, followed by a field lens (Q9), which is necessary to compensate for the dispersion at the end of the achromat. The beam is then further deflected by BV2 before passing through a

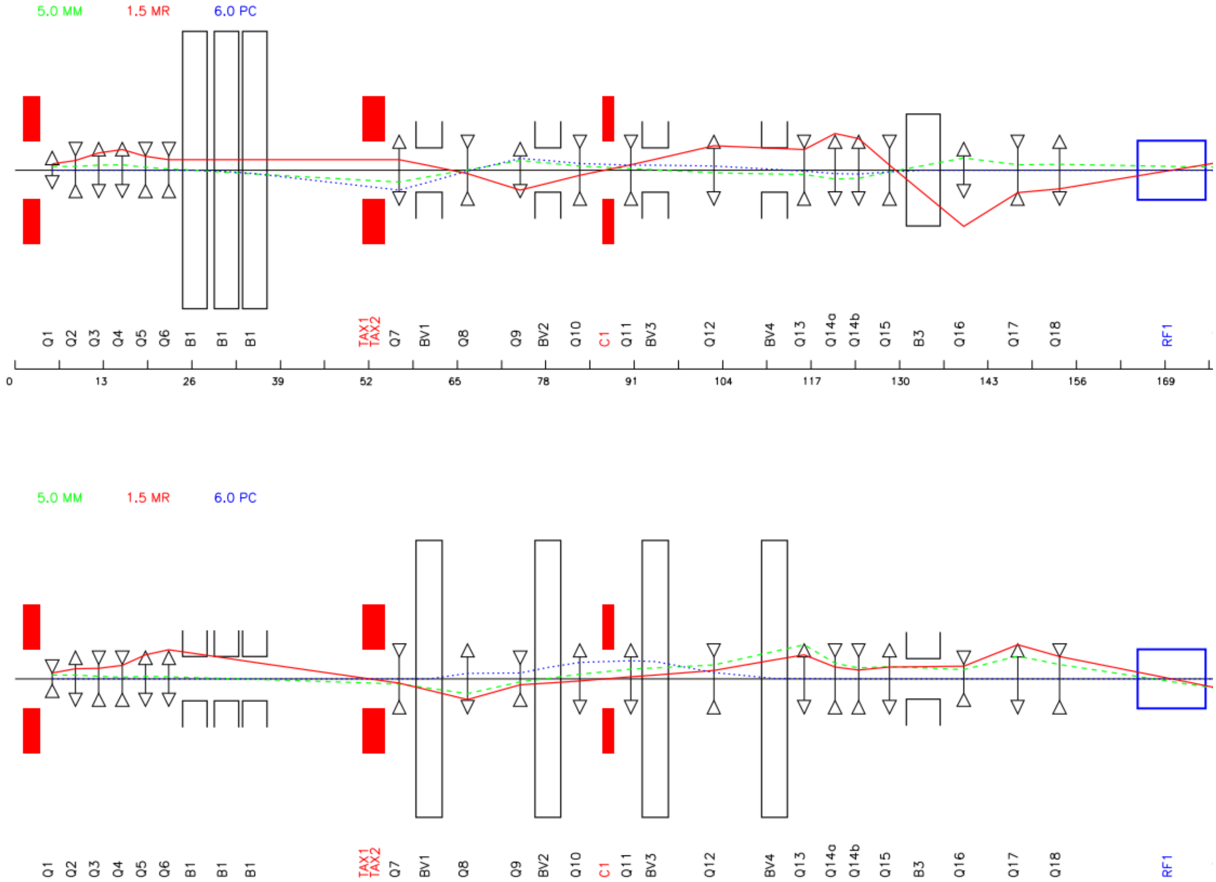

Fig. 42: Preliminary front-end optics up to the first RF cavity (RF1) for an RF-separated beam.

momentum slit (C1), after which the dispersion is re-matched using another field lens (Q8) and additional vertical bending magnets BV3 and BV4. The next steps were focused on the integration of the two RF cavities, with the goal of determining the expected beam spot size at these locations. This information is necessary to provide the required parameters of the RF cavities and the corresponding RF frequency, which in turn defines, together with the distance between RF1 and RF2, the maximum momentum possible.

After the first set of cavities, RF1, a quadrupole triplet is used to match the beam into a long FODO section for transport towards RF2. Due to the changes in the vertical tunnel slopes, the presence of two vertical bending magnets, BEND4 and BEND5, is necessary in between. The vertical dispersion that arises due to BEND4 is fully recombined in BEND5, ensuring a well-defined trajectory for all beam particles. The beam is then properly shaped on RF2, which is followed after some lever arm by a beam dump for unwanted particles. Following this section, the bending magnets BEND6 and BEND8 level the beam and make it dispersion-free. A final beam section accommodates the kaon particle identification which may involve the two CEDAR detectors. Finally, a quadrupole quadruplet is used to focus the beam in both, the horizontal and vertical, planes onto the experimental target.

4.5.4 RF System Requirements

From this layout and optics design we can determine the RF system requirements. It is evident that only superconducting cavities will will be able to sustain the slow extraction and the corresponding long spill duration, over which the system must be powered. Given the results of the initial study, frequencies in the range of 4 to 10 GHz seemed to be favourable. Following discussions with RF experts at CERN and at the Cockcroft Institute, an RF frequency of 3.9 GHz, or potentially 5.2 GHz, has been identified as a reasonable compromise between performance, feasibility and cost. The cavity iris could have a diameter of about 30 mm, with a kick strength of $\mathcal{O}(5\,\mathrm{GeV\,m^{-1}})$. The large duty cycle of the slow-extracted beams in the North Area imposes constraints on these parameters. For the final studied design we opted for 3.9 GHz cavities, which are the common industry standard.

4.5.5 Integration

As an initial step, the existing 2D layout of the M2 tunnel has been converted into a 3D model that includes the tunnel geometry. Once the complete design of the RF-separated beam was available, all beamline elements were incorporated into the model, allowing for a comprehensive assessment of service requirements and potential civil engineering modifications.

4.5.6 Review of the Completed RF-separated Beam Studies

The completed studies on RF-separated beams for the M2 beamline have been published as comprehensive reports in Refs. [82, 83]. The beam optics through the RF cavities has been optimised for highest transmission and separation of the particle species. Given the relatively small aperture size of the cavities compared to typical beam sizes, an initial approach focused on beam optics with a strongly focused beam. In this configuration, the R_{12} and R_{34} terms of the R matrix were set to zero, ensuring that the initial beam divergence in the x and y plane does not contribute to the beam size at the RF cavity location. Since beam emittance is conserved, the resulting phase space ellipse in this configuration is compressed in x and expanded in x'. This ensures maximal transmission of the beam through the cavities. This setup has the disadvantage that the relative kick from the cavity is small compared to the large beam divergence, resulting in suboptimal separation of the desired and the unwanted particle species.

As shown in Fig. 43, the best separation is achieved having a parallel beam configuration (blue curve), where a large R_{12} value results in an almost parallel beam. This setup ensures that separation is primarily influenced by the beam momentum spread, limited to 1 %. Unfortunately, this option comes at the cost of having a very low absolute rate of kaons. A compromise was therefore made between the beam size and divergence, as illustrated by the black curve in Fig. 43, where the beam optics was tuned to $R_{12} = 7.5\,\mathrm{m\,rad^{-1}}$. This value was chosen because of the cavity's iris radius of 15 mm and the 2 mrad horizontal acceptance of the M2 front-end. This configuration ensures that a particle at the edge of the angular acceptance of the beamline can still be transported through the cavity. While this setup is less effective in terms of angular separation compared to the fully parallel option, it provides better transmission. Interestingly, for cases requiring the highest purity, a larger beam should be considered, as the intensity remains constant even with a wider beam dump. The separation achieved with the $R_{12} = 7.5\,\mathrm{m\,rad^{-1}}$ configuration is shown in Fig. 44.

The intrinsic divergence of the mixed hadron beam results in smearing, affecting the particle separation, as shown in Fig. 44, and leading to potential losses of desired particles at the beam dump due to insufficient deflection. This effect is further amplified by the non-zero momentum spread of the beam. Any deviation from the nominal momentum causes phase mismatches, which in turn smear the angular distribution after the beam passes through the RF-separator. To effectively separate the different particle species, the difference in their angular divergence must be converted into a spatial separation. This is achieved by allowing the particles to drift freely after exiting R. In the final layout a 20 m drift length has been implemented. Maximising this drift length is essential to reach the best separation, while also ensuring that the beam remains clear of the yoke of the quadrupole aperture that refocuses the now separated beam onto the optical axis. The phase space distributions after the drift for kaons as the desired and pions as the unwanted species are shown in Fig. 45. Since antiprotons follow a similar phase space distribution as pions, their behaviour is expected to be identical in this context.

The current configuration yields a kaon intensity of approximately 3×10^6 per spill with a purity of 20 %. Following discussions with the AMBER Collaboration, it has been confirmed that while these

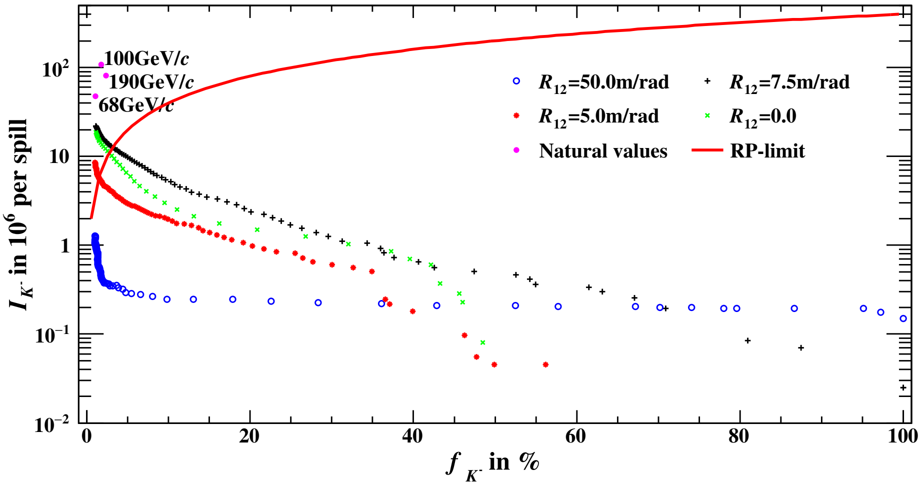

Fig. 43: Kaon intensity as a function of the kaon fraction in the beam for different beam optics. The solid red line represents the maximum kaon intensity allowed in EHN2 by radio-protection. The purple dots indicate the theoretical number of kaons that could reach the hall if only decay processes were considered. From Refs. [82–84]; modified.

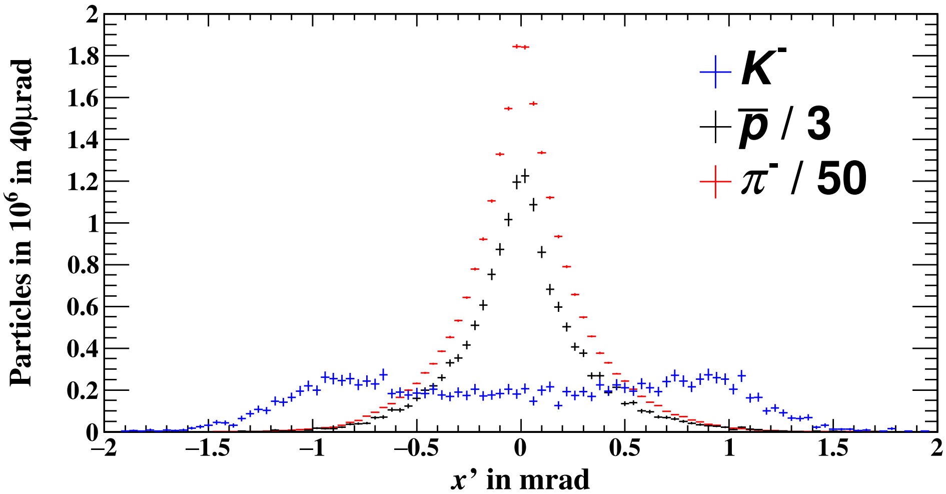

Fig. 44: Angular distribution of the mixed negative hadron beam after passing through the RF-separator. The pion and antiproton intensities are scaled. From Refs. [82–84]; modified.

results are promising for certain parts of their programme, such as kaon spectroscopy runs, the intensity achieved with RF-separation remains largely insufficient for the envisaged Drell–Yan measurements. Considering the significant investment that would be needed to establish an RF-separated beam, the gain in kaon yield and purity compared to the conventional hadron beam used so far is negligible.

As discussed in Section 4.6, a more effective approach to enriching the identifiable kaon sample can be achieved by completing the vacuum along the beamline, optimising beam optics accordingly and modifying the collimation scheme. While the total kaon abundance in the beam remains unchanged from previous runs, these improvements will significantly enhance the fraction of identifiable kaons at AMBER. The investment required to achieve full vacuum is minimal compared to the cost of implementing

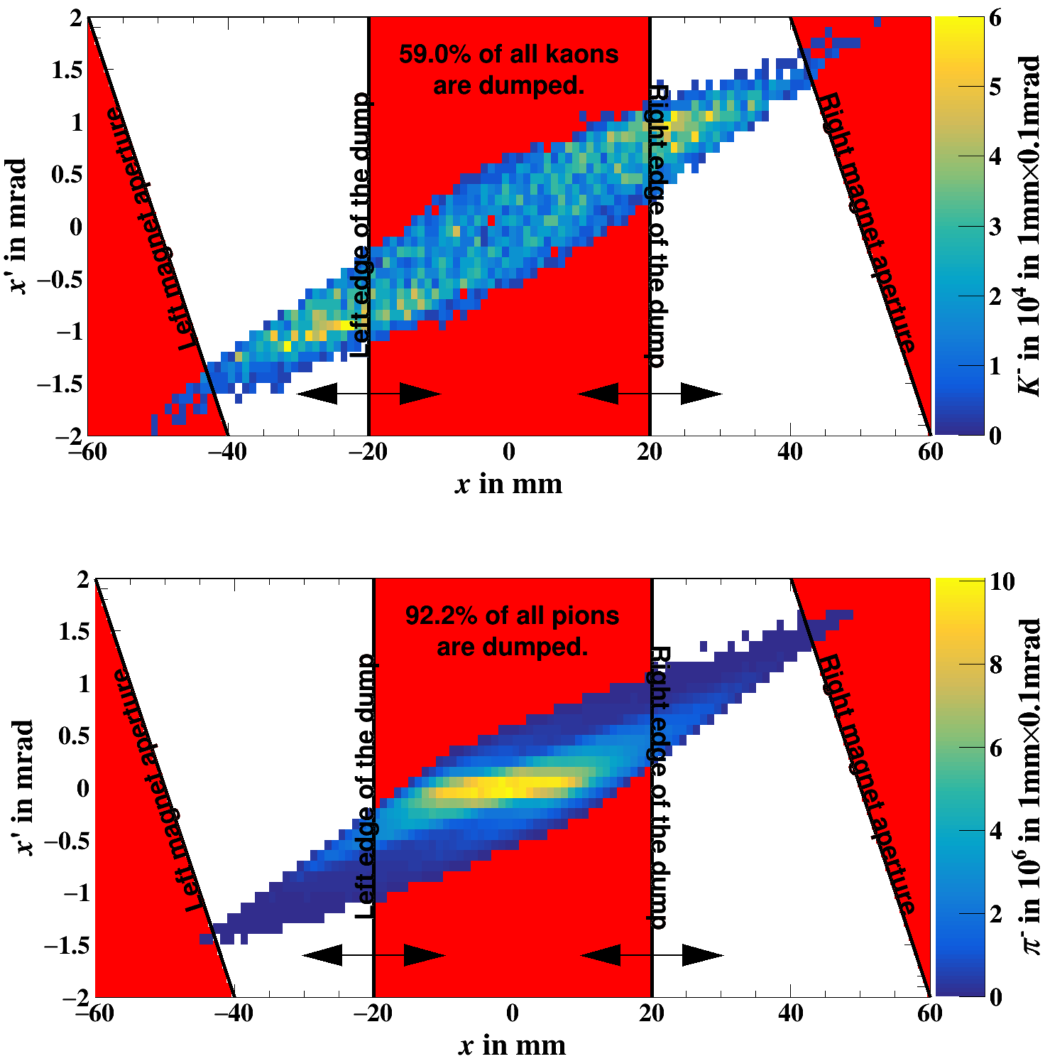

Fig. 45: In the top plot, the phase-space distribution of kaons after the drift is shown, while on the bottom, the corresponding distribution for pions is presented [82–84]. The beam dump, as indicated, would remove approximately 95 % of the unwanted pions and antiprotons, while allowing around 40 % of the desired kaons to bypass it.

RF-separation. Consequently, the decision has been made to stop the RF-separated beam studies at this point and pursue studies for improvements to the conventional beamline instead.

4.6 Upgrades for Conventional Hadron and Electron Beams

In previous Drell–Yan runs, the COMPASS Collaboration focused primarily on the pion component of the hadron beam. Since the pion fraction is significantly higher than the kaon component, the particle identification efficiency with the CEDAR detectors was sufficient. With kaon beams, it is crucial to maximise the particle tagging efficiency in order to minimise losses in the accepted kaon intensity. The CEDAR performance is highly sensitive to beam divergence at its location. In the current M2 beamline configuration there are a large number of long sections in air. These sections at atmospheric pressure sum up to about 100 m of air, including nine 5 m long magnetic collimator (Scraper) sections that are not under vacuum. The multiple scattering in air increases beam emittance and divergence, which cannot be mitigated by beam optics. Since the CEDAR detectors are positioned only 40 m upstream of the experiment, strong collimation in the CEDAR region is not a viable solution, as it would increase background levels at the experiment. The beam divergences in the horizontal and vertical planes as measured during the 2018 COMPASS Drell–Yan run are shown in Fig. 46, along with a comparison to a fully vacuum-sealed beamline configuration. To ensure efficient particle identification, the combined divergence in both planes must be limited to 60 µrad, which corresponds to the approximate angular separation of the Cerenkov rings produced by kaons and pions. As shown in Fig. 46, completing the vacuum system does not significantly alter the standard deviation of the divergence distributions, but the beam rate increases by 20 % for the same number of protons on the T6 target. Additionally, the peak in the divergence distribution is 35 % higher, implying that the number of kaons within the 60 µrad window increases by 50 %.

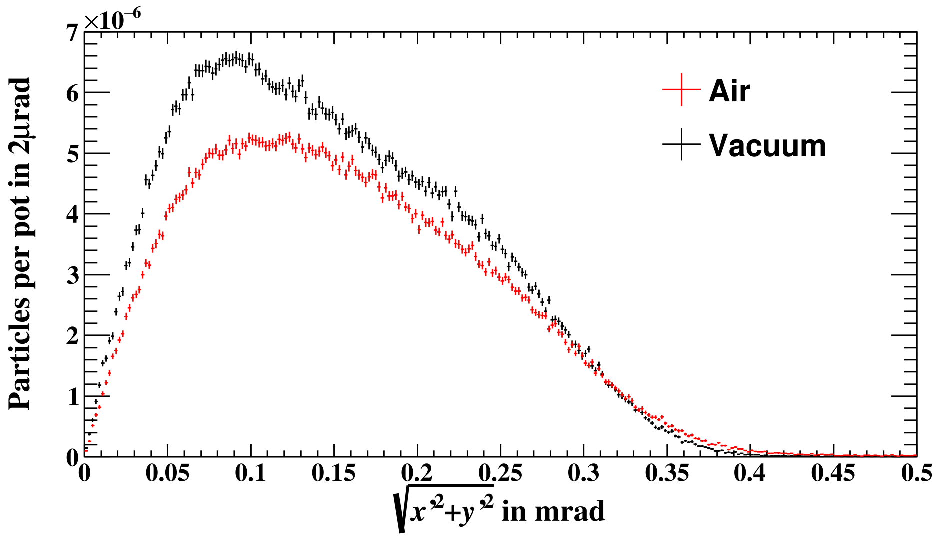

Fig. 46: Beam divergence for the optics used for the 2018 COMPASS run, compared to a fully vacuum-integrated beamline. The fully vacuum-sealed setup increases the beam rate by 20 % compared to the 2018 configuration from [84].

With continuous vacuum, collimation along along the beamline can be further improved. Continuous beam vacuum minimises multiple scattering which in turn improves angle and position correlations between the collimator locations in the upstream and downstream parts of the beamline. A good correlation would allow for more precise beam shaping by collimation only in the upstream collimators. Figure 47 shows the beam divergence at the CEDAR location with improved upstream collimation. This optimisation leads to an additional gain of 80 % in the number of kaons within the 60 µrad acceptance window. The combined enhancements from all these upgrades lead to a total kaon yield increase by a factor of 2.7 compared to the current beamline configuration.

In addition to vacuum and collimation upgrades, the number of units on T6 can be increased from 120 units in 2018 to 150 units of 10^{11} protons/spill, yielding an additional 25 % increase in intensity. To keep the total intensity within the radiation protection limits, stronger upstream collimation is required. Therefore, the effect of installing an additional collimator with a large maximum gap (for the muon beam mode) 290 m downstream of the T6 target has been studied, and the results are shown in Fig. 48.

Since this additional collimation removes only the beam tails that are anyway outside the CEDAR acceptance, the number of tagged kaons remains unaffected. As seen in Fig. 48, the collimator reduces the overall beam intensity while simultaneously decreasing horizontal divergence, effectively eliminating unidentifiable particles. A similar vertical collimator study was performed, but no significant improvement was observed in terms of limiting the vertical divergence. This is expected, as M2 is predominantly a

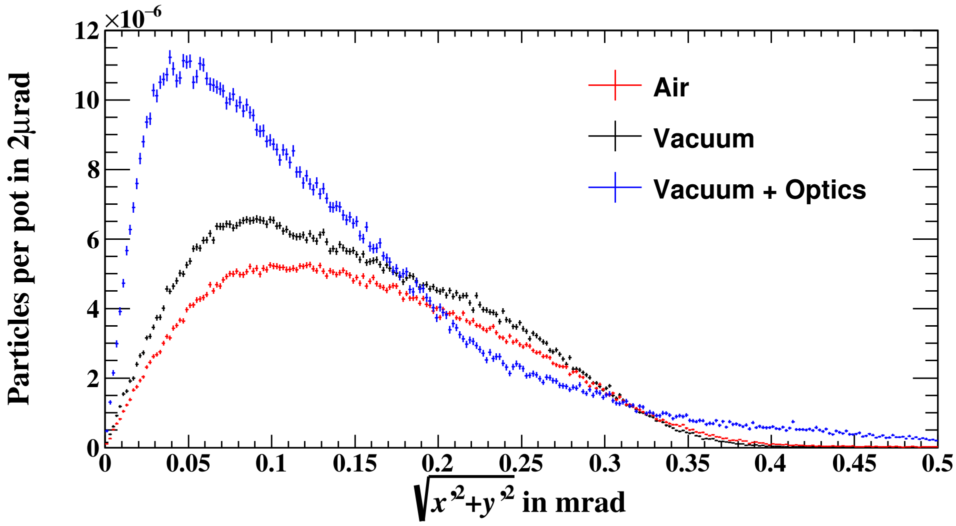

Fig. 47: Beam divergence at the CEDAR location with completed vacuum and optimised collimation, compared to the previous optics - with and without vacuum, from [84].

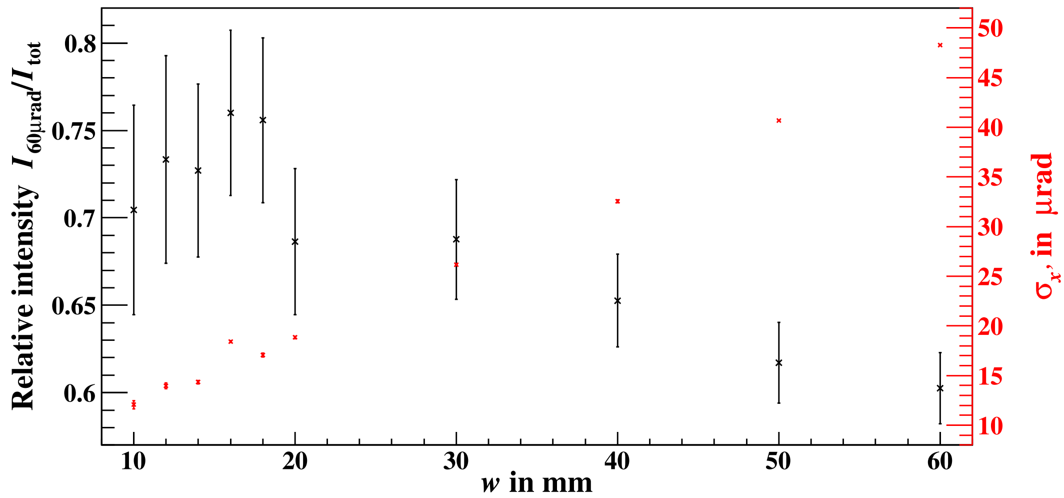

Fig. 48: Horizontal divergence and beam intensity as a function of the aperture of the additional collimator [84].

vertical beamline with vertical bends and the dispersion in the y-plane inherently limits further divergence reduction.

4.6.1 Higher Intensity Hadron Beams

The high-intensity hadron beam used for previous Drell–Yan measurements at COMPASS was limited to approximately 4×10^8 hadrons per 4.8 s spill due to radiation protection constraints. These high intensities were only permitted under a special configuration of the COMPASS spectrometer, which included a hadron absorber directly installed behind the polarised target and additional layers of concrete added to the shielding wall on the control room (Salève) side. To explore the possibility of further increasing the allowable beam intensity, a FLUKA study was launched in collaboration with HSE-RP. This study aimed to improve the understanding of radiation sources originating along the beam tunnel and taking into account the material composition of the two installed CEDAR detectors. The details of these studies and the proposed shielding upgrades are summarised in Ref. [85]. A preliminary cost estimate and tentative schedule have been outlined, with installation proposed during LS3, contingent upon approval of the AMBER Drell–Yan run. With these proposed changes, AMBER will be able to achieve the requested accumulated intensity of 3×10^{14} hadrons on target per year, with an intensity kept below 10^9 hadrons per 4.8 s spill.

4.7 Beam Instrumentation

4.7.1 CEDAR upgrade

Two CEDAR detectors, used for beam particle identification, are positioned at the exit of the M2 beamline tunnel, at the entrance to the EHN2 experimental hall. This location exposes them to significant temperature gradients between the tunnel and the hall, with considerable fluctuations between day and night as well as across seasons. These variations cause dynamic temperature changes and density variations over the gas volume of the CEDAR detectors, affecting their stability by altering the effective refractive index over time and along the detector. Even a constant temperature gradient degrades performance by smearing the Cherenkov light opening angle, whereas the internal CEDAR optics requires a precisely defined angle for optimal detection. To mitigate these effects, an actively controlled thermal shielding system was proposed and implemented by BE-EA and EN-CV at the beginning of 2018. The new system consists of an improved insulating layer around the gas vessel, designed to allow air circulation within the system. Cooled air is continuously circulated, maintaining a temperature gradient below 0.1 °C, as displayed in Fig. 49. A test conducted during the summer of 2018 further demonstrated the importance of this upgrade. During a controlled period when air circulation was deliberately stopped for a few days, significant temperature variations were measured along the CEDAR gas vessels. As shown in Fig. 50, measurements from multiple temperature probes revealed significant temperature differences along the vessel, along with a pronounced day/night cycle.

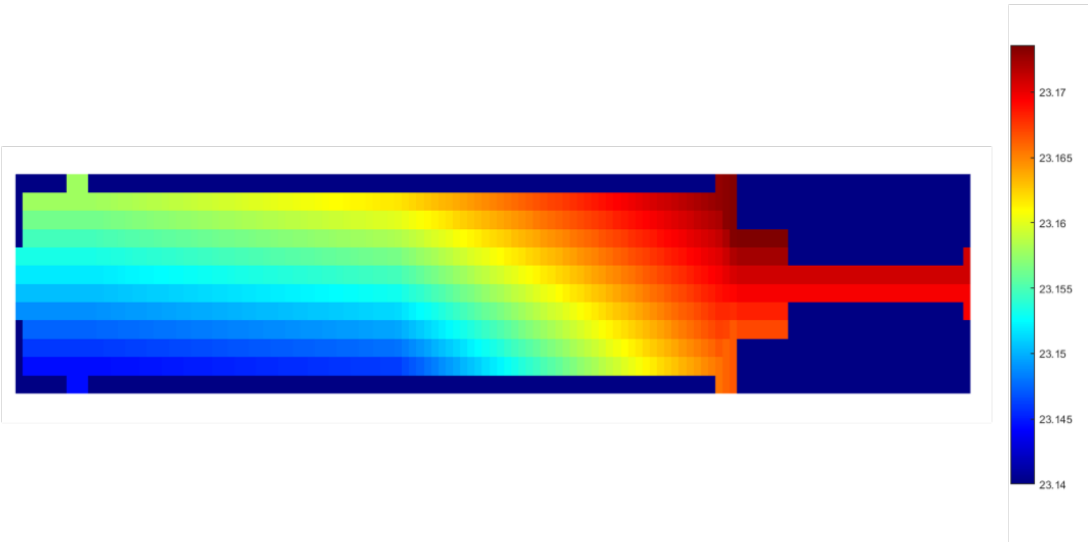

Fig. 49: Measured temperature gradient along the CEDAR1 gas vessel. The temperature fluctuates by less than 0.1 °C between minimum and maximum values.

Beyond thermal improvements, the CEDAR detectors were also upgraded with new multi-anode photomultiplier tubes and enhanced readout electronics to accommodate the increased beam intensity required for COMPASS Drell–Yan data taking.

As part of the NA-CONS project, the ongoing refurbishment of the CEDAR detectors includes enhancements to the mechanical alignment control, diaphragm precision, and gas control system. To facilitate these upgrades, a new clean room in EHN1 will become operational by the end of 2025.

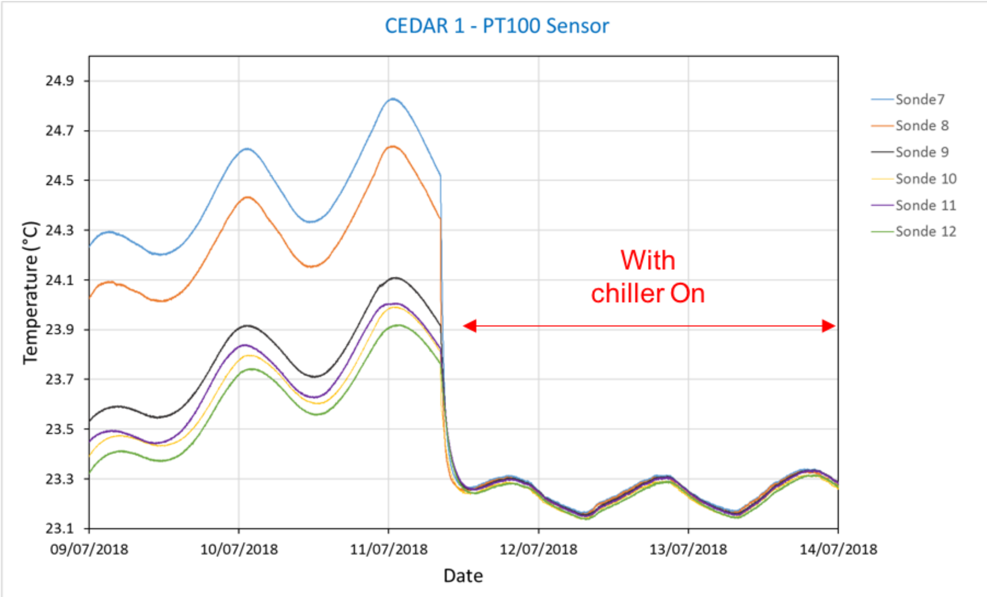

Fig. 50: Temperature stability of CEDAR1 during a test phase in the summer of 2018. When cooled air circulation was stopped, significant temperature variations were observed along the CEDAR gas vessels, as indicated by the differences between multiple temperature probe measurements. The day/night temperature cycle is also clearly visible.

Significant progress has been made in improving the precision of the diaphragm opening, with accuracy now approaching the experimental requirement, as demonstrated in Fig. 51. It shall be noted that some planned performance refinements are pending and the diaphragm opening precision is therefore expected to improve even further. The upgraded CEDAR detectors were successfully tested during a 2024 AMBER test run, yielding promising results. Additionally, ongoing studies by the experiment aim to further enhance the tagging efficiency of the CEDAR detectors.

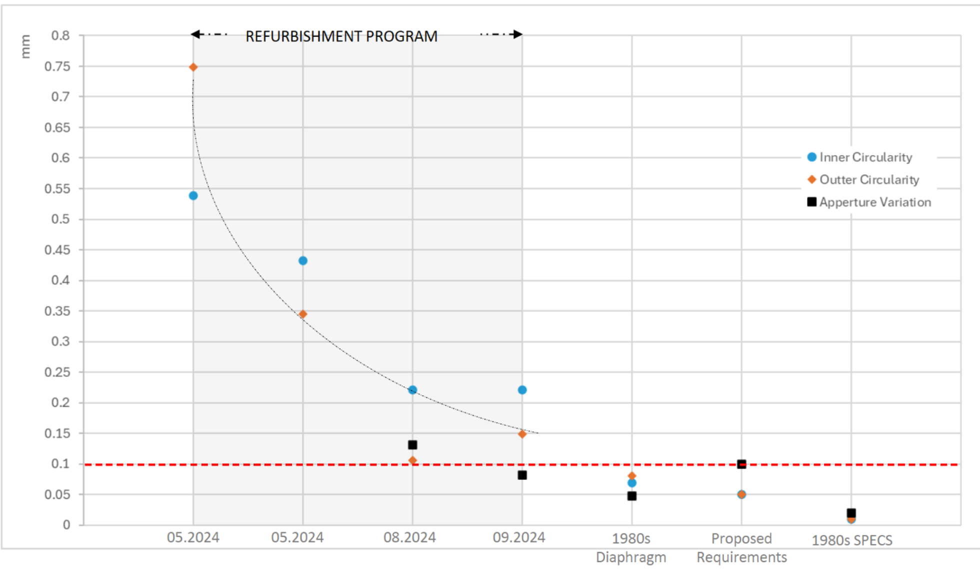

Fig. 51: Control of the CEDAR diaphragm opening, approaching the required precision of 0.1 mm.

4.7.2 Possible Upgrades to Beam Momentum Measurements

In the context of the NA64μ Phase 1 studies, simulations were performed with HALO and Geant4 to check the performance of the BMS and MS1 detectors to define the momentum of the incoming beam particles. The BMS consists of beam defining hodoscopes, labelled BM01 to BM06 as shown in Fig. 52. The entire beamline was simulated with HALO and the particle hits were scored at the BMS hodoscope positions. The BMS hodoscopes have a spatial resolution of 1.3 mm for BM01–BM04 and 0.7 mm and 0.4 mm for BM05 and BM06, respectively. The hodoscopes measure positions only in the vertical (y) co-ordinate. The system of bending magnets (BEND6) consists of three 5 m vertical bends with 3.3 T m bending power each.

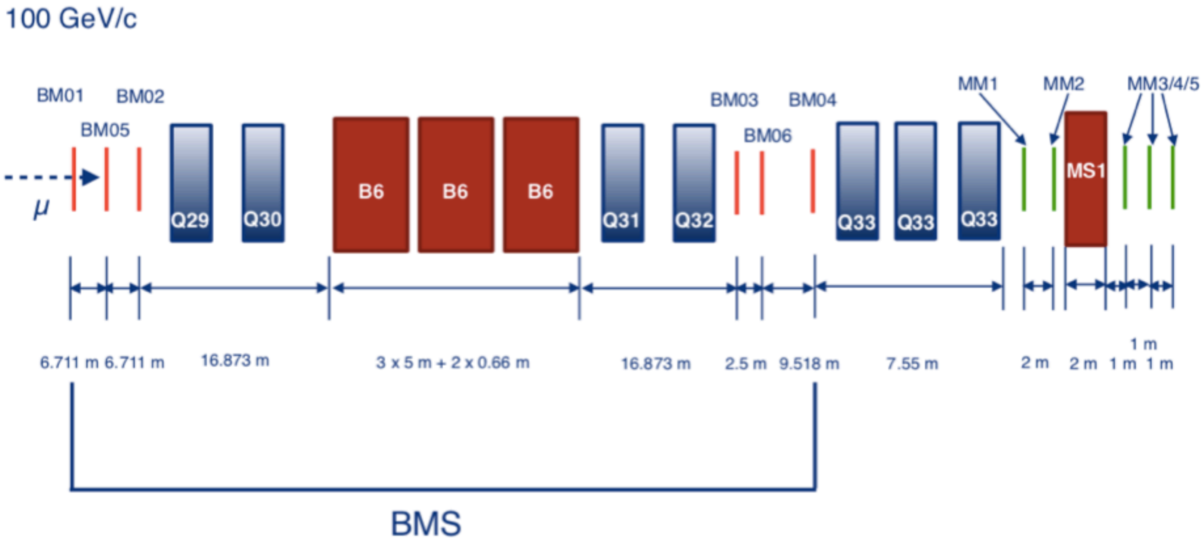

Fig. 52: Schematic of the beamline showing the BMS and MS1.

The momentum reconstruction with the BMS was estimated using the TMVA analysis package in ROOT [86] using the Boosted Decision Tree method. The vertical hit positions and the direction of the particles in the parts upstream and downstream of BEND6 were chosen as the input variables. The detector resolution was taken into account. Figure 53, top, shows the momentum resolution of 1 % as calculated with this method for a 160 GeV/c incoming beam. In order to further improve the BMS resolution, a BMS upgrade could be envisaged by replacing the existing hodoscopes with detectors of much better spatial resolution, such as Silicon detectors ($\sigma_y = 10$ to 50 μm) or gas strip detectors with very high rate capability ($\sigma_y = 100$ to 200 μm). Figure 53, bottom, shows the improvement in the momentum resolution for a 160 GeV/c incoming beam using the above momentum reconstruction method for different detector resolutions, keeping the detector positions and the number of detectors constant. For a detector resolution of 50 μm, achievable with a silicon detector, a resolution of 0.35 % can be expected. The fit function has been extrapolated to a 500 μm resolution in case a detector based on scintillating fibres would be considered.

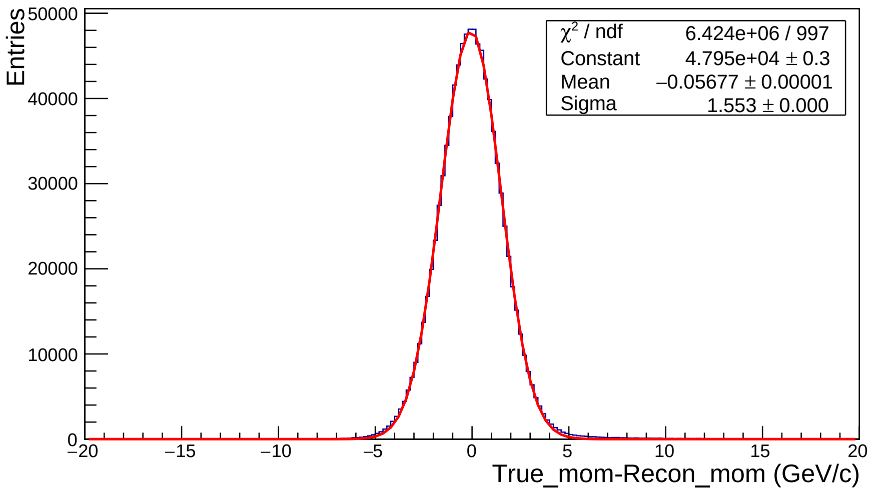

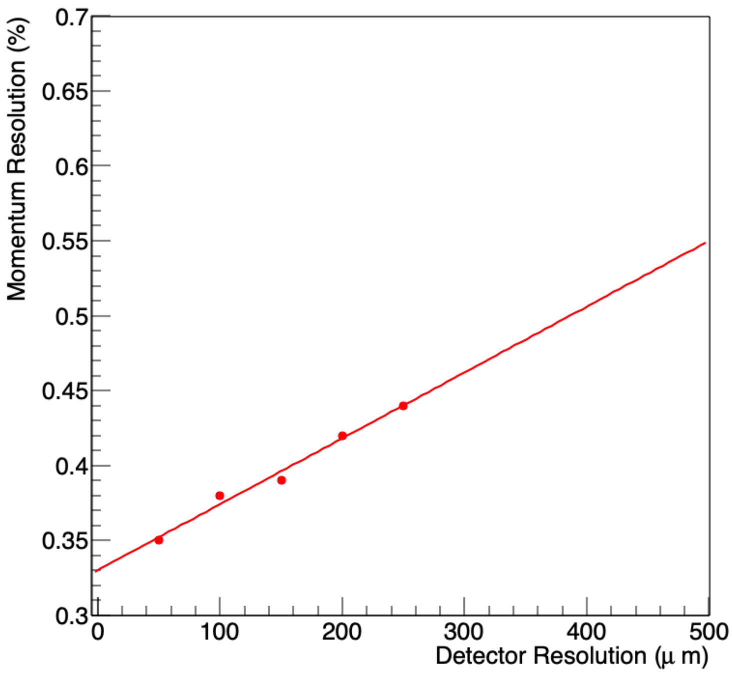

Fig. 53: Top: Momentum resolution of 1 % estimated for the current BMS set-up with simulation. Bottom: Estimated momentum resolution $\Delta p/p$ in % as a function of detector resolution.

Chapter 5

Projects in ECN3

Anna Baratto Roldan, Johannes Bernhard, Maarten van Dijk, Lau Gatignon, Rob Murphy, Laurence James Nevay, Florian Stummer

5.1 Introduction

For ECN3, a number of project ideas have been assigned to the Conventional Beams working group: HIKE, a proposal for a set of High Intensity Kaon Experiments [23], DICE/NA60+ [25], DIRAC++ [87], and SHADOWS [38]. Presently, the NA62 experiment [42] is the sole user of the ECN3 cavern and is approved to take data until LS3 to precisely study the ultra-rare decay $K^+ \to \pi^+ \nu\bar{\nu}$. First studied within the Beam Dump Facility (BDF) working group [88], a new underground facility (ECN4) has been proposed to host the SHiP experiment that aims to search for feebly interacting particles, foremost Heavy Neutral Leptons (HNLs) and candidates for Dark Matter [20]. After the 2020 European Strategy for Particle Physics Update, the BDF/SHiP proponents searched for an alternate, already existing underground cavern, and identified ECN3 as a viable alternative. In the following, we will shortly introduce the proposals and experiments mentioned above and their goals together with the studies that CBWG provided. The final decision by CERN management and Council was to select SHiP as the next experiment in ECN3.

The HIKE proposal was originally structured in three phases. The first phase, HIKE-K^+, would have been a follow-up experiment of the currently running NA62 experiment, with upgrades of the target complex and beam delivery to cope with a 4 to 6 times increased intensity with respect to the present conditions. The aim was a measurement of the same ultra-rare decay $K^+ \to \pi^+ \nu\bar{\nu}$ with a precision of about 5 %, in line with the improvement of the precision of the theoretical predictions. This measurement was planned to be interleaved with runs in beam dump mode (HIKE-BD). In a second phase, the experiment aimed to run a first version of a neutral K_L beam, employing the available space and detectors of the K^+ experimental set-up. This HIKE Phase 2, tentatively named HIKE-KL, was proposed at a later stage and only studied conceptually within CBWG. In case of a positive decision for HIKE, more detailed studies would have been done in the preparation phase for a technical design report. Finally, not part of the proposal, but studied in more detail by CBWG, the so-called KLEVER[1] experiment was originally supposed to be the follow-up experiment of NA62. It was aiming at collecting a useful sample of $K_L \to \pi^0 \nu\nu$ decays in a new set-up in ECN3. This required the design of a completely new, neutral beamline in place of the existing K12 line, as well as a potential extension of the ECN3 hall by about 150 m to cope with backgrounds.

SHADOWS was proposed as a beam dump experiment that could have been installed just behind the TAX dump after the T10 target, offset horizontally to the beam. It would have run parasitically to HIKE-BD without impact on HIKE operations. The lateral offset is helpful to reduce the muon background from the TAX, but further background suppression still turned out to be necessary, for which studies can be found in this chapter.

Both DIRAC++ and DICE/NA60+ require high-intensity primary beams. DIRAC++ requests high-intensity proton beams, while DICE/NA60+ requires conventional proton beams for reference measurements and high-intensity lead ion beams for its main measurements. While these beam types are available at the SPS, evolving radiation protection requirements restrict their provision to underground areas such as ECN3. These can only be provided if no other experiments are present in the hall. New beamlines for primary beam delivery into the hall would need to be constructed, although rather standard ones. Studies for the installation of DICE/NA60++ in ECN3 have been performed [1], but the Collaboration has now shifted its baseline to an implementation at lower beam intensity in EHN1, see

[1] KLong Experiment to detect VEry Rare decays

Chapter 3. The study on DIRAC++ was finally stopped because of the strong competition for ECN3.

5.2 NA62/HIKE Beam Dump

Being part of the HIKE proposal, the K12 beamline already offers currently the possibility for operation in beam dump mode to search for feebly interacting particles when the K12 TAX is moved vertically into dump position and the T10 target head is moved out of the beam. Both devices are motorised, so changing NA62 from Kaon to beam dump operation is typically done within minutes. After LS2 and based on CBWG studies in the first phase of PBC, the experiment successfully took data and published already first results. Many details of the original CBWG study can be found in the former editions of this report [1, 2]. Here, we give only a rather short summary of the final beam dump configuration and the achieved suppression of muon background together with a short introduction to the K12 beamline, which will be useful to describe also the changes that would have been needed for HIKE and SHADOWS.

The K12 beamline for NA62 [42] roughly follows a straight line from the K^+ production target T10 to the NA62 main detectors. This potentially exposes the NA62 detectors to a high muon background flux, for which a muon sweeping system has been designed and optimised. The K12 beamline with its optics is schematically shown in Fig. 54. The mixed beam is produced in the 400 mm long beryllium production target T10. The outgoing particles are captured and focused by a quadrupole triplet onto a pair of dump collimators (XTAX) with two 10 mm diameter holes each. Upstream of the TAX two dipoles produce a parallel downward displacement of 75 GeV/c beam particles by 110 mm. The TAXs are positioned and offset such that an overall ± 2.5 mm aperture provides a 1 % RMS momentum selection for the transmitted beam. Another pair of dipole magnets puts the beam back on the original horizontal axis for further transport and collimation. This section of dipoles, together with the TAX, is called first achromat due its functionality to cancel the effect of the introduced momentum spread on the beam trajectory. The rest of the beamline serves to clean the beam, identify the kaons and measure the momentum, position and direction of each beam particle at a rate of up to 2.2×10^9 particles per 4.8 s spill.

Muons originate mostly from the decay of pions and kaons produced by interactions in the T10 target and TAX. Muons can thus be positively or negatively charged. A first stage of muon sweeping consists of a series of three 2 m-long dipoles (BEND3) which have their gap filled with iron, except for a 40 mm diameter hole that is almost field free to allow the passage of the beam. Both positively and negatively charged muons are swept sideways out of the detector acceptance by the field in the yokes. From there, only positive hadrons are transported and the muons from their decays are only positive.

The second achromat is a set of 4 dipoles named BEND4 (two magnets), BEND5, BEND6, constituting the momentum spectrometer. In its centre, a toroid magnet, often denominated as the scraper, sweeps the left-over positive muons outside the main beam, away from the detector. The remaining muon background is dominated by unavoidable pion and kaon decays downstream of the scraper. As the rates in the detectors also comprise a significant rate of other particles (hadrons, electrons, photons, etc.), background estimates for dark sector searches must account for those rates as well.

In the first PBC phase, a G4Beamline simulation [89] had been implemented and subsequently used to optimise settings and possibly an optimised layout for dark matter searches. Based on a comparison to measured data sample provided by B. Döbrich and T. Spadaro from the NA62 Collaboration, scaling factors have been introduced in the MC simulation. Results are shown in Fig. 55 for positive and negative muons. The characteristics of the data are reproduced to a large extent. Both, positive and negative muons contain a large accumulation at larger radii and lower momenta, which originate from the TAX, while the cluster at about $R = 200$ mm and $p = 75$ GeV/c for positive muons originating from upstream decays can be also seen in the data. Given the satisfactory qualitative agreement, a modification of the four magnets of the first achromat has been proposed and implemented. Until LS2, BEND2 referred to the second of the four magnets and the other three were interconnected in series with the appropriate polarities as BEND1. From 2021 on, the first three magnets are in series and controlled as BEND1,

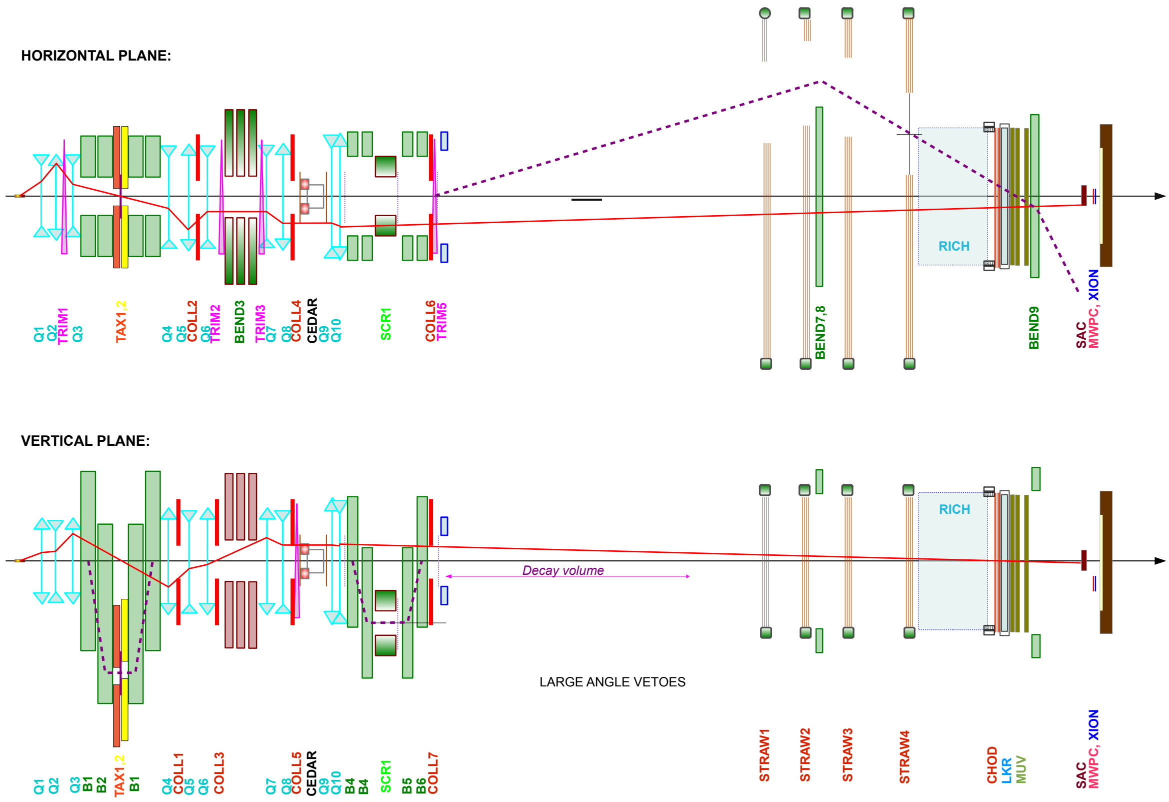

Fig. 54: Schematic layout and optics of the K12 beam for the NA62 experiment.

whereas BEND2 is now the fourth dipole. This allows to implement the above scenarios by just remotely changing settings, without hardware intervention. A first beam dump data taking has been performed by NA62 in 2021. While setting-up, the three first achromat magnets have been set to their maximum value and the current of the fourth magnet, now denominated BEND2, has been varied while the total muon rate in the NA62 detectors was recorded. As expected, Fig. 56 shows a drop of the measured muon flux for a reversed polarity (negative current values) in the MUV3 detector, which is sensitive to the overall muon background. The magnitude and position of the minimum is compatible with the predicted values of our G4Beamline simulation. In the second PBC phase, there has been a substantial effort to update the K12 G4Beamline model for both beam dump and standard kaon modes and move it to BDSIM, resulting in an even better agreement with experimental data.

5.3 HIKE-K+

For their first experimental phase, HIKE planned a measurement of the ultra-rare decay $K^+ \rightarrow \pi^+ \nu\bar{\nu}$ with a precision of about 5 %. Compared to the current NA62 experiment, this implies an increase of the kaon statistics by a factor of 4. For this, the T10 target complex in TCC8, including the K12 TAXs, would need a major upgrade. The upgrade should ensure compatibility with all further HIKE phases and should be in line with radiation protection needs as well as best practices for maintenance and operation. The P0-SURVEY machine protection against wrong magnet currents, problems with XTAX and target cooling, and closed vacuum valves must be improved, which is foreseen in the framework of the North Area Consolidation project. Already during LS2, the existing protection system was sped up such that the interlock is always triggered before the next extraction. In addition to these already implemented changes, major upgrades to the experimental set-up were under consideration to cope with the higher rates in the

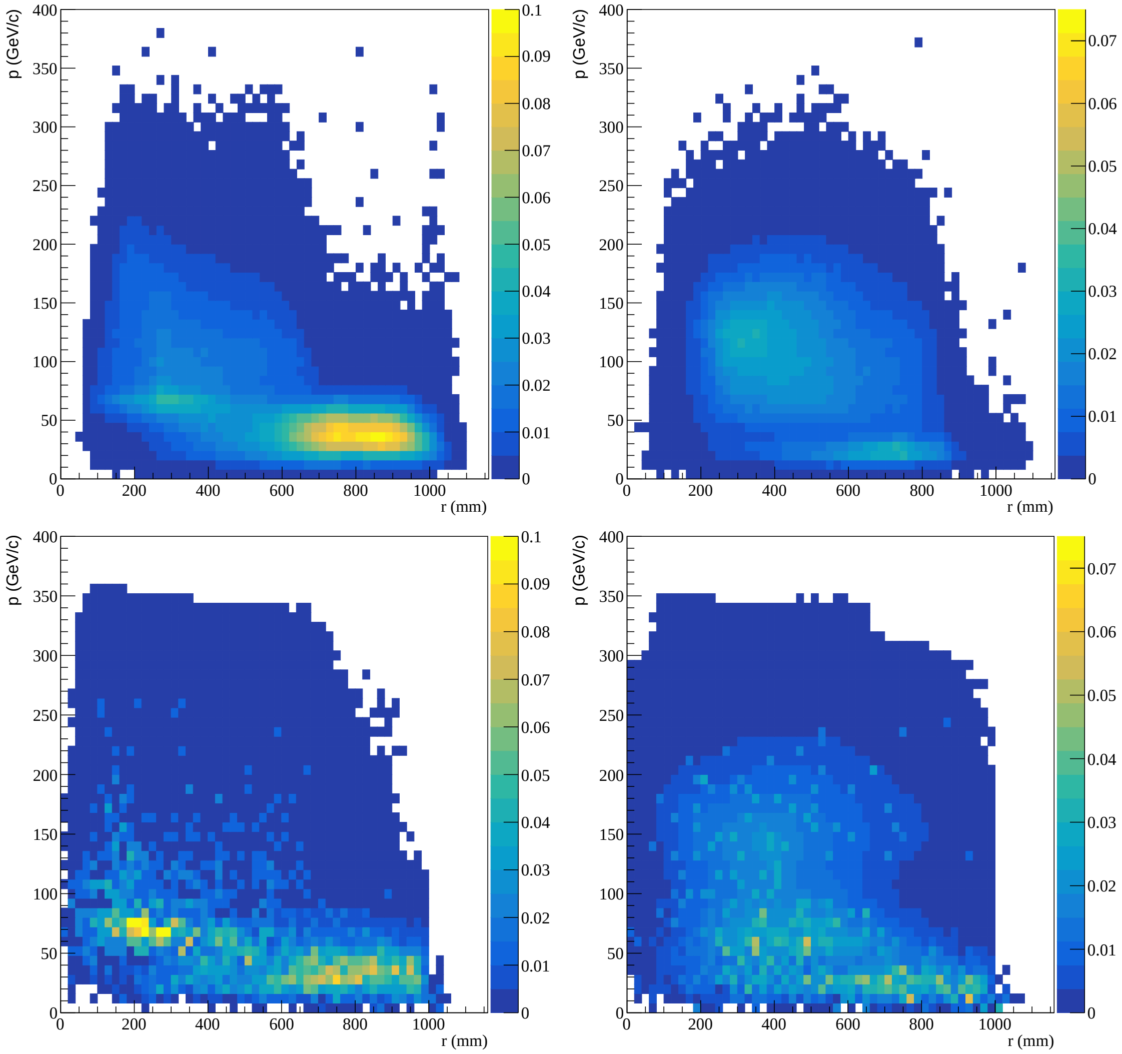

Fig. 55: Measured distribution of charged tracks (left) and simulated distribution of muons at $s = 180$ m and within NA62-CHOD acceptance (right) in beam dump mode. The upper (lower) row represents the positive (negative) charged particles. The colour scale indicates the number of muons per billion PoT per bin. The data has been downscaled by a factor 5.

detectors. The K12 beamline as such would not have needed a specific upgrade in this first phase, but consolidation and exchanges of irradiated magnets would have been envisaged. Studies for a new target and K12 TAX have been done first in synergy with the KLEVER study, see Section 5.4.

5.4 KLEVER

KLEVER, which aimed to measure the branching ratio of the ultra-rare decay $K_L \to \pi^0 \nu\bar{\nu}$, would have served as the counterpart of the Phase 1 HIKE-K^+ measurement of $K^+ \to \pi^+ \nu\bar{\nu}$. This decay mode is even rarer with a Standard Model prediction of about 3×10^{-11}.

Initially foreseen as a follow-up of NA62 immediately after LS3, it was, at the time of the HIKE EoI, considered as a third phase of HIKE, HIKE Phase 3. Finally, the HIKE Collaboration submitted a proposal only for Phases 1 and 2, and KLEVER was no longer part of this proposal.

As the neutral beam acceptance cannot profit from focusing, the angular acceptance is smaller than for a charged beam. Consequently, the required proton flux for KLEVER is at least 2×10^{13} protons per 4.8 s spill, about a factor 7 higher than for the nominal NA62 beam.

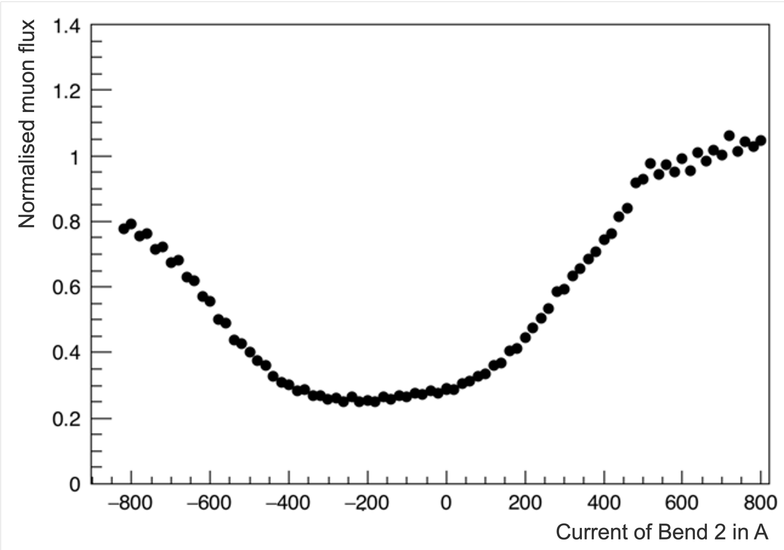

Fig. 56: Measured muon rate at MUV3 for different currents of BEND2. The normalisation, i.e. 100 % muon flux, corresponds to +770 A, respectively a bending power $Bl = 1.82$ T m, which is the nominal value of BEND2 for the kaon beam.

The beam will transport all long-lived or stable neutral particles, including K_L but also K_S, Λ, neutrons, and photons. A non-zero production angle will reduce the fraction of Λs and neutrons in the beam, relative to the K_L component, but also the K_L rate per proton on target. In addition, a larger production angle will soften the spectra of the particles. For a start of the decay volume at a sizeable distance from the production target (about 100 m), a larger angle implies an increase of the K_L decay rate per produced K_L over the length of the fiducial volume, but a decrease of K_S and Λ decays over that same length, as they will more often decay before the start of the fiducial volume.

A first study addresses the optimal production angle, based on FLUKA [90, 91] and Geant4 simulations, starting with benchmarking compared to (sparse) existing data. The baseline target material will be beryllium, but in the future alternative materials could be studied. A benchmark study for the simulation performance and the impact of the production angle for the beam to KLEVER has been completed [92]. High-Z target materials would reduce the photon content in the beam (relative to the K_L), but suffer from higher local temperature rise. In general, all questions related to the high intensities and their impact on equipment and radiation protection will be addressed in Section 5.5.2.

The production angle must be implemented in the last section of the P42 beamline, which transports the primary proton beam over almost 900 m from the T4 target in TCC2 to the kaon production target T10 in TCC8 (in its present location). The proposal is to have the protons impinging onto the T10 target downward at the required angle (the neutral beam axis being horizontal). This is an also essential factor in reducing the prompt muon flux outside of ECN3, above and behind the ECN3 cavern.

Finally, the study addresses the design and optimisation of the neutral beam itself, in particular the background reduction, collimation and muon sweeping.

Many aspects of the beam design for KLEVER have been retained for HIKE Phase 2, as discussed in Section 5.6.

5.4.1 Conclusions on targeting

The initial proposal for the design of KLEVER, as described in [48], had the protons impinging on the target at an angle of 2.4 mrad, in other words the neutral beam is derived at a production angle of 2.4 mrad. It was found that under these conditions, the rate of background Λ^0 decays (in particular into

π^0n) occurring in the fiducial volume of the detector was prohibitive. A solution was found by using a larger production angle, and in parallel opening up the angular acceptance of the neutral beam (from 0.3 to 0.4 mrad) to compensate for the reduced K_L flux per proton at this higher production angle.

The effect of the production angle on the particles emerging from the target was studied extensively. To ease and speed up studying the particle spectra, in particular the impact of decays over the long distance between the target and the detector, a series of fits was made to the produced particle spectra. These were fitted over the full angular and momentum space simultaneously, using the Malensek parametrisation, described in [93]. A detailed description of the methods used, as well as the fit parameters extracted from the Geant4 and FLUKA simulations, can be found in the full note [92]. It was found that this model reasonably describes the simulated production of all hadron species. The use of this parametrisation then allows for quick refactoring of the impact of lifetime of the particle (notably in the case of the Λ^0, which in its rest frame only has a lifetime of 263 ps. The change to higher production angle has several different important consequences the total production rate reduces, but also the momentum spectrum changes. The production at the target and the average momentum of Λ^0 and K_L are shown in Fig. 57.

The impact of the change in production angle is large: The production of K_L drops by a factor of 2.6, and the production of Λ drops by a factor of 8.3. However, the fraction of K_L that decays inside the fiducial volume actually goes up by a factor 1.6, owing to the smaller decay length at lower momenta combined with the specific long lifetime of the K_L of 51 ns. The fraction of Λ^0 decays in the fiducial volume goes down by a factor 48. The net effect of the change in opening angle (0.3 to 0.4 mrad) and production angle (2.4 to 8 mrad) is generating 10 % more K_L decays in the fiducial volume and suppressed the number of Λ^0 decays by a factor 220. With this additional suppression, the amount of background represented by the Λ^0 was (at the time of the first PBC CBWG report) considered acceptable for the KLEVER measurements. The total number of decays in the fiducial volume after the change to 8 mrad is 4.1×10^{-6} and 1.3×10^{-10} per proton on target, for K_L and Λ^0 respectively. The remaining suppression required comes from kinematic cuts applied in the detector and has been shown to adequately reduce the number of background decays of the K_S and Λ [94].

Simultaneously with the studies concerning the production angle, an assessment was made of the impact of the target material. For targets of identical length in terms of nuclear interaction length λ, no large differences were found in terms of hadronic production. However, there is strong suppression of the photon content of the beam, since higher-Z materials have a significantly smaller conversion and radiation length. With the current rate of high energy photons above 5 GeV/c in the beam, it is necessary to put a significant quantity of material directly in the beam as a photon absorber, which then simultaneously adds extra scattering for the incident K_L. However, if the choice is made for a higher-Z target, this absorber could be made substantially thinner. Two target materials (lead and copper) were assessed in the same way as the beryllium target benchmarking described above and it was found that they are similarly well-simulated in FLUKA and Geant4. It is expected that tungsten would be a more suitable high-Z material than lead because of its superior thermomechanical properties. However, the technical feasibility remains to be studied, as the energy deposit per unit of volume is much higher than in beryllium. The impact of the target material on the thickness of the photon absorber is studied further by means of a full beamline simulation in the next but one section.

5.4.2 P42 modifications

The P42 beam transports primary protons traversing and not interacting in the T4 target to the T10 target, located almost 900 m further downstream. At the end of the present P42 beam three dipoles allow to control the vertical angle of incidence onto the T10 target and therewith the production angle of the secondary beam. However, in the present layout this angle is limited to less than about 3 mrad. The charged kaon beam for NA62 is operated at 0 mrad production angle and the K_L beam for the NA48 experiment at 2.4 mrad. Both options can thus comfortably be covered with the present layout. The production angle can be controlled by adjusting the fields in the three last dipoles. However, for the

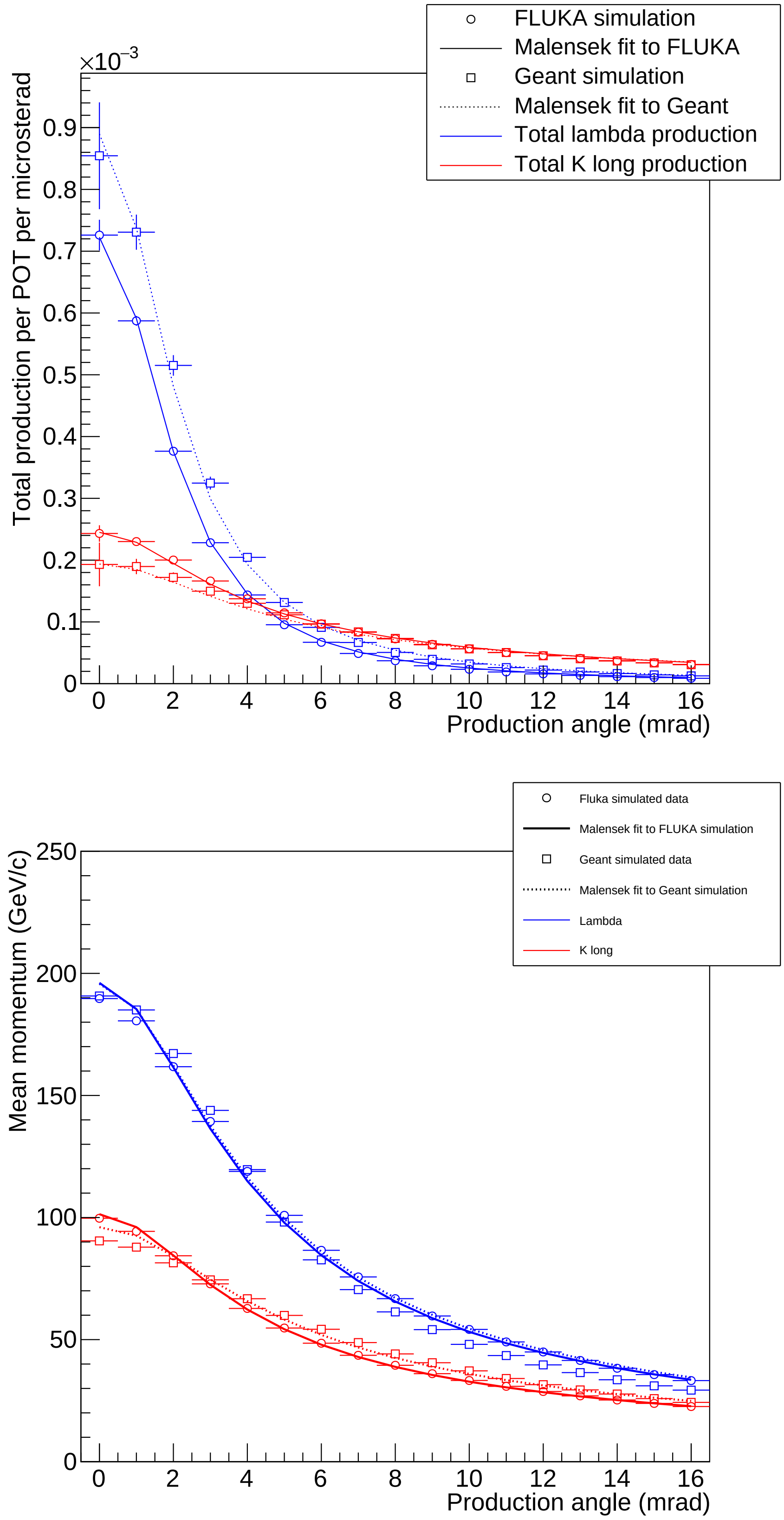

Fig. 57: Production per proton on target (top) and mean momentum (bottom) of K_L and Λ^0.

KLEVER experiment the required production of 8 mrad implies a downward slope of the incoming beam of 8 mrad with respect to the horizontal beam axis of the outgoing kaons, as an upward slope would be unfavourable for radiation protection reasons. A possible solution to this issue has been demonstrated in the 2018 edition of this report [1].

5.4.3 Neutral beam design

Following the change of production angle to 8 mrad for the 'short' version of KLEVER that keeps an upgraded NA62 detector at the same location in ECN3, an optimised design was made for the neutral beamline after the target. This design uses four collimators. The first of these is the TAX (Target Attenuator) collimator (located about 5.6 m downstream of the target), which serves the dual purpose of absorbing the primary proton beam emerging from the target and initial preselection of the beam particles. Second is the defining collimator, at 40 m distance from the target, which defines the beam acceptance by stopping all particles beyond a certain radius. This generates additional background [95] (in particular at the edge of the aperture), which is removed by a third collimator, the cleaning collimator, located at 80 m from the target. The active final collimator is at the same time a detector, with a LYSO inner ring extending outward from 60 to 100 mm radius and a lead / plastic shashlik calorimeter extending out to a radius of 1 m. It serves to define the upstream limit of the fiducial volume, and vetoes all unwanted particles from the upstream region that would otherwise trigger the detector. The current beamline design is shown in Fig. 58.

It should be noted that with the 8 mrad production angle, the design calls for a calorimeter at around $s = 250$ m from the target, extending from 130 mm radius outward; this implies that the existing krypton calorimeter,featuring a vacuum pipe of 80 mm radius, will not be suitable for KLEVER.

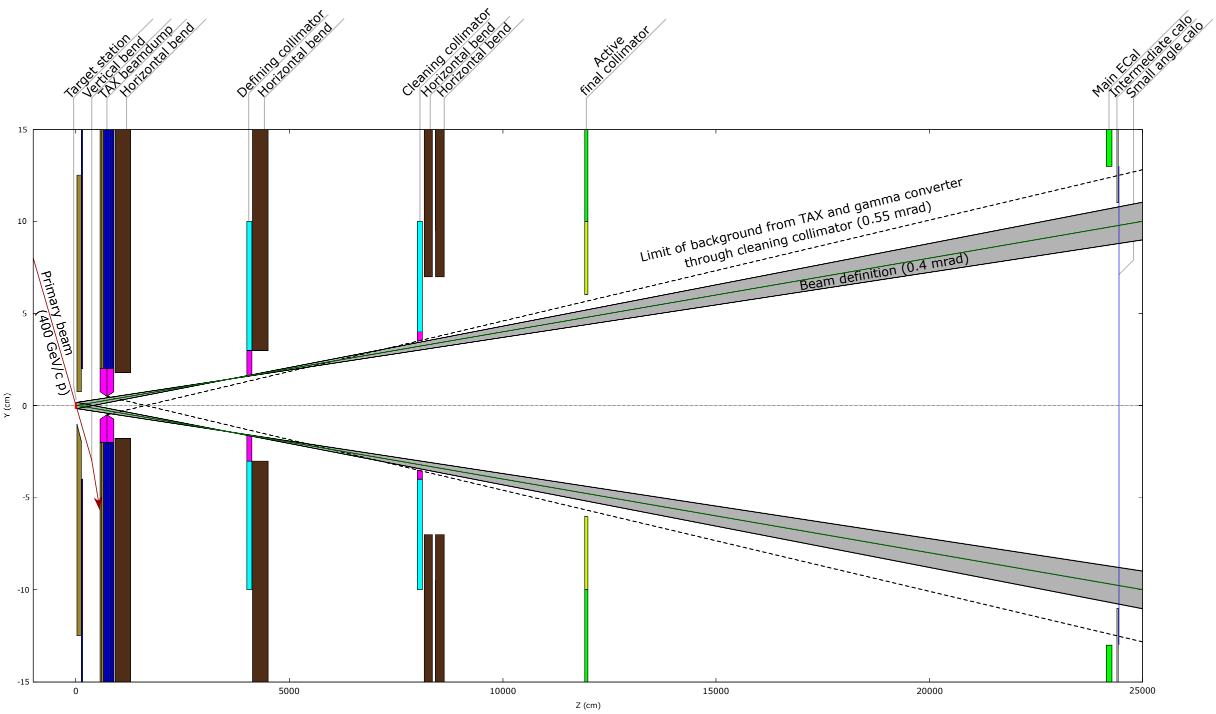

Fig. 58: Schematic layout of the beamline and collimators for KLEVER by N. Doble.

The decay fiducial region extends from about 130 to 170 m from the target. The KLEVER detector consists of a large number of large angle photon vetoes (LAVs), constituting hermetic coverage as viewed from the fiducial region, which reject any decay for which a photon is detected that would not hit the main detectors at the end of the beamline.

At the end of the beamline, about 250 m from the target, three calorimeters are located. The inner small angle calorimeter (SAC) extends out to a radius of 100 mm, set by the angular definition of the beam, 0.4 mrad. It covers the phase space with a direct line of sight to the target. The second is referred to as the main electromagnetic calorimeter (MEC), extending out to 1250 mm radius, which records the signals of the photons that have a sufficiently large opening angle relative to the beam, allowing π^0 particles that are generated and decay in the fiducial volume to be reconstructed. An intermediate ring-shaped calorimeter (IRC) sits in between the MEC and the SAC to ensure that no particles escape through the gap between the MEC and the SAC. Figure 59 shows the detector design.

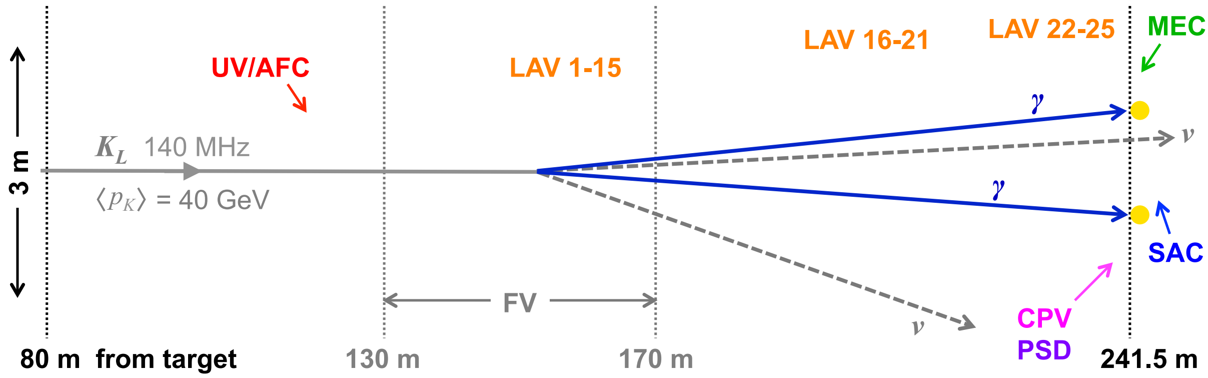

Fig. 59: Schematic layout of the KLEVER detector by M. Moulson.

As discussed in the previous section, KLEVER is expected to operate with 2×10^{13} protons per spill. With the early NA62 definition of a so-called effective spill, taken at the time as 3 s, while currently rather in the order of 4.5 s, the instantaneous rate would be around 6.7×10^{12} protons on target/s, which needs accounting for intensity fluctuations. The rate requirement set on the small angle calorimeter (SAC) is 10^8 particles/s, of which about 4×10^7 s^{-1} are assumed from high-energy photons with an energy above 5 GeV. This design parameter implicitly determines the thickness of the photon absorber to be integrated in between the TAX, see Fig. 60. A simulation was performed using three different target materials and a photon absorber made of tungsten. For tungsten, the radiation length X_0 is about 3.5 mm. The effective photon conversion length (for pair creation, referred to as X_{eff}) is a factor 9/7 times longer, i.e. about 4.5 mm. For each target material (beryllium, copper and tungsten) eleven simulations were made, stepping from zero to ten effective conversion lengths of tungsten photon absorber, and the rate of particles passing into the volume occupied by the SAC was recorded. In Fig. 60, a detail from the FLUKA simulation shows the TAX region of the beamline design for KLEVER, with the photon absorber inset in the centre. Figure 61 shows the rate of photons above 5 GeV passing into the SAC for the three target materials, as a function of photon absorber thickness.

The effect of the photon absorber is twofold: it removes high-energy photons from the beam but also scatters K_L. We found that for the beryllium, copper, and tungsten targets, respectively, a photon absorber of length $7.3/5.2/3.8X_{\mathrm{eff}}$ ($32.9/23.3/16.9\,\mathrm{mm}$ tungsten) is needed. This simultaneously degrades the number of K_L passing the final collimator. Using the copper (tungsten) target, 15 % (28 %) more K_L passes through the hole in the active final collimator.

To assess the effect of the stages of collimation, the momentum spectrum of three particle species after each collimation stage is shown in Fig. 62. The spectrum of photons and neutrons is shown in Fig. 63.

The amorphous photon absorber could be replaced by an oriented crystal converter, which would have an increased photon conversion rate per unit of length. As a result, the length of the absorber can then be reduced and along with the length its impact on the hadron component of the neutral beam. A test of such a crystal converter has been performed in the H2 beamline in the North Area in August 2018 [96].

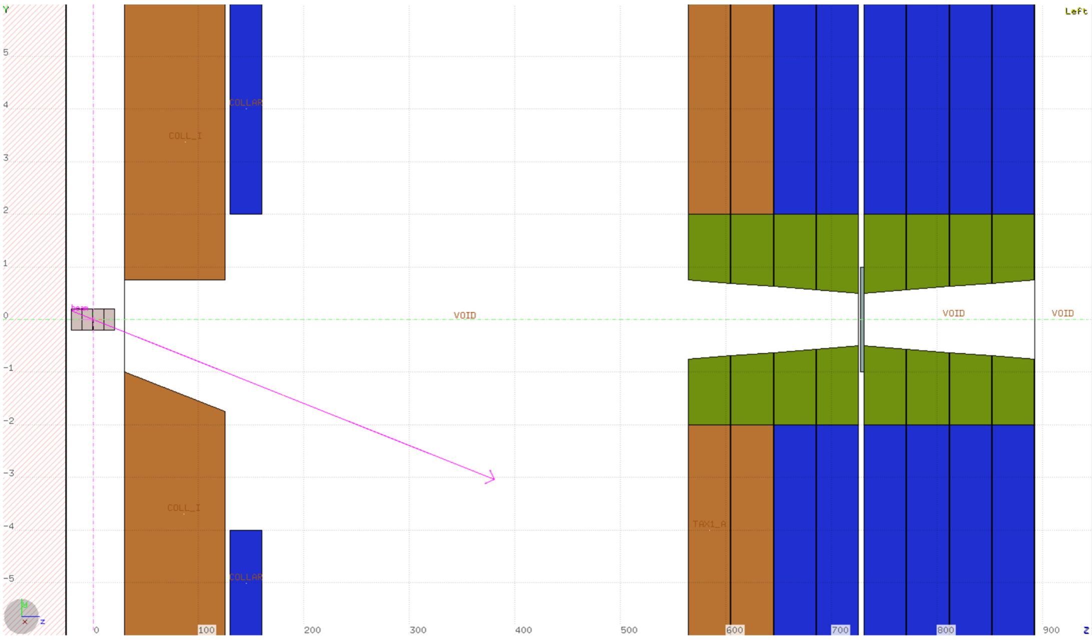

Fig. 60: Detail from FLUKA showing the target region featuring the T10 target station internal collimator and steel collar, and the TAX, composed of 2×400 mm of copper and 6×400 mm of steel. The photon absorber is inset in the middle of the tungsten TAX inserts.

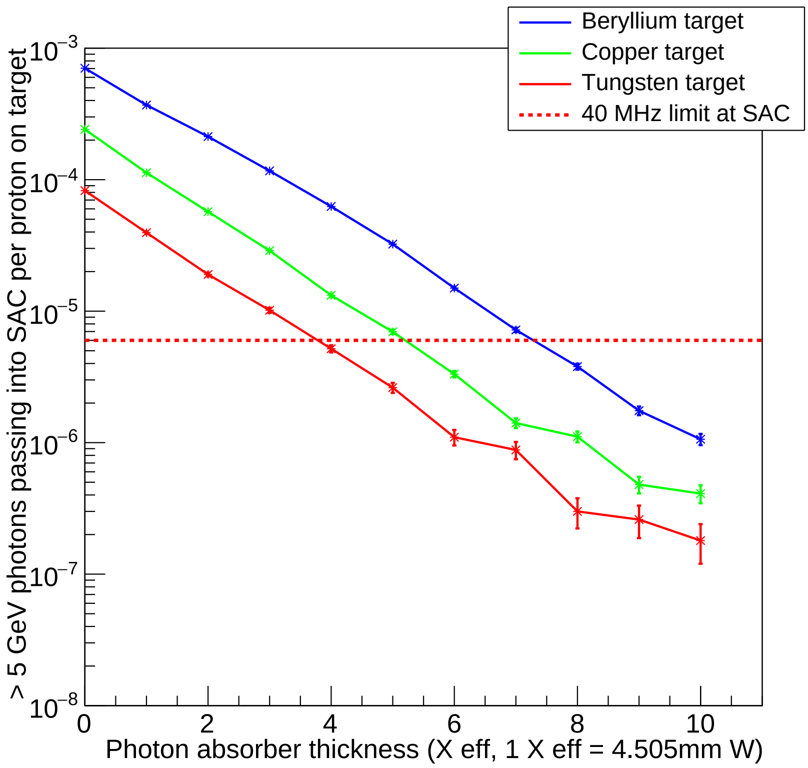

Fig. 61: Impact of choice of target material on required thickness of the photon absorber.

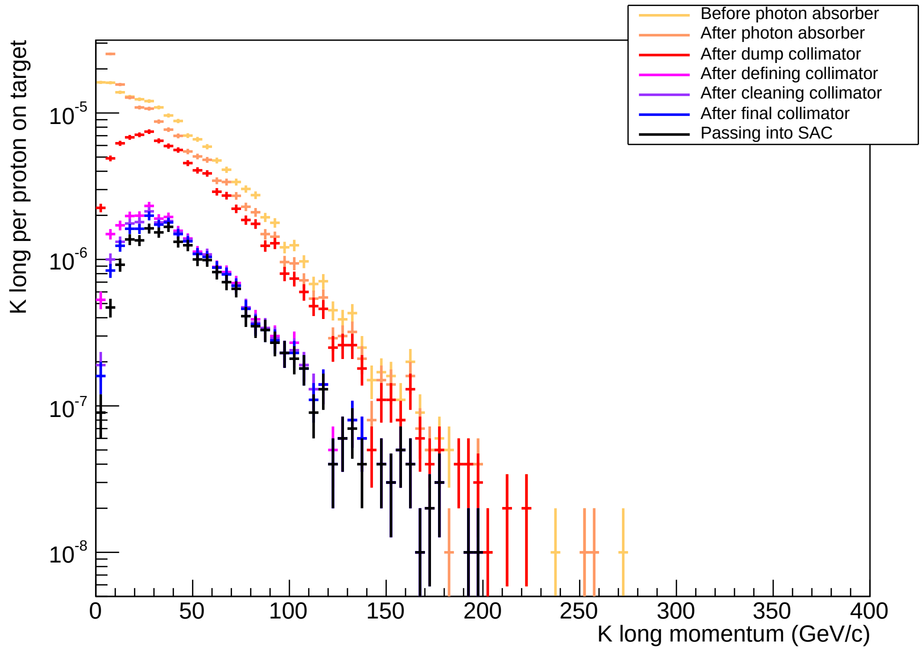

Fig. 62: The momentum spectra of the K_L after each collimation stage.

As a final step, several magnetic elements are expected to be part of the beamline. The first of these is an MTR with a bending power of 7.5 T m, directly after the target station, giving the primary proton beam an additional 5.6 mrad downward angle before being dumped in the TAX at a sufficient distance from the neutral beam. The other purpose of the magnetic sweeping is to sweep away the charged secondary particles. It is expected that the TAX itself also creates additional charged background, which is to be swept by another MTR with a bending power of 7.5 T m. The defining collimator is to be followed by an MTN magnet, which has also a bending power of 7.5 T m but with a larger gap to fit the beam. Finally, the cleaning collimator has two MBPL magnets with 3.8 T m bending power each. These magnets serve to sweep out of the main detector acceptance any background produced on the collimators. The final collimator is not followed by a magnet since it is already an active detector which would thus anyway veto particles crossing it. All the dipole magnets quoted here are already part of the K12 beamline for NA62 and in principle could be reused after refurbishment.

An important background for the experiment is formed by muons being swept into the acceptance by the magnets, both through the field in their gap and by the return field in the yoke. To this end, a simulation of reduced scope was performed to assess the muon flux passing into the AFC and the MEC. A brief test run of the simulation indicated that the majority of the muons are generated from decays occurring in the upstream region before the TAX.

To reduce computational cost, a cut was implemented in the simulation, removing non-muon particles hitting material, and leaving the photon absorber transparent. This removes the cascade of the primaries in the collimator inside the target station and in the TAX. A computational cost reduction of around a factor 30 was achieved. This allowed for a more detailed exploration of magnet parameter space. The magnets should be positioned as close to the collimators as possible. The first (vertical) sweeping magnet serves for dumping the primary beam, and its position is assumed to be fixed. This leaves the magnets after the TAX, defining and cleaning collimators. Of these, the two MBPLs are varied together; since they have no lever arm with respect to each other. Varying both would just lead to partial cancellations and adding complexity without benefits. It was also assumed that the magnets should be run at maximal field, to optimise the removal of unwanted (non-muon) charged components. Three (sets of)

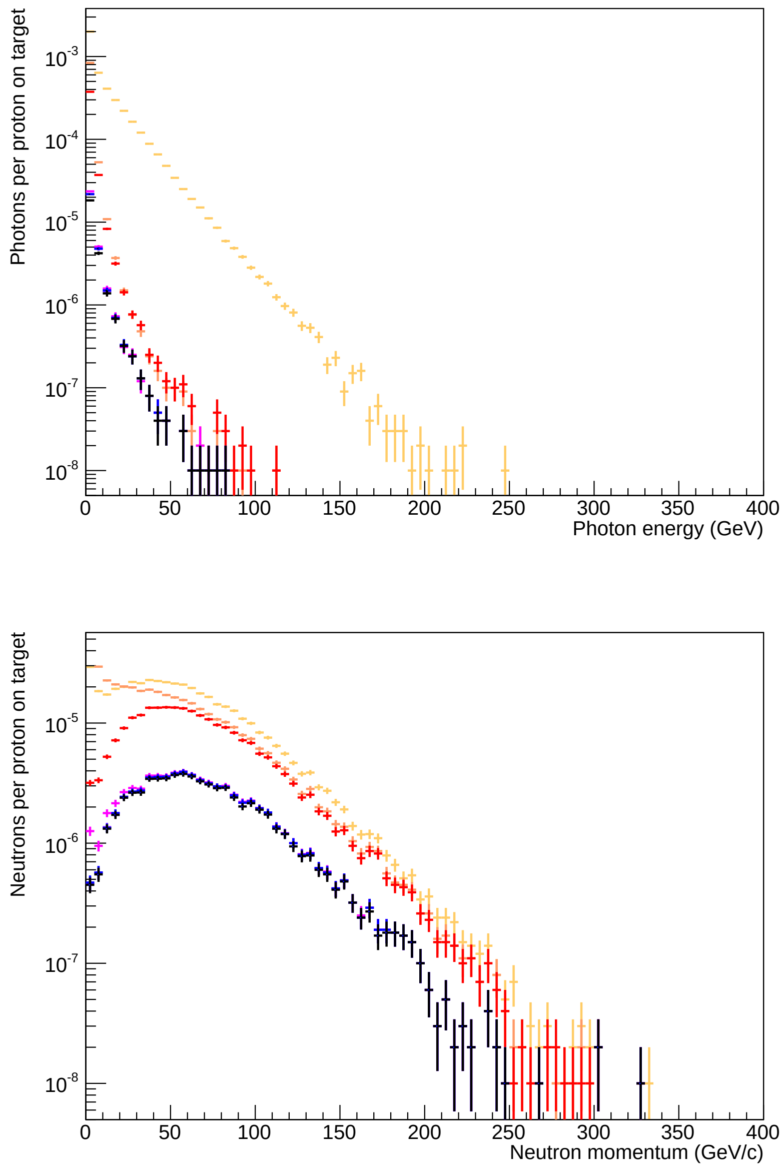

Fig. 63: Momentum distribution of photons (top) and neutrons (bottom) at the various stages of collimation.

magnets remain, and for each of these there are four cardinal rotations, for a total of 64 combinations.

To represent all of these in a relatively simple fashion, a vertical and horizontal weight was attributed to each of these magnets, a factor 4 for the first, a factor 2 for the second, and a factor 1 for the final set. Together with an orientation (+1 vertical, 0 horizontal for up, 0 vertical and -1 horizontal for sweeping towards negative x) these weights now form a two-dimensional parameter space, allowing the total muon rates to be plotted on a colour scale. The result, showing the muon rate for all combinations of rotations, in the AFC and in the MEC, can be seen in Fig. 64.

These plots are divided into four quadrants; each of which represents an orientation for the sweeping magnet following the TAX, which has the largest weight. It is observed that placing this magnet in a vertical orientation (top and bottom quadrants), has a severe detrimental effect. There is also a local maximum for the far left and right tips of these plots, indicating that placing all the magnets in the same horizontal orientation results in a local maximum. The minimum is found at the points just left and right

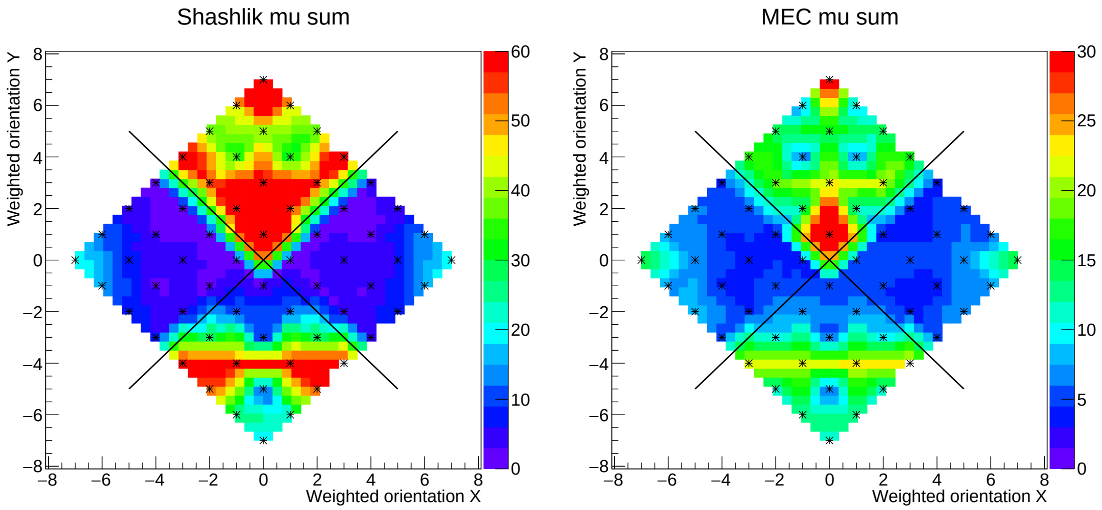

Fig. 64: Muon background rate in $10^6\,\mathrm{s}^{-1}$ (total for positive and negative) found in the AFC (left) and in the MEC (right), as a function of geometrically weight of the magnets.

of the origin; representing a fully horizontal set of orientations with the magnet after the TAX sweeping in the opposite direction of the two (sets of) magnets following it. The better of these two is then picked on the basis of considerations of radiation protection. Figure 65 shows the (local) rate of positive and negative muons, for a plane extending to ± 4 m horizontally and vertically, placed just before the AFC (at $s = 119$ m). For this particular case, the magnet following the TAX sweeps positive particles to positive x, and the remaining magnets to negative x. The size of the AFC is indicated.

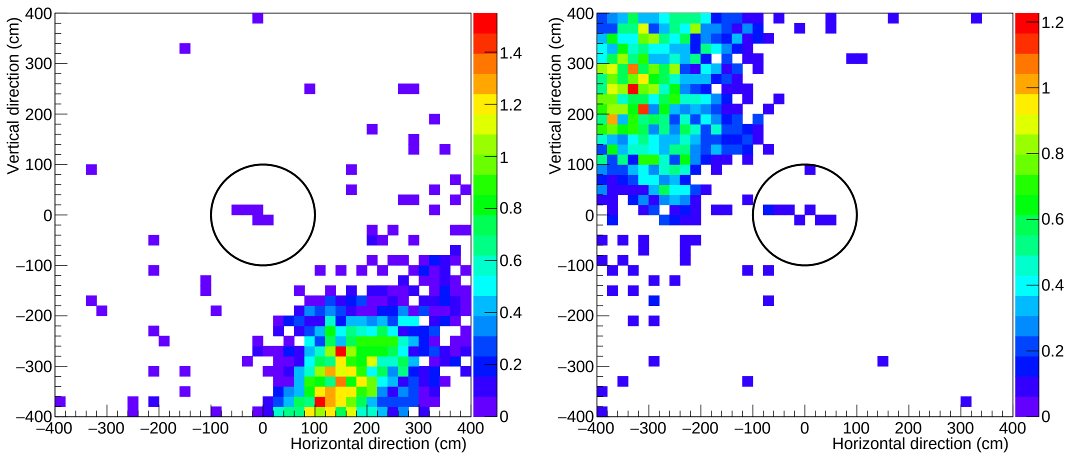

Fig. 65: Local muon rate (in $10^6\,\mathrm{s}^{-1}$) at $s = 119$ m, in front of the AFC, for positive muons (left) and negative muons (right). The black circle indicates the coverage of the AFC.

The directionality of these two groups of muons are set by the first (vertically sweeping) magnet just after the target station and that following the TAX. The first is fixed; thus the positive muons acquire a downward orientation, and the negative muons upward. The magnet following the TAX adds a horizontal component to this, in this case sweeping positive particles to positive x. The critical consideration is that the control room (currently hosting NA62) is located at positive x. As such, out of the two orientations that were found to be optimal earlier, the one that sweeps the positive muons away from the control room is chosen. After the optimisation, the total muon rates found in the AFC and MEC are about 2.5 and $4.9 \times 10^6\,\mathrm{s}^{-1}$ respectively, with the increase in the latter being mostly attributed to decays between the two.

Beam-gas interactions of the neutral beam require to maintain a vacuum level of 10^{-7} mbar as demonstrated in the 2022 edition of this report [2].

5.4.4 New results during LS2

In 2019 KLEVER realised that up to then its background rejection capability against $\Lambda^0 \to \pi^0 n$ decays was in fact overestimated by several orders of magnitude. This finding has important consequences for the design of the beam and experiment. Several ideas were considered to reduce this background to acceptable values. A further increase of the production angle (to about 20 mrad) would decrease the number of Λ^0 decays and soften their spectrum, but also very (too) significantly lower the rate of kaon decays.

The most promising option retained for the moment is to lengthen the K_L beam by about 100 to 150 m. This can be achieved by moving the production target upstream by that amount or by prolonging the ECN3 cavern accordingly. The move of the production target would cause major radiation protection issues, in particular at the passage of the Lion river. A mitigation would be extremely complicated, if at all possible, and costly with major civil engineering and iron shielding costs. Also it would mean that the KLEVER experiment would have to be installed on a 10 mrad slope. The prolongation of ECN3 will also have a high cost, but at first sight this solution would be much cleaner from the radiation protection and integration point of view. In this scenario the concept of the K_L beam design can be preserved, but most of the lengths must be scaled. Additional stages of collimation and sweeping may be considered. This long beam option was addressed during the second phase of the PBC studies on a conceptual level and is included in the rough cost estimate we made in the executive summary of this document.

5.5 Intensity Limitations

5.5.1 The existing situation

For NA62, the nominal beam flux on T10 is 3×10^{12} ppp. The nominal beam intensity of the 75 GeV/c secondary beam is 2.2×10^9 ppp. These intensities are quite similar to the nominal primary and secondary beam intensities for the NA48 experiment (last run in 2002). However, in between the approval of NA48 and operation of NA62 the radiation protection rules and guidelines have changed considerably.

In an underground area like ECN3, with a hermetic zone perimeter physically excluding any access with beam on, the secondary beam intensity for NA62 does not pose particular problems. Activation is limited to the region of the final beam dump and only a part of the small tunnel leading towards that dump is locked with a RP veto. However, the primary beam intensity onto the T10 target leads to significant activation around the target, TAX dump collimators and in general to the front-end of the K12 beamline. Also, the air around the front end of the beamline gets activated and might escape into the part of ECN3 where NA62 is installed and, via the access shafts, into the control rooms and into the environment. After weeks of running, the air activation in ECN3 would impose moderately long cool-down times before allowing access into ECN3 (about 24 hours or more). Therefore, several mitigation measures had to be implemented before the start of NA62 operation.

A double wall with over-pressure inside had to be installed to separate the air volumes of the target zone in TCC8 from the detector zones in the downstream part of the TCC8 cavern and in ECN3. This reduces the waiting time before access to just the time it takes to access anyway. On top of that air locks were installed in the access galleries towards the control rooms on the surface. In addition, it was considered crucial to install massive shielding around the target region in order to restrict air activation mostly to the air volume inside the shielding. However, it was not clear how quickly the activated air could escape into the environment. The initial conservative estimate was that the system would be sufficient for NA62 operating conditions, but with only a small safety margin.

Also, the front-end shielding should help reduce the prompt muon dose outside ECN3 by stopping pions and kaons before they decay into muons. For KLEVER-like intensities a study was needed.

The beam elements and also the experiment itself are protected against beam excursions by a system called P0-survey. It checks the magnet currents and their references with respect to a surveillance reference and moves one of the TAX to dump position in case of discrepancy. The acquisition of the currents and the closing of the TAX hole may take more than one spill and this may become critical with much higher intensities than now.

Yet another issue is the delivery of sufficient protons onto the T10 target in the presence of other users of the T4 target (H6 and H8 beams) and at the same time high intensities on T2 and T4. The T4 target serves as an attenuator for the P42 beam to T10 but also to produce the H6 and H8 secondary beams. The longer the target, the higher the production rates for H6 and H8, but the stronger the attenuation for the primary proton beam towards T10 and the higher the radiation dose produced around the T4 target. The high rate needed on T10 would suggest a short T4 target head, but even then, a proton crisis could occur. One solution could be a by-pass beam, where the vertical beam size at T4 would be made much larger than the thickness of the target plate. In that case most of the beam would pass by the T4 target unattenuated. As the overall rate is high, the small fraction hitting the target would still be sufficient for H6 and H8.

5.5.2 Radiation Protection Aspects: Shielding and Ventilation

Air Activation and Shielding Measures

FLUKA studies from 2011 [97] estimated air activation for NA62 operation, assuming an intensity of 2×10^{11} protons/s over 150 operational days per year. The primary isotope production occurs in the target-TAX zone, which is now enclosed by concrete shielding, as shown in Fig. 66.

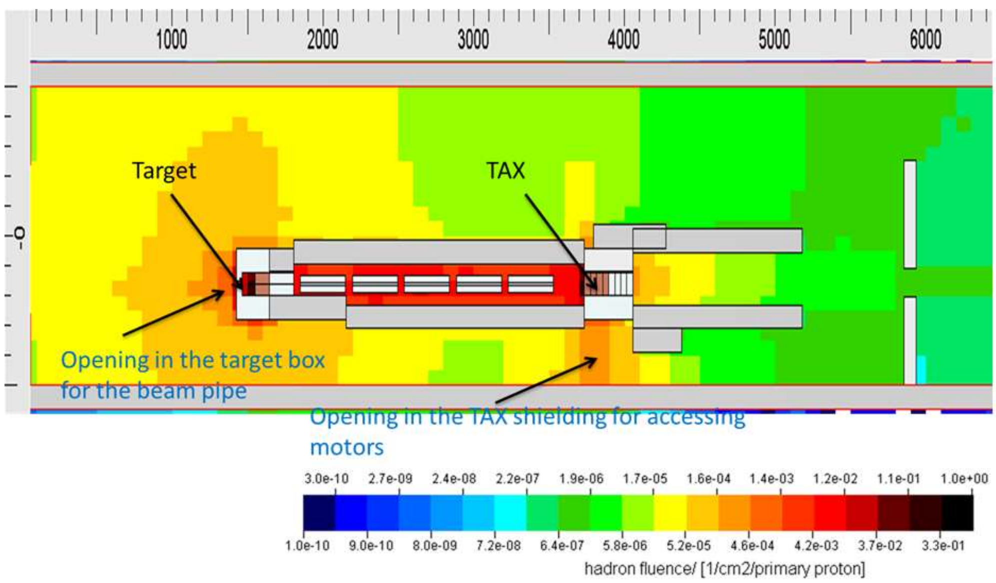

Fig. 66: Hadron fluence per primary particle on T10.

Initially, without a ventilation barrier, a waiting time of 7.5 hours was required for access to ECN3, as illustrated in Fig. 67. To reduce this, an air separation system was installed, including a double-walled containment with overpressure and a controlled ventilation strategy. This system minimises the recirculation of activated air, ensuring that access is possible without additional waiting beyond the standard cool-down period.

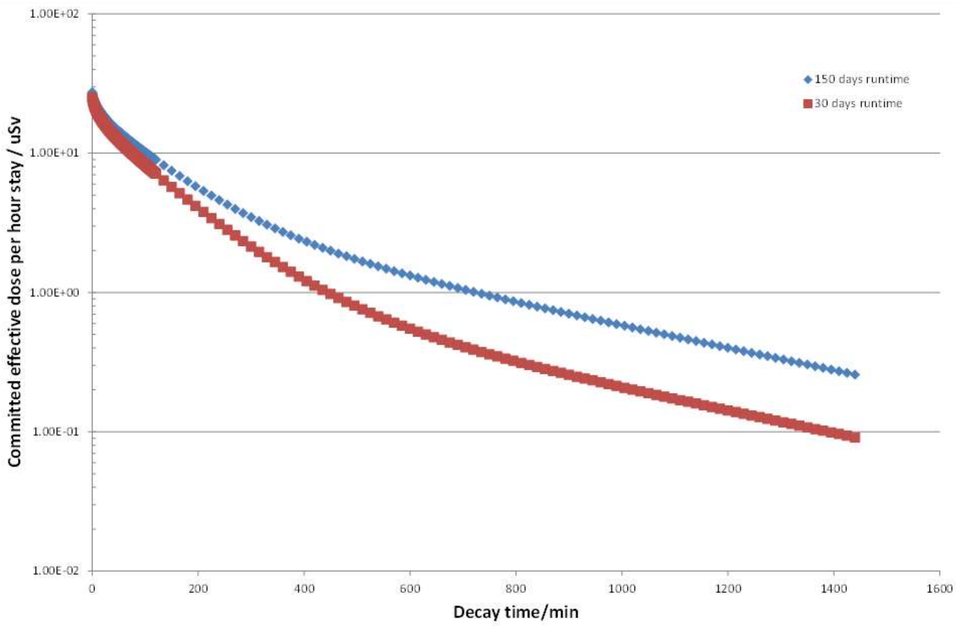

Fig. 67: Effective dose rate per hour in TCC8 and ECN3 after 30 and 150 days of NA62 operation.

Environmental Impact and Air Releases

Simulations [98] predicted an annual release of 59 TBq in TCC8 and 4.2 GBq in ECN3. To meet the public dose objective of less than 10 μSv yr^{-1}, air leakage between these areas was eliminated, and a minimum release delay of 0.5 hours was implemented. This reduced the effective release to 6 TBq, ensuring that 99 % of short-lived isotopes decay before emission.

Measured values in 2017 showed only 0.2 TBq of short-lived isotopes, corresponding to 3 % of the predicted level. The discrepancy can be attributed to a lower actual proton flux of 7.7×10^{17} protons in 2017, which was a factor of 3.4 below the assumption in simulations. Additionally, isotope decay during machine stops and air drift delays contributed to the difference. Simulation uncertainties in geometry and isotope transport may also play a role. Even with the planned increase in beam intensity to 2×10^{13} protons/s for KLEVER, expected doses remain well below the 10 μSv yr^{-1} threshold.

Prompt Dose Considerations

Muon production in the beamline contributes significantly to prompt dose levels above ECN3. FLUKA simulations for 2×10^{11} protons/s were conducted using a conservative soil density of 1.2 g cm^{-3}. Surface dose rates peaked at 6 to 7 μSv h^{-1}, leading to an annual dose estimate of 22 mSv for 150 operational days. With a more realistic soil density of 1.9 g cm^{-3}, expected hadron fluence was reduced by a factor of approximately 30, resulting in a maximum surface dose of only 0.045 mSv yr^{-1}, as shown in Fig. 68.

For KLEVER, updated simulations confirmed manageable dose rates in critical areas, except for the PP851 access building, where neutron dose rates of 20 μSv h^{-1} were found (Fig. 69). To mitigate this, additional shielding will be required. The downward beam steering at 8 mrad will help, but further localised shielding solutions must be implemented.

Muon dose rates were highest at the exit from the ground, reaching 70 μSv h^{-1}, as illustrated in Fig. 70. Several shielding options are under study, including additional shielding above the TAX and the use of magnetised iron blocks similar to those in the M2 beamline.

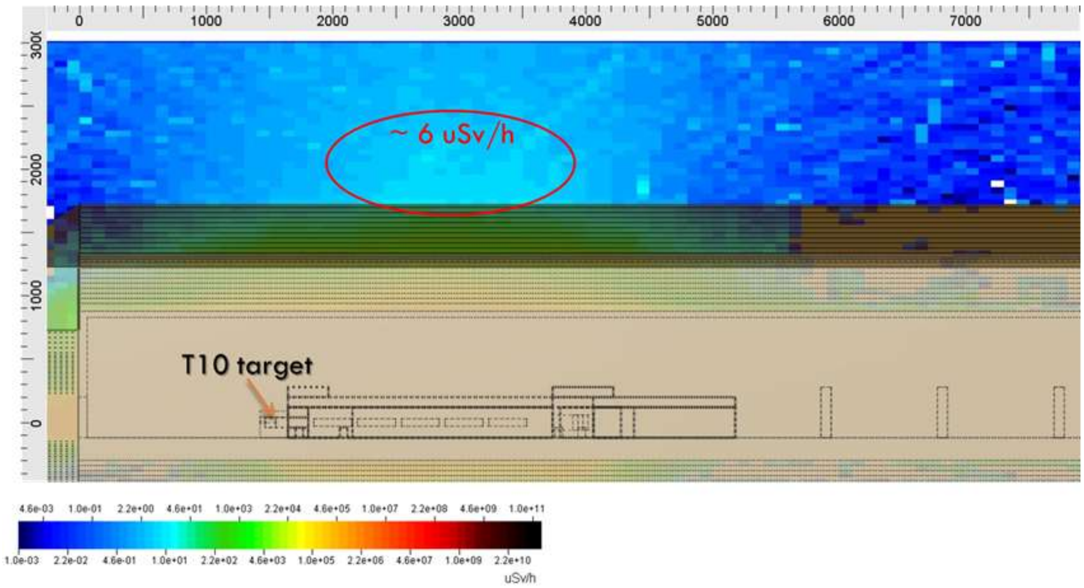

Fig. 68: Dose rates above TCC8.

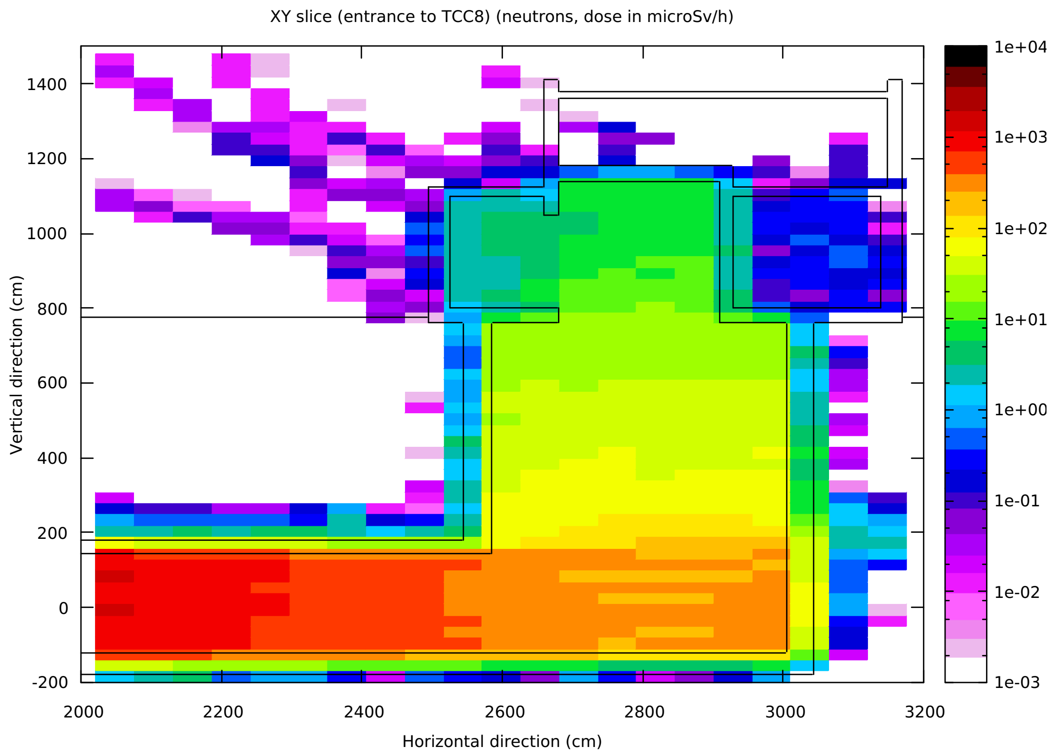

Fig. 69: Dose rates at the TCC8 access shaft.

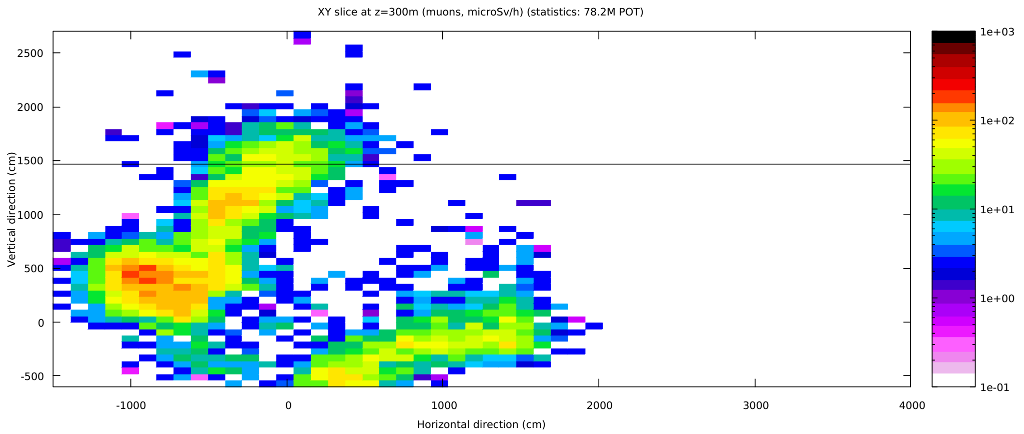

Fig. 70: Muon equivalent dose rates at the ECN3 ground shield exit.

Measured Prompt Dose and Monitoring

Environmental monitoring confirmed compliance with public dose limits. In 2017, the highest recorded dose was 0.27 mSv at the SMS816 monitoring station. The dose contribution was split evenly between neutrons and muons. If scaled to KLEVER beam intensities, this dose would exceed public safety thresholds in transfer lines, requiring further shielding. Additional studies of accidental beam loss scenarios are necessary, and an interlocked monitoring system is under consideration.

Survival of K12 TAX

The K12 TAX, a large collimator 24 m downstream of the T10 target, would need to be relocated to 5.5 m for KLEVER. It absorbs beam components not directed toward the detector, including primary protons that do not interact in the target. The existing TAX consists of two vertically movable modules, each with four shielding blocks (two copper, six cast iron) mounted on water-cooled plates (see Fig. 72).

FLUKA simulations (Fig. 73) show significant energy deposition in the TAX, particularly in the first copper block, which absorbs most of the beam power. ANSYS analysis of thermal stress identifies two critical scenarios:

– Initial Beam Impact: A single 4.8 s pulse raises the first copper block above 160 °C (Fig. 74, left side), exceeding the 100 °C operational limit for copper and the 250 MPa stress threshold.
– Steady-State Operation: Sustained beam exposure raises temperatures further (Fig. 74, right side). The copper blocks remain well above safe limits, while the iron blocks also heat up significantly, approaching 727 °C, where structural modifications occur.

These findings confirm that the current TAX design is unsuitable for KLEVER and would require modifications:

– Moving the cooling plate closer to the beam impact zone and extend the coil to enhance heat dissipation.
– Replacing pure copper with CuCrZr alloy, which withstands higher temperatures.
– Removing tungsten inserts from the first and potentially second block to prevent thermal deformation.
– Exploring embedding cooling channels directly into the TAX modules.

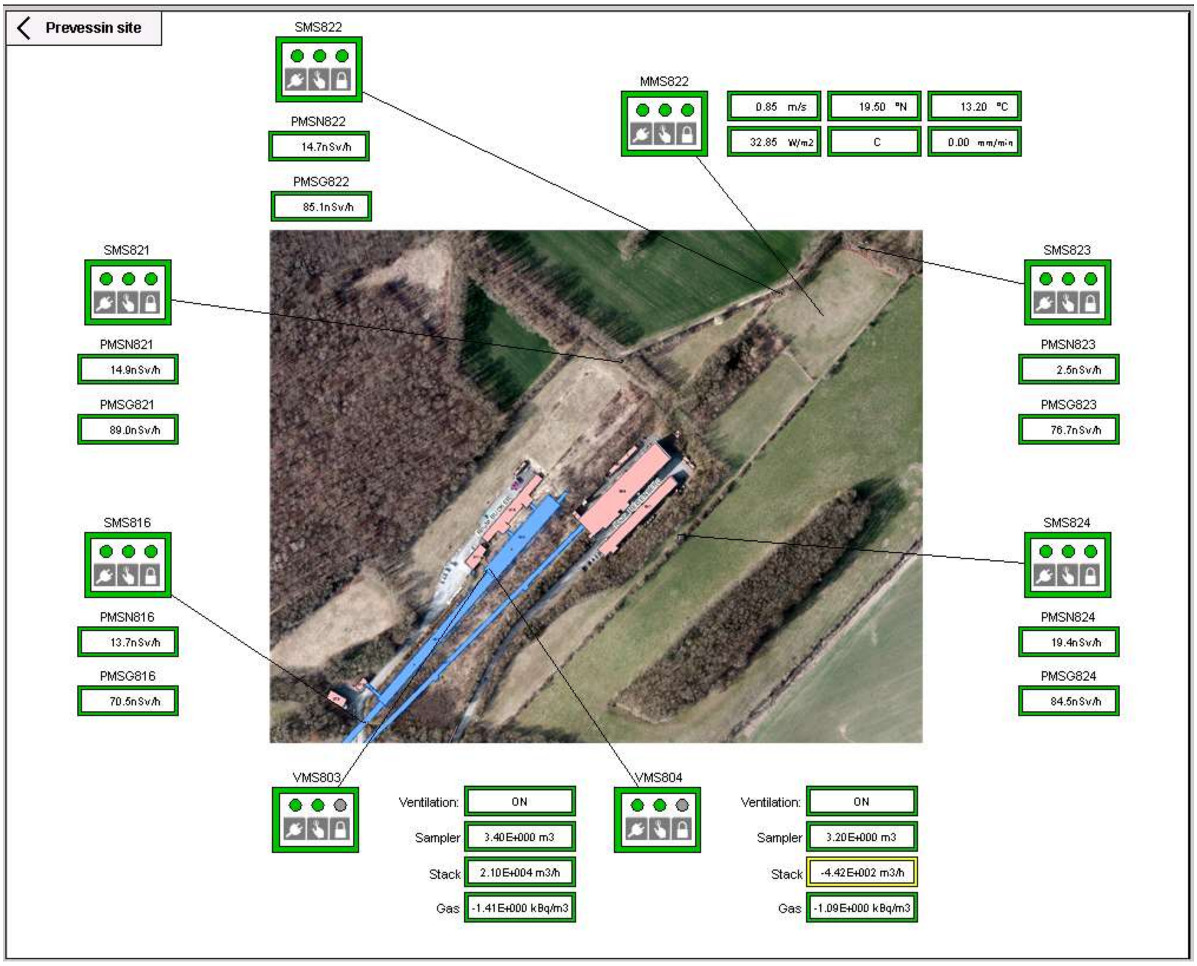

Fig. 71: Stray radiation monitoring stations.

5.6 HIKE Phase 2

Until the time of preparing the Letter of Intent [24] for the HIKE experiment in 2022, KLEVER was the baseline for a next kaon experiment in ECN3. Due to the background issue from $\Lambda \to \pi^0 n$ decays, the mitigation of which could not be sufficiently elaborated within the deadline for a full Proposal to the SPSC, the Collaboration decided to rather concentrate on a second phase proposal concentrating on $\Lambda \to \pi^0 e^+ e^-$ and $\Lambda \to \pi^0 \mu^+ \mu^-$ decays, complemented with a rich programme of other rare decays [23]. This phase could be performed with a neutral beamline very similar to the one described for KLEVER in Section 5.4, with a production angle of 2.4 mrad. The detailed layout of this beam is shown in Fig. 75 and documented in detail in Ref. [99].

Special care has been given to the shaping of the collimator jaws as shown in Fig. 76. The collimators are designed such that any possible scattered particle 'reflected' from the surface does not intercept a downstream collimator, which would in turn create a tertiary background.

A complete 3D model of the HIKE Phase 2 beamline including the surrounding shielding and cavern using BDSIM is shown in Fig. 77. Particle spectra at the end of the beamline are shown in Fig. 78. The equipment and radiation protection studies are very similar to the ones described for KLEVER.

Following the Research Board's decision to allocate ECN3 to BDF/SHiP, the studies were concluded and documented at this point.

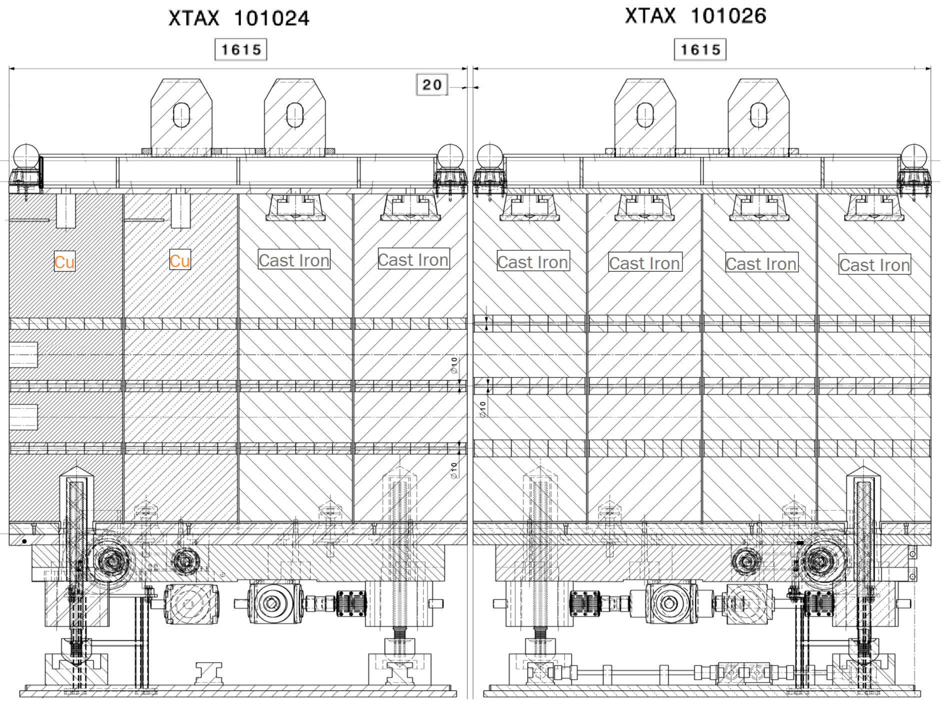

Fig. 72: Layout of the K12 TAX collimator currently used for the NA62 experiment.

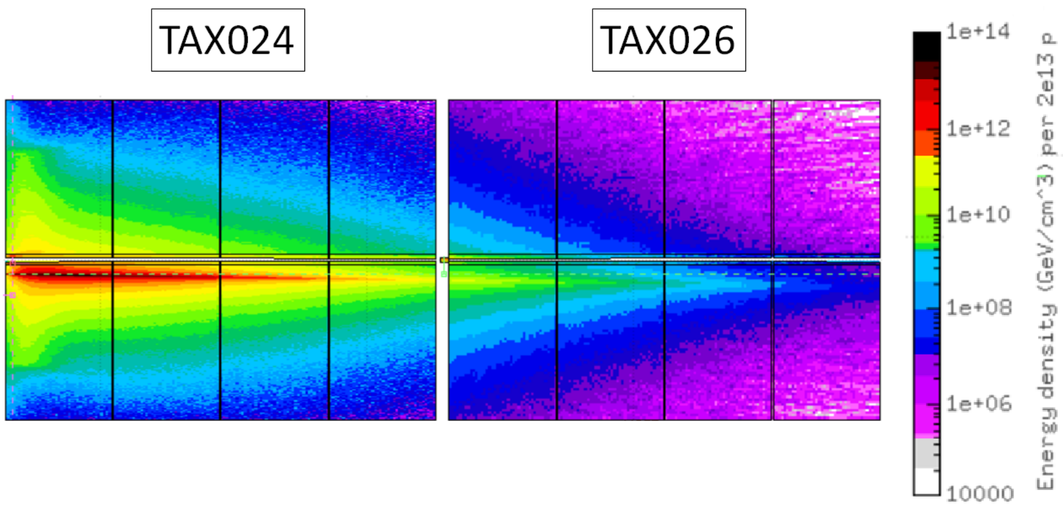

Fig. 73: Energy deposition of one pulse for KLEVER beam in the two modules of the current K12 TAX design.

5.7 SHADOWS

Feebly-interacting particles (FIPs) are particles with masses below the electro-weak scale that may belong to a rich dark sector. They represent a promising avenue for exploring physics beyond the Standard Model (SM), and could help us answer many open questions in modern particle physics. These include the baryon asymmetry of the universe, the nature of dark matter, the origin of neutrino masses and oscillations, cosmological inflation, the strong CP problem, and the hierarchy of scales [100].

The SHADOWS project [39, 101, 102] aimed to be a leader in the search for FIPs in the mass range from a MeV to a few GeV. It planned to use the existing infrastructure and CERN North Area complex, including the TCC8 and ECN3 experimental caverns currently hosting the NA62 experiment. The experiment uses the 400 GeV proton beam from the P42 beamline which will impinge on the closed

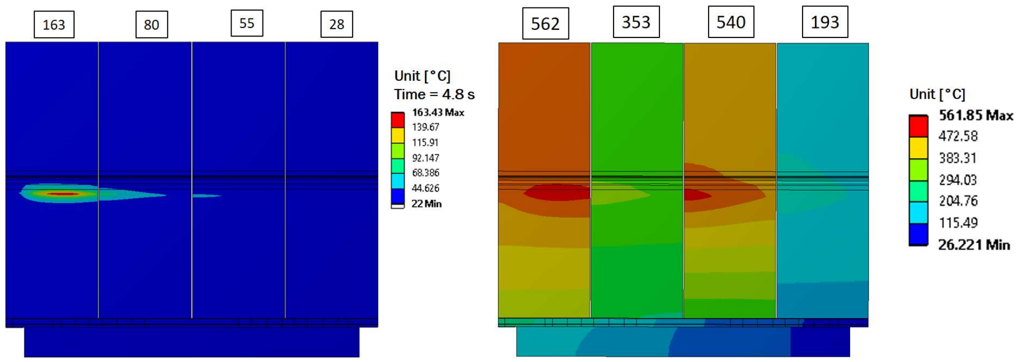

Fig. 74: The temperature distribution in the four blocks and the cooling plate of the first TAX module. Left: At the extraction end of one 4.8 s KLEVER pulse. Right: during the steady state operation of KLEVER. The maximal temperature reached in each of the four blocks is displayed above the block.

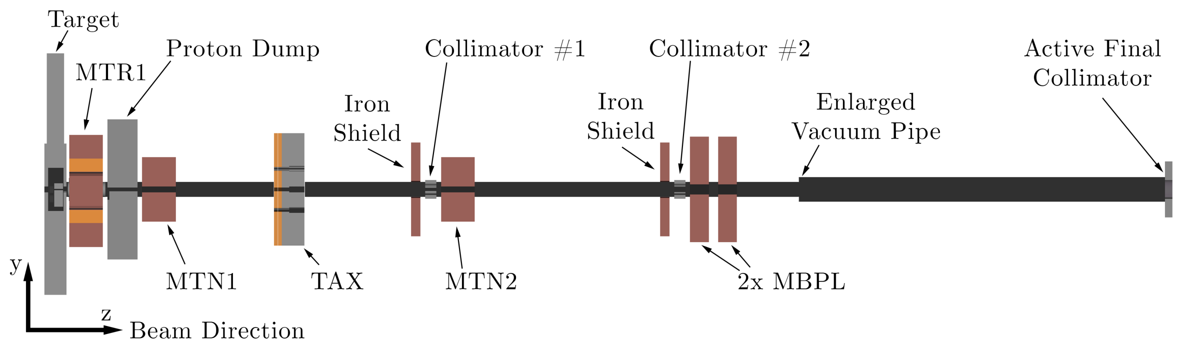

Fig. 75: Overview of complete beamline with the beam travelling from left to right. The view has the longitudinal (z) scale compressed by a factor of 10 with respect to the vertical (y) scale.

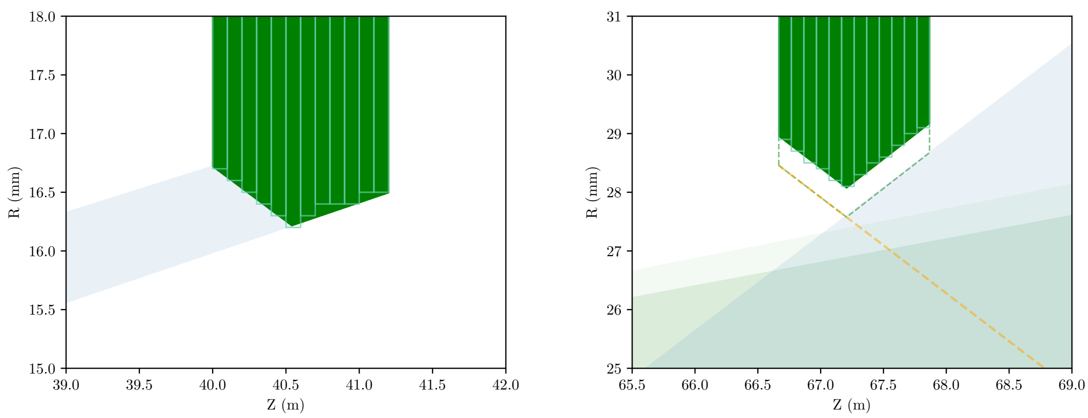

Fig. 76: Close-up views of the design of the first (left) and second (right) collimator jaws on one side. The possible reflections are shown in blue and the nominal cones of the surface in orange.

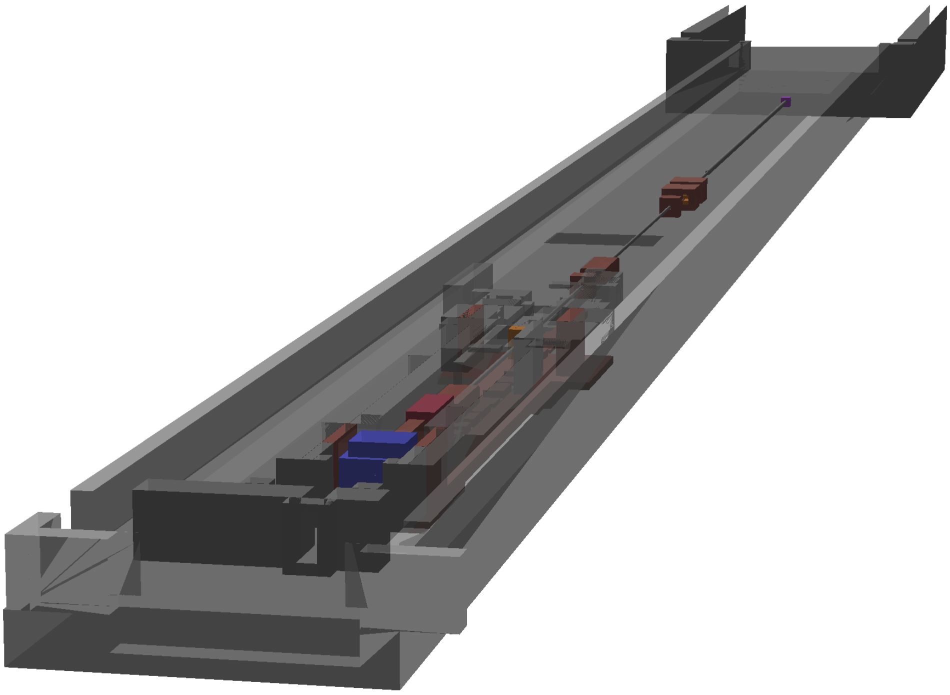

Fig. 77: A 3D view of the HIKE Phase 2 BDSIM model with shielding included. The target housing is shown in blue and the proton dump in red. The beam goes from bottom left to top right. The final active collimator at $s = 120$ m is shown in purple in the distance.

TAX dump-collimator of the K12 beamline (XTAX), which effectively acts as a beam dump and as a potential source of FIPs. By definition, FIPs are feebly coupled to the Standard Model and could thus decay into Standard Model particles [100]. The data taking can be done concurrently with the proposed HIKE experiment when operating in beam dump mode. The off-axis location of SHADOWS allows the experiment to move much closer to the beam dump as the majority of the background, including muons, is created in forward direction and misses the SHADOWS detectors. The NaNu detector [39, 103], downstream of SHADOWS, will in parallel perform neutrino cross-section measurements, particularly of tau neutrinos, in a phase space complementary to that explored by the SND and FASER experiments currently running at the LHC. A conceptual drawing of the detector alongside the K12 beamline is shown in Fig. 79.

5.7.1 The Magnetised Iron Block (MIB) System

The SHADOWS Muon Shield system [104, 105] aims to further reduce the muon background at the SHADOWS detector. Background muons originate from the XTAX beam dump and are pushed off-axis into the SHADOWS acceptance by the return yokes of two dipole magnets directly downstream of this dump. These magnets are part of the muon sweeping system for HIKE when K12 is running in beam dump mode. Figure 80 shows the illumination by the muon flux immediately after the beam dump and Fig. 81 after the first dipole magnet. A dedicated muon shield is needed to mitigate this off-axis background for SHADOWS.

Three options are available to shield against muons:

– Passive mitigation: Muons loose momentum when they move through dense material due to its stopping power (dE/dx). Especially low-momentum muons can loose enough momentum to be effectively stopped or to fall below the SHADOWS sensitivity. Additionally, multiple scattering causes deviations in their trajectories.

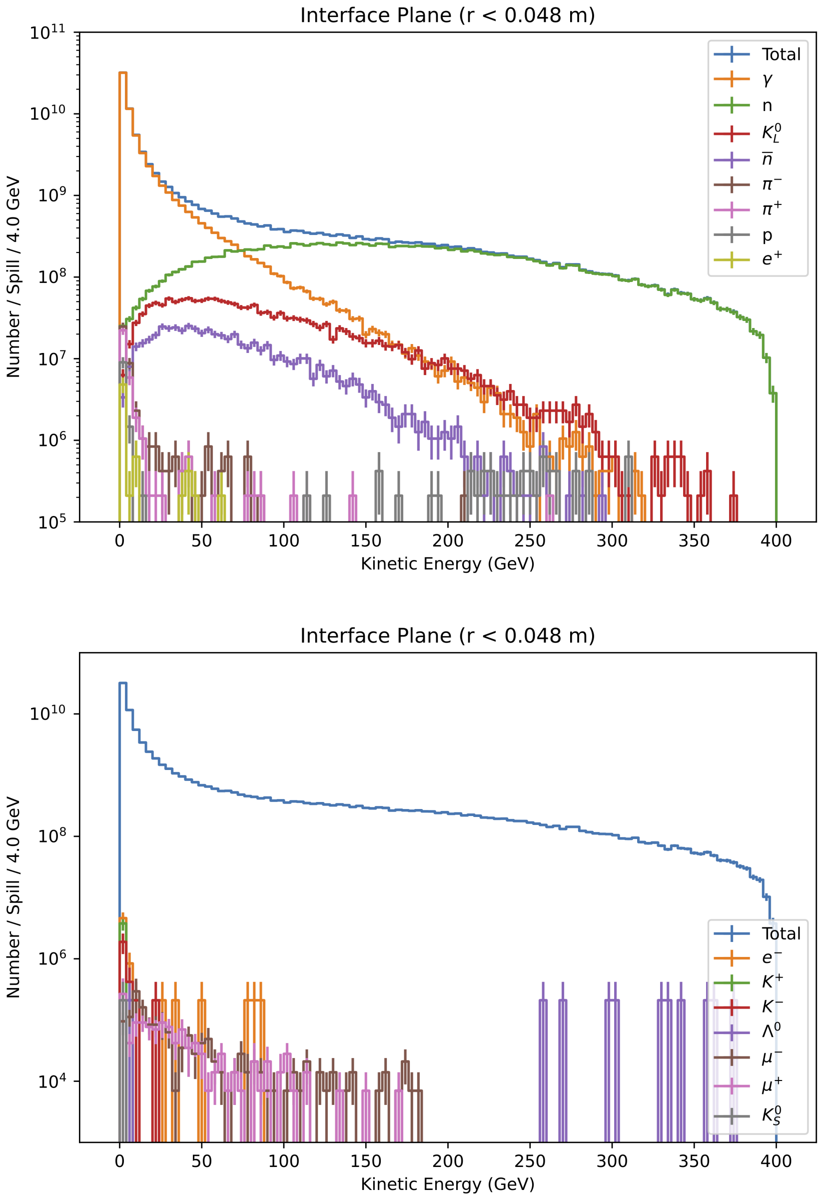

Fig. 78: Momentum spectra at $s = 120\,\mathrm{m}$ at interface plane after collimator #3 with a radial cut of 4.8 cm corresponding to the 0.4 mrad acceptance cone.

– Active mitigation: Magnetic fields can be used to deflect the muons away from the SHADOWS detectors.
– Distance: Muons that emerge from the beam dump have a (predominantly small) transverse momentum. If the detector is placed sufficiently far sideways from the dump, the muon flux within the SHADOWS angular acceptance is reduced.

The SHADOWS muon sweeping system integrates all three approaches by positioning Magnetised Iron Blocks (MIBs) between the beam dump and the detector. This setup enhances the positive effect of the distance between the beam dump and the first tracking detector of the spectrometer, which naturally arises from the length of the SHADOWS decay volume.

The most effective background mitigation in the off-axis region was found to be achieved in two steps. First, positively and negatively charged muons are separated from each other in step 1. In the

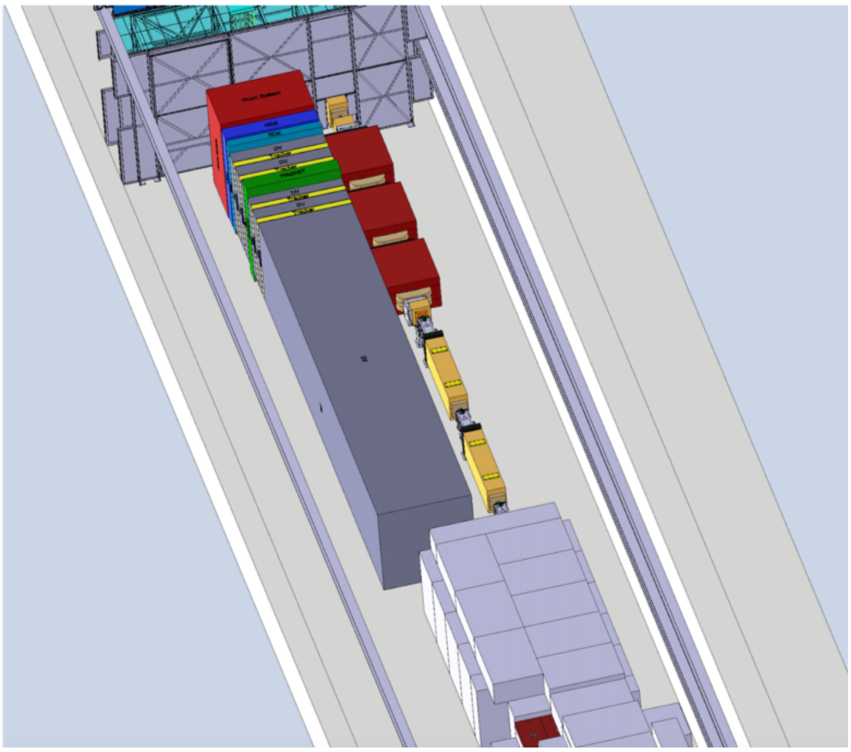

Fig. 79: 3D view of the SHADOWS detector.

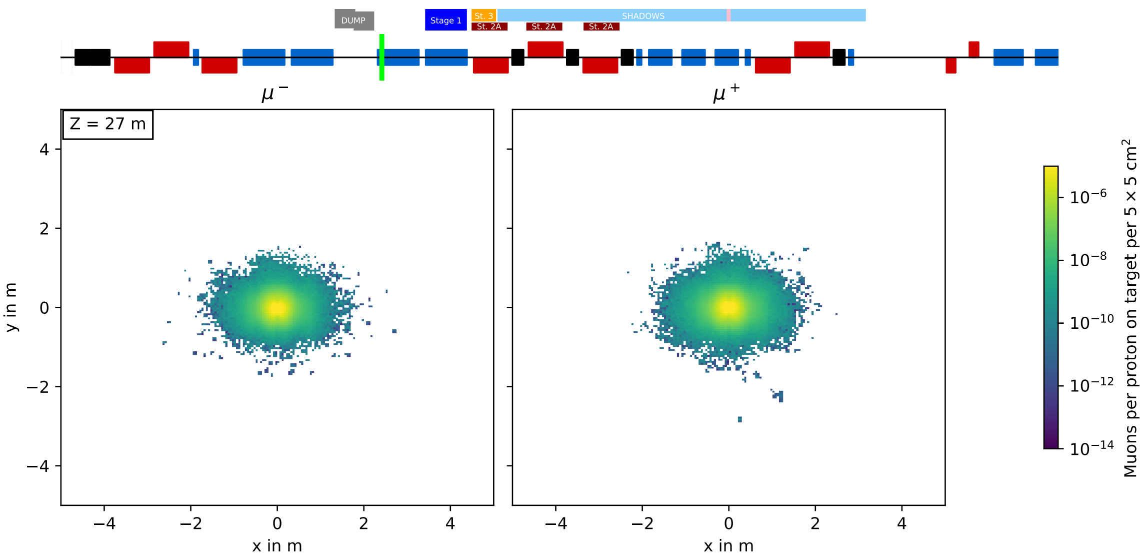

Fig. 80: Muon illumination at the plane corresponding to $s = 27$ m with respect to the usual K12 target location (after the beam dump, see green line in lattice diagram, left: positive muons, right: negative muons).

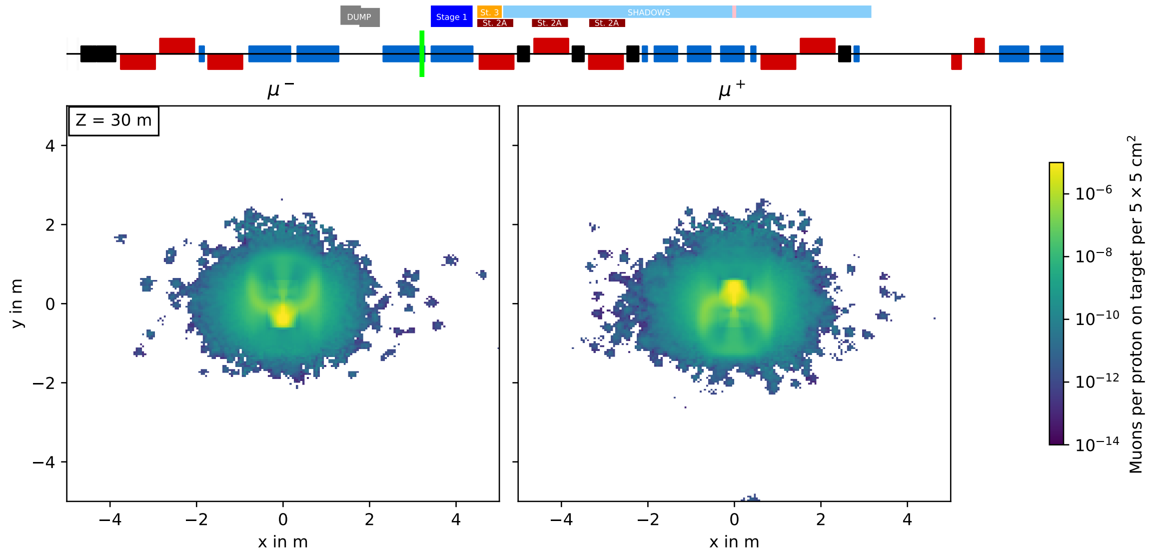

Fig. 81: Muon illumination at the plane corresponding to $s = 30$ m with respect to the usual K12 target location (after the first dipole magnet downstream of the dump, see green line in lattice diagram, left: positive muons, right: negative muons).

second step , the separated muon charges can be effectively swept off-axis. Each of these two steps can be done using figure-8 shaped magnetised iron blocks. The first step is performed by the Stage 1 MIB, and the second step is carried out by the Stage 2 and Stage 3 MIBs. Figure 82 shows a schematic layout of the shape of these three MIBs, along with their design parameters that are optimised separately for each Stage.

Moreover, the magnets are most effective when placed as close as possible to the beamline to ensure maximum coverage close to the beamline and maximum passive mitigation, while at the same time sweeping the muons that enter the MIBs sideways.

Figure 83 shows the setup of the SHADOWS MIB system in top-view. The muons created in the beam dump (purple) are pushed off-axis by the two beamline dipoles just downstream of the TAX (yellow) that reduce the muon background for HIKE in beam dump mode. The 3.5 m-long Stage 1 MIB (blue) is placed alongside the second dipole as simulations show that after the first dipole the muons are already far enough off-axis for Stage 1 to be effective. Stage 2 (red) consists of three MIBs and three passive iron shielding blocks. The first of the three MIBs is placed directly after Stage 1 to move the now charge-separated muons further off-axis. Due to its slim design with a width of only 40 cm, Stage 2 can be placed alongside the SHADOWS detector without having to move the detector further away from the beamline. Stage 3 was added later on in the study and supports Stage 2 in the upstream region before the start of the detector. It pushes the remaining background that is too far off-axis to be in the acceptance of Stage 2 MIBs away from the detector. For this approach to work, the Stage 1 MIB must be run with a polarity that is opposite to that of Stage 2 and 3. The passive iron shielding blocks after each of the Stage 2 MIBs can be easily removed by crane to allow access to the beamline elements when needed. This concept was developed together with an integration expert [106]. Simulations were carried out with a benchmarked BDSIM model of the K12 beamline in beam dump mode [104, 107, 108]. They show that the Muon Shield reduces the muon background at the SHADOWS detector dramatically by a factor of 70.

The impact of Stage 1 on the muon flux is shown in Fig. 84. When comparing this figure to Fig. 81

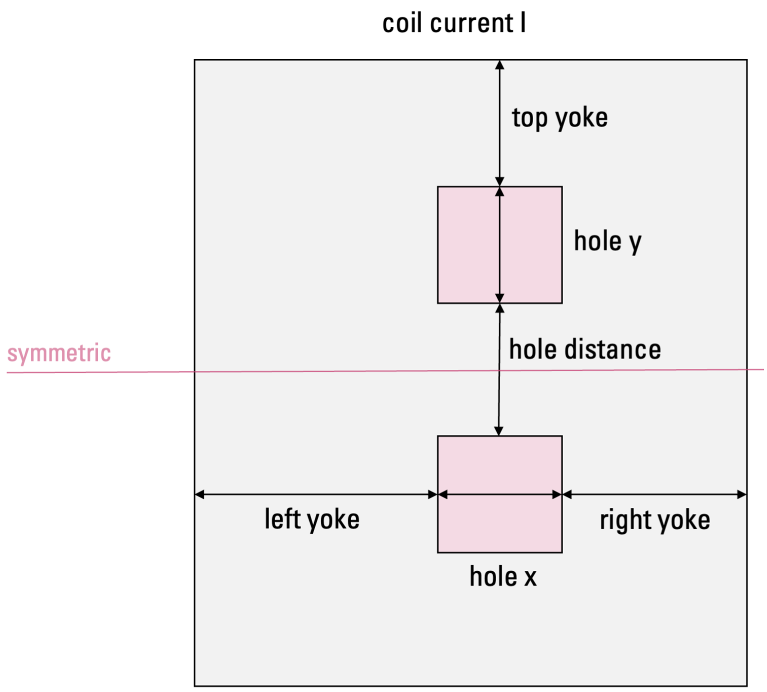

Fig. 82: Conceptual layout of the magnetised iron blocks and their 7 design parameters.

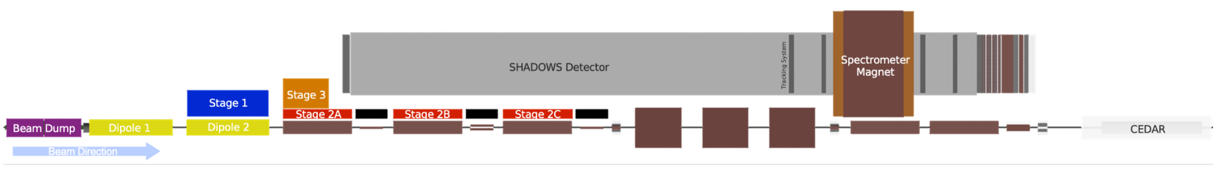

Fig. 83: Conceptual layout of the SHADOWS setup including the muon sweeping system in top view.

one sees clearly that the two muon charges were pushed into separate transverse regions. This allows for more effective sweeping with the Stage 2 and Stage 3 MIBs. Their locations are depicted in Fig. 85. In the current design, Stage 2 impacts the muon background in three ways. Firstly, the separated muon charges from Stage 1 are pushed further off-axis by the far-away side of the yoke. Secondly, the side of the yoke close to the beamline will push back muons that enter the MIBs from the side. Thirdly, Stage 2 acts as a passive shielding for all muons that enter either from the front or from the side. Due to its combined length of about 13 m, i.e. $3{\times}3$ m MIBs and $3{\times}1.4$ m shielding, the stopping power of the iron (about 1 to 2 GeV/m of iron for muons between 1 to 100 GeV) can decrease the energy of these muons by up to about 13 to 26 GeV. This is sufficient to completely eradicate the background component from the side. The length of Stage 3 was studied in detail and was found that 3 m is sufficient to reduce the muon flux sufficiently. To maximise the length of the decay volume, a length of 2 m was finally chosen.

The muon reduction factor of 70 is evaluated by comparing the muon illumination at the start of the SHADOWS Tracking Detector ($1.5\,\mathrm{m} < x < 4\,\mathrm{m}$, $-1\,\mathrm{m} < y < 1.5\,\mathrm{m}$, $s = 57\,\mathrm{m}$). The illumination with the MIB system in place is shown in Fig. 86.

Table 8 provides information on the muon reduction factor for both charges together and for each charge separately. The overall muon reduction factor of 70 results in a decrease of the muon rate within the acceptance from $(166 \pm 17) \times 10^6\ \mathrm{s}^{-1}$ to $(2.37 \pm 0.24) \times 10^6\ \mathrm{s}^{-1}$. Specifically, positive muons are reduced

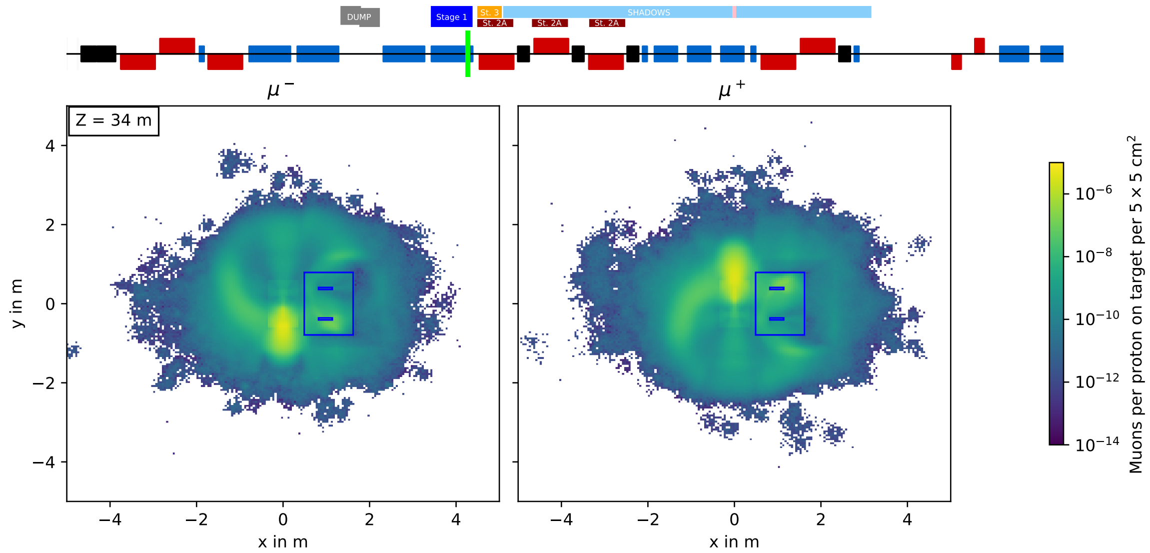

Fig. 84: Muon illumination at the plane corresponding to $s = 34\,\mathrm{m}$ with respect to the usual K12 target location (at the end of Stage 1, see green line in lattice diagram, left: positive muons, right: negative muons).

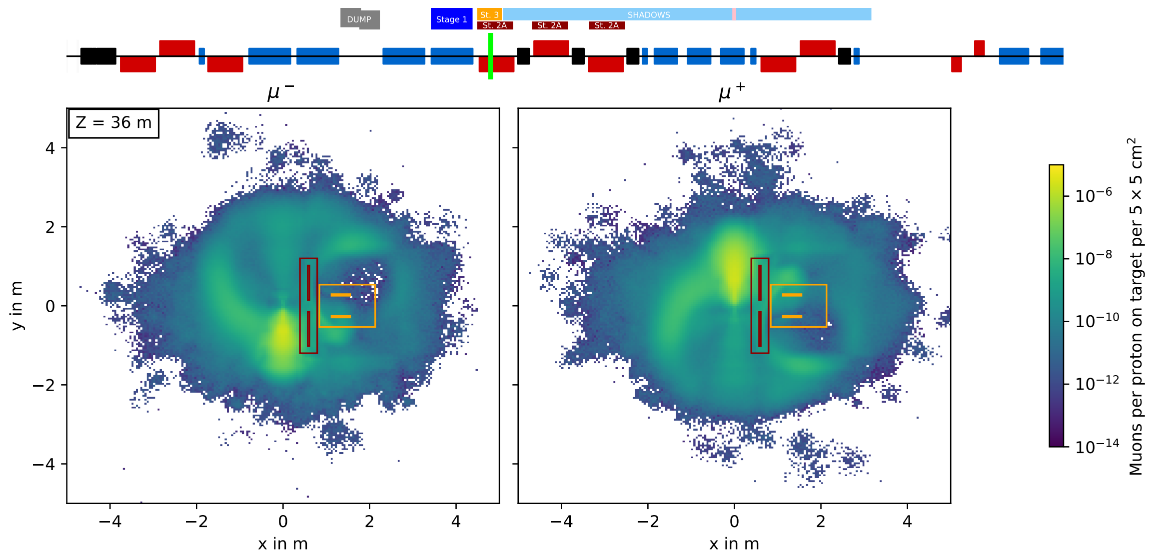

Fig. 85: Muon illumination at the plane corresponding to $s = 36\,\mathrm{m}$ with respect to the usual K12 target location (after the end of Stage 3, see green line in lattice diagram, left: positive muons, right: negative muons).

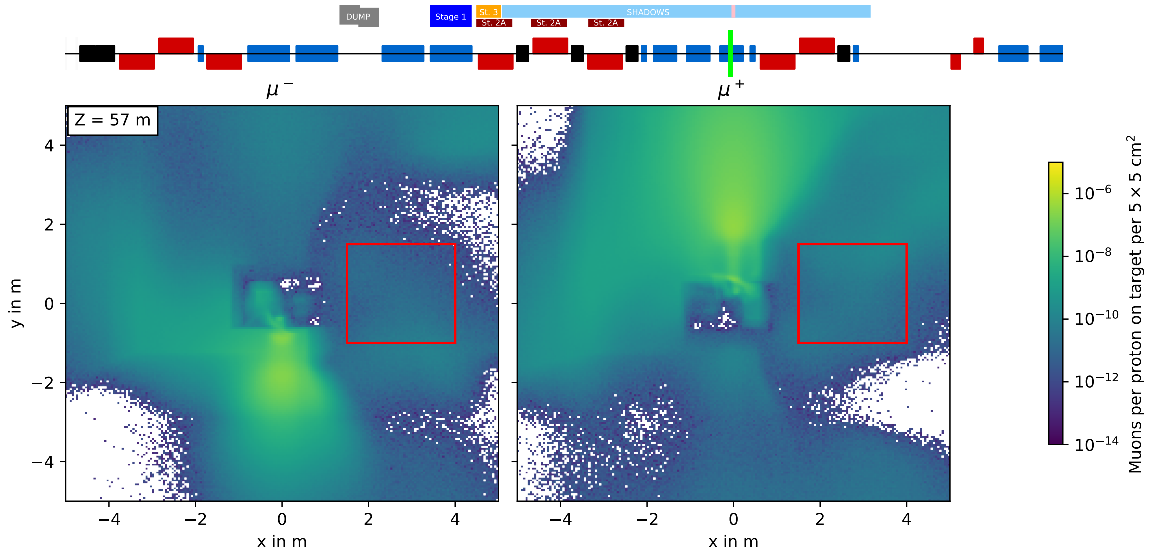

Fig. 86: Muon illumination at the plane corresponding to $s = 57\,\mathrm{m}$ with respect to the usual K12 target location (at the start of the tracking system, see green line in lattice diagram, left: positive muons, right: negative muons).

Table 8: Muon flux rate in SHADOWS acceptance at the level of the first tracking station without and with the MIB for the two charges together and for each charge separately. The calibration factor of 3.39 ± 0.35 between data and simulation that has been found in the off-axis measurement was taken into account in the rate evaluation.

	$\mu^+ + \mu^-$	μ^+	μ^-
Rate without Muon Shield in $10^6\ \mathrm{s}^{-1}$	166 ± 17	91 ± 9	75 ± 8
Reduction Factor	70	58	94
Rate with Muon Shield in $10^6\ \mathrm{s}^{-1}$	2.37 ± 0.24	1.58 ± 0.16	0.79 ± 0.08

by a factor of 58, while negative muons are reduced by a factor of 94. These significant reduction factors were considered sufficient by the experiment. It is worth mentioning that other versions of the muon shield would have allowed reaching background reduction factors up to about 150. However, as these would lead to both higher cost and some decrease in physics discovery potential, a compromise at a factor of 70 reduction is the solution preferred by the Collaboration.

Additionally, the effect of quadrupoles and BEND3 magnets on the muon background for SHADOWS has been studied and was found negligible due to their downstream position with respect to the SHADOWS decay volume. The impact of the MIBs on the background in the HIKE detectors has been investigated, both for kaon and beam dump mode, and was found negligible.

5.7.2 Optimisation of the MIB Designs

In this section, we describe in detail our approach to designing the magnetised iron blocks and the optimisation process that we use. To understand the design choices, it is important to recall the purpose of Stages 1,2, and 3.

Stage 1 aims to achieve efficient vertical charge separation of the muon background, which demands a strong magnetic field in the horizontal direction (x-direction) alongside the K12 beamline. Stages 2 and

3 must provide a strong magnetic field in any direction that pushes the muons away from the SHADOWS detector while simultaneously preventing the separated muon charges from recombining. Also, Stage 3 should avoid pushing any muons back into the Stage 2 acceptance. All magnetic fields must be symmetric in the vertical direction (y-direction) and aligned at the same height as the dipole magnets and the K12 beamline to treat both muon charges symmetrically.

To satisfy these requirements, we propose using figure-8 shaped magnetised iron blocks. They consist of an iron yoke with two holes that leave space for the passage of copper coils to magnetise the iron block. Apart from its length in the z-direction, a MIB of this kind can be fully described by 7 design parameters, as shown in Fig. 82. For each MIB, these design parameters need to be optimised separately. The length is then chosen to maximise the passive mitigation while staying within any limitations arising from integration considerations [106]. These include the space available alongside the beamline within TCC8 and ECN3, the weight limit given by the crane and they ensure easy accessibility of beamline elements for interventions.

We used the finite element method code FEMM [109] to model the figure-8 shaped MIB and calculate its magnetic field for any given set of design parameters. The field map was then extracted and utilised to accurately describe the magnet within Monte Carlo frameworks such as `BDSIM` [110, 111]. We used ARMCO iron as material for the yoke and copper for the coils in our simulations, which should be close to the final materials chosen.

A Python framework was created that enabled us to generate FEMM models to simulate a wide range of parameter constellations and extract the respective magnetic field composition. These were used to create a dataset with 40000 figure-8 shaped MIB field map samples with different parameter constellations.

In order to rank them, a measure for the efficiency in mitigating the muon background was defined that combines the energy-weighted muon distribution at the MIB location (from the BDSIM simulation) and the magnetic field (from FEMM) that these muons would traverse. Stage 1 serves to separate the muon charges and Stages 2 and 3 to sweep away the muons. Instead of using the best performing MIB sample, the data-set was used to train a Deep Neural Network (DNN) to predict the efficiency for any given set of MIB design parameters, which could then be used to fine-tune the design. We made sure that the loss function of the DNN converged and that common quality metrics for regression were met to guarantee that the DNN makes reliable predictions. The DNN was used to optimise the design parameters even more. The optimal design parameters as predicted by the DNN were then forwarded to FEMM to validate that the efficiency really increased due to this process. Once the Stage 1 MIB was optimised, the process was repeated for Stage 2 and 3, whose muon distribution then already took into account the impact of Stage 1.

The optimised MIBs were then implemented in the final BDSIM model to evaluate the impact of the MIB system on the muon background. The optimised parameters for all three Stages are presented in Table 9. Fig. 87 shows these optimised MIBs for each Stage and their magnetic fields. The beamline would be located at the left hand side. More details on this optimisation study can be found in Ref. [104].

Table 9: New MIB design and dimensions compared with the ones used in the LoI. The current is always assumed to be 100 A and the size is given in the format (x,y,z).

Design	Stage 1	Stage 2	Stage 3
active	1.1 m×1.6 m×3.5 m	3×(0.4 m×2.4 m×3 m)	1.3 m×1.1 m×2 m
passive	–	3×(0.4 m×2.4 m×1.4 m)	–

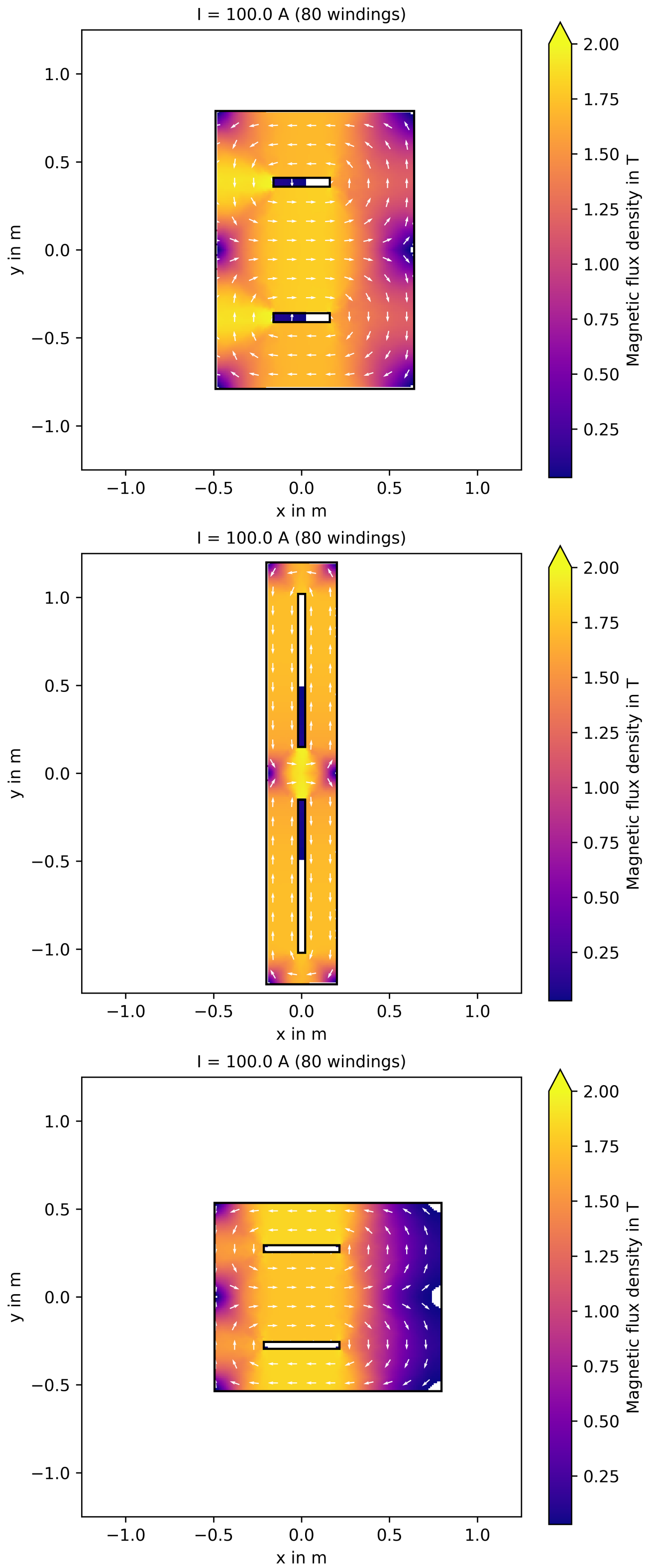

Fig. 87: Preliminary design of the Stage 1 (top), Stage 2 (middle) and Stage 3 (bottom) MIBs. Magnetic field computed using FEMM. The K12 beamline would be located at the left-hand side of the magnets.

5.7.3 Dedicated Muon Shield for NaNu

The NaNu experiment is a proposed neutrino detector that was included in the SHADOWS proposal [39]. Its aim is to study neutrino interactions using an emulsion detector positioned immediately downstream of SHADOWS as shown in Fig. 88. Given that tau neutrinos remain the least experimentally explored Standard Model particle, NaNu seeks to enhance the detection of tau and anti-tau neutrinos produced in the high-energy proton collisions with the beam dump. The experiment would operate alongside HIKE and SHADOWS when K12 runs in beam dump mode, complementing other neutrino research efforts like DUNE, FASER, and SND.

Similarly to SHADOWS, a major challenge for the experiment is the presence of muon backgrounds, which leave tracks in the emulsion detector that incrementally increase the track density over time. This necessitates frequent emulsion exchanges and therefore increases operational costs.

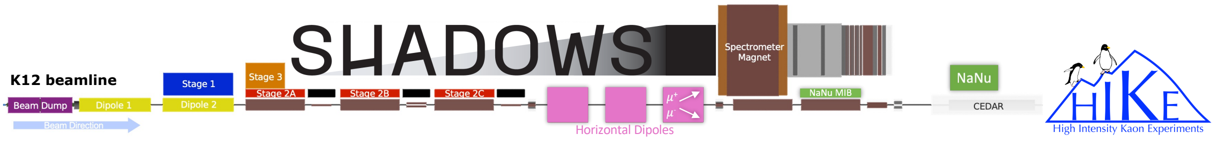

Fig. 88: Experiment setup from the beam-dump (purple) downstream (beam direction left to right). The NaNu setup is shown in green and the horizontal dipoles relevant for the muon background are pink.

While the off-axis muons from the proton dump have been eradicated by the SHADOWS Muon Shield, the dominant background component at the NaNu detector ($0.6\,\mathrm{m} < x < 1.6\,\mathrm{m}$, $-0.25\,\mathrm{m} < y < 0.25\,\mathrm{m}$, $s = 73\,\mathrm{m}$) arises from the K12 muon sweeping dipoles, BEND3, as can be seen in Fig. 89. These dipoles sweep positive muons into the acceptance of the NaNu detector and negative ones to the other side of the K12 beamline.

Studies were performed to mitigate this, concluding that the most effective and feasible solution is the implementation of an additional figure-0 shaped MIB (see Fig. 90). This MIB actively deflects positive muons away from the NaNu location through its magnetic field, while at the same time passively absorbing low momentum muons in its dense material.

The design of the NaNu MIB required careful optimisation and was carried out in the same fashion as for the SHADOWS MIBs considering factors like power constraints, spatial limitations, and weight restrictions due to crane capacity. Using finite-element and BDSIM simulations, we found that an optimal MIB design could reduce muon backgrounds by 55 %, significantly decreasing the frequency of required emulsion exchanges.

The reduction in muon background rates achieved by the SHADOWS and NaNu muon shields demonstrates the feasibility of the NaNu concept. This improvement would even enable the experiment to consider positioning its emulsion detectors closer to the beamline, where muon rates are typically higher. This version is normally referred to as Super-NaNu.

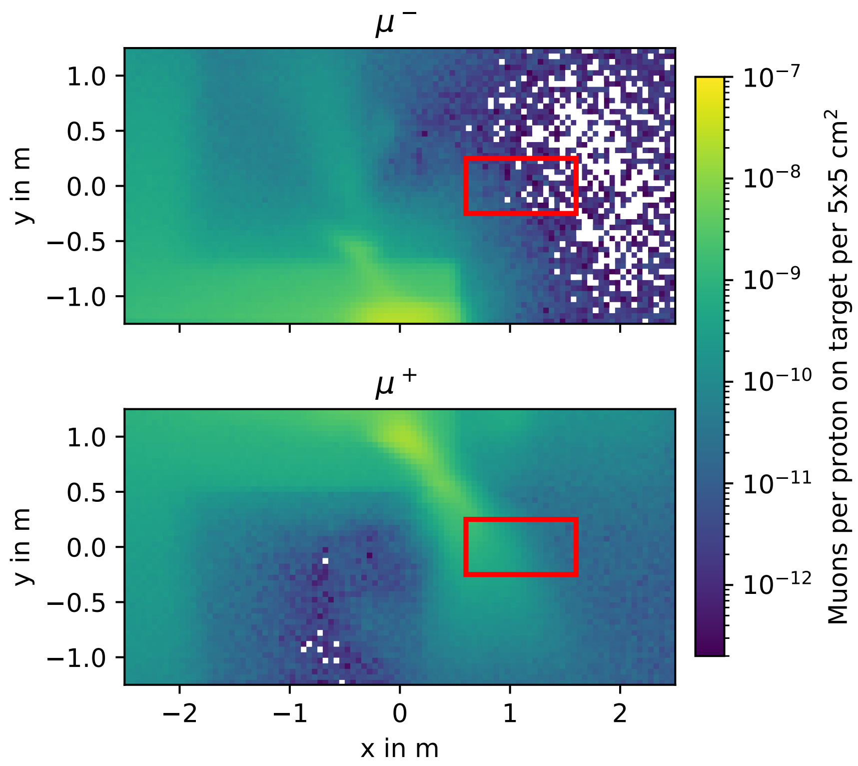

Fig. 89: Simulated muon flux at the NaNu detector (red) without the NaNu MIB. Dominant component: μ^+.

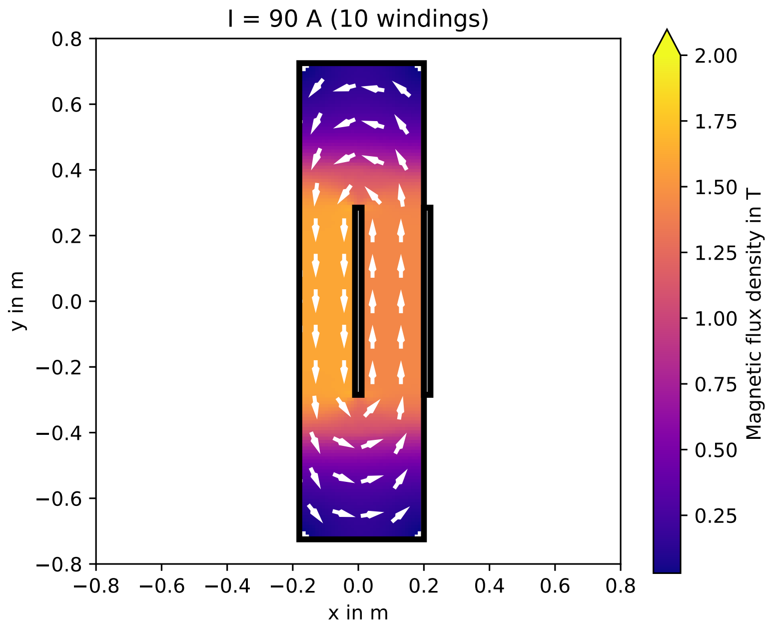

Fig. 90: NaNu MIB with optimised design. The beam axis would be at the left.

5.8 High-intensity Beam Delivery to ECN3

At the end of 2022, three Letters of Intent were submitted to the SPSC Committee: HIKE [23], SHADOWS [39] and BDF/SHiP [20]. In view of the importance and urgency of the final choice of future experiment in ECN3, the CERN management set up the ECN3 Beam Delivery Taskforce [112] in the technical and accelerator sector to study with highest priority all options and complications of providing the requested beam intensities in ECN3 and firmly confirm the feasibility for all choices. The Conventional Beams Working Group continued to work on the HIKE and SHADOWS design downstream of the T10 target, but at lower priority imposed by the requirements of the taskforce. In parallel, the SPSC set up a taskforce to asses the scientific merits of all three proposals.

One important deliverable of the ECN3 Beam Delivery Taskforce for HIKE and SHADOWS was assessing the feasibility of increasing proton beam intensity to the ECN3 experimental cavern. These studies were necessary given that all experiments, including BDF/SHiP, rely on significantly higher beam intensities than those used in previous operations at ECN3, with HIKE aiming at a direct continuation of the charged kaon programme of NA62, while SHADOWS proposed performing searches for Feebly Interacting Particles (FIPs) in beam dump mode. The key challenges identified include the optimisation of proton delivery cycles, the impact of higher intensities on radiation protection, modifications to the beamline infrastructure, and shielding requirements.

5.8.1 Proton Delivery Scenarios and Cycle Structure

The primary consideration for delivering protons to ECN3 is the integration of the HIKE and SHADOWS programmes within CERN's existing accelerator complex, ensuring compatibility with other ongoing experiments and minimising impact on their operations. The study examined different scenarios for proton extraction from the SPS, balancing the need for high beam power while avoiding excessive activation of accelerator components and surrounding infrastructure. The proposed scenarios are summarised in Fig. 91.

Currently, the primary proton beam needed for ECN3 is in the order of 3×10^{12} protons/pulse (ppp) for NA62 operations. However, HIKE and SHADOWS require significantly higher intensities, with the goal of reaching up to 2×10^{13} ppp. The task force evaluated the feasibility of these intensities while considering operational constraints imposed by LHC fills, other SPS users, and the impact on machine protection.

5.8.2 Challenges in Beam Transport and Infrastructure Modifications

To accommodate the increased proton flux, several modifications to the P42 and K12 beamlines were deemed necessary, such as new magnets replacing the old, irradiated ones to ensure a stable operation over the life time of the facility.

For SHADOWS, which operates in beam dump mode, the main requirement is maximising acceptance for particles emerging from the proton interactions while minimising background from hadronic showers. The placement of the SHADOWS detector must ensure a balance between these constraints while maintaining compatibility with HIKE operations. A preliminary integration study confirmed that SHADOWS could be positioned off-axis from the primary beam dump to minimise direct exposure to high-energy hadrons while still capturing the FIP decay signatures it aims to detect.

5.8.3 Radiation Protection Considerations

As stated before, with higher intensities, radiation protection becomes a central concern, particularly regarding prompt dose rates, air activation, and environmental impact. The ECN3 task force proposed significant shielding enhancements that would significantly reduce the radiation footprint, in particular to outside the facility, e.g. through ground activation and muon radiation at the CERN fence. Additional measures would be required to handle activated air and potential contamination in the target area.

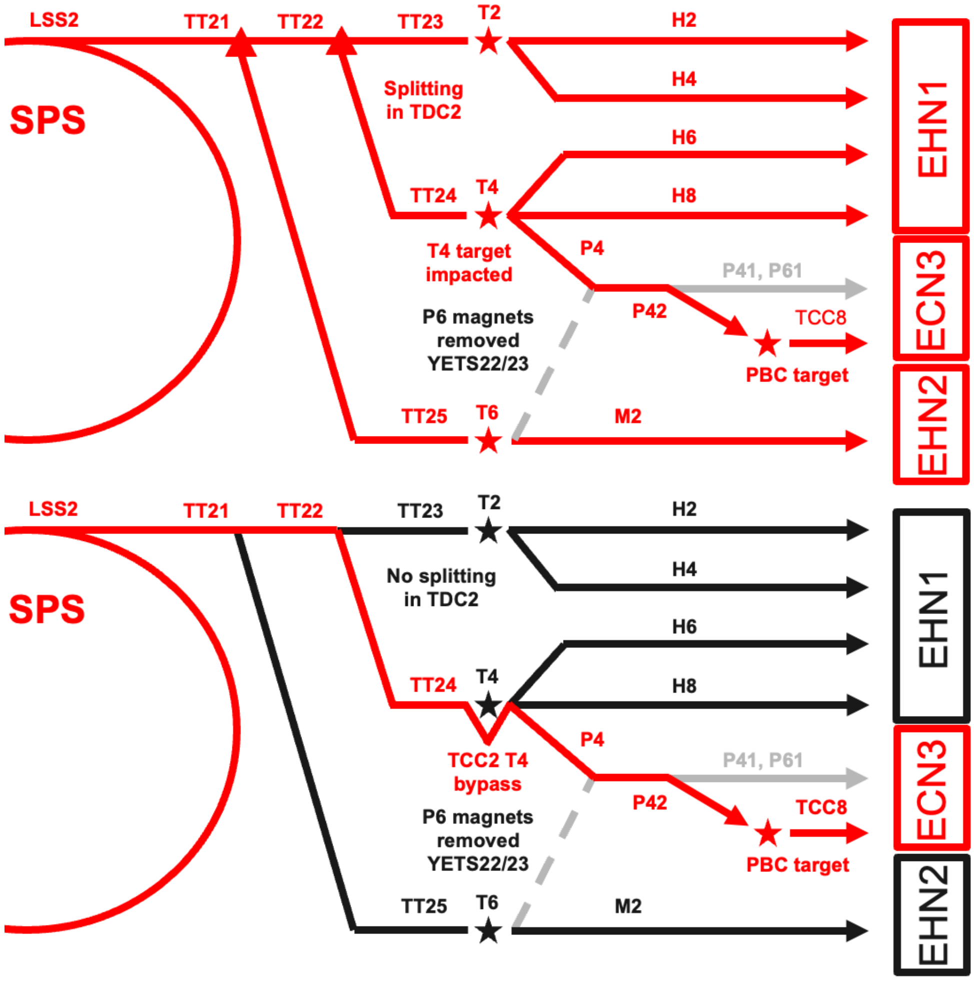

Fig. 91: Schematic diagram of the two ECN3 beam delivery scenarios considered. Top: Shared ECN3 scenario, similar to today's operational scenario. Bottom: Dedicated ECN3 scenario.

Additionally, the impact of increased intensity on residual radiation in beamline components was assessed. The higher fluence of secondary particles will lead to increased activation of accelerator components, necessitating stricter access protocols for maintenance. The task force recommends improved remote handling capabilities for highly irradiated components, ensuring safe operation and maintenance in the long term.

5.8.4 Feasibility of HIKE and SHADOWS Coexistence

The task force concludes that both HIKE and SHADOWS could operate within ECN3, provided that the necessary infrastructure upgrades are implemented. However, several technical challenges would remain. The optimisation of beam-sharing schedules, the refinement of shielding configurations, and the integration of enhanced radiation protection measures would need to be studied in detail during a TDR phase to allow for a realistic implementation. The recommendations outlined in the task force report form the basis for further design refinements and preparatory work required for a potential full implementation of HIKE and SHADOWS in ECN3.

In summary, the task force confirms that high-intensity proton delivery to ECN3 is feasible, but requires significant infrastructure modifications and upgrades, which would need to be compatible with the North Area Consolidation project (NA-CONS). The proposed cycle structure ensures compatibility with other SPS users, while shielding and radiation protection upgrades are essential to maintain safe operation. The full report can be found under Ref. [113]. A comprehensive summary including the physics potential of HIKE and SHADOWS can be found in a dedicated PBC report [114].

5.9 Continuation of the Studies

The three experiments submitted their full Proposals to the SPSC Committee towards the end of 2023. The science cases of all three experiments were considered outstanding but a objective comparison between BDF/SHiP and HIKE plus SHADOWS was difficult for the committee, due to the very different nature of the projects. In the end the CERN management decided to select BDF/SHiP as the future experiment in the TCC8 and ECN3 caverns. The technical implementation of the beam and infrastructure upgrades has now been mandated to the HI-ECN3 project, which works in close synergy with the North Area consolidation project. Following this decision, the studies for HIKE, SHADOWS, and NaNu were discontinued.

A further study on a continued CERN kaon programme at the SPS or at another, future accelerator remains a possibility. Should there be interest, such a study could be pursued within PBC-CBWG.

Chapter 6

Projects Related to Neutrino Physics

Anna Baratto Roldan, Nikolaos Charitonidis, Marc Jebramcik, Carlo Alberto Mussolini, Elisabetta Giulia Parozzi

6.1 Introduction

At the 2021 PBC annual workshop [8], two proposals for respectively monitored and tagged neutrino beams were presented: ENUBET [115] and NuTag [116]. ENUBET aims for a precise flux measurement (1 % precision) of electron and muon neutrinos stemming from respective K^+ and π^+ decays. NuTag focuses (mostly) on the tagging, i.e. exact measurement of the neutrino kinematics, of muon neutrinos stemming from the two-body $\pi^{\pm}$ decay. Neutrino tagging is considered very helpful for measuring CP violation in the neutrino sector. Both projects are new additions to PBC and to the Conventional Beams working group.

During the 2024 PBC Annual Workshop [117], a combination of ENUBET and NuTag into a single beamline proposal, the Short Baseline Neutrino beamline (SBN), was announced since both proposals have nearly identical beamline requirements and clear synergies. The SBN proposal is strongly based on the ENUBET beamline design and is currently under active development. A beamline layout has been designed and the possible implementation of the beamline at CERN is currently under investigation. Apart from the two new concepts of ENUBET and NuTag, the NA61++ experiment proposes the construction of a classic low-energy beam, dedicated to measurements for neutrino beams. This project has been transferred from the EHN1 subgroup to the new CBWG-NB subgroup due to the targeted physics goals.

6.2 Low-Energy Beamline for NA61++

In order to provide a low-energy beam for NA61++, a short tertiary beam branch is necessary. An implementation of a similar branch has been done elsewhere in the past for the CMS [118] and ATLAS [119] experiments. The low-energy branch for NA61++ would be located in zone PPE132 and PPE142, just upstream of NA61++, which is already a fully shielded zone allowing high intensities on a secondary target. A possible location depicting the position of this tertiary beamline is shown in Fig. 92.

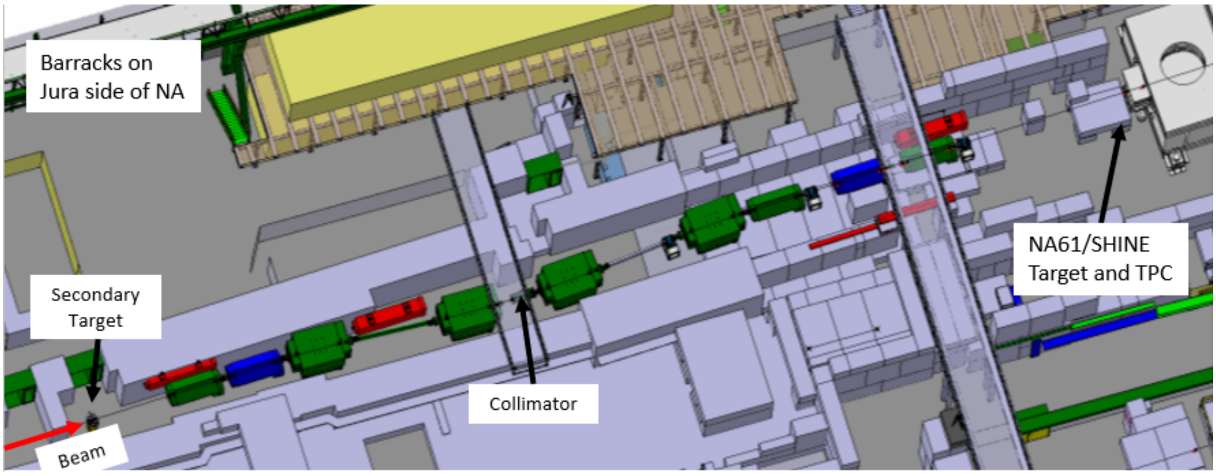

Fig. 92: A possible location for a tertiary low-energy beamline serving NA61++, located in PPE132. The zone is already shielded, thus allowing for intensity required on the secondary target.

A preliminary design of such a tertiary branch has been studied and the corresponding preliminary optics design is shown in Fig. 93.

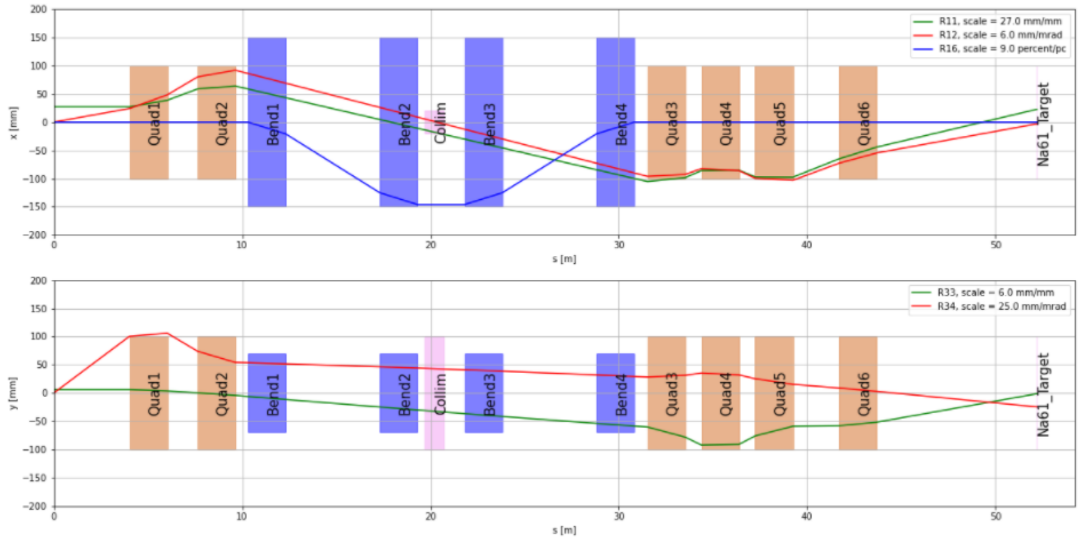

Fig. 93: The proposed first-order optics design for the low-energy tertiary beamline branch serving NA61++. The red line corresponds to the sine-like ray, the green and blue lines are the magnification and dispersive terms, respectively. The deflection angle of the bends is 120 mrad.

The design process has included the study and optimisation of the secondary target for this beamline, as well as the momentum of the secondary or attenuated primary beam impinging on it. The target would be a cylinder of copper or tungsten, with a length of about 200 mm and a diameter of about 30 mm, while studies have shown that a high-momentum beam of 380 to 400 GeV/c impinging on the target is more favourable for the wanted particle rates. Downstream of the target, a quadrupole doublet consisting of large-aperture QPL-type quadrupoles with an aperture radius of 100 mm will focus the low-energy particles at the centre of a momentum-selection collimator. A so-called dogleg configuration, consisting of four MBPL dipole magnets with an aperture of 420 mm $\times$ 140 mm will define the central momentum of the low-energy particles, with a maximum momentum of 13 GeV/c. The total length of the beamline is only about 55 m, thereby allowing most of the low-energy particles to reach the experiment without decaying beforehand. A beam dump consisting of iron and concrete would be placed at the side of the collimator, to stop off-momentum particles and dump any high-energy secondary or primary particles that have not interacted with the target, thereby blocking them or their interaction products from reaching the experiment. A tracking-simulation result of particles transported to NA61++ is shown in Fig. 94.

The beamline has been designed to meet the experimental requirements set out in [120], in terms of particle rates, beam-spot sizes, and momentum resolution. These are summarised in Table 10. For this purpose, extensive simulations of the beamline have been performed in G4BeamLine to ensure that the requirements are met.

In these simulations, an accurate description of the beam produced in TCC2 was used. This beam was then transported throughout the whole H2 beamline until reaching the newly placed secondary target. The simulations used the FTFP_BERT physics list and consisted of 10^6 initial primary 400 GeV/c protons, a reasonable, albeit likely underestimated spill intensity to stay within radiation protection limitations. The expected yields of particles at the NA61++ target, when operating at nominal momenta ranging from 2 to 13 GeV/c and with a $\pm$ 3 cm collimator aperture can be seen in Fig. 95.

In order to meet the experimental requirements, the background must be minimised in each of NA61++'s 50 ns detection windows. For this beamline, the most important source of background will be the high-energy muons produced by the secondary pion decays. These particles ($>$ 30 GeV), which

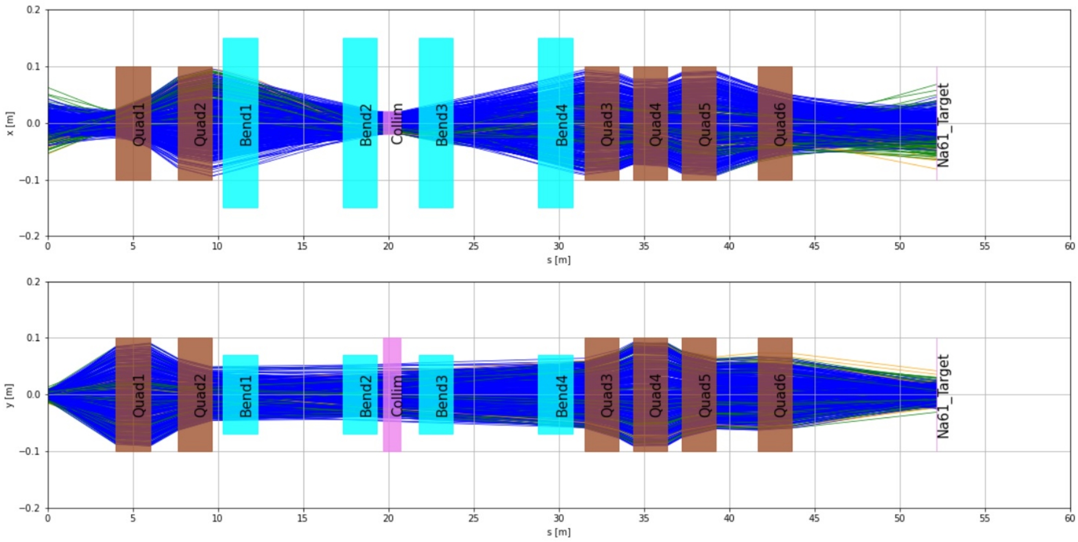

Fig. 94: Accepted particles at a nominal beamline momentum of $p = 13\,\mathrm{GeV}/c$ from their production at the new secondary target to the NA61++ target. The momentum selection collimator is open at $\pm$ 3 cm. Different colours indicate particles with momenta different from the nominal momentum. For blue tracks $\delta p/p < 5\,\%$, for green tracks $5\,\% < \delta p/p < 10\,\%$ and for yellow tracks $10\,\% < \delta p/p < 20\,\%$.

Table 10: NA61++ requirements for the low-energy beamline for future measurements.

Parameters	Requirements
Desired particles	p, $\pi^{\pm}$, $K^{\pm}$
Particle momentum p	2 to 13 GeV/c
Relative momentum spread $\Delta p/p$	< 5 %
Minimum rate	50 particles/s
Maximum rate	< 1.5×10^4 particles/s
RMS beam size in both planes at NA61++ target	20 mm

practically cannot be stopped by any reasonable shielding, have been simulated and they correspond to only about 3 % of the triggering particles. At the same time, lower energy halo muons originating in the last straight section of the secondary beamline and travelling outside the beam pipe could be hitting the detector. In addition, some low-energy muons from the decay of low-energy pions within the apertures of the VLE line dipoles can also find their way into the detector. For these latter, low-energy muons could, however, be deflected away by optimising the shielding or implementation of magnetised iron blocks (MIBs). However, the first studies that are considering the 50 ns timing window of the NA61++ TPC, are indicating that very few dangerous background particles are detected in the experiment.

The momentum resolution of the beamline has also been calculated, including the effect of modifying the collimator's aperture on the particle rates. The beamline is able to achieve the desired momentum resolution of a $\Delta p/p$ of less than 5 % already with a collimator opening of $\pm$ 3 cm, however, better resolutions can also be achieved at the cost of particle rate, by further closing the collimator jaws. The effects of closing these on the achievable momentum resolution can be seen in Fig. 96.

The requirements for the beam-spot size, can be met at both, 2 and 13 GeV/c, as can be seen in Fig. 97. The same stands for all intermediate momenta. It can be concluded that the proposed beamline design is suitable to meet all the requirements of NA61++.

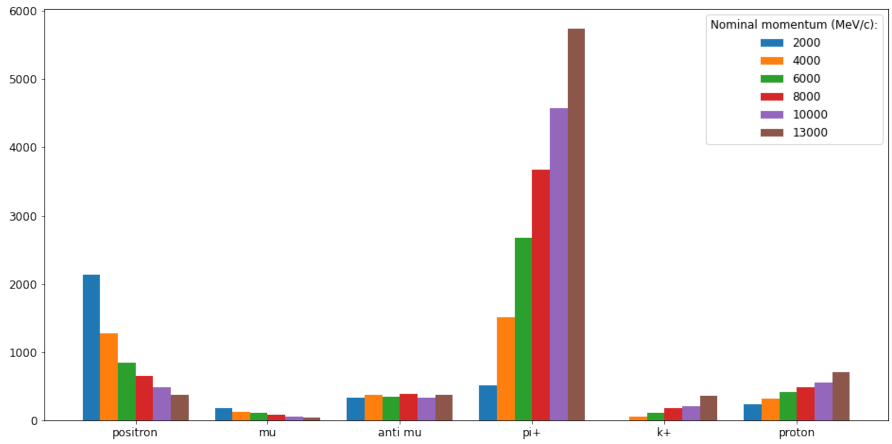

Fig. 95: The number of particles from 2 to 13 GeV/c reaching the NA61++ target from one SPS spill of 10^6 primary protons.

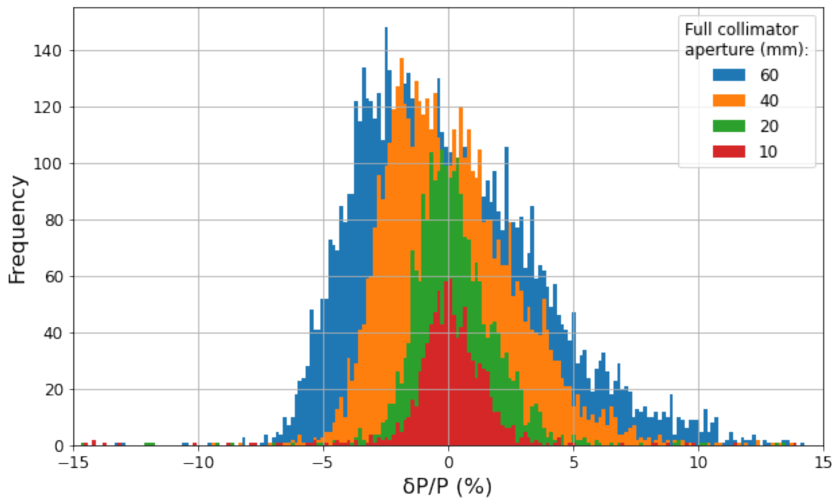

Fig. 96: The momentum resolution of protons, pions, kaons, and positrons reaching the NA61++ target as different collimator jaw openings are used to perform momentum selection.

6.2.1 Particle Identification Techniques

All the delivered particles to the experiment must be tagged and identified to be used in later analyses. To this end, significant studies have been performed to come up with a particle identification detection (PID) scheme that will enable particle-by-particle identification in the whole available momentum range from as low as 2 GeV/c up to the upper limit of 13 GeV/c.

The specific range of momenta at which the beamline will operate has proven to be particularly challenging, as two different types of technologies will need to be used to ensure full particle identification. Specifically, the lower end of the momentum range can be addressed using a time of flight (ToF) system with a 500 ps time resolution, which can be achieved by using only NA61++'s silicon detectors, while for the upper end a system of Cherenkov counters can be used. The intermediate energies will need to be

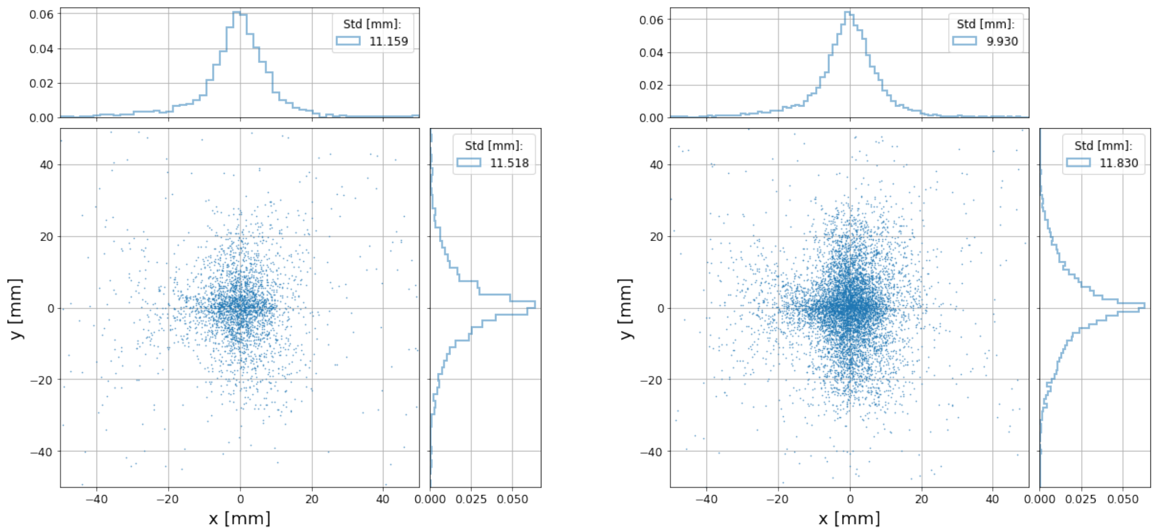

(a) 2 GeV/c (b) 13 GeV/c

Fig. 97: The beam spot size at the NA61++ target at (a) p = 2 GeV/c and (b) p = 13 GeV/c.

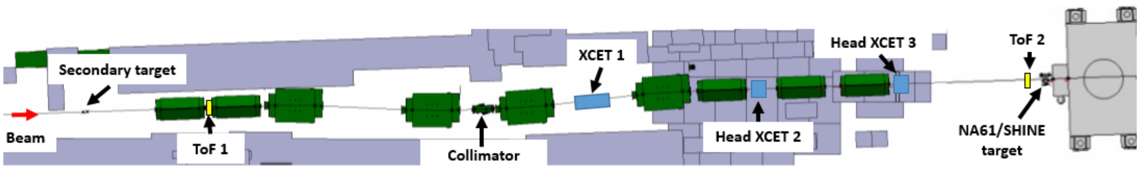

Fig. 98: Position of the instrumentation which will equip the low-energy beamline branch.

covered by the use of a combination of the two systems. This combination has been designed specifically to address the requirements of NA61++ while also minimising the material budget in the beamline, as this may otherwise cause a spot size enlargement at the position of the NA61++ target. The placement of this instrumentation can be seen in Fig. 98, while the settings of the various Cherenkov counters and which detector will be used for each particle can be seen in Table 11.

The studies concerning this beamline cannot continue further unless the project is approved. The proposal for the necessary Engineering Change Request (ECR) is documented in Ref. [121].

6.3 ENUBET

ENUBET [21, 22] has already been approved at CERN as a Neutrino Platform experiment (NP06) and has received funding via an ERC grant. The physics scope of this project has been the preparation of a site-independent design of a kaon and pion-tagged neutrino beam in the GeV/c range that will vastly improve the systematic uncertainties on the $\nu_{e/\mu}$ cross-sections. It includes a new beamline design that allows the exploration of cross-section measurements in a broad energy range, such as the region of interest at T2K, Hyper-Kamiokande, and DUNE. This new beamline design is labelled REF design in the following and serves as the starting point of the aforementioned SBN beamline (see Section 6.5). The ENUBET Collaboration has performed significant R&D work on novel detector designs for beam monitoring and kaon tagging [122] through a fully instrumented decay tunnel. Numerous test beam campaigns in the East Area have been performed and are planned for the coming future, with the goal to characterise and develop further the designs. ENUBET has been been a proposal within the PBC Conventional Beams Working Group (Neutrino Beams subgroup); however, it has now transitioned to be

Table 11: Proposed particle identification scheme for the NA61++ low-energy line.

Momentum (GeV/c)	Detector	Gas type, pressure	Identified particles
2	Time of flight	-	π^+, K^+, p
	Cherenkov Counter 1	CO_2, 8 bar	e^+
	Cherenkov Counter 2	-	
	Cherenkov Counter 3	-	
4	Time of flight	-	p
	Cherenkov Counter 1	CO_2, 1.1 bar	e^+
	Cherenkov Counter 2	CO_2, 2.3 bar	π^+
	Cherenkov Counter 3	-	
6	Time of flight	-	
	Cherenkov Counter 1	He, 8 bar	e^+
	Cherenkov Counter 2	CO_2, 2.5 bar	π^+
	Cherenkov Counter 3	CO_2, 10 bar	K^+
8	Time of flight	-	
	Cherenkov Counter 1	He, 8 bar	e^+
	Cherenkov Counter 2	CO_2, 1.5 bar	π^+
	Cherenkov Counter 3	CO_2, 6 bar	K^+
10	Time of flight	-	
	Cherenkov Counter 1	He, 8 bar	e^+
	Cherenkov Counter 2	CO_2, 1.3 bar	π^+
	Cherenkov Counter 3	CO_2, 4 bar	K^+
13	Time of flight	-	
	Cherenkov Counter 1	He, 8 bar	e^+
	Cherenkov Counter 2	CO_2, 1.2 bar	π^+
	Cherenkov Counter 3	CO_2, 3 bar	K^+

part of the ENUBET-NuTag fusion — the SBN beamline [123].

6.3.1 Target Optimisation

Secondary hadrons are produced via the interaction of a proton beam with a fixed target. Various target optimisation studies [124] were necessary in order to determine the re-interaction and absorption probability of the secondary particles, as a function of the beamline's downstream elements and acceptance. The cross-analysis of various target materials, such as graphite (2.2 g cm^{-3}), beryllium (1.81 g cm^{-3}), Inconel (8.2 g cm^{-3}), and several high-Z materials, in different geometry configurations and subjected to different primary energies, has identified the optimum candidate.

From the study shown in Fig. 99, it can be concluded that the maximum yields are different for different particle momenta and target radii, therefore a compromise between all different configurations must be chosen. For the moment, a 70 cm length and 20 mm radius are considered (as good compromise between all three different momenta). Currently, a more detailed optimisation of the target material is taking place in the framework of the SBN project.

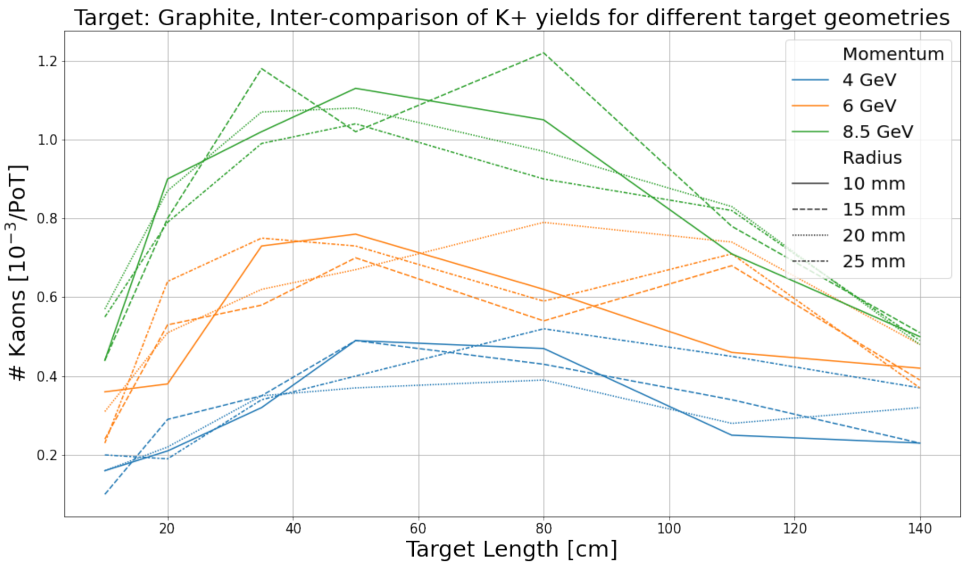

Fig. 99: Kaon yields as a function of the graphite target length. The primary beam simulated is a 400 GeV/c proton beam. The figure of merit for this study is the number of kaons of given energy with 10 % momentum bite that enters an ideal beamline with $\pm$ 20 mrad angular acceptance in both planes, placed 30 cm downstream of the target. The error bars have been omitted to improve readability; statistical errors are negligible (1 %), while the systematic error from Monte-Carlo simulations amounts to about 20 %. Colours refer to the momenta of different kaons while the line style identifies the target radius.

6.3.2 Optics Layout

The studies of beam optics and background reduction are finished. The novel REF beamline design differs from the existing baseline in its ability to transport a higher rate of secondary particles of 4, 6, and 8.5 GeV/c K^+ momenta [125]. The layout and optics of the REF design are shown in Figs. 100 and 101.

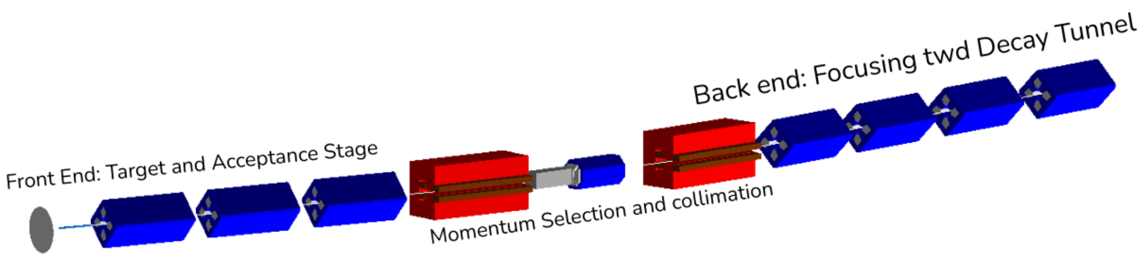

Fig. 100: Beamline visualisation, as modelled with G4Beamline. Downstream from the target, a ‘Q200‘ quadrupole triplet is placed. The bending and momentum selection section comprises two large dipole magnets, a collimator of 9×9 cm^2 aperture followed by a QFL focusing magnet. Downstream this section, and before the decay tunnel, a final large-aperture (Q200 type) quadrupole quadruplet has been placed to shape the beam before the ENUBET tagger.

6.3.3 Shielding

Secondary particle decays as well as particle interactions with beamline elements, are a source of background that can be transported toward the entrance of the decay tunnel. To prevent this, proper shielding is placed strategically to absorb particles outside the acceptance of the main beam. Shielding

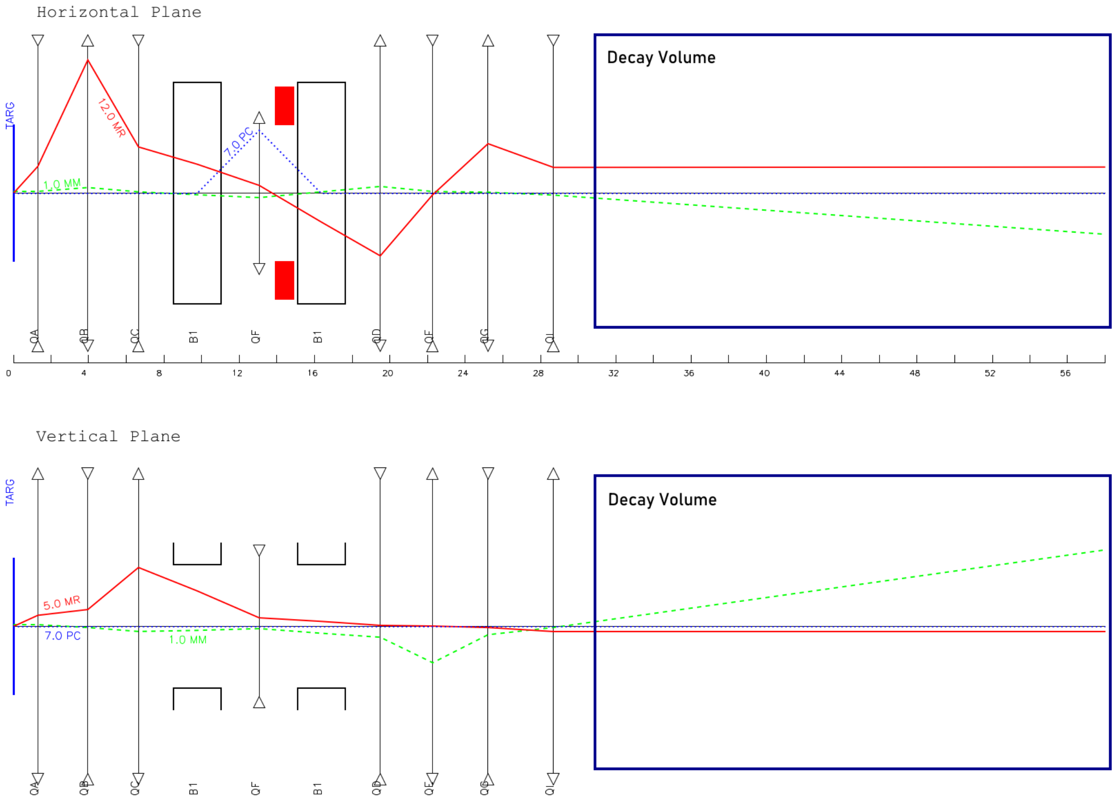

Fig. 101: Beamline optics designed with TRANSPORT.

design is significant in experimental halls where users need to operate close to the experiments. For this study, high-density blocks of material (high-Z) have been employed similar to the ones already present at CERN in the experimental halls. The analysis was carried out through G4Beamline studying the dependency of the particles' momentum spectra on the function of the shielding block location.

Since the beamline is placed at an angle to the target, the proximity of the primary beam with the third quadrupole yoke constitutes today the main source of background. The beam dimensions, both in x and in y, are such that interactions of the beam with the magnet edges are non-negligible. Two other important background sources are the beam's interaction with the so-called field lens quadrupole (located between the two dipole magnets). For this reason, custom shielding needs to be placed around the secondary target and the collimator, but also in other places in the beamline.

The shielding optimisation was performed by studying the momentum spectrum of the particles at the tunnel entrance for the 8.5 GeV/c configuration. The primary source of background is shown in the form of a low-energy peak of off-momentum particles around 4 GeV/c, which originates mainly in the magnet's apertures downstream of the momentum selection.

6.3.4 Results

The beamline's performance has been evaluated by counting the number of particles transported to the lepton tagger, the fully instrumented decay tunnel. The lepton tagger is a 40 m-long tunnel with a 1 m radius. The beam envelope needs to be fully contained within the walls of the tunnel to avoid background that could compromise the reconstruction of the signal produced by the decay of pions and kaons. The momentum spectra of the particles transported by both the REF beamline and the old baseline beamline are shown in Fig. 102.

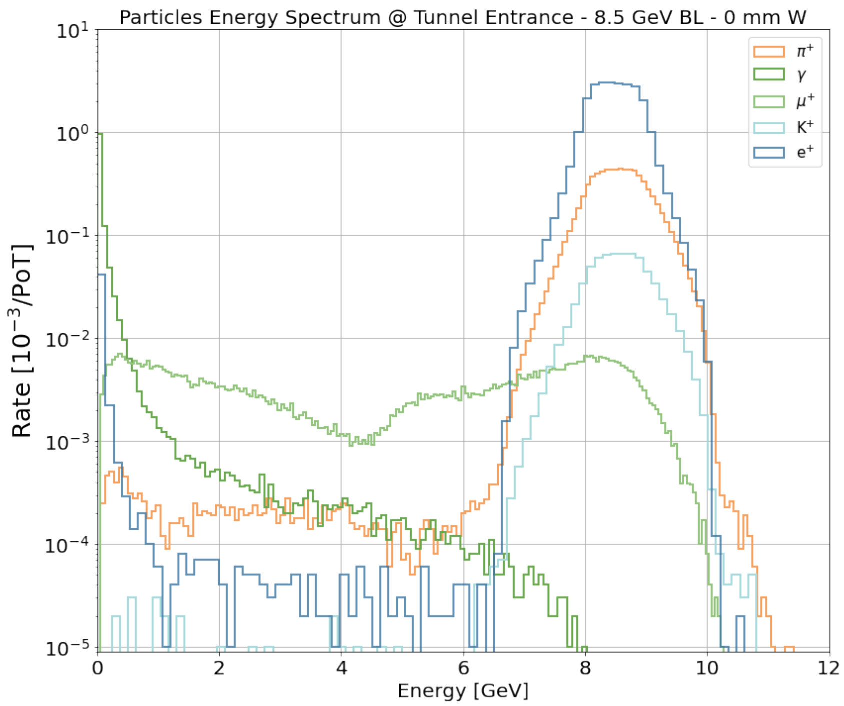

(a) REF Beamline

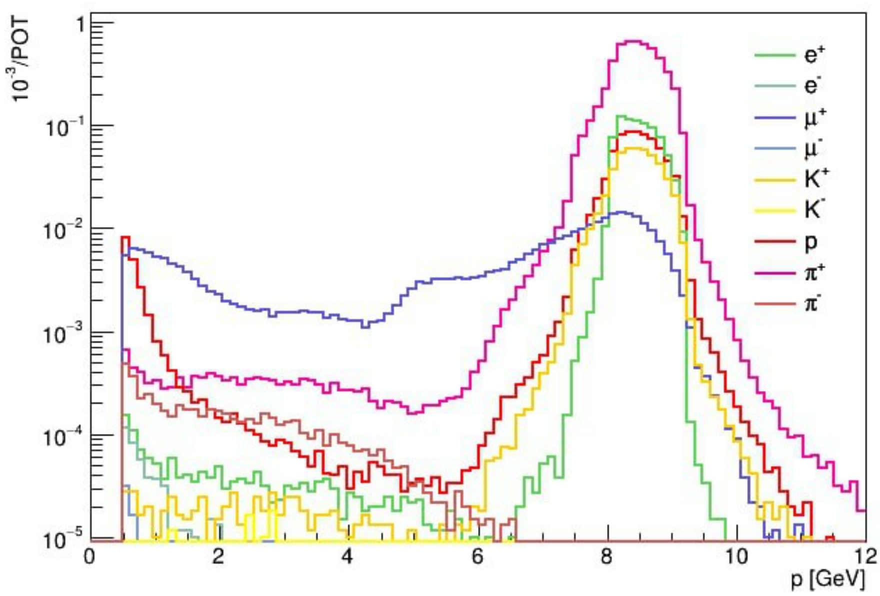

(b) Standard Beamline

Fig. 102: Comparison of the momentum spectra at the tunnel entrance for various charged particles of both beamlines in the 8.5 GeV/c configuration.

Table 12: Particle rates at the lepton tagger entrance for 8.5 GeV/c for both beamline proposals, and for 6 and 4 GeV/c for the REF design.

Particle momentum	8.5 GeV/c	6 GeV/c	4 GeV/c
REF beamline design			
K^+/ PoT (10^{-4})	7	0.28	0.08
π^+/ PoT(10^{-3})	10	4.1	1.7
Baseline beamline			
K^+/ PoT (10^{-4})	0.36	–	–
π^+/ PoT (10^{-3})	3.97	–	–

Finally, muon and electron neutrinos are producing the forward direction by the decay of pions and kaons. While the decay-charged leptons are detected within the decay tunnel, a fraction of the neutrinos interact within a large mass neutrino detector located approximately 50 m from the end of the tagger. A comparison of the neutrinos weighted by the cross-section and normalised by the number of primaries reaching the far detector for both beamline layouts is shown in Figs. 103 and 104.

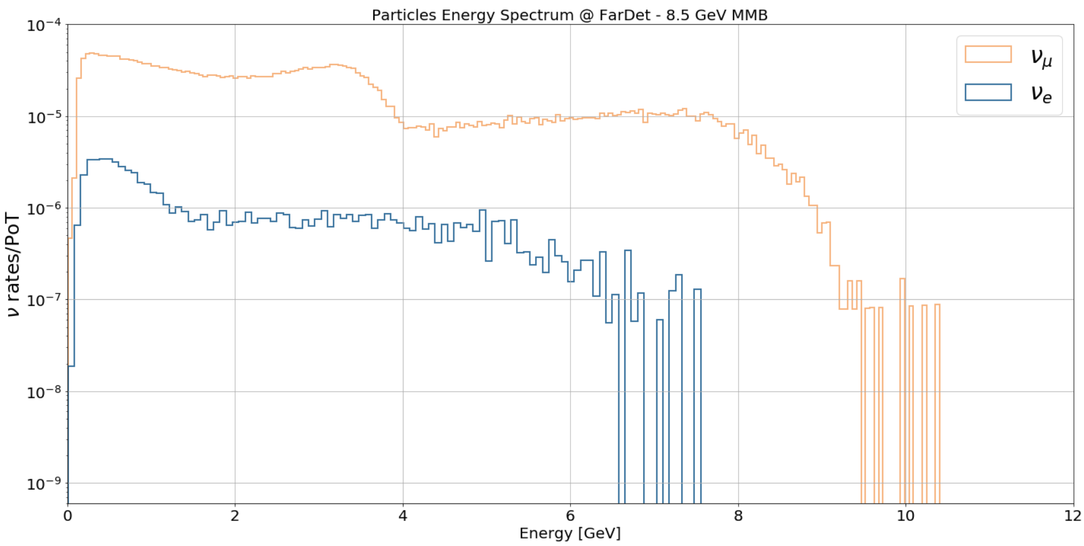

Fig. 103: Logarithmic momentum spectrum of the neutrinos reaching the neutrino detector for a beamline momentum of $p = 8.5\,\mathrm{GeV}/c$ of the REF beamline design. The spectra are weighted by the cross-section and energy.

The first spectrum, shown in Fig. 103, is the one calculated for the REF beamline design, while Fig. 104 shows the equivalent spectrum calculated with the ENUBET baseline version. The simulation of the baseline design was carried out with a low-energy cut at 500 MeV/c. The cross-section weighted flux is thus proportional to the events observed by the neutrino detector at the end of the ENUBET data taking. In the case of the baseline design, the muon neutrino spectrum has a sharper separation between the neutrino peaks produced by K and π. Conversely, the electron neutrino spectrum is more prominent in the 8.5 GeV/c for the new design. As shown in Table 12, the REF design demonstrates a kaon and pion yield that is approximately twice as high as that of the baseline ENUBET beamline at the tagger entrance. Using the 4 and 6 GeV/c runs, the recent beamline design enables the required degree of adaptability to increase the number of detected neutrino interactions in the 1 GeV/c range for both ν_e and ν_μ at the detector.

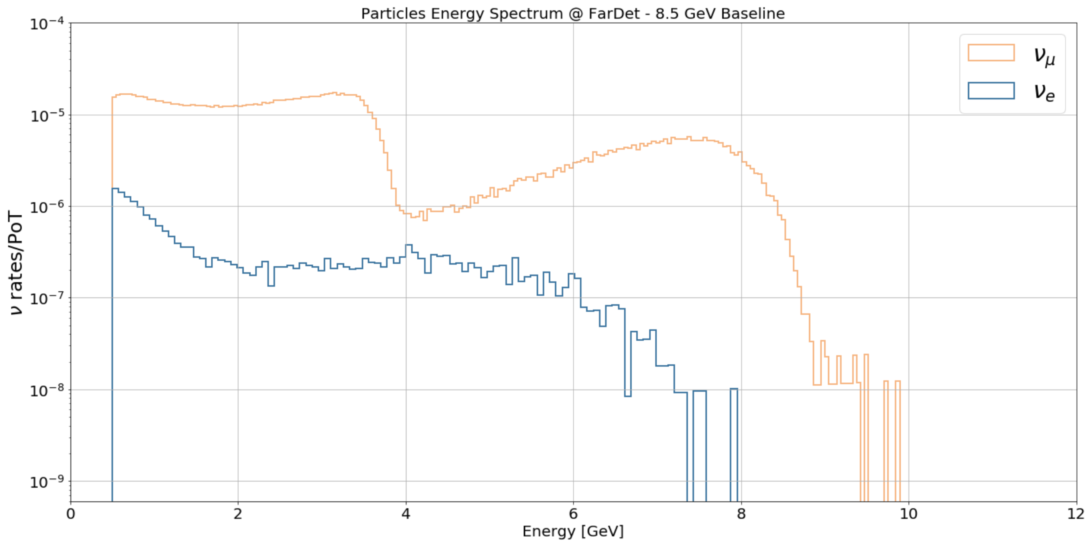

Fig. 104: Logarithmic momentum spectrum of the neutrinos reaching the neutrino detector for original ENUBET beamline design at the beamline momentum $p = 8.5\,\mathrm{GeV}/c$. The spectra are weighted by the cross-section and energy.

6.4 NuTag

NuTag is a completely new proposal, at first presented at the PBC workshop at the beginning of 2021, that has evolved to a new idea of a tagged neutrino beam [34] making use of silicon pixel detectors to measure the beam on a particle-by-particle basis. The aim of this new project is similar to ENUBET's goal: reforming the concepts of conventional neutrino beams by exploiting tagged neutrino beam techniques. The NuTag Collaboration proposes a fully-tagged secondary pion beam. By using high-resolution and fast-readout pixel detectors, the particle kinematics are fully determined. Neutrino tagging with a similar technique using special trackers developed for the NA62 experiment, the so-called GigaTracker [126] is done today, at a smaller scale. This technique would allow for an event-by-event reconstruction of the pion decay kinematics in the $\nu_\mu/\bar{\nu}_\mu$ decay mode. Specifically, based on time and angular coincidences, each neutrino interacting in the detector could be associated with a single "tagged" neutrino. The physics goals for this project are better flux knowledge, improved background suppression at the neutrino detector, and more accurate energy reconstruction. On top, since the tagged neutrino energy reconstruction is independent of the neutrino interaction final state, by comparing the tagged neutrino energy with the "visible" energy deposited in the detector, the process undergone can be determined. This would lead to improved flavour identification.

A conceptual, site-agnostic long-baseline beamline design has been developed by the study team. The beamline momentum-selects both the π^+ and the π^- and transports them towards a long ($\mathcal{O}(100\,\mathrm{m})$) decay region. The transverse optics of the proposal are shown in Fig. 105. The non-interacting primary beam impinges onto the two-hole collimator that is centred in first achromat. Detailed FLUKA simulations [90, 127] have been performed, as shown in Fig. 106. The long-baseline design for NuTag is in a quite preliminary study phase. The very first analysis of the possibilities of such a long-baseline project has been investigated and published [35]. The study is discontinued within the PBC; however, the NuTag proposal has merged with ENUBET into the SBN beamline [128] that is under active development.

6.5 The Short Baseline Neutrino Beamline Study (SBN)

Recently, the ENUBET and NuTag Collaborations decided to join forces under the umbrella of the Conventional Beams Working Group, to develop a beamline that serves both experiments' physics

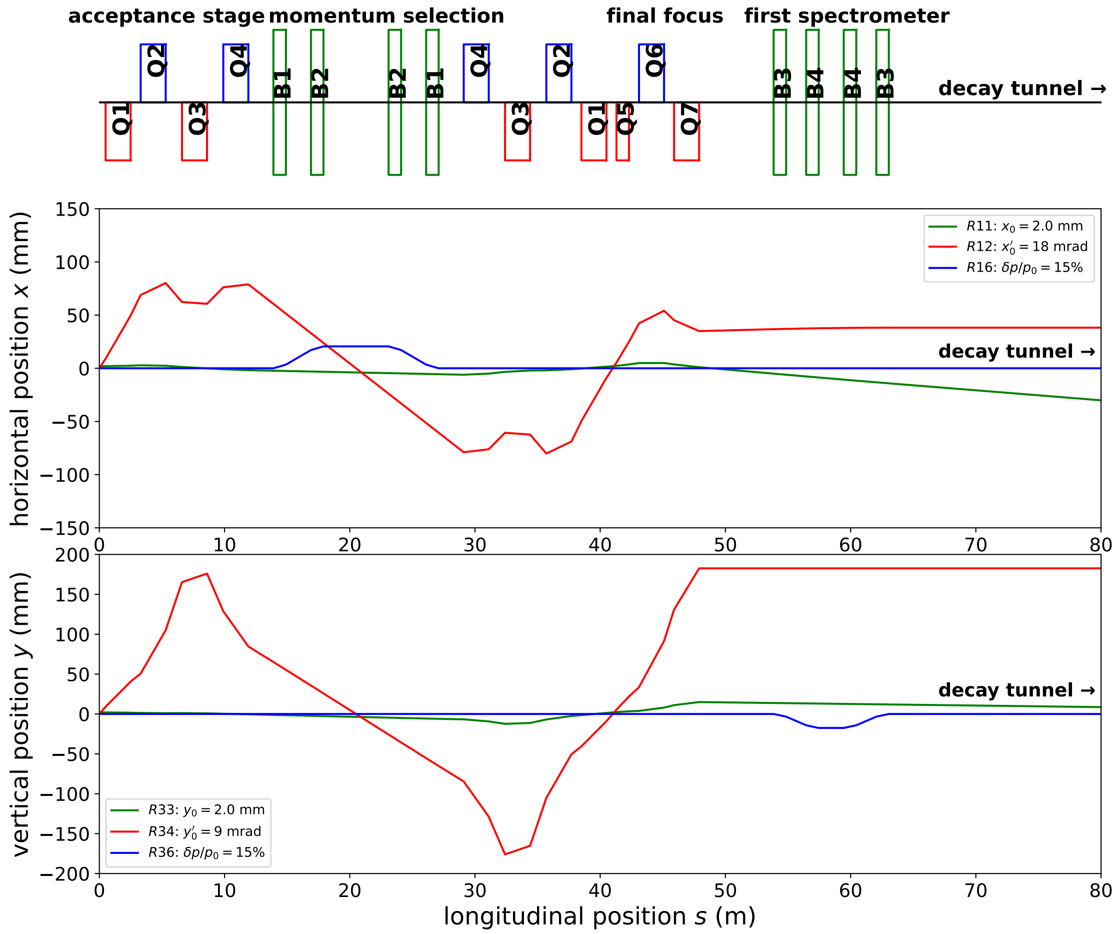

Fig. 105: Linear optics of the NuTag long-baseline proposed beamline. The top sketch indicates the quadrupoles and their focusing (red) or de-focusing (blue) action on a positive particle, while the green boxes indicate bending magnets. Only the first 80 meters of the beamline are shown. Below, the top plot displays the horizontal optics while the bottom plot shows the vertical optics. The red lines correspond to the sine-like rays, the green lines to the cosine-like rays, and the blue lines to the dispersive ray (particle has a momentum offset, indicated in the legend as a percentage of the central momentum). The tracking detectors are installed in the second achromat, just before the decay region as discussed in the text.

.

purposes [37], i.e., producing monitored or even fully-tagged K^+ and π^+ beams and subsequently a 'tagged' neutrino beam in the 1 to 10 GeV/c momentum range. While the methodology of ENUBET focuses on the measurement of leptons to infer the $\nu_{e/\mu}$ flux to ultimately measure the respective cross section, NuTag follows a different approach by investigating the two-body decay of π^+ instead: Here, a full kinematic reconstruction (direction and momentum) of the parent meson, as well as that of the μ^+ emerging from the decay enables a full reconstruction of the $\bar{\nu}_\mu$ kinematics. In addition, it appears likely that a neutrino interaction within a respective near detector, e.g., a ProtoDUNE equivalent liquid-argon detector, can be associated with the respective measurement of the parent meson and the produced lepton. Such capabilities will also provide the opportunity to measure the ν_μ cross-section with unprecedented precision. Hyper-Kamiokande as well as DUNE have indicated great interest in the experiment as it will provide viable information to their respective physics case.

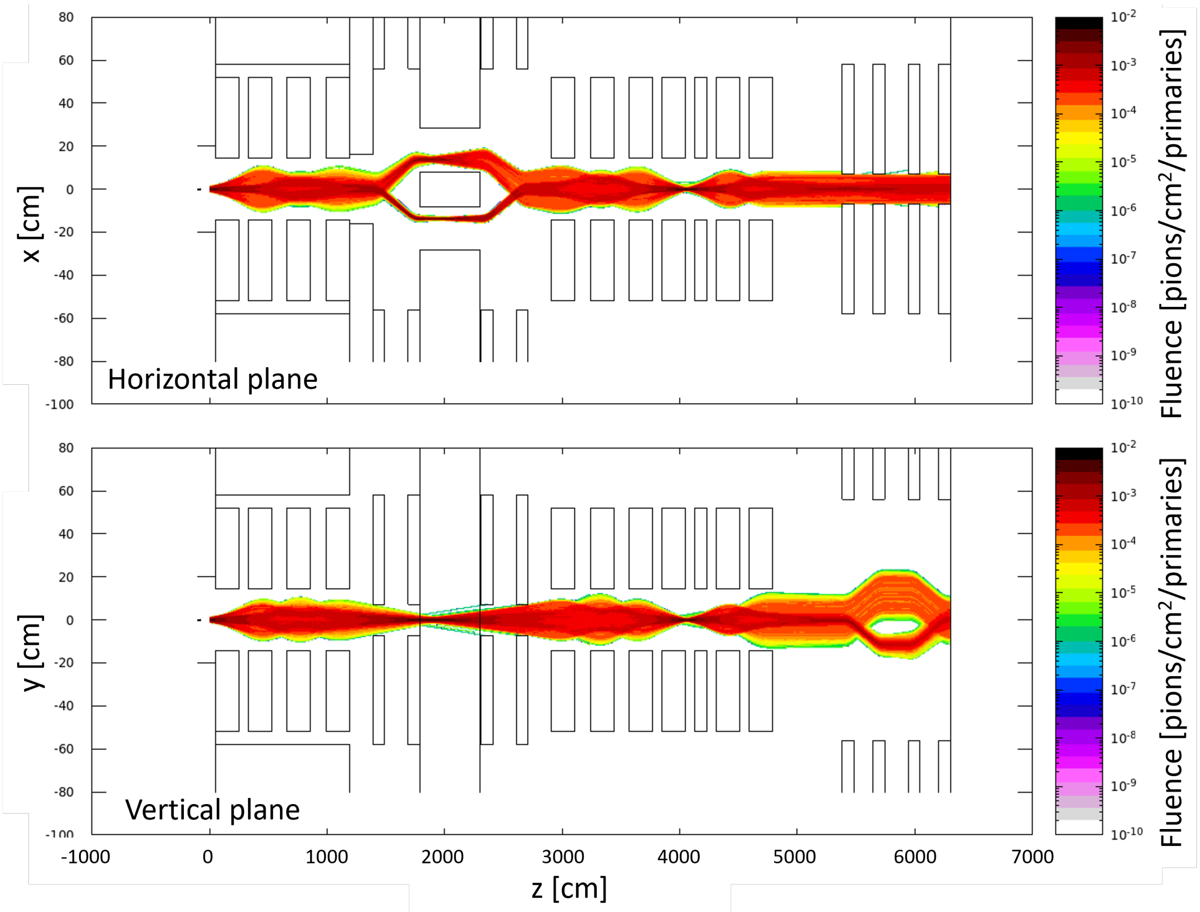

Fig. 106: FLUKA simulation of π^+ and π^- that are within the linear acceptance in phase space [129]. The horizontal (top) and the vertical planes (bottom) are depicted. All results are normalised to the number of primary protons. The trajectories of the particles inside the decay region are not shown.

6.5.1 The Beamline Design

The starting point of the beamline design is the ENUBET REF design that has been developed within CBWG (see Section 6.3) and outperforms the ENUBET baseline design in terms of transmission [124]. Within the scope of the SBN study, a comprehensive optimisation of the beamline has been performed, ultimately including the silicon pixel detectors required for the NuTag physics case. As a result of this optimisation, a new beamline layout has emerged with the difference to the previous design, described in the next paragraph. Moreover, in view of a conceptual feasibility study, the beamline must be optimised for maximum efficiency in terms of protons on target (PoT) from CERN's injector complex to minimise direct competition with experiments such as BDF/SHiP.

6.5.2 Multi-Objective Optimisation of the Beamline

One key element of the fusion of the two designs is the introduction of NuTag's silicon pixel detectors into the beamline. These pixel detectors ideally have a read-out rate of $\mathcal{O}(10^8\,\mathrm{s}^{-1}\,\mathrm{mm}^{-2})$, assuming a HL-LHC-like technology [130]. Hence, the beam particle flux should optimally be of $\mathcal{O}(10^7\,\mathrm{s}^{-1}\,\mathrm{mm}^{-2})$ to avoid being too heavily reliant on the successful R&D and implementation of that future technology. To increase the transmission of the beamline and to include the NuTag pixel detectors (with their limitations), the proposed SBN beamline has the following characteristics (see Fig. 107):

– The beamline now features a quadrupole triplet upstream and downstream of the momentum-

Table 13: Comparison of the optimised SBN beamline with the previously developed REF design (see Section 6.3) and the ENUBET baseline design [21] at $p = 8.5\,\mathrm{GeV}/c$ within a $\Delta p/p_0 \in [-10\,\%; 10\,\%]$ momentum selection. The last column contains the optimised beamline considering a 25 GeV/c beam from the PS as the driver.

Particle yield	ENUBET design	REF design	SBN (opt.)	SBN (opt.) PS energy
K^+ / PoT (10^{-4})	3.6	7.0	12.6	0.31
π^+ / PoT (10^{-2})	0.4	1.1	1.9	0.047

selection section, resulting in a reduced overall length compared to the REF design;

- A 1.2 cm-thick Pb plate, inserted into the beamline right after the Q4 quadrupole, in order to energy-degrade and eventually remove unwanted positrons from the beam. Without such a positron countermeasure, the particle flux of the monitors easily exceeds $10^8\,\mathrm{s}^{-1}\,\mathrm{mm}^{-2}$ and the momentum measurement on a particle-by-particle basis becomes impossible. Analogously to NA62, it may turn out useful to be able to change the thickness of the positron absorbing Pb plate in order to effectively tune the flux on the pixel detectors.
- Instead of sticking to so-called QPL magnets (2 m length and 20 cm aperture diameter) in the upstream and downstream triplets, an optimisation of the quadrupole specifications was carried out. This does not necessarily imply that new magnets have to be designed; instead, it points to the most suitable quadrupoles that come close to the ideal design.

With these changes, the beamline is optimised using a multi-objective genetic algorithm (MOGA). The algorithm has the capability of optimising 26 beamline parameters simultaneously. These parameters, displayed in Fig. 107, are as follows:

- A total of seven drift spaces in the upstream and downstream quadrupole triplets,
- For each quadrupole in both triplets, the aperture, length and gradient (18 parameters),
- The target type (length, radius and density).

The optimiser is capable of changing the graphite production target and choose another target type from a pre-calculated list that contains a total of 18 different targets. The list includes the T2K, CNGS, ENUBET and NuMi targets and variations of these [131–133].

6.5.3 Optimisation Results

The optimisation has been carried out using the NSGA-III [134], SMS-EMOA [135] and AGE-MOEA [136] implementations within the PyMoo Python library [137]. The optimised beamline is verified by a full start-to-end BDSIM simulation. The results of the respective BDSIM simulation are listed in Table 13. The table clearly shows the distinct improvement of the beamline performance in comparison to the REF as well as the final ENUBET design. These improvements are achieved even though obstacles like a Pb plate and silicon pixel detectors have been inserted into the beamline.

The main reasons for these transmission enhancements are the following:

- The optimal target has been found to be a variation of the CNGS target with a length of 1.25 m, a radius of 6 mm and a density of 2.26 g cm^{-3}. It is important to stress that there is a chance that this particular graphite density cannot be achieved in this particular application. For this reason, a conservative density of 2.0 g cm^{-3} is used in all simulations. A future study may find the necessity of reducing the graphite density.

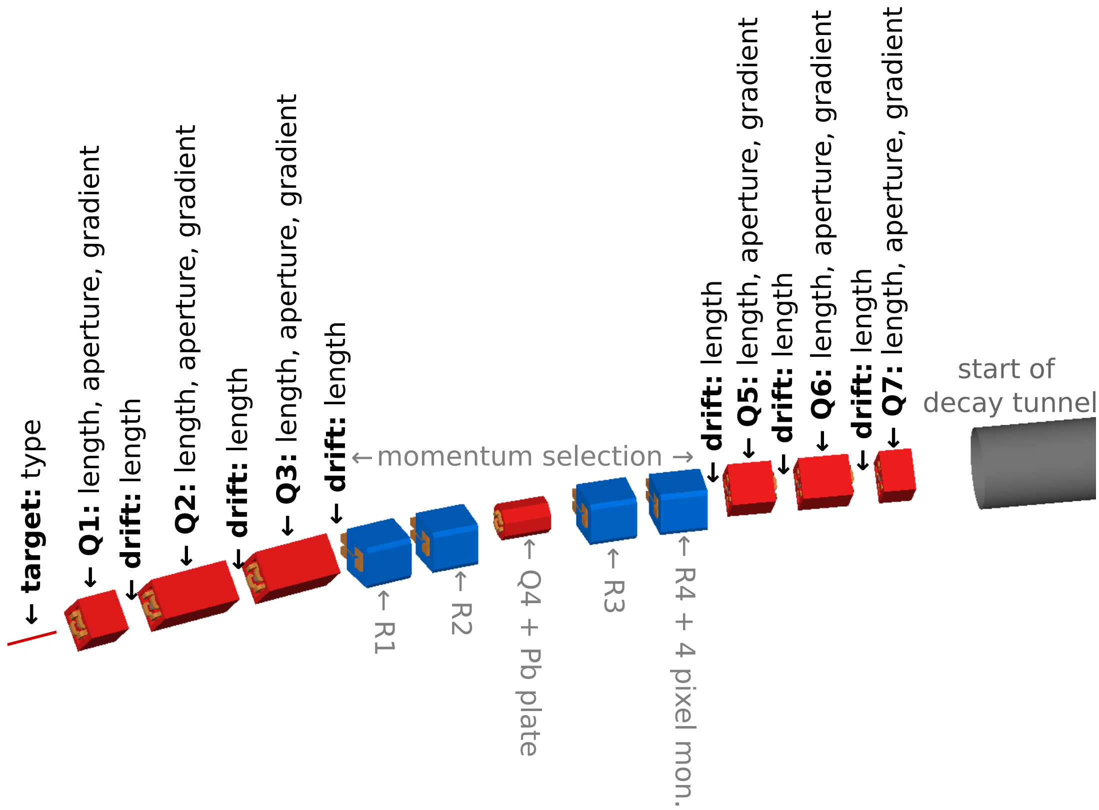

Fig. 107: The sketch shows the new layout of the SBN beamline with the parameters that can be varied by the MOGA optimisation algorithm printed in black on top while the parameters that are fixed and are not part of the optimisation process are printed in grey. In contrast to the ENUBET design, the bending magnets have been split and a quadrupole in the final triplet has been removed.

– The beamline has become shorter by more than 5 m. Hence, fewer K^+ mesons (π^+ to a smaller degree) decay in the beamline before they reach the decay tunnel.
– The most significant improvement comes from a modified beamline acceptance that captures more of the K^+ and π^+ mesons that emerge from the production target.

It appears likely that most of the optimised quadrupoles share significant similarities with the QPL and QPS magnet design. It therefore appears likely that no new designs are required with the potential exception of the bending magnets.

The spectrum of the particles transmitted by the beamline to the start of the decay tunnel is shown in Fig. 108 (left). The NuTag pixel monitors could add an additional and effective veto for the ENUBET physics case since two pixel detectors would be deployed right in front of the entrance to the decay tunnel (part of the NuTag setup). This way, leptons entering the decay tunnel from the beamline can be potentially excluded from the analysis, ultimately enhancing the signal-to-noise ratio of the measurement.

A very important parameter for the beamline is the instantaneous particle flux of the pixel detectors that are used for the momentum reconstruction at the R4 bending magnet (see Fig. 107). The limit of these detectors in terms of flux is $10^8\ \mathrm{s}^{-1}\ \mathrm{mm}^{-2}$. In the proposed design, the flux on the first pixel detector upstream of the R3 bending magnet is shown in Fig. 108 (right). With a spill intensity of 10^{13} PoT within 4.8 s, the particle rate is in the range of 10^7 to $4 \times 10^7\ \mathrm{s}^{-1}\ \mathrm{mm}^{-2}$—a rate that is fully acceptable. Any increase of the SPS spill duration would of course lead to an additional reduction of the instantaneous rate, assuming a constant overall spill intensity.

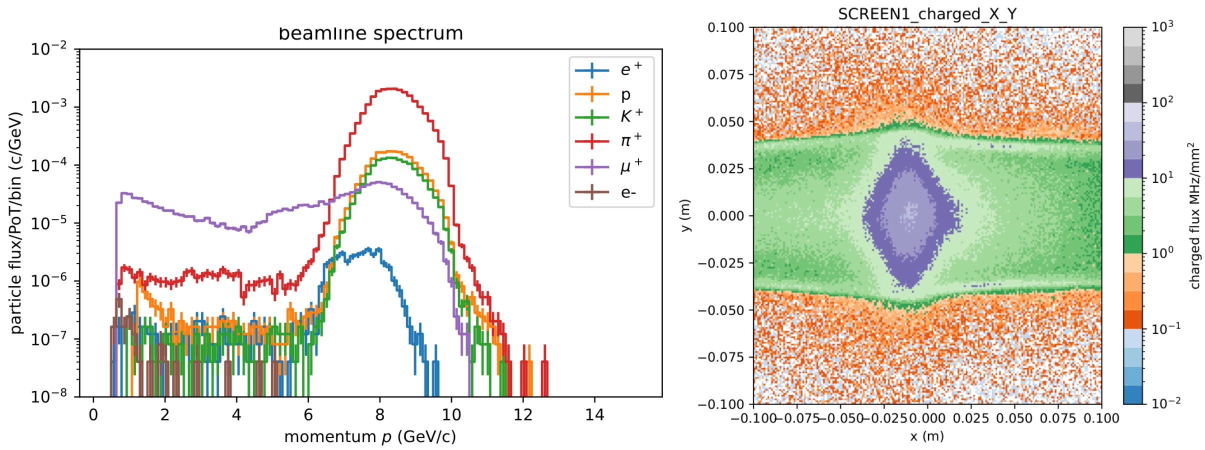

Fig. 108: Left: Beamline momentum spectrum after the optimisation process. Compared to any previous design, the positron transmission is strongly suppressed due to the Pb plate followed by two bending magnets. Studying the noise level of low-energy leptons is still pending. Right: Flux of charged particles on the first pixel detector at the R4 bending magnet of the beamline with a spill intensity of 10^{13} PoT within a spill length of 4.8 s.

6.5.4 Feasibility Analysis of the SBN Beamline at the PS

Within the scope of the study we evaluated whether the beamline can be effectively driven by the PS. In addition to the beamline optimisation at SPS energies ($p = 400\,\mathrm{GeV}/c$), the optimisation framework has also been applied to determine the optimal K^+ and π^+ yields achievable using the PS beam with a momentum of 25 GeV/c.

The target was optimised in isolation[1] by evaluating the particle yield in the vertical and horizontal transverse phase space in a $\pm$ 10 cm range in x and y respectively, with a limit on the transverse angles x' and y' of $\pm$ 10 mrad at the exit plane of the target. The volume in transverse phase space that is enclosed by these constraints easily comprises the beamline acceptance. In contrast to the setup at SPS beam energy, the production angle has been removed for this optimisation at the PS proton energy to maximise the meson yield. Several target configurations have been analysed:

- Material: The set {Au, Fe, Be, Al, W, C} was considered,
- Length: varied in the range 0.1 to 1.3 m,
- Radius: varied in the range 0.002 to 0.040 mm.

The optimal target was found to be a 1.06 m long carbon (C) target with a radius of 4.1 mm, While the target was optimised in isolation, the quadrupoles and drift spaces outside the double-bend achromat have been optimised in a second optimisation step using the aforementioned MOGA optimisation framework. The meson yield after the optimisation is 3.1×10^{-5} K^+/PoT and 4.7×10^{-4} π^+/PoT in the relative momentum range $\Delta p/p_0 \in [-10\,\%, +10\,\%]$ at $p = 8.5\,\mathrm{GeV}/c$ (see Table 13). These numbers are more than an order of magnitude smaller than those of the optimised beamline at SPS energies. The spectra of the π^+ and K^+ at the SPS and those at the PS (both after a respective MOGA optimisation) are shown in Fig. 109.

Given the resulting kaon and pion yield, a significantly larger (between one and two orders of magnitude) number of protons on target is required to achieve the sample of 10^4 ν_e necessary for a precise ν_e cross-section measurement (statistical uncertainty at the 1 % level). With a neutrino detector mass of 1 kt of liquid argon, the estimated required number of PoT is roughly 5×10^{20} PoT. This number is two

[1]The target was optimised in a first optimisation step. The remaining parts of the beamline (drift spaces and quadrupole parameters) have been optimised in a second optimisation step.

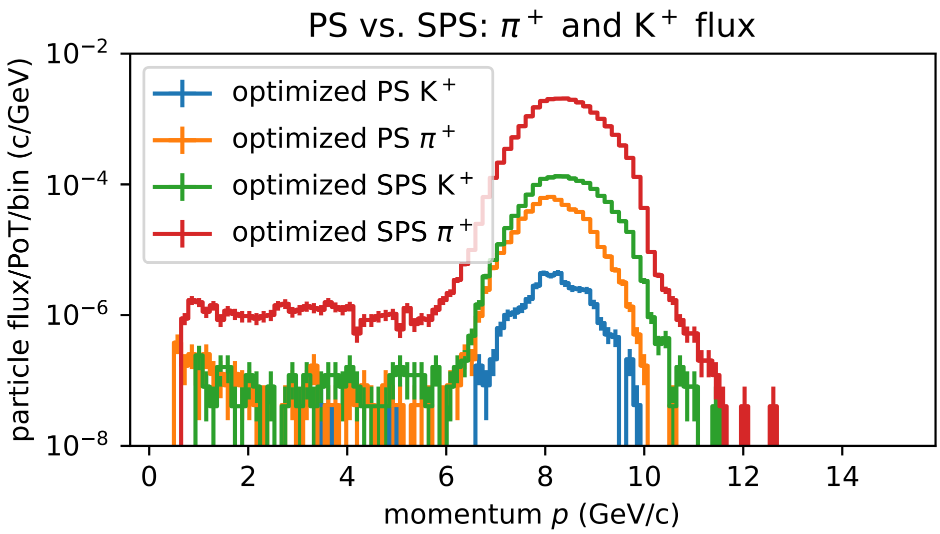

Fig. 109: Comparison of the SPS and the PS π^+ and K^+ spectra. The meson production at PS energies is more than one order of magnitude smaller than at the SPS. Both beamlines (PS and SPS) have each been optimised with the customised MOGA routine.

orders of magnitude larger than the requirement at SPS energies for an optimised beamline. Accumulating this number of PoT within a reasonable time span (shorter than 20 years) is extremely challenging. The PS intensity will have to significantly increase during the BDF/SHiP era. Studies, however, indicate that cycles dedicated to ECN3 would require an additional 7 to 11 % of the PS time to maintain the yearly intensity for the other PS users. Even in the best-case scenario of an SFTPRO-equivalent intensity at the PS level for a future neutrino beamline (assuming the 4.8 s SPS cycle with the annual intensity of 1.24×10^{19} PoT, excluding any heavy-ion runs), it would take about 40 years to meet the ENUBET physics case requirements.

In summary, the PS is not efficient enough to drive the beamline at a design momentum up to $p = 8.5\,\mathrm{GeV}/c$ due to the low kaon and pion production rates.

6.5.5 A Possible Implementation of the SBN Beamline at the SPS

The implementation of the beamline has been documented in more detail in Ref. [128]. In this report we discuss the studies for the three following locations at the SPS:

- ECN4: Similarly to the BDF/SHiP study [113], a new underground facility could be constructed to house SBN.
- SPS LSS6 (TT61/TNC): The beamline could be placed at SPS LSS6 if a slow extraction is established in this direction. The existing TNC/TT61 tunnel infrastructure could be repurposed, reducing the need for extensive civil engineering.
- SPS LSS4 (TTC6): Alternatively, the beamline could be served via a new slow extraction from SPS LSS4, taking advantage of the existing experimental cavern in TCC4.

Two additional locations, TT4/TT5 (former West Area) and EHN2, have not been considered in the analysis since they are close to the surface and the placement of the beamline in a straight tunnel is not possible without extensive excavation due to the significant bending angle of 18° in the beamline.

The following presents the solution that is currently favoured in terms of cost and feasibility: placing the beamline in the TT61 and TNC tunnels (HiRadMat in the TNC tunnel would remain fully operational). For other studied placement scenarios of the beamline, the reader is referred to Ref. [128].

A Slow Extraction towards SPS LSS6

Since SBN requires a slow extraction from the SPS, any placement of the beamline outside the North Area (where a slow extraction already exists) requires the implementation of an additional slow extraction setup in the SPS. A conceptual feasibility study regarding the implementation of a second slow-extraction setup in the SPS has been performed and was reported in Ref. [138]. It was found that a slow extraction from the Long Straight Section 6 (LSS6) of the SPS can be achieved by installing new Electrostatic Septa (ZS) wire septa in either LSS4 or LSS5 in a non-local extraction (where wire septa and magnetic septa are not located in the same straight section). Figures 110–112 shows the behaviour of the on-resonance beam as well as the extracted beam fraction in case the ZS are placed in LSS4 to then extract in LSS6. A bent crystal could replace the ZS wire septa to reduce setup cost; however, R&D would be needed to assess its feasibility. The proposed setup does not influence the extraction to the LHC since existing hardware is not touched. Instead, only the wire septa and one or two pulsed bumper magnets would have to be added to achieve the correct orbit bump at the location of the wire septa. The solution using wire septa would be achievable using existing technology. More details are available in Ref. [138].

A Potential Location of the Beamline in TT61 and TNC

A potential location of the beamline in the TNC and TT61 tunnels (see Fig. 113) has the advantage of the primary production target being deep underground. The former TCC6 cavern (see Fig. 113; cavern upstream of TNC and TT61) housed the T9 target (neutrino-beam target) for the former West Area receiving large numbers of proton on a yearly basis (more than 10^{19} PoT/year). HiRadMat also features a beam dump in the TNC tunnel; however, here it is worth noticing that HiRadMat can only receive 10^{16} PoT/year due to RP constraints. The TNC tunnel with a width of 5.6 m is slightly wider than the TT61 tunnel (4 m wide).

At this point in time, a placement of the beamline target, primary beam dump, as well as most of the magnetic structure is envisaged to be placed within TT61 as can be seen in Fig. 113. The bending angle within the beamline, that is required for momentum selection, transports the beam to the TNC tunnel. The end of the decay tunnel and the location of the neutrino detector require excavation. Further studies will be aimed at reducing the overlap of the detector setup and the decay tunnel with the soil north of the TNC tunnel.

The implementation of each part of the beamline will have its own challenges and requirements:

- Slow extraction: As explained in Section 6.5.5, the scheme that is proposed here requires the installation of the ZS septa in LSS4 of the SPS and the other aforementioned modifications (additional bumper magnet(s), operation with two orbit bumps etc.).
- Transfer line: The beamline continues via a nearly straight transfer line from TCC6 into TT61. It requires a bending magnet to steer the beam away from the HiRadMat beam in TCC6. After refurbishment, existing magnets can be used for the transfer line.
- Target complex: With the initial part of the beamline being placed in TT61, it requires a K12-like target complex and a beam dump similar to the existing XTAX, that today are widely used in TCC2 for the North Area slowly extracted beams. The installation of the target complex will require excavation to acquire sufficient space for hoists and other machinery to pass by and to access the target.
- Secondary beamline: The beamline requires excavation of the decay tunnel on the North side of TT61 (see Fig. 114 bottom). The floor difference between TT61 and TNC will allow to vertically bypass TNC. A part of the decay tunnel will intersect the soil north of the TNC tunnel. Here, major excavation will be required. The passage of the decay tunnel through the soil can be further reduced by optimising the beamline trajectory.
- Experimental Area: In the scenario of Fig. 114 also the experimental area must be excavated. This setup envisages a short distance between decay tunnel and the detectors. Consequently, the

htbp

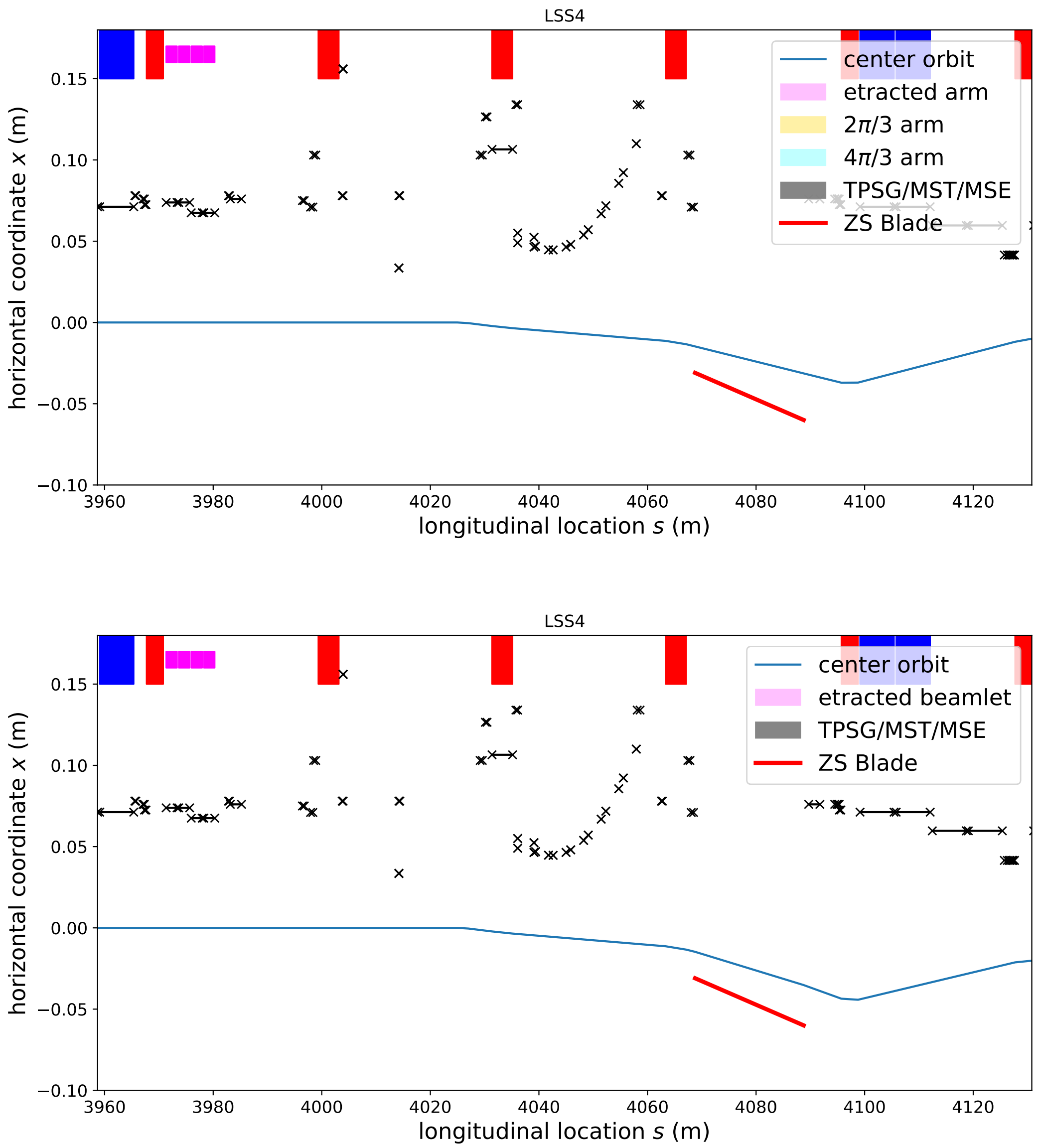

Fig. 110: Plots of the 3 arms of the stored beam (top) and the extracted beam fraction (bottom) in LSS4. Figures taken from Ref. [138].

ProtoDUNE-like detector acceptance can be reduced from $6 \times 6\,\mathrm{m}^2$ to about $4 \times 4\,\mathrm{m}^2$ with a length of roughly 22 meters. This corresponds to a neutrino detector mass of 500 t of liquid argon.

6.5.6 Requirement for Protons on Target

A preliminary analysis evaluated the proton on target (PoT) requirements for the SBN beamline. This study is published in a PBC note [128].

In the first scenario, the beamline is considered to be operated within a shared SFTPRO cycle, independently of the specific beamline location (this scenario is also possible in TT61/TNC). A neutrino detector mass of 500 t of liquid argon at a distance of 25 m from the end of the decay tunnel is assumed, requiring 1.4×10^{19} PoT to achieve the desired 10^4 ν_e sample. The SPS flattop duration is assumed

htbp

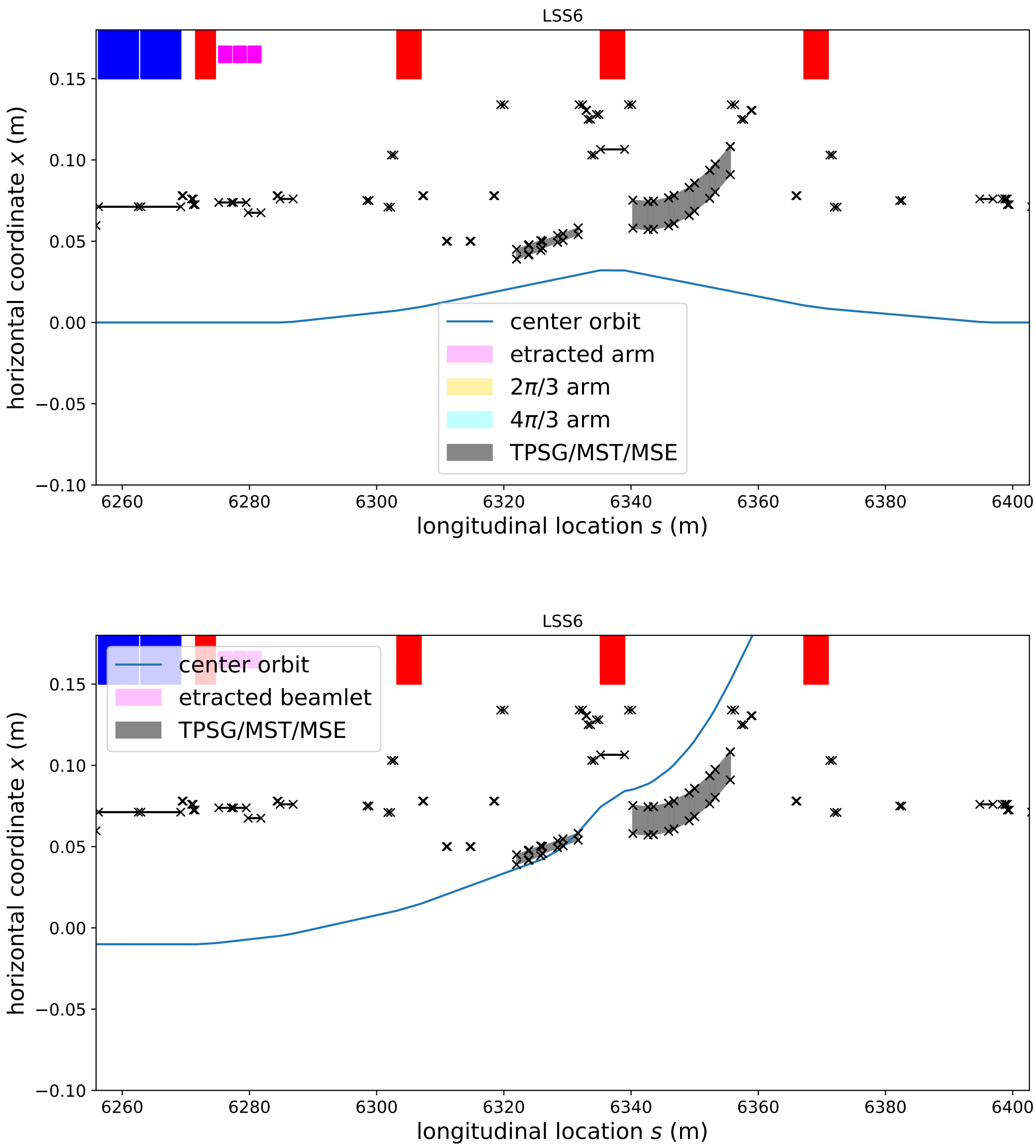

Fig. 111: Plots of the 3 arms of the stored beam (top) and the extracted beam fraction (bottom) in LSS6. Figures taken from Ref. [138].

to be 9.6 s, delivering 10^{13} PoT per spill to the SBN beamline in a shared cycle. ECN3 (BDF/SHiP) receives the maximum requested 4×10^{19} PoT/year. The SBN runtime would then be between 5.7 to 7.3 years, depending on the number of heavy-ion runs, with a yearly PoT consumption of 1.8×10^{18} to 2.4×10^{18} PoT. This corresponds to 25 % of the TCC2 intensity.

In case the SPS flattop duration would remain at the current value of 4.8 s (see Ref. [113]), the SBN beamline would still consume roughly 25 % of the TCC2 intensity (10^{13} PoT/spill) and would reach the physics goal of 10^4 ν_e within 4.3 to 6.5 years.

It is important to mention the possibility of an enhanced number of spills for TCC2 in case the BDF/SHiP spill intensity is increased from 4×10^{13} to 5×10^{13} PoT/spill. This would increase the number of spills for the North Area (BDF/SHiP excluded) by roughly 25 %. Under the assumption of a 9.6 s spill duration from the SPS, the experiment's runtime would reduce to a time span of roughly 5 years.

htbp

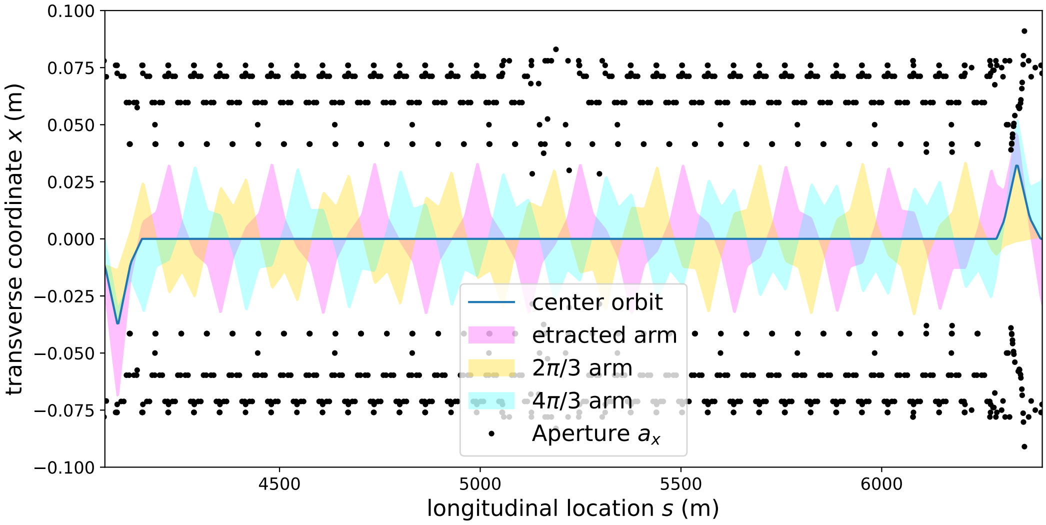

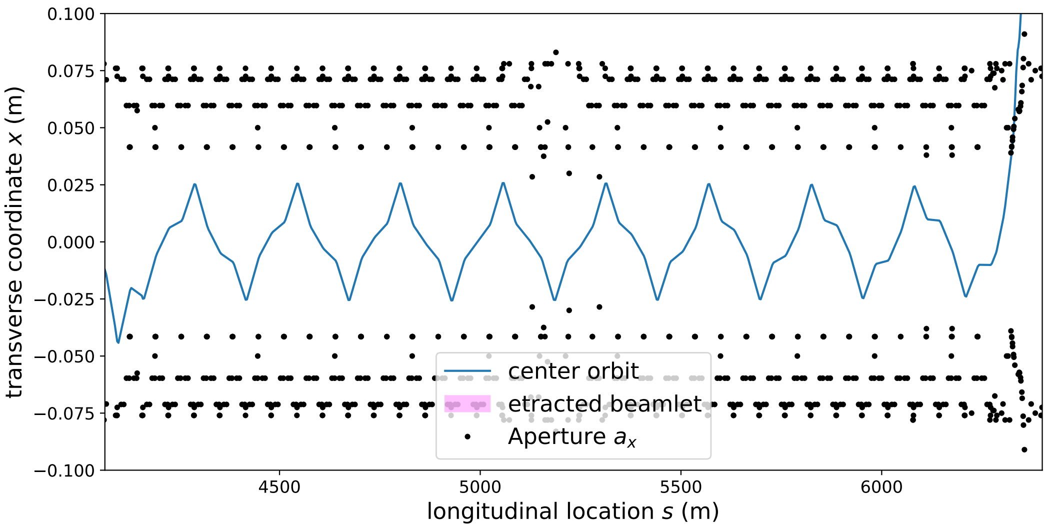

Fig. 112: Oscillation of the 3 stored arms (top) and the extracted beam fraction (bottom) from LSS4 up to LSS6. One can see the two local orbit bumps in LSS4 and LSS6. Figures taken from Ref. [138].

In a different scenario, a second slow-extraction setup for a respective extraction either at LSS4 or LSS6 of the SPS could provide the necessary flexibility to achieve simultaneous extractions to the SBN as well as the North Area (SFTPRO and SHiP cycle). This possibility is described more thoroughly in the PBC note that analyses a potential second slow-extraction setup in the SPS [138]. This would enable the extraction of a tiny part of the beam of a SHiP cycle in a simultaneous slow extraction, which in turn reduces the number of PoT taken from the SFTPRO cycle. Any such complex sharing scenario requires further study.

As the total number of protons is intrinsically limited, co-existence of SBN with other experiments automatically implies minimising competition for PoT and therefore, the SBN beamline may never be operated in a dedicated cycle.

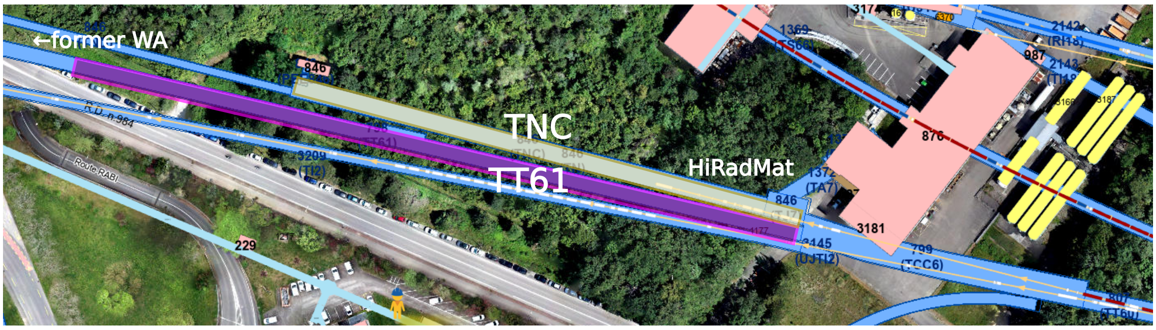

Fig. 113: View of the TNC (yellow frame) and TT61 (purple frame) tunnels downstream of the extraction location in SPS LSS6. The first part of the TNC tunnel is occupied by the HiRadMat test facility; however, the downstream tunnel (approximately 120 m) could be used for the beamline. The TT61 tunnel, although slightly narrower than the TNC tunnel, is currently not occupied.

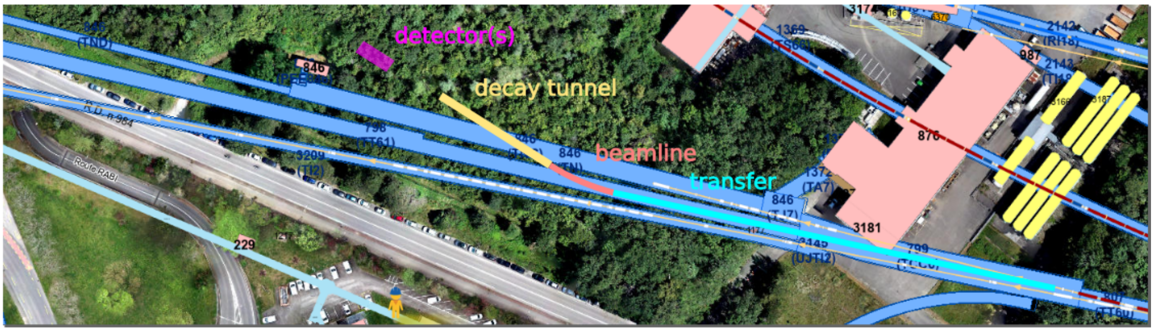

Fig. 114: The solution that is currently considered to be the easiest to achieve has a straight transfer from the TCC6 cavern into TT61. From there, the beamline intersects the wedge between TT61 and TNC and penetrates the soil north of TNC. Excavation for the neutrino detectors and for the beamline will be required; however, existing infrastructure is leveraged more effectively compared to any other solution.

6.5.7 Conclusions and Outlook

The study of the SBN at CERN is well on track. The beamline optimisation was highly successful despite the challenges of introducing the NuTag tracker hardware into the beamline. The transmission improvements achieved by the optimisation process were successfully confirmed by respective BDSIM simulations. As currently designed, the SBN beamline reduces the total PoT required by the ENUBET Collaboration to reach its physics goals by a rough factor of three to four. The study has found that the PS cannot drive the beamline effectively due to the reduced meson yield at PS energies — SPS energies are required. With the yearly intensity of roughly 25 % of the yearly TCC2 intensity and a 9.6 s spill duration, the experiment would reach its physics goals in six to seven years depending on the number of heavy-ion runs. An increased SFTPRO intensity per year as a result of increasing the SHiP cycle intensity would reduce the experiment's runtime to 5 years or less, depending on the SPS spill duration. Different locations at the SPS have been analysed [128]. Currently, the implementation in the TT61/TNC tunnels is favoured. This implementation, however, requires a second slow-extraction setup in the SPS [138]. The next steps will include the start of the potential technical integration of the experiment.

Chapter 7

Interfaces with Other Working Groups

Dipanwita Banerjee, Johannes Bernhard, Nikolaos Charitonidis, Matthew Fraser, Yacine Kadi, Laurence James Nevay, Maarten van Dijk

Introduction

The Conventional Beams Working Group has greatly benefited from the insights and discussions with other PBC working groups, as well as various CERN working groups. Proton delivery is a key issue and there is a significant potential impact from BDF/SHiP operation due to a reduction of the duty cycle for North Area operation. This has been studied originally by the Complex Performance study group [139] within the PBC Accelerators and Facilities study [9] and in synergy with the Beam Dump Facility working group (BDF) [3, 4, 88]. With the approval of BDF-SHIP for the Technical Design Report phase in March 2024, these studies have been extended to two new working groups bSAC (Beam Sharing Across Complex) and SOX (Spill Optimisation for Experimental Areas) with a mandate to summarise the studies by Q1/2025.

In the course of the second PBC phase, an ECN3 task force has been installed, providing a first concept for providing proton beams with higher intensities to ECN3, agnostic to the then later chosen experiment. After BDF/SHiP was selected, the new project, HI-ECN3, took over with the goal of working out the details for both delivering high-intensity beams and transforming TCC8 and ECN3 into a new beam dump facility that will serve the BDF/SHiP experiment. The deliverable will be a technical design report that is currently being prepared. These upgrades rely on a thorough consolidation of the North Area and its infrastructure. HI-ECN3 thus works in close synergy with the NA-CONS consolidation project.

Another restriction comes from high radiation doses at critical locations such as extraction septa, splitters and primary targets. In this domain we profit from excellent progress made by the SPS Losses and Activation Working Group, SLAWG [140].

7.1 North Area Consolidation Project (NA-CONS)

A consolidation of the North Experimental Area has been approved in 2021 (NA-CONS project) and will see a major two-phased facelift in the upcoming years, covering the renovation of beamline equipment, infrastructures and services to recover reliability and bring the facility into compliance with modern safety requirements. The first phase of the consolidation programme is targeting the single-point-of-failures with particular focus on the primary beam delivery systems. The second phase of the consolidation will guarantee flexibility for, and compatibility with, future upgrades and experiments.

Figure 115 gives an overview of the locations that are targeted by both consolidation phases: Phase 1 of NA-CONS (2019–2029), in blue, aims at the consolidation of the primary beam areas including TT20, TDC2, TCC2, BA2, BA80 and the high-intensity beamline towards TCC8 and ECN3. Phase 2 (2030–2035), in orange, will address the consolidation of the Experimental Halls EHN1 and EHN2 together with their associated beamlines and technical buildings BA81 and BA82. The North Area Consolidation project is fully funded, and its Cost-To-Completion amounts to 89.2 MCHF for Phase 1 and 81.8 MCHF for Phase 2, corresponding to a total cost of 171 MCHF, excluding CERN staff. All work packages of Phase 1 are globally validated and ready for LS3. No showstoppers have been identified so far except the availability of storage space which will be critical.

Return of experience from operating the North Area in the last years indicates clearly the need for a full consolidation. Nearly all major breakdowns and downtimes in the last years stems from faults in TCC2 and from BA80 power converters with an increasing trend. Some faults had the potential to stop operation

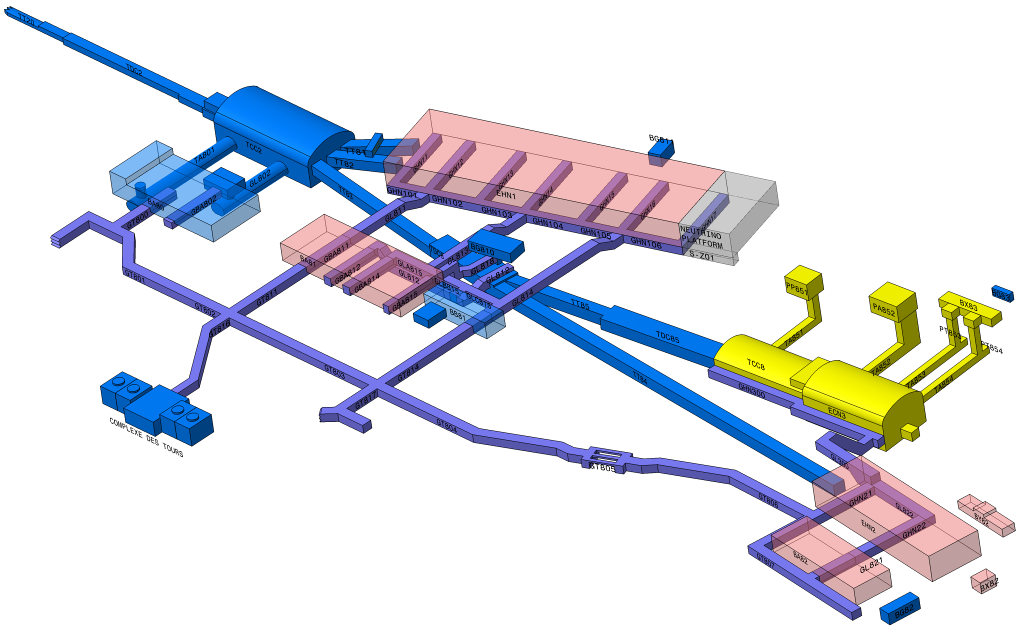

Fig. 115: Overview of the experimental areas, beam tunnels, target caverns, and technical galleries in the CERN North Area. The locations affected by Phase 1 of NA-CONS are depicted in blue (caverns, tunnels, service buildings) and in violet (technical galleries), areas targeted by Phase 2 are shown in light red, and locations under HI-ECN3 are in yellow.

for specific beamlines and experiments for a long time, however it was just about possible to mitigate the consequences so far. The observed sudden increase of magnet faults in TCC2 hints to a potential end-of-life scenario, in particular as there are not enough spares currently available to cover magnets at risk. Realistically, one would expect longer downtimes and/or reduced performance of beamlines now. While the original NA-CONS baseline did not cover a full renovation, in particular of the TCC2 target cavern, discussions are progressing well to extend the scope and address these concerns.

A shifted and longer LS3 offers a unique opportunity to address the situation. It is proposed to carry out a full renovation of the TCC2 area including the entire re-alignment of the beamlines, the replacement of the old MTN, MTS, MSN and QSL magnets and production of additional spares, the replacement of plug-in supports and damaged magnet supports, extensive cabling/de-cabling, shielding removal and re-routing of all the services to provide better accessibility. Such an extension of scope will ensure a safe and reliable operation throughout the next 20 years and maximise the combined Run4/Run5 physics and test-beam availability.

7.2 HI-ECN3 Project and Former BDF Working Group

The consolidation efforts go hand in hand with the recent decision to host a new experimental facility to search for hidden sector particles, for which an original Expression of Interest [14] was submitted to the SPSC in October 2013, identifying underground locations around the SPS (TCC4, TNC, ECN3, and TT61) locations [141]. At that time, all the suitable locations had recently approved programmes (AWAKE, HiRadMat, and NA62, respectively) and TT61 was disfavoured for environmental reasons. Studies continued with a focus on the construction of an entirely new facility at a new underground cavern in the NA, coined ECN4. Following a Technical Proposal [15, 16] submitted to the SPSC in 2015, a three-year Comprehensive Design Study (CDS) was carried out under the auspices of the CERN PBC initiative to prepare a proposal for the Beam Dump Facility (BDF) [17] and the SHiP experiment [18, 19] to the 2020 European Strategy for Particle Physics Update. The BDF/SHiP proposal was recognised as one of the leading candidates among the new facilities explored in the PBC study. However, due to cost considerations, the project could not, as of 2020, be recommended for construction in the near future in light of the overall recommendations from the Update of the European Strategy for Particle Physics [142]. Following a thorough assessment of alternative sites [143], focus moved to ECN3 to reduce the investment cost for the implementation of the facility. After a competitive process via the SPSC, in which several experimental proposals were compared [114], the CERN Research Board selected the BDF/SHiP experiment [20] for the future exploitation of the ECN3 experimental cavern after LS3 including an upgrade of the facility to higher beam intensity. Figure 116 shows an overview of BDF/SHiP in ECN3.

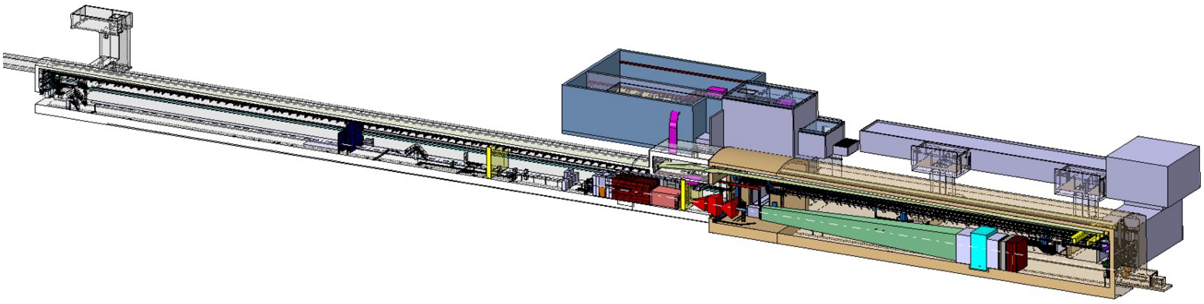

Fig. 116: BDF/SHiP integrated inside the ECN3 experimental cavern.

The cost of upgrading and implementing BDF in ECN3 for SHiP came in at approximately 100 MCHF lower than the original ECN4 proposal by removing the need for major civil engineering works and by re-using existing infrastructure, as well as profiting from the ongoing investment in the consolidation of the North Area. Alongside the NA-CONS project, the upgrade of ECN3 will secure the long-term future of the SPS Fixed Target physics programme at CERN. The HI-ECN3 project is presently in a rapid technical design phase with the delivery of the Technical Design Report (TDR) expected mid-2026. The project is working in close synergy with the NA-CONS project to upgrade the required accelerator infrastructure as part of the foreseen consolidation programme during LS3, 2026–2029. The TDR for BDF/SHiP is expected around mid-2027. The construction plan foresees commissioning of the facility in 2031 and detector in 2032 with at least one year of initial physics data taking before LS4, marking the start of a programme of exploration until the mid of this century.

7.3 Complex Performance Study Group

A common feature of most of the proposals received is the request for higher intensities. In the first phase of PBC, the Complex Performance Study Group was formed to study proton sharing scenarios across the CERN accelerator complex and possible optimisations, including the proton flux requirements, for future operation of the proposed PBC experiments.

After CNGS operation stopped in December 2012, the North Area fixed-target experiments receive spills with 4.8 s flat top at the highest possible repetition rate. The working group studied a possible scenario for simultaneous operation of BDF/SHiP in the same super-cycle, for which the NA fixed-target cycles are alternated with 4 cycles of 7.2 s each for the SHiP Beam Dump Facility (BDF), as shown in Fig. 117, assuming CNGS-like cycles. Depending on the number of BDF/SHiP cycles, the proton flux sharing per year between BDF and the other NA fixed-target experiments is shown on the left side of Fig. 118.

In this scenario, the FT programme would receive about 10^{19} protons on target per year. This, for instance, would have corresponded to the request of KLEVER alone. The overall FT request is probably by a factor 1.5 higher. Therefore, and in this scenario, some prioritisation by the scientific committees would be necessary in the proton flux attribution.

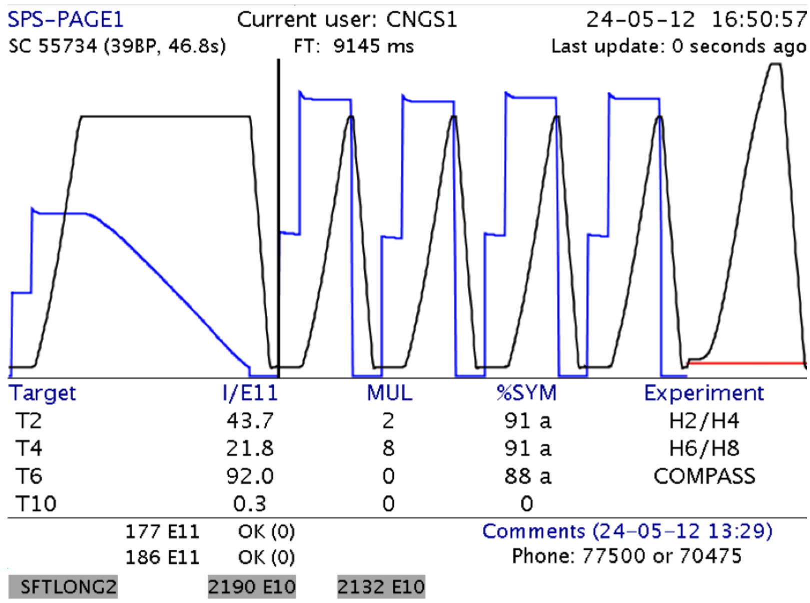

Fig. 117: An example of running the NA fixed-target programme and CNGS cycles in the same super-cycle. BDF cycles were assumed to be similar to CNGS cycles, but with a 1 s flat-top in a slow-extracted spill instead of a fast extraction.

The scale on the right-hand side of Fig. 118 indicates the number of 4.9 s spills per year. With an increasing number of spills for BDF, the duty cycle and hence the number of spills available for the existing North Area fixed-target programme decreases by up to about a factor 3. This is still the favoured scenario in case the available proton flux is the main limiting factor and concern. In case the request for proton flux extracted to the North Area would be lower than 4×10^{13} protons per spill, a solution (also adopted during CNGS operation) would be to lengthen the flat top and increase the proton flux per spill in proportion. The extra spill duration has only a marginal effect on the overall super-cycle length. As an extreme example, the spill length could be doubled, at a slight reduction of the overall proton flux available but with much increased duty cycle. The right side of Fig. 118 shows the proton sharing between BDF and North Area physics for this scenario. The number of spills is still the same, but can also be expressed in "equivalent spills" (periods of 4.9 s with beam): the number of equivalent spills is doubled and much closer to the number from 2018. Details of these schemes are described in the report of the Proton Performance working group [139].

In March 2024, the Research Board approved the Technical Design Report Phase for BDF/SHiP, following which the task of finalising the proton sharing studies and spill optimisation for the North Area was taken over by the Beam Sharing Across the Complex (bSAC) and Spill Optimisation for eXperiments (SOX) Working Groups as described below.

7.4 Beam Sharing Across the Complex (bSAC)

In March 2024, SHiP was approved for its Technical Design Report (TDR) phase, with the aim of being housed in the future High-Intensity ECN3 facility. SHiP requests 4×10^{19} protons on target (pot) annually, which will substantially reduce the number of available spills for the North Area, as outlined above. This reduction also affects upstream machines, impacting their supercycle compositions and the availability of beam time for other users, such as ISOLDE and n_TOF.

To ensure a coherent proton-sharing strategy across CERN's facilities, the bSAC working group

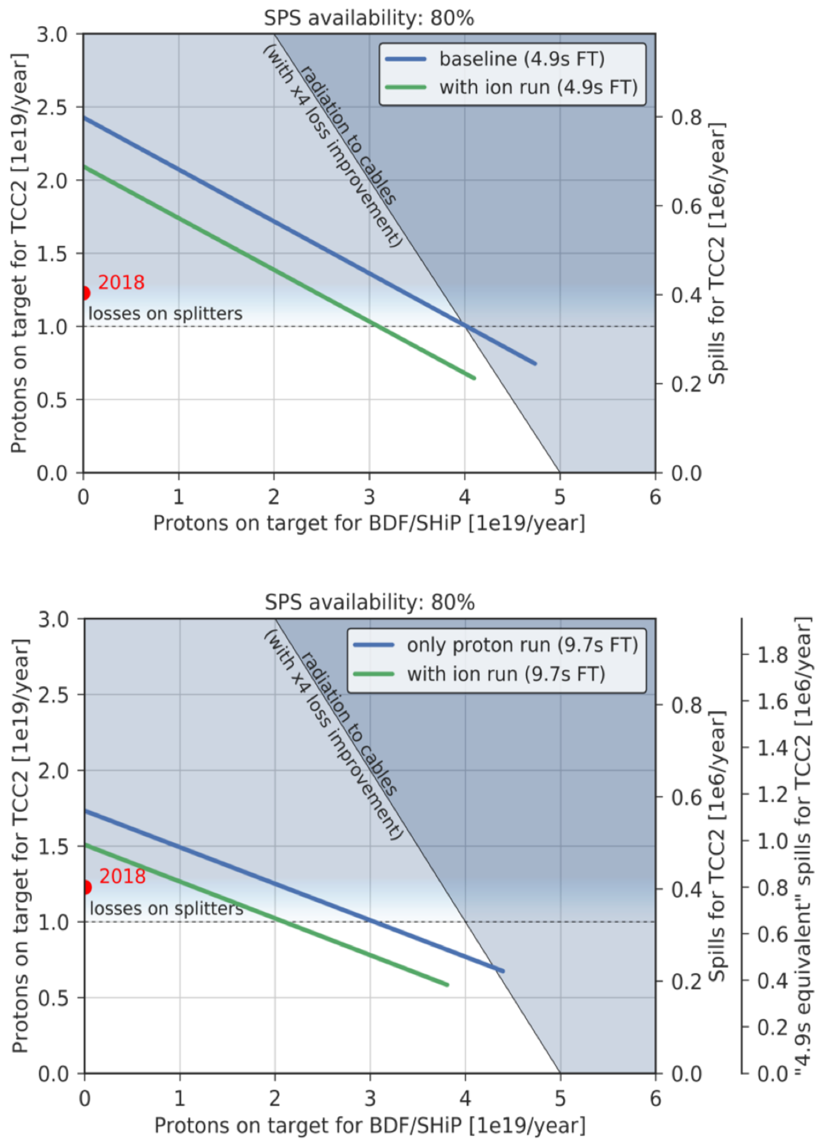

Fig. 118: Possible scenarios for proton sharing between SHiP/BDF and the North Area physics programme, with a spill duration of 4.9 s (top) and 9.7 s (bottom) for the North Area operation.

has been mandated by the IEFC to study, analyse and document various proton-sharing scenarios within the CERN accelerator complex as a whole. Additionally, bSAC is responsible for developing quantitative models to assess the impact of potential optimisation measures, identify possible limitations, and propose mitigation strategies for any bottlenecks. The group's work is expected to be completed by Q1/2025.

7.5 Spill Optimisation for eXperiments (SOX)

Beyond the critical challenge of proton sharing, ensuring the spill quality and intensity required by current and future experiments and test beam users is similarly essential. With the expected reduction in available spills for the North Area, optimising the delivered spills will be crucial for maintaining the statistical precision of data collected by experiments.

To address this, the SOX working group has been mandated by the IEFC to investigate and document requirements for slow extraction spill quality, intensity and spill length for users in the North and East

Areas. The group will propose necessary measures to optimise beam transport and delivery, including potential R&D efforts for accelerators and experimental areas to overcome existing limitations. The work is scheduled for completion by Q1 2025.

7.6 SPS Losses and Activation Working Group (SLAWG)

The SLAWG working group in the Accelerator and Technical sector is aiming to provide proposals for the reduction of losses and activation at extraction, splitting and beam transfer to the North Area. The total requirement for protons to the North Area is well above the maximum considered feasible today. The working group proposed very promising solutions to reduce the losses at extraction and in the proton transfer to the North Area, for instance, through local and non-local crystal shadowing and the use of octupoles.

7.7 Beam Instrumentation for Fixed Targets (BIFT)

Many of the experiments quoted in this document require significant increases of the beam intensity. This implies a need for robust and reliable equipment, especially beam instrumentation, that meets these requirements and simultaneously minimises interventions in radiation areas. The BIFT working group (Beam Instrumentation for Fixed Targets) has taken over this mandate from the former EABI working group [144]. The mandate was extended to include instrumentation for primary beamlines, target regions, and secondary beamlines. A key series of items is being followed by this working group in the context of the North Area consolidation NA-CONS [145], requiring substantial overhaul and improvement across many equipment families. Similarly, many experiments followed under the PBC mandate will require specific instrumentation, which is taken up by the BIFT following approval of the respective experiment. Minutes of all BIFT meetings can be found on the respective Indico category [146].

Chapter 8

Summary and Outlook

Dipanwita Banerjee, Johannes Bernhard, Markus Brugger, Nikolaos Charitonidis, Silvia Schuh

8.1 Further Studies

In the preceding chapters, we have shown many study results relevant for the evaluation of the long list of proposals submitted to the Conventional Beams Working Group. There is an impressive progress that happened since the first phase of Physics Beyond Colliders and many studies evolved from concepts to implemented experiments. In the following, we indicate what still needs to be studied further in the coming years, in case their respective proposals are approved and shall be implemented.

DICE/NA60+

The DICE/NA60+ Collaboration will soon be ready to submit a proposal for an experiment at the H8 beamline to the CERN SPS Committee. Should the review yield a positive outcome, the next step will be the preparation of a Technical Design Report, detailing the technical implementation of the experiment. A key focus will be on studying critical aspects of beam delivery, particularly ensuring stable and reliable operation of ion beams at all requested energies, as well as developing a detailed proposal for the safe extraction of primary proton beams at different momenta for reference measurements.

ENUBET, NuTag and the PBC-SBN beamline

While conceptual studies for ENUBET and NuTag study were successfully completed, the new SBN idea is currently taking shape, combining the strengths of both original proposals. Feasibility studies for hosting the SBN beamline at CERN made quick progress and show already that such a concept could be implemented given adequate resources and priorities. The next step would require a preparation phase for a conceptual design report, concentrating on further studies of a new slow extraction from the SPS and the identification of a potential site. In the meantime, studies for hosting such a beamline outside of CERN are being pursued, with the possibilities being Fermilab and J-PARC.

High Intensity Upgrades

As discussed also in Section 3.3, the suppression of halo particles reaching the NA64e trigger system and the simultaneous electron intensity increase is quite important for the physics scope of the experiment. Based on dedicated beam measurements taken during 2024, an optimisation of the final focusing section of the beamline is currently being studied. This optimisation of the line using multi-objective optimisation algorithms examines the installation of new, or the re-organisation of existing quadrupole magnets.

These modifications must come in-tandem with an increased intensity (150–200 units) on the T2 target, that will allow a better collimation and therefore control of the halo arriving to the experimental area. In particular for the ERC-funded project POKER [56], part of NA64e, that focuses on exploiting the resonant annihilation channel $\mathrm{e}^+ + \mathrm{e}^- \to \mathrm{A}' \to \chi\overline{\chi}$, very pure positron beams are necessary. The fraction of positrons in beams is always smaller and decreases faster with momentum than that of electrons in negative beams due to the strong proton production in the former case. Despite the very nice spectrometer resolution of the H4 line, the protons mainly from the Λ decay before the electron/positron converter constitute a contamination source that is quite challenging to be removed. The veto of the hadrons is possible at the level of the experiment; however this also necessitates the higher intensities at the level of the T2 target in order to reach similar statistics of e^+ as for the e^-. Other experimental users would also profit from increased intensity.

For the period after LS3, MUonE and AMBER request high intensity muon and hadron beams in EHN2. Currently, the muon beam is limited to 2×10^8 μ per 4.8 s spill with 150 units of 10^{11} protons/pulse on the T6 target. Following the measurements performed with HSE-RP, mitigations are possible for the radiation to increase the muon intensity by nearly a factor 3. In order to achieve this, studies have been initiated to improve the acceptance of the M2 beamline. In addition increasing the number of units on the T6 target, e.g., up to 200 units of 10^{11} ppp per 4.8 s spill will help gain another 30 %. Similarly, for AMBER higher intensity hadron beams, increasing the number of units on the T6 target will help collimate further the beam upstream, thus reducing the tails in the beam divergence. This will increase the relative fraction of identifiable kaons for their Drell–Yan programme. Studying the feasibility of increasing the intensity, as well as determining the limits on the North Area targets, is therefore very critical. For these high intensity requests the longest target lengths will always be used to maximise the production of the secondary beam. Thus, the XTAX will never see the full intensity of the beam. However, as the XTAX will be limited to 150 units post-LS3 following the consolidation of the element, a target interlock should be envisaged with these increased intensities to prevent more than 150 units reaching the XTAX. Studies to check the conditions for this interlock and its implementation are also needed.

Experiments at the FCC-ee injectors

A future CERN FCC-ee injector chain (see Fig. 119) could provide a combined experimental and test-beam programme for the CERN North Area. Developing effective methods to extract electron and positron beams at intermediate injection energies back into the North Area complex would address key test-beam requirements essential for future FCC detector designs while simultaneously extending CERN's physics programme on the precision and intensity frontier.

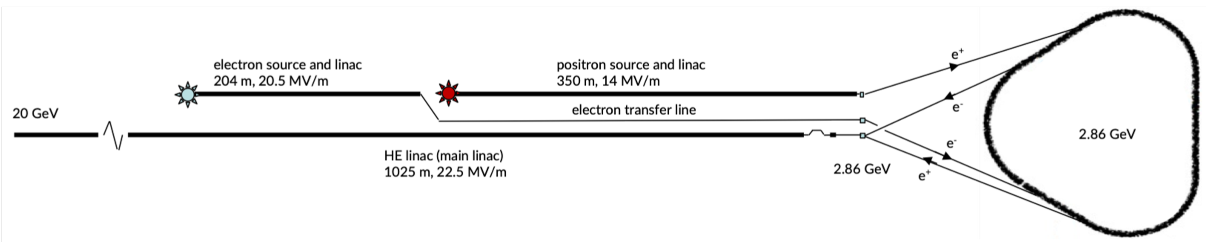

Fig. 119: Schematic layout of the proposed FCC-ee injector complex [147].

The FCC-ee injector could deliver an unprecedented flux of up to 20 GeV electrons, surpassing current LDMX designs at SLAC and offering competitive combined electron/positron beams in the range of a few to 20 GeV to a global user community. The beam parameters in Table 14 illustrate the achievable performance. This could enable future experiments with enhanced sensitivity to rare dark matter production channels, as well as setups benefiting from bremsstrahlung photons or hadron conversions with time-of-flight capabilities. Some first ideas have been discussed at a recent workshop at CERN [148].

To explore these possibilities further and develop a platform that enhances the global dark-sector exploration programme, a PBC-driven physics and facility "think tank" should be envisaged during the pre-TDR phase of the FCC-ee project.

Table 14: Beam parameters of the FCC-ee injector complex [147].

Parameter	FCC	PBC FT users
Beam Energy (GeV)	20	$\leq$ 20
Max. bunch charge (nC)	4	4
Max. bunch population	0.1–2.5	2.5
Bunches per pulse	2–4	1–4
Linac repetition rate (Hz)	50–100	100
Norm. emittance x/y (mm mrad)	$\leq$ 20/2	$\leq$ 20/2
Physical emittance x/y (nm rad)	$\leq$ 0.5/0.05	$\leq$ 0.5/0.05
Bunch length rms (mm)	4	1–4
Energy spread (%)	0.1	0.1–0.75
Bunch spacing (ns)	25	25 or 50
Pre-injector duty cycle (%)	5–73	27–95

8.2 Cost Estimates

Cost estimates remain largely preliminary. Table 15 lists the current estimates, categorised into four cost groups as an initial reference. Notably, consolidation costs, such as those for electrical systems, cooling, ventilation, and civil engineering infrastructure, are not included. Additionally, these estimates pertain solely to beam and infrastructure upgrades and do not account for the costs of the experiments themselves. The cost categories are defined as follows:

- C0: Up to 300 kCHF
- C1: From 300 kCHF to 2 MCHF
- C2: From 2 to 10 MCHF
- C3: Above 10 MCHF

Please note that some of these upgrades have already been partly or completely implemented, including the new shielding for NA61++, the newly established PPE144 zone with NA64e already taking data in it, and the re-cabling of the first achromat in the K12 beam.

8.3 Summary

In almost all cases, the available studies give good indications of the feasibility and implications of the beams and infrastructure modifications associated with the proposed experiments. However, in view of an actual implementation, more time and resources are required. These resources include budget for R&D studies, industrial manpower (e.g. for integration studies), as well as staff, fellows and/or project associates.

Table 15: Preliminary cost estimates for the initial proposals where available. The definition of cost categories is explained in the text.

Location	Proposal	Foreseen upgrades	Cost category	Comment
EHN1	NA61++	Shielding, interlocks	C1	Done.
	DICE/NA60+	Shielding, magnets, power, beam instrumentation (TT20+H8)	C2	
	NA64e	Semi-permanent location	C0	Done.
EHN2	NA64μ	New location in beamline	C0	Done.
	NA64μ	Phase 2, detector installation in SM2	C0	
	MUonE	Installation in M2 beamline	C1	
	AMBER	Static vacuum improvements	C1	Ongoing.
	AMBER	Magnetic collimator upgrade	C2	
	AMBER	New RF-separated beam	C3	
ECN3	NA62/HIKE-BD	Re-cabling for μ sweeping	C0	Done.
	HIKE-K+	Compatibility with high intensity operation	C3	
	HIKE-KL	Replacement of K12 with neutral beamline	C2	
	HIKE-KLEVER	Upgrades, civil engineering, and new beamline	C3	
	SHADOWS	Integration of experiment	C2	
	DIRAC++	New K12 beamline	C2	
other	ENUBET[1]	New beamline (site-independent)	N/A	
	NuTag[1]	New beamline (site-independent)	N/A	
	SBN	New slow extraction from SPS	C3	

[1]Conceptual design, now superseded by SBN.

Acknowledgements

We have profited from and are grateful for important input from a large number of experts, in particular C. Ahdida, P. Avigni, H. Bartosik, M. Battistin, L. Bellantoni, P. Boisseaux-Bourgeois, K. Buffet, G. Burt, M. Calviani, S. Cholak, A. Ciccotelli, M. Dos Santos, A. Ebn Rahmoun, L.S. Esposito, R. Folch, M.A. Fraser, Y. Gaillard, F. Gerigk, S. Girod, R. Jacobsson, D. Jaillet, V. de Jesus, Y. Kadi, M. Lazzaroni, J. Lehtinen, A. Lafuente Mazuecos, V. Marchand, E. Nowak, S. Pagan, T. Prebibaj, B. Rae, G. Romagnoli, F. Sanchez-Galan, P. Schwarz, K. Sidorowski, N. Solieri, F.M. Velotti, Heinz Vincke, Helmut Vincke, and T. Zickler.

Parts of this report build upon material prepared in the previous edition, for which we gratefully acknowledge the contributions of the earlier authors G.L. d'Alessandro, A. Gerbershagen, E. Montbarbon, and M. Rosenthal.

The studies included in this report have been performed in close collaboration with the representatives of the proposals submitted to the group, in particular A. Aduszkiewicz, V. Andrieux, G. Arduini, A. Ceccucci, P. Crivelli, O. Denisov, B. Döbrich, J. Friedrich, S. Gninenko, E. Goudzovski, J. Jäckel, E. Kabuß, S. Kowalski, G. Lanfranchi, C. Lazzeroni, A. Longhin, G. Mallot, C. Matteuzzi, L. Molina Bueno, M. Moulson, L. Nemenov, M. Perrin-Terrin, S. Pulawski, G. Ruggiero, G. Schnell, E. Scomparin, T. Spadaro, F. Terranova, G. Usai, C. Vallée, B.M. Veit, G. Venanzoni, W. Wuensch, and E.D. Zimmerman.

We thank A. Papageorgiou Koufidou for her outstanding editing work on the first edition of this report. Finally, we acknowledge the excellent collaboration with and support from the PBC management and the other PBC working groups, contributing CERN working groups, as well as of the ECN3 task force, the NA-CONS project, and the HI-ECN3 project.

Glossary

BDF Beam Dump Facility
BSI Beam Secondary emission Intensity monitor
BSM Beyond Standard Model
CCC CERN Control Center
CEDAR differential Cherenkov counter with achromatic ring focus
CNGS CERN Neutrino to Gran Sasso beamline
DIRAC Di-meson Relativistic Atom Complex experiment
ECN3 Experimental Cavern North 3
EHN1/2 Experimental Hall North 1/2
FIPs Feebly Interacting Particles
FT Fixed Target
GPD Generalised Parton Distribution
HIKE High Intensity Kaon Experiments
HL-LHC High Luminosity Large Hadron Collider
KLEVER KLong Experiment to detect VEry Rare decays LDM Light Dark Matter
LHC Large Hadron Collider
LKr Liquid Krypton
PBC Physics Beyond Colliders
pot protons on target
ppp protons per pulse, i.e. protons per spill
PID Particle Identification Detection
PS Proton Synchrotron
PDF Parton Distribution Functions
PSB Proton Synchrotron Booster
PSD Projectile Spectator Detector of the NA61 experiment
QCD Quantum ChromoDynamics
QGP Quark Gluon Plasma
SHADOWS Search for Hidden And Dark Objects With the SPS
SPS Super Proton Synchrotron
SPSC Super Proton Synchroton Committee
TAX Target Attenuator eXperimental areas, a movable collimator and beam dump combination
TBIU Target Box Instrumentation Upstream
TPC Time Projection Chamber

Tables

Figures

References

[1] D. Banerjee et al., Report from the Conventional Beams Working Group to the Physics Beyond Colliders Study and to the European Strategy for Particle Physics, CERN-PBC-REPORT-2018-002 (CERN, Geneva, Dec 2018).

[2] D. Banerjee et al., Report from the Conventional Beams Working Group to the Physics Beyond Colliders Study and to the European Strategy for Particle Physics, CERN-PBC-REPORT-2022-002 (CERN, Geneva, Dec 2022).

[3] C. Ahdida et al., SPS Beam Dump Facility - Comprehensive Design Study, CERN-PBC-REPORT-2019-005 ; CERN-2020-002 (CERN, Geneva, 2020).

[4] O. Aberle et al., Study of alternative locations for the SPS Beam Dump Facility, CERN-ACC-NOTE-2022-0009 ; CERN-PBC-Notes-2022-002 (CERN, Geneva, 2022).

[5] Physics Beyond Colliders Working Group Meeting, `https://indico.cern.ch/event/827066/`, Nov 2019.

[6] D. Banerjee et al., The North Experimental Area at the CERN Super Proton Synchrotron, CERN-ACC-NOTE-2021-0015 (CERN, Geneva, Jul 2021).

[7] Physics Beyond Collider study website, `http://pbc.web.cern.ch/`, last accessed 31 March 2025.

[8] Physics Beyond Colliders Annual Workshop 2021, `https://indico.cern.ch/event/1002356/`, Mar 2021.

[9] Accelerators and Technology Domain, `https://pbc.web.cern.ch/acc/`.

[10] The Physics Beyond Colliders Kickoff Workshop, `https://indico.cern.ch/event/523655/`, Sep 2016.

[11] O. Denisov, COMPASS, a Universal Facility for Hadron Structure and Spectroscopy Studies, Presented at the Physics Beyond Colliders Kickoff Workshop (CERN, Geneva, Sep 2016).

[12] J. Friedrich, O. Denisov and A. Vorobyev, Addendum to the COMPASS-II Proposal, CERN-SPSC-2017-034; SPSC-P-340-ADD-1 (CERN, Geneva, Apr 2018).

[13] B. Adams et al., Letter of Intent: A New QCD facility at the M2 beam line of the CERN SPS: COMPASS++/AMBER, CERN-SPSC-2019-003; SPSC-I-250; SPSC-I-250 (CERN, Geneva, Aug 2018).

[14] W. Bonivento et al., Proposal to Search for Heavy Neutral Leptons at the SPS, CERN-SPSC-2013-024, SPSC-EOI-010, SPSC-EOI-010 (CERN, Geneva, Oct 2013).

[15] M. Anelli et al., A Facility to Search for Hidden Particles (SHiP) at the CERN SPS, CERN-SPSC-2015-016, SPSC-P-350 (CERN, Geneva, Apr 2015), Technical Proposal.

[16] M. Anelli et al., A Facility to Search for Hidden Particles (SHiP) at the CERN SPS (Addendum to Technical Proposal), CERN-SPSC-2015-040, SPSC-P-350-ADD-2 (CERN, Geneva, Oct 2015), Technical Proposal.

[17] C. Ahdida et al., SPS Beam Dump Facility - Comprehensive Design Study, CERN-2020-002 (CERN, Geneva, Jan 2020), doi:10.23731/CYRM-2020-002.

[18] C. Ahdida et al., SHiP Experiment - Progress Report, CERN-SPSC-2019-010, SPSC-SR-248 (CERN, Geneva, Jan 2019).

[19] C. Ahdida et al., SHiP Experiment - Comprehensive Design Study report, CERN-SPSC-2019-049, SPSC-SR-263 (CERN, Geneva, Dec 2019).

[20] R. Albanese et al., BDF/SHiP at the ECN3 high-intensity beam facility, CERN-SPSC-2023-033; SPSC-P-369 (CERN, Geneva, Oct 2023).

[21] F. Acerbi et al., Design and performance of the ENUBET monitored neutrino beam, *Eur. Phys. J. C* **83** (2023) 964, doi:10.1140/epjc/s10052-023-12116-3.

[22] F. Acerbi et al., The ENUBET project, CERN-SPSC-2018-034, SPSC-I-248 (CERN, Geneva, Oct 2018).

[23] M.U. Ashraf et al., High Intensity Kaon Experiments (HIKE) at the CERN SPS: Proposal for Phases 1 and 2, CERN-SPSC-2023-031; SPSC-P-368 (CERN, Geneva, Oct 2023).

[24] E. Cortina Gil et al., HIKE, High Intensity Kaon Experiments at the CERN SPS, CERN-SPSC-2022-031, SPSC-I-257 (CERN, Geneva, 2022).

[25] G. Usai, Investigating the QCD phase transitions with dileptons: new opportunities at the CERN SPS, Presented at the Physics Beyond Colliders Kickoff Workshop, CERN, Sep 2016.

[26] C. Ahdida et al., Letter of Intent: the NA60+ experiment, CERN-SPSC-2022-036 (CERN, Geneva, 2022).

[27] N. Abgrall et al., NA61/SHINE facility at the CERN SPS: beams and detector system, *JINST* **9** (2014) P06005, doi:10.1088/1748-0221/9/06/P06005.

[28] M. Gazdzicki and P. Seyboth, Search for critical behavior of strongly interacting matter at the CERN Super Proton Synchrotron, *Acta Phys. Pol. B* **47** (2015) 1201, doi:10.5506/APhysPolB.47.1201.

[29] M. Gazdzicki, NA61/SHINE: physics and facility beyond 2020, Presented at the Physics Beyond Colliders Kickoff Workshop, CERN, Sep 2016.

[30] A. Aduszkiewicz, Study of Hadron-Nucleus and Nucleus-Nucleus Collisions at the CERN SPS: Early Post-LS2 Measurements and Future Plans, CERN-SPSC-2018-008. SPSC-P-330-ADD-10 (CERN, Geneva, Mar 2018).

[31] S. Gninenko, Search for dark sector physics in missing energy events at the CERN SPS, Presented at the Physics Beyond Colliders Kickoff Workshop, CERN, Sep 2016.

[32] S. Gninenko, Addendum to the NA64 Proposal: Search for the $A' \to invisible$ and $X \to e^+e^-$ decays in 2021, CERN-SPSC-2018-004, SPSC-P-348-ADD-2 (CERN, Geneva, Jan 2018).

[33] S. Gninenko, Addendum to the Proposal P348: Search for dark sector particles weakly coupled to muon with NA64μ, CERN-SPSC-2018-024, SPSC-P-348-ADD-3 (CERN, Geneva, Sep 2018).

[34] M Perrin-Terrin, Neutrino tagging: a new tool for accelerator based neutrino experiments, *Eur. Phys. J. C* **82** (2022) doi:10.1140/epjc/s10052-022-10397-8.

[35] A. Baratto-Roldán et al., NuTag: a proof-of-concept study for a long-baseline neutrino beam, *Eur. Phys. J. C* **84** (2024) 1024, doi:10.1140/epjc/s10052-024-13324-1.

[36] G. Venanzoni, MUonE, Presented at the Physics Beyond Colliders Annual Workshop, CERN, Nov 2017.

[37] F. Acerbi et al., SBN@CERN: A short-baseline neutrino beam at CERN for high-precision cross-section measurements, arXiv:2503.21589 (CERN, Geneva, March 2025).

[38] G. Lanfranchi, SHADOWS, Presented at the Physics Beyond Colliders Annual Workshop, Mar 2021.

[39] M. Alviggi et al., SHADOWS Technical Proposal, CERN-SPSC-2023-029; SPSC-P-367 (CERN, Geneva, 2023).

[40] P. Crivelli, True muonium in fixed target experiments at the current and future CERN facilities, Presented at the Physics Beyond Colliders Annual Workshop (CERN, Geneva, Mar 2021).

[41] N.T. Doble, L. Gatignon, G. Von Holtey and F.N. Novoskoltsev, The upgraded muon beam at the SPS, *Nucl. Instrum. Meth. Phys. Res. A* **343** (1993) 351, doi:10.1016/0168-9002(94)90212-7.

[42] E. Cortina Gil et al., The beam and detector of the NA62 experiment at CERN. The Beam and detector of the NA62 experiment at CERN, *JINST* **12** (2017) P05025, doi:10.1088/1748-0221/12/05/P05025.

[43] D. Banerjee et al., Search for invisible decays of sub-GeV dark photons in missing-energy events at the CERN SPS, *Phys. Rev. Lett.* **118** (2016) 011802, doi:10.1103/PhysRevLett.118.011802.

[44] E. Depero et al., High purity 100 GeV electron identification with synchrotron radiation, *Nucl. Instrum. Meth. Phys. Res. A* **866** (2017) 196, doi:10.1016/j.nima.2017.05.028.

[45] W. Scandale et al., Electromagnetic processes in strong crystalline fields, CERN-SPSC-2005-030, SPSC-P-327 (CERN, Geneva, Jun 2006).

[46] S.P. Møller et al., High efficiency bending of 450 GeV protons using channeling, *Phys. Lett. B* **256** (1991) 91, doi:10.1016/0370-2693(91)90224-E.

[47] N. Doble, L. Gatignon and P. Grafström, A novel application of bent crystal channeling to the production of simultaneous particle beams, *Nucl. Instrum. Meth. B* **119** (1996) 181, doi:10.1016/0168-583X(96)00141-3.

[48] M. Moulson, Prospects for an experiment to measure BR$(K_L \to \pi^0 \nu\bar{\nu})$ at the CERN SPS, *J. Phys.: Conf. Ser.* **800** (2016) 012037, doi:10.1088/1742-6596/800/1/012037.

[49] N. Charitonidis and I. Efthymiopoulos, Low energy tertiary beam line design for the CERN neutrino platform project, *Phys. Rev. Accel. Beams* **20** (2017) 111001, doi:10.1103/PhysRevAccelBeams.20.111001.

[50] C. Ahdida, Radiation Protection Assessment of the NA61 High Intensity Pb Run Post-LS2, EDMS 2125733 (CERN, Geneva, 2024), restricted access.

[51] N. Charitonidis, Modifications in PPE142/52 zones for NA61 operation after LS2, EDMS 2093072 (CERN, Geneva, 2020), CERN internal access.

[52] I. Efthymiopoulos et al., Development of Fragmented Low-Z Ion Beams for the NA61 Experiment at the CERN SPS, CERN-ATS-2011-226 (CERN, Geneva, Nov 2011).

[53] Yu. M. Andreev et al., Shedding light on dark sectors with high-energy muons at the NA64 experiment at the CERN SPS, *Phys. Rev. D* **110** (Dec 2024) 112015, doi:10.1103/PhysRevD.110.112015.

[54] Yu. M. Andreev et al., Dark-sector search via pion-produced η and $\eta^{'}$ mesons decaying invisibly in the NA64h detector, *Phys. Rev. Lett.* **133** (2024) 121803, doi:10.1103/PhysRevLett.133.121803.

[55] Yu. M. Andreev et al., First constraints on the $l_\mu - l_\tau$ explanation of the muon $g-2$ anomaly from NA64-e at CERN, *JHEP* **2024** (2024) 212, doi:10.1007/JHEP07(2024)212.

[56] A. Marini et al., Status and perspectives of the poker detector for dark sector searches, *Nucl. Instrum. Meth. Phys. Res. A* **1067** (2024) 169677, doi:10.1016/j.nima.2024.169677.

[57] Yu. M. Andreev et al., Measurement of the intrinsic hadronic contamination in the NA64$-$e high-purity e$^+$/e$^-$ beam at CERN, *Nucl. Instrum. Meth. Phys. Res. A* **1057** (2023) 168776, doi:10.1016/j.nima.2023.168776.

[58] R. Gargiulo, S. Palmisano and E. Di Meco, Feasibility study of true muonium discovery with the CERN-SPS H4 positron beam, *Phys. Rev. D* **110** (2024) 092015, doi:10.1103/PhysRevD.110.092015.

[59] E. Scomparin and G. Usai, Need of reference proton data for the DICE/NA60+ experiment, CERN-PBC-NOTES-2025-003 (CERN, Geneva, 2025).

[60] L.A. Dyks, E.G. Parozzi and M. Van Dijk, Proton beam delivery study for the NA60+ experiment in the H8 beamline at the CERN SPS North Area, CERN-PBC-Notes-2025-001 (CERN, Geneva, 2025).

[61] E. Scomparin and G. Usai, Possible use of MNP33 by the NA60+ experiment, Presented at the 18th EP Magnet Working Group Meeting (CERN, Geneva, Jun 2024).

[62] E. Scomparin, NA60+ status update, Presented at the 21st EP Magnet Working Group Meeting (CERN, Geneva, Jan 2025).

[63] F. Stummer, Computational Studies and Simulation of the MNP33 and MEP48 Magnets for DICE/NA60+, CERN-PBC-Notes-2025-002 (CERN, Geneva, 2025).

[64] C. Ahdida and E. Nowak, Update on RP assessment of NA60+ 40 GeV Pb ion run in EHN1, EDMS 3170937 v1 & v2 (CERN, Geneva, 2025), restricted access.

[65] C. Ahdida, Update on RP assessment of NA60+ 150A GeV Pb ion run in EHN1, EDMS 3231421 (CERN, Geneva, 2025), restricted access.

[66] J. Wenninger, Introduction to slow extraction to the north targets, EDMS 2883124 (CERN, Geneva, 2023).

[67] A. Gerbershagen et al., Design of beam optics and radiation protection concept for NA60+ heavy-ion experiment at CERN, *Nucl. Instrum. Meth. Phys. Res. A* **1047** (2023) 167887, doi:10.1016/j.nima.2022.167887.

[68] J. Bernhard, K. Li, F. Roncarolo and F. Velotti, NA target station beam instrumentation functional specification, EDMS 2897766 (CERN, Geneva, 2024), CERN internal access.

[69] A. Goldblatt, NACONS-HI 3 new BSGs in TT23-24-25 lines, EDMS 3175515 (CERN, Geneva, 2024), CERN internal access.

[70] J. Sanders on behalf of the NA62 collaboration, A new hydrogen-filled Cherenkov detector for kaon tagging at the NA62 experiment at CERN, *JINST* **19** (2024) C05026, doi:10.1088/1748-0221/19/05/C05026.

[71] E. Gousiou, I. Kozsar and G. Kruk, White Rabbit timing—Renovation of the general machine timing, EDMS 3088857 (CERN, Geneva, 2025), CERN internal access.

[72] C. Matteuzzi, Mu-e, Presented at the PBCacc - Conventional Beams WG - 1st Meeting, CERN, Feb 2017.

[73] U. Marconi, Review of the experimental apparatus and systematic errors, Presented at The Evaluation of the Leading Hadronic Contribution to the Muon Anomalous Magnetic Moment, Mainz Institute for Theoretical Physics, Johannes Gutenberg University, Feb 2018.

[74] G. Hall, U. Marconi, C. Matteuzzi and D. Pocanic, Proposal for phase 1 of the MUonE experiment, CERN-SPSC-2024-015 (CERN, Geneva, Aug 2024).

[75] F. Aberle, EHN2 high intensity muons radiation survey, EDMS 3190012 (CERN, Geneva, Geneva, Nov 2024), restriced access.

[76] P. Coet and N. Doble, An Introduction to the Design of High-Energy Charged Particle Beams, CERN/SPS 86-23 (EBS) (CERN, Geneva, 1986).

[77] P. Bernard, P. Lazeyras, H. Lengeler and V. Vaghin, Particle separation with two-and three-cavity RF separators at CERN, CERN-68-29 (CERN, Geneva, 1968), doi:10.5170/CERN-1968-029.

[78] C. Adolphsen et al., Design of the ILC crab cavity system, SLAC-PUB-12751, FERMILAB-TM-2388, EUROTEV-REPORT-2007-010 (SLAC, Jun 2007).

[79] R. Appleby et al., Considerations for a RF separated K^+ beam for NA62, CERN-ACC-NOTE-2021-0013, Note NA62-21-04, CERN-PBC-Note-2021-001 (CERN, Geneva, 2021).

[80] RF-separated beams for AMBER kickoff meeting, `https://indico.cern.ch/event/1069879/`, Sep 2021.

[81] RF-separated beams for Amber- Follow-up Workshop, `https://indico.cern.ch/event/1133376/`, Mar 2022.

[82] A. Gerbershagen et al., Design of beam optics for RF-separated kaon and antiproton beams in the M2 beamline of the CERN North Area, *Nucl. Instrum. Meth. Phys. Res. A* (2022) 168004, doi:10.1016/j.nima.2022.168004.

[83] A. Gerbershagen et al., RF-separated beam project for the M2 beam line at CERN, CERN-PBC-Notes-2022-004 (CERN, March 2022).

[84] Fabian Metzger, Studies for current and future high-intensity operation of CERN's secondary M2 beamline, Dissertation, Rheinische Friedrich-Wilhelms Universität Bonn, 2024, CERN-THESIS-2024-145.

[85] A. Devienne, C. Ahdida and F. Malacrida, Radiation protection assessment of shielding improvements at EHN2 for AMBER Drell–Yan run, EDMS 2670569 (CERN, Geneva, Feb 2023), CERN internal access.

[86] A. Höcker et al., TMVA : The Toolkit for Multivariate Data Analysis eith ROOT, CERN-2008-001.184 (CERN, Geneva, 2008).

[87] L. Nemenov, Experimental checks of precise QCD predictions by studying the $\pi^+K^-, K^+\pi^-, \pi^+\pi^-$ atoms, Presented at Physics Beyond Colliders Kickoff Workshop, CERN, Sep 2016.

[88] Beam Dump Facility working group, `http://pbc.web.cern.ch/bdf/`.

[89] T.J. Roberts et al., G4beamline particle tracking in matter-dominated beam lines, Presented at EPAC08, Genoa, Italy, Conf.Proc.C 0806233 (2008) WEPP120, 2008.

[90] C. Ahdida et al., New capabilities of the FLUKA multi-purpose code, *Front. Phys.* **9** (2022) doi:10.3389/fphy.2021.788253.

[91] Giuseppe Battistoni et al., Overview of the FLUKA code, *Ann. Nucl. Energy* **82** (2015) 10, doi:10.1016/j.anucene.2014.11.007.

[92] M. Van Dijk and M. Rosenthal, Target studies for the proposed KLEVER experiment, CERN-ACC-NOTE-2018-0066 (CERN, Geneva, Oct 2018).

[93] A.J. Malensek, Empirical formula for thick target particle production, FERMILAB-FN-341 (Fermilab, Batavia, IL, Oct 1981).

[94] F. Ambrosino et al., KLEVER: An experiment to measure BR($K_L \to \pi^0 \nu\bar{\nu}$) at the CERN SPS, arXiv:1901.03099, KLEVER-PUB-18-02 (KLEVER collaboration, Jan 2019).

[95] L. Gatignon, Design and tuning of secondary beamlines in the CERN North and East Areas, CERN-ACC-NOTE-2020-0043 (CERN, Geneva, Oct 2020).

[96] M. Soldani et al., Strong enhancement of electromagnetic shower development induced by high-energy photons in a thick oriented tungsten crystal, *Eur. Phys. J. C* **83** (2023) 101, doi:10.1140/epjc/s10052-023-11247-x.

[97] C. Theis et al., Requirements for the TCC8/ECN3 ventilation system due to air activation, EDMS 1176875 (CERN, Geneva, 2011), CERN internal access.

[98] P. Vojtyla and F. Malacrida, Environmental constraints on a ventilation system of NA-62, EDMS 1163163 (CERN, Geneva, 2011), restricted access.

[99] L. J. Nevay, M. Van Dijk, L. Gatignon and J. Bernhard, Conceptual design of a neutral beam line phase 2 of the HIKE experiment, CERN-PBC-Notes-2023-006 (CERN, 2023).

[100] P. Agrawal et al., Feebly-interacting particles: FIPs 2020 workshop report, *Eur. Phys. J. C* **81** (2021) 1015, doi:10.1140/epjc/s10052-021-09703-7.

[101] M. Alviggi et al., SHADOWS Letter of Intent, CERN-SPSC-2022-030, SPSC-I-256 (CERN, Geneva, November 2022).

[102] W. Baldini et al., SHADOWS (Search for Hidden And Dark Objects With the SPS): Expression of Interest, CERN-SPSC-2022-006, SPSC-EOI-022 (CERN, Geneva, January 2022).

[103] D. Chouhan et al., Nanu: Proposal for a neutrino experiment at the SPS collider located at the North Area of CERN, *Nucl. Instrum. Meth. Phys. Res. A* **1064** (2024) 169327, doi:10.1016/j.nima.2024.169327.

[104] F. Stummer, AI-Enhanced Muon Shield Design for Background Mitigation in Next-Generation Intensity Frontier Experiments at CERN, Dissertation, Royal Holloway, University of London, 2025.

[105] F. Stummer et al., Conceptual design of the magnetised iron block system for the shadows experiment, *J. Phys. Conf. Ser.* **2687** (2024) 022030, doi:10.1088/1742-6596/2687/2/022030.

[106] L. Krzempek, Integration studies for the proposed SHADOWS experiment at the CERN North Area, EDMS 3017491 v.0.3 (CERN, Geneva, 2023), CERN internal access.

[107] G.L. D'Alessandro, Studies for current and future high intensity experiments at the cern P42 and K12 beam lines, PhD thesis, Royal Holloway, University of London, 2022, Dissertation.

[108] F. Stummer, Studies and Optimization for Future Beam Dump Experiments in the K12 and P42 Beams at CERN, Master's thesis, Vienna University of Technology, 2021, CERN-THESIS-2021-194.

[109] D.C. Meeker, Finite Element Method Magnetics (FEMM), 2022, `https://www.femm.info`.

[110] L.J. Nevay et al., BDSIM: An accelerator tracking code with particle–matter interactions, *Comput. Phys. Commun.* **252** (2020) 107200, doi:10.1016/j.cpc.2020.107200.

[111] S. Agostinelli et al., Geant4—A simulation toolkit, *Nucl. Instrum. Meth. Phys. Res. A* **506** (2003) 250, doi:10.1016/S0168-9002(03)01368-8.

[112] M. Brugger et al., Mandate of the PBC ECN3 Task Force, EDMS 2790130 (CERN, October 2022).

[113] C. Ahdida et al., Findings of the Physics Beyond Colliders ECN3 Beam Delivery Task Force, CERN-PBC-REPORT-2023-001 (CERN, Geneva, 2023).

[114] C. Ahdida et al., Post-LS3 Experimental Options in ECN3, CERN-PBC-REPORT-2023-003 (CERN, Geneva, 2023).

[115] F. Terranova, ENUBET and synergies with NUSTORM, Presented at Physics Beyond Colliders Annual Workshop, Mar 2021.

[116] M. Perrin-Terrin, Pion decay tagged muon neutrino beam (NuTag), Presented at the Physics Beyond Colliders Annual Workshop, Mar 2021.

[117] Physics Beyond Colliders Annual Workshop 2024, https://indico.cern.ch/event/1369776/, Mar 2024.

[118] S. Abdullin et al., The CMS barrel calorimeter response to particle beams from 2 to 350 GeV/c, CMS-NOTE-2008-034 (CERN, Geneva, Jun 2008).

[119] E. Abat et al., Study of the response of the ATLAS central calorimeter to pions of energies from 3 to 9 GeV, *Nucl. Instrum. Meth. Phys. Res. A* **607** (2009) 372 , doi:10.1016/j.nima.2009.05.158.

[120] Y. Nagai and the NA61/SHINE collaboration, Addendum to the NA61/SHINE proposal: A low-energy beamline at the SPS H2, CERN-SPSC-2021-028, SPSC-P-330-ADD-12 (CERN, Geneva, 2021).

[121] C. Mussolini and N Charitonidis, Engineering change request: H2-LE: New tertiary branch of the H2 beamline for low-energy particle beams, EDMS 2803011 (CERN, Aug 2023), CERN internal access.

[122] F. Acerbi et al., Decay tunnel instrumentation for the ENUBET neutrino beam, *JINST* **15** (2020) C05059, doi:10.1088/1748-0221/15/05/c05059.

[123] M. Jebramcik et al., Beam line designs for ENUBET/NuTag, Presented at Physics Beyond Colliders Annual Workshop, Mar 2024.

[124] E.G. Parozzi, Design and optimisation of a variable momentum secondary beamline for the NP06/ENUBET project, Dissertation, Milan Bicocca U., 2023, CERN-THESIS-2023-265.

[125] E.G. Parozzi et al., The ENUBET multi momentum secondary beamline design, presented at the 12th Int. Particle Accelerator Conf. (IPAC'21). JACoW Publishing, May 2021, pp. 3053–3056, doi:10.18429/JACoW-IPAC2021-WEPAB187.

[126] G. Aglieri Rinella et al., The NA62 gigatracker: a low mass high intensity beam 4D tracker with 65 ps time resolution on tracks, *JINST* **14** (2019) P07010, doi:10.1088/1748-0221/14/07/P07010.

[127] T. T. Böhlen et al., The FLUKA code: Developments and challenges for high energy and medical applications, *Nucl. Data Sheets* **120** (2014) 211, doi:10.1016/j.nds.2014.07.049.

[128] Marc Andre Jebramcik and Nikolaos Charitonidis, Conceptual comparative analysis of the SBN beamline implementation at CERN, CERN-PBC-Notes-2025-004 (CERN, Geneva, March 2025).

[129] Anna Baratto Roldan et al., NuTag: A proof-of-concept study for a long-baseline neutrino beam, CERN-PBC-Notes-2024-004 (CERN, Geneva, January 2024).

[130] A. Lai, A system approach towards future trackers at high luminosity colliders: the timespot project, 2018 IEEE Nuclear Science Symposium and Medical Imaging Conference Proceedings (NSS/MIC). IEEE, November 2018, doi:10.1109/nssmic.2018.8824310.

[131] N. Simos et al., 120 gev neutrino physics graphite target damage assessment using electron microscopy and high-energy x-ray diffraction, *PRAB* **22** (2019) 041001, doi:10.1103/physrevaccelbeams.22.041001.

[132] B. Densham et al., Design of the T2K target for a 0.75-MW proton beam, Presented at 46th ICFA Advanced Beam Dynamics Workshop on High-Intensity and High-Brightness Hadron Beam, Morschach, Switzerland, October 2010, 2010, pp. 560–562.

[133] M. Calviani, CNGS target operation and modified design, Presented at the 8th International Workshop on Neutrino Beams and Instrumentation, Nov 2012.

[134] K. Deb and H. Jain, An evolutionary many-objective optimization algorithm using reference-point-based nondominated sorting approach, Part I: Solving problems with box constraints, *IEEE Trans. Evol. Comput.* **18** (2014) 577, doi:10.1109/TEVC.2013.2281535.

[135] N. Beume, B. Naujoks and M. Emmerich, SMS-EMOA: Multiobjective selection based on dominated hypervolume, *Eur. J. Oper. Res.* **181** (2007) 1653–1669, doi:10.1016/j.ejor.2006.08.008.

[136] A. Panichella, An adaptive evolutionary algorithm based on non-euclidean geometry for many-objective optimization, Proceedings of the Genetic and Evolutionary Computation Conference. ACM, July 2019, GECCO '19, pp. 595–603, doi:10.1145/3321707.3321839.

[137] J. Blank and K. Deb, pymoo: Multi-objective optimization in python, *IEEE Access* **8** (2020) 89497, doi:10.1109/ACCESS.2020.2990567.

[138] M.A Jebramcik, N. Charitonidis and P. Arrutia, Ideas for a slow extraction via SPS LSS4 or LSS6 to a future PBC-SBN beamline, CERN-PBC-NOTE-2024-006 (CERN, Geneva, 2024).

[139] H. Bartosik et al., SPS operation and future proton sharing scenarios for the SHiP experiment at the BDF facility, CERN-ACC-NOTE-2018-0082, CERN-PBC-Notes-2021-008 (CERN, Geneva, Dec 2018).

[140] SPS Losses and Activation Working Group (SLAWG), SLAWG Indico pages, CERN internal access.

[141] G. Arduini et al., A new Experiment to Search for Hidden Particles (SHIP) at the SPS North Area, EDMS 1369559 (CERN, July 2014).

[142] The European Strategy Group, Deliberation document on the 2020 Update of the European Strategy for Particle Physics, CERN-ESU-014 (CERN, Geneva, 2020), doi:10.17181/ESU2020Deliberation.

[143] O. Aberle et al., Study of alternative locations for the SPS Beam Dump Facility, CERN-SPSC-2022-009 (CERN, Geneva, 2022).

[144] L. Gatignon, I. Ortega and J. Tan, Final report of the EABI Working Group, EDMS 2222321 v1.2 (CERN, 2019), restricted access.

[145] Y. Kadi et al., Strategy for the consolidation and upgrade of the North Experimental Area, NA-CONS-REPORT-001, EDMS 2042932 v2.1 (CERN, Geneva, 2020), CERN internal access.

[146] Beam Instrumentation for Fixed Target Facilities (BIFT) WG, BIFT meetings, https://indico.cern.ch/category/16541/, Mar 2023.

[147] R. Alemany Fernandez et al., Summary report of the Physics Beyond Colliders study at CERN, CERN-PBC-REPORT-2025-003 (CERN, Geneva, 2025).

[148] Other Science Opportunities at the FCC-ee, https://indico.cern.ch/event/1454873/, Nov 2024.